ALLOMETRIC RELATIONSHIPS AND THE EVOLUTION OF THE AVIAN BRAIN

FELIPE BARROS DA CUNHA
Master of Science, Universidade Federal do Rio de Janeiro, 2016

A thesis submitted
in partial fulfilment of the requirements for the degree of

DOCTOR OF PHILOSOPHY

in

NEUROSCIENCE

Department of Neuroscience
University of Lethbridge
LETHBRIDGE, ALBERTA, CANADA

ALLOMETRIC RELATIONSHIPS AND THE EVOLUTION OF THE AVIAN BRAIN

FELIPE BARROS DA CUNHA

Date of Defence: August 6, 2021

Dr. A. Iwaniuk	Associate Professor	Ph.D.
Dr. D. Wylie Thesis Co-Supervisors	Professor	Ph.D.
Dr. S. Pellis Thesis Examination Committee Member	Professor	Ph.D.
Dr. T. Burg Thesis Examination Committee Member	Professor	Ph.D.
Dr. I. Whishaw Internal External Examiner Department of Neuroscience Faculty of Arts and Science	Professor	Ph.D.
Dr. P. Němec External Examiner Charles University Prague, Czech Republic	Associate Professor	Ph.D.
Dr. M. Tatsuno Chair, Thesis Examination Committee	Professor	Ph.D.

ABSTRACT

A relatively larger brain is thought to have relatively more neurons and thus higher processing capacity. However, to what extent brain region volumes, and numbers and sizes of neurons vary with brain size remains uncertain. Here, I provide quantitative measurements on the cerebellum, telencephalon, and oculomotor nuclei across different bird species. Within the cerebellum, different neuronal populations increase in number and size at different rates relative to brain size, but there is little variation across clades. Using evolutionary path analysis, I show that the relationship between telencephalon and cerebellum size is a function of migration. Last, the oculomotor nuclei differ in volume across clades, but these differences are not driven by neuron numbers. I conclude that grade shifts in brain size are not always driven by changes in neuron numbers. I suggest that neuron size better explains changes in the size of brainstem motor nuclei than neuron number.

ACKNOWLEDGMENTS

I would like to begin saying a big thank you to Dr. Andrew Iwaniuk for offering me all the opportunities I had during this PhD. The "PhD journey" was not an easy pathway (I think he knows that!), and Andy was always there promptly giving me useful insights, comments, feedback on my Chapters, advice on statistical analyses, and ideas for future projects. Even when the storm was up in my head, Andy was there to help and give me the guidance. Thanks for all the patience, Andy. All the opportunities he provided throughout these years were incredible for my learning and formation as a critical scientist: from sending me to workshops, to discussing papers in the lab, encouraging and supporting myself to present at conferences, and introducing me to other professors and colleagues. Everything that I learned with him goes way beyond of what is written, published, and reported in this thesis, no doubt! Thank you so much, Andy.

I would also like to mention here my committee members: Dr. Theresa Burg, Dr. Sergio Pellis and Dr. Douglas Wylie. Thank you all for hearing about my projects almost every six months, and still – even when it was probably super tedious to hear about my results over and over again, you were there giving helpful and useful comments. A special shout out thank you to Doug, my co-supervisor: the interpretation of some of my results were not an easy thing to do, and I appreciate every comment and discussion on the results. I also have to say a big thank you to Dr. Cristian Gutiérrez-Ibáñez – he is the person that first introduced R to me and taught me how to perform most of the analyses done in this thesis. Thank you so much for the patience and guidance, for reviewing chapters, and connecting online with me so many times in moments of desperation with all the analyses and doubts I had.

I cannot forget to mention everyone in the lab, they were always the best! All of them made my days less stressful, even when I had no idea what they were talking about (the unforgettable day of a “sorry guys, I don’t get it, I don’t think this is part of my culture”, after some of the many jokes thrown in the lab). Ben Brinkman (or beef boi, even though *he* should be the *sweet* Ben!), thank you so much for being so supportive during all these 4 years! Our chats in the lab during lunchtime were the best way to make my day lighter, and you were always an amazing and friendly source for advice and help with anything in the lab. If you are not so sure on how to fix the scope, Ben will probably know it! I also have to emphasize here all the help that I got from Kelsey Racicot: as a great independent student (and now she is a great MSc), she helped me so much with the non-ending data and measurements collected for the cerebellum chapters. Thank you, Ben and Kelsey! Michelle Martin (hey Mike!) was a great company that arrived later in the lab, thanks for the chats and for being the “birder” introducer. I also need to mention other people that were members of the lab at some point during these 4 years, and made a difference (even if it’s indirect) for this thesis to come out: Lauren Williams, Ryaan ElAndari, Krista Fjordbotten, Olivia Stephen and Christina Popic. I extend here my thanks to Dr. Maurice Needham (always there helping when the microscope suddenly decided to give a break on us) and Naomi Cramer for all the support. Finally, I would like to say a “hugfull” thank you to my friends – the old ones from Brasil, and the more recent ones I met in Canada (international fam, Tres Leches, Lafafa House, Sandhya, Mahmud, Vanja, Camilla, Miche, Brenton, Mila, Wael, Edberto, Sahar), and my family. Y’all were always there supporting and encouraging me, and I’m so grateful for it. Many thanks!

TABLE OF CONTENTS

ABSTRACT .... **iii**

ACKNOWLEDGMENTS .... **iv**

LIST OF TABLES .... **ix**

LIST OF FIGURES .... **xi**

LIST OF SUPPLEMENTARY INFORMATION .... **xv**

LIST OF ABBREVIATIONS .... **xvi**

CHAPTER ONE: GENERAL INTRODUCTION **1**
- An Integrative Approach to Testing the Principle of Proper Mass 6
- Hypotheses 7

References **11**

CHAPTER TWO: A QUANTITATIVE ANALYSIS OF CEREBELLAR ANATOMY IN BIRDS **17**

Abstract **17**

Introduction **18**

Material and Methods **22**
- Specimens 22
- Volumetric measurements 22
- Surface area of the Purkinje cell layer 23
- Cerebellar Foliation Index (CFI) 24
- Cell counts 24
- Cell sizes 26
- Variation across orders 27
- Model selection and hypothesis testing 28

Results **28**
- Allometric relationships of the cerebellum volume 28
- Allometric relationships among neuronal populations 30
- Allometry of cerebellar foliation and surface area 31

Discussion **32**
- Allometric scaling within the cerebellum 34
- Cerebellar volume, surface area of the Purkinje cell layer, and foliation 37
- Conclusions 38

References **40**

CHAPTER THREE: EVOLUTION OF CEREBELLUM SIZE IN BIRDS: THE EFFECTS OF DEVELOPMENT, FLIGHT, MIGRATION AND TELENCEPHALON SIZE **63**

Abstract 63
Introduction 64
Material and Methods 67
Data collection 67
Statistical analyses 69
Results 71
Path analysis 72
Discussion 72
Altricial vs. Precocial Species 73
Flight behaviour and the cerebellum 75
Migratory birds: a trade-off between the cerebellum and telencephalon 77
Conclusions 80
References 81
CHAPTER FOUR: VARIATION IN THE VOLUME AND NUMBER OF NEURONS OF THE OCULOMOTOR NUCLEI ACROSS BIRD SPECIES 108
Abstract 108
Introduction 109
Material and Methods 112
Specimens 112
Stereological measurements 114
Retinal topography 115
Data analyses 115
Results 116
Cytoarchitecture of the oculomotor nuclei 116
Oculomotor nucleus (nIII) 117
Trochlear nucleus (nIV) 117
Abducens (VI) 118
Edinger-Westphal (EW) 119
Discussion 120
Nucleus VI and EW in Songbirds 120
Pursuit diving 122
Smaller oculomotor nuclei in owls 123
Larger VI in falcon, hawks and vultures 124
Conclusions 127
References 129
CHAPTER FIVE: GENERAL DISCUSSION 161
Recapitulation 161
Brain size and neuron numbers: more complex than what we think 162
Are there “allometric scaling rules” in the brain? 166
2-in-1: concerted and mosaic brain hypotheses 167

Future directions 170

References **175**

SUPPLEMENTARY INFORMATION **179**

LIST OF TABLES

Table 2.1. A list of the avian species analyzed and their respective brain volumes, cerebellum volumes, molecular layer volumes, granule cell layer volumes, white matter volumes, surface area of the Purkinje cell layer, and cerebellar foliation index (CFI). 45

Table 2.2. Numbers (#) of Purkinje cells, granule cells and cerebellar nuclei neurons across species analyzed. 48

Table 2.3. Soma sizes (μm ^{2}) of Purkinje cells, granule cells and cerebellar nuclei neurons across species analyzed (±SD). 50

Table 2.4. Summary of the clade differences for the measurements examined relative to brain volume (vol.) or cerebellum volume. Down arrow indicates relative reduction, up arrow indicates relative increase, and hyphen indicates no difference between a given clade and other birds. 52

Table 3.1. Details of the allometric relationships between brain region sizes. Brain remainder corresponds to total brain size minus the volumes of the telencephalon and cerebellum. λ = Pagel's lambda; p = p-value; r^2 = coefficient of determination. 89

Table 3.2. Model comparison for our hypothesized causal relationships (see Fig. 3.4). We report: K, number of independence claims; q, number of parameters; C, Fisher's C statistics; p-values; CICc, C statistic information criterion corrected for small sample sizes; ΔCICc, difference in CICc from the best-fitting model; w, CICc weights. 90

Table 3.3. A list of the bird species analyzed and their respective orders, brain volumes (=brvol), telencephalon volumes (=telenvol), cerebellum volumes (=cbvol), and remaining brain structures volumes (=RBrvol), and sources from which data were extracted. Order abbreviations: Acc=Accipitriformes; Ans=Anseriformes; Apod=Apodiformes; Apt=Apterygiformes; Buce= Bucerotiformes; Capr=Caprimulgiformes; Casua=Casuariiformes; Cath=Cathartiformes; Cico=Ciconiiformes; Colum=Columbiformes; Cora=Coraciiformes; Cucu=Cuculiformes; Fal=Falconiformes; Galli=Galliformes; Gavi=Gaviiformes; Grui=Gruiformes; Otidi=Otidiformes; Passe=Passeriformes; Pelec=Pelecaniformes; Phoe=Phoenicopteriformes; Pici=Piciformes; Podic= Podicipediformes; Proce=Procellariiformes; Psi=Psittaciformes; Rhei=Rheiformes; Sphen=Sphenisciformes; Stri=Strigiformes; Strut=Struthioniformes; Suli=Suliformes; Tin=Tinamiformes. 91

Table 3.4. List of the species analyzed and their respective behaviours. Dev.=developmental mode; Altr.=altricial; prec.=precocial; Y=yes; N=no. For flight, rank is based on Norberg's (2012) as: 0 = flightless, 1 = slow, poor manoeuvrable birds that soar, 2 = fast, poorly manoeuvrable fliers, 3 = slow manoeuvrable fliers, 4 = fast manoeuvrable fliers. Order abbreviations: Acc=Accipitriformes; Ans=Anseriformes; Apod=Apodiformes; Apt=Apterygiformes; Buce= Bucerotiformes; Capr=Caprimulgiformes; Casua=Casuariiformes; Cath=Cathartiformes; Cico=Ciconiiformes; Colum=Columbiformes; Cora=Coraciiformes; Cucu=Cuculiformes; Fal=Falconiformes; Galli=Galliformes; Gavi=Gaviiformes; Grui=Gruiformes; Otidi=Otidiformes; Passe=Passeriformes; Pelec=Pelecaniformes;

Phoe=Phoenicopteriformes; Pici=Piciformes; Podic= Podicipediformes; Proce=Procellariiformes; Psi=Psittaciformes; Rhei=Rheiformes; Sphen=Sphenisciformes; Stri=Strigiformes; Strut=Struthioniformes; Suli=Suliformes; Tin=Tinamiformes. 98

Table 4.1. Published data on eye movements. EOG=electro-oculogram; N/D=not detected; NR=values not reported. Notes: [1]=anectodal observation; [2]=animal's head was immbolized; [3]=technique cannot detect small amplitude of eye movements. 137

Table 4.2. Volumes of the brain, brainstem, abducens (VI), trochlear (IV), III-dorsolateral, III-dorsomedial, III-dorsoventral, and Edinger-Westphal nuclei for the species analysed. Grid sizes varied between 20 - 50 μm. 140

Table 4.3. Numbers of neurons (n) of the abducens, trochlear, III-dorsolateral, III-dorsomedial, III-ventral, and Edinger-Westphal nuclei for the species analysed. For every species, grid size was 50 μm and frame size was 40 μm. 144

Table 4.4. Details of the allometric relationships among the variables from the oculomotor nuclei examined. λ = Pagel's lambda; p = p-value; r^2 = coefficient of determination; CI = confidence interval. 147

Table 4.5. Data collated in the literature on retinal topography for the species in our sample. Notes: for species highlighted with "1", data on retinal topography was assumed based on available data of congeners; for species highlighted with "2", data is still insufficient, another area or fovea could be present (see Lisney et al., 2015). 148

LIST OF FIGURES

Figure 1.1. In rodents (brown), when the brain increases in size it does not gain as many neurons as a primate's brain (yellow). Species depicted are agouti (*Dasyprocta primnolopha; Dp*), capybara (*Hydrochoerus hydrochoeris; Hh*), owl monkey (*Aotus trivirgatus; At*), and crab-eating macaque (*Macaca fascicularis; Mf*). *Data from Herculano-Houzel et al., 2006, 2007.* 16

Figure 2.1. Phylogeny of the species analyzed in this study. The clades Passeriformes (songbirds), Psittaciformes (parrots), Anseriformes (waterfowls), and Galliformes (chicken-like birds) are indicated on the branches.. 53

Figure 2.2. Midsagittal sections of Nissl-stained cerebella of: **A** peaceful dove (*Geopelia placida*), **B** grey partridge (*Perdix perdix*), **C** lesser scaup (*Aythya affinis*), **D** brown thornbill (*Acanthiza pusilla*), **E** sulphur-crested cockatoo (*Cacatua galerita*), and **F** Australian bustard (*Ardeotis australis*). Note the difference in cerebellar size and shape across avian species. For example, while the sulphur-crested cockatoo has a CFI of 5.56, the peaceful dove has a CFI of 2.97. For the peaceful dove (A), cerebellar folia are represented as roman numerals, from I (anterior) to X (posterior), as suggested by Larsell (1967). The black continuous line follows the Purkinje cell layer. The ratio between the length of the Purkinje cell layer (continuous black line) and the envelope length of this same layer (dotted black like) is referred to as the cerebellar foliation index (CFI). ml=molecular layer; gr = granule cell layer, and "wm+cn" = white matter layer and cerebellar nuclei. Scale-bars: A-C = 1mm, D = 0.5mm, E-F = 2mm. 54

Figure 2.3. Scatterplots of the log-transformed volumes (mm^3) of: **A** molecular layer (mm^3) against rest of cerebellum and **B** granule cell layer against rest of the cerebellum, **C** white matter layer plus cerebellar nuclei neurons against rest of the cerebellum. Clades with significant differences from other birds are indicated in the graph. See allometric equations and statistical data in Table S2.2. The rest of the cerebellum refers to as total cerebellum size minus the size of the cerebellar layer in the y-axis. 55

Figure 2.4. Scatterplots of the log-transformed of: **A** Purkinje cell number, **B** granule cell number, **C** cerebellar nuclei neuron number, **D** Purkinje cell size (mm^2), **E** granule cell size (mm^2), and **F** cerebellar nuclei neuron size (mm^2) against the log-transformed volume (mm^3) of the cerebellum. Clades with significant differences from other birds are indicated in the graph. See allometric equations and statistical data in Table S2.2. CbN=cerebellar nuclei. 56

Figure 2.5. Distribution of cell soma sizes (μm^2) of Purkinje cells (A, D, G, J, M), granule cells (B, E, H, K, N) and cerebellar nuclei neurons (C, F, I, L, O) within the following specimens: brown thornbill (*Acanthiza pusilla,* A-C), lesser scaup (*Aythya affinis,* D-F), galah (*Cacatua roseicapilla*, G-I), collared sparrowhawk (*Accipiter cirrocephalus*, J-L) and emu (*Dromaius novaehollandiae*, M-O). The depicted bars represent the summed-up counts of cells within the following ranges: 25-50 μm for Purkinje cells and cerebellar nuclei neurons, and 0.75-1.50 μm

for granule cells. The distribution of cell soma sizes followed a normal distribution curve. Although the distribution of the granule cell sizes in the emu appears to be slightly different than a normal curve, most of the measurements were still restricted to a narrow range of sizes (e.g., 16-22 μm)... 57

Figure 2.6. Scatterplots of the log-transformed of: **A** granule cell number against Purkinje cell number, **B** cerebellar nuclei neuron number against Purkinje cell number, **C** cerebellar nuclei neuron number against granule cell number, **D** granule cell size (μm^2) against Purkinje cell size (μm^2), **E** cerebellar nuclei neuron size (μm^2) against Purkinje cell size and **F** cerebellar nuclei neuron size against granule cell size. Clades with significant differences from other birds are indicated in the graph. See allometric equations and statistical data in Table S2.2. CbN=cerebellar nuclei. 59

Figure 2.7. Scatterplots of the log-transformed of: **A** Purkinje cell number against Purkinje cell size (μm^2), **B** granule cell number against granule cell size (μm^2), and **C** cerebellar nuclei neuron number against cerebellar nuclei neuron size (μm^2). See allometric equations and statistical data in Table S2.2. 60

Figure 2.8. Scatterplots of the log-transformed of: **A** cerebellum volume (mm^3) against rest of the brain volume (mm^3), **B** surface area of Purkinje cell layer (mm^2) against rest of the brain volume, and **C** Purkinje cell number against rest of the brain volume. Clades with significant differences from other birds are indicated in the graph. See allometric equations and statistical data in Table S2.2. 61

Figure 2.9. Scatterplots of the log-transformed of: **A** cerebellum volume (mm^3) against rest of the brain volume (mm^3), **B** surface area of Purkinje cell layer (mm^2) against rest of the brain volume, and **C** Purkinje cell number against rest of the brain volume. Clades with significant differences from other birds are indicated in the graph. See allometric equations and statistical data in Table S2.2. 62

Figure 3.1. Scatterplots of log-transformed volumes (mm^3) of: **A.** cerebellum against brain remainder, **B.** telencephalon against brain remainder, and **C**. cerebellum against telencephalon. Altricial and precocial species are depicted in different colors, as shown in the legend. The brain remainder refers to brain size minus the sizes of the telencephalon and cerebellum. 104

Figure 3.2. Scatterplots of log-transformed volumes (mm^3) of: **A.** cerebellum against brain remainder, **B.** telencephalon against brain remainder, and **C.** cerebellum against telencephalon. Migratory (red) and non-migratory (gray) species are depicted in different colors, as shown in the legend. The brain remainder refers to brain size minus the sizes of the telencephalon and cerebellum.. 105

Figure 3.3. Scatterplots of log-transformed volumes (mm^3) of: **A.** cerebellum against brain remainder, **B.** telencephalon against brain remainder, and **C.** cerebellum against telencephalon. Aerial (yellow) and non-aerial (gray) species are depicted in different colors, as shown in the legend. The brain remainder refers to brain size minus the sizes of the telencephalon and cerebellum.. 106

Figure 3.4. Hypothetical models (M1-M10) based on our trait predictors, and brain region sizes. The best-fitting model ('Best fit model, M10') is depicted in the figure. Arrows represent hypothetical causal links, and values represent the standardized average coefficients of the causal links from the best-fitting model 107

Figure 4.1. A. Oculomotor (III) and Edinger-Westphal (EW), **B.** trochlear (IV), and **C.** abducens (VI) nuclei of a ring-necked pheasant (Phasianus colchicus). Subnuclei of nIII are depicted in **A.**, III-m = dorsomedial III, III-l = dorsolateral III, III-v = ventral III. Scale-bar = 200 µm. 151

Figure 4.2. Oculomotor and Edinger-Westphal nuclei of: **A.** brown-headed cowbird (Molothrus ater), **B.** white-headed pigeon (Columba leucomela), **C.** Swainson's hawk (Buteo swainsoni), **D.** red-breasted merganser (Mergus serrator), **E.** barn owl (Tyto alba), and **F.** great horned owl (Bubo virginianus). EW = Edinger-Westphal; III-m = dorsomedial III; III-l = dorsolateral III; III-v = ventral III. Scale-bar = 200 µm.. 152

Figure 4.3. Scatterplots of log-transformed volumes (mm^3) of: **A.** dorsomedial III against brainstem, **C.** dorsolateral III against brainstem, and **E.** ventral III against brainstem. Residuals distribution across avian orders from each scatterplot performed are shown for: **B.** relative size of dorsomedial III, **D.** relative size of dorsolateral III, and **F.** relative size of ventral III. Significant differences found among bird orders by pANCOVAs are shown with an asterisk (*). Residuals boxplots are only a visual depiction of the differences found in graphs **A**, **C**, and **E**. III = oculomotor nucleus. 153

Figure 4.4. Scatterplots of log-transformed of: **A.** number of neurons of dorsomedial III against brainstem volume (mm^3), **C.** number of neurons of dorsolateral III against brainstem volume, and **E.** number of neurons of ventral III against brainstem volume. Residuals distribution across avian orders from each scatterplot performed are shown for: **B.** relative number of neurons of dorsomedial III, **D.** relative number of neurons of dorsolateral III, and **F.** relative number of neurons of ventral III. Significant differences found among bird orders by pANCOVAs are shown with an asterisk (*). Residuals boxplots are only a visual depiction of the differences found in graphs **A**, **C**, and **E**. III = oculomotor nucleus. 154

Figure 4.5. Scatterplots of log-transformed of: **A.** number of neurons of dorsomedial III against dorsomedial III volume (mm^3), **C.** number of neurons of dorsolateral III against dorsolateral III volume (mm^3), and **E.** number of neurons of ventral III against ventral III volume (mm^3). Residuals distribution across avian orders from each scatterplot performed are shown for: **B.** relative number of neurons of dorsomedial III, **D.** relative number of neurons of dorsolateral III, and **F.** relative number of neurons of ventral III. Significant differences found among bird orders by pANCOVAs are shown with an asterisk (*). Residuals boxplots are only a visual depiction of the differences found in graphs **A**, **C**, and **E**. III = oculomotor nucleus.................................... 155

Figure 4.6. Scatterplots of log-transformed of: **A.** IV volume (mm^3) against brainstem volume (mm^3), **C.** number of neurons of IV against brainstem volume, and **E.** number of neurons of IV against IV volume. Residuals distribution across avian orders from each scatterplot performed are shown for: **B.** relative volume of IV, **D.** number of neurons of IV relative to brainstem size,

and **F.** number of neurons of IV relative to IV volume. Significant differences found among bird orders by pANCOVAs are shown with an asterisk (*). Residuals boxplots are only a visual depiction of the differences found in graphs **A**, **C**, and **E**. IV = trochlear nucleus. 156

Figure 4.7. Scatterplots of log-transformed of: **A.** VI volume (mm^3) against brainstem volume (mm^3), **C.** number of neurons of VI against brainstem volume, and **E.** number of neurons of VI against VI volume. Residuals distribution across avian orders from each scatterplot performed are shown for: **B.** relative volume of VI, **D.** number of neurons of VI relative to brainstem size, and **F.** number of neurons of VI relative to VI volume. Significant differences found among bird orders by pANCOVAs are shown with an asterisk (*). Residuals boxplots are only a visual depiction of the differences found in graphs **A**, **C**, and **E**. VI = abducens nucleus................... 157

Figure 4.8. Scatterplots of log-transformed of: **A.** EW volume (mm^3) against brainstem volume (mm^3), **C.** number of neurons of EW against brainstem volume, and **E.** number of neurons of EW against EW volume. Residuals distribution across avian orders from each scatterplot performed are shown for: **B.** relative volume of EW, **D.** number of neurons of EW relative to brainstem size, and **F.** number of neurons of EW relative to EW volume. Significant differences found among bird orders by pANCOVAs are shown with an asterisk (*). Residuals boxplots are only a visual depiction of the differences found in graphs **A**, **C**, and **E**. EW = Edinger-Westphal. 158

Figure 4.9. Scatterplots of log-transformed of: **A.** EW volume (mm^3) against brainstem volume (mm^3), **B.** number of neurons of EW against brainstem volume, and **C.** number of neurons of EW against EW volume across waterfowls. The red-breasted merganser (Mergus serrator) is highlighted in blue. Confidence intervals (95%) of the allometric regressions are indicated as gray shades in the graphs. 159

Figure 4.10. Scatterplots of log-transformed of: **A.** total III volume (mm^3) against brainstem volume (mm^3), **C.** number of neurons of total III against brainstem volume, and **E.** number of neurons of total III against total III volume. Residuals distribution across avian orders from each scatterplot performed are shown for: **B.** relative volume of total III, **D.** number of neurons of total III relative to brainstem volume, and **F.** number of neurons of total III relative to total III volume. Residuals boxplots are only a visual depiction of the differences found in graphs **A**, **C**, and **E.** 160

LIST OF SUPPLEMENTARY INFORMATION

Table S2.1 Sampling interval and grid size used for each neuronal population examined: Purkinje cells, granule cells, and cerebellar nuclei neurons. For Purkinje cells and cerebellar nuclei neurons, frame size was 80 x 80 µm. For granule cells, frame size was 10 x 10 µm…179

Table S2.2. Details of the allometric relationships among the cerebellar measurements examined………………………………………………………………………………...181

Table S2.3. Multiple allometric models with number of Purkinje cells as the dependent variable, and surface area of the Purkinje cell layer, and cerebellar volume as the predictor variables. #PC = number of Purkinje cells; PCL area = surface area of the Purkinje cell layer; Cbvol = cerebellum volume…………………………………………………………………………182

Figure S2.1. A comparison of the sizes of Purkinje cells, granule cells, and cerebellar nuclei neurons in two species, **A-C** the brown thornbill (Acanthiza pusilla), and **D-F** the little penguin (Eudyptula minor). For each species, Purkinje cells are shown in **A** and **D** (scale-bar = 50 µm); granule cells in **B** and **E** (scale-bar = 10 µm), and cerebellar nuclei neuron in **C** and **F** (scale-bar = 30 µm)……………………………………………………………………………………….183

LIST OF ABBREVIATIONS

μm – micrometers “microns”
vol – volume
kg – kilograms
g – grams
mg – milligrams
ANCOVA – analysis of covariance
AIC – Akaike information criterion
CIC – C statistic information criterion
CICc – C statistic information criterion adjusted for small samples
w – CICc weights
Cb, cb – cerebellum/cerebellar
Cbvol – cerebellum volume
telenvol – telencephalon volume
RBrvol – remaining brain structures volume
CbN – cerebellar nuclei
wm+cn – white matter + cerebellar nuclei
ml – molecular layer
gr, gl – granule cell layer
CFI – cerebellar foliation index
PC – Purkinje cell
PCL – Purkinje cell layer
Dev. – developmental mode
altr. – altricial
prec. – precocial
RA - robust nucleus of the arcopallium
III – oculomotor nucleus
III-m – dorsomedial III nucleus
III-l – dorsolateral III nucleus
III-v – ventral III nucleus
IV – trochlear nucleus
VI – abducens nucleus
EW – Edinger Westphal nucleus

CHAPTER ONE: GENERAL INTRODUCTION

Brain size varies greatly among vertebrate species, possibly moreso than any other organ. In mammals, for example, this mass variation reaches 100,000 times, ranging from 60 mg in an Etruscan shrew (*Suncus etruscus*) to 9 kg in a blue whale (*Balaenoptera musculus*) (Fons et al. 1984; Pearce 2013). Not only mammals, but birds also have an impressive range of brain sizes; from the 0.2 g brains of hummingbirds to 40 g brains of ostriches (*Struthio camelus*) (Portmann 1947; Rehkämper et al. 1991b). This difference is still great if we consider brain size relative to body size. Humans (*Homo sapiens*), for instance, have a brain seven times larger than that expected from their body mass, whereas rats (*Rattus norvegicus*) have brains that are only 0.4 times larger than expected (Jerison 1973; Jerison 1977). This variation also extends to other vertebrates, including birds: parrots, owls and corvids have the largest relative brain sizes among birds (Bennett and Harvey 1985; Iwaniuk et al. 2005; Fristoe et al. 2017; Ksepka et al. 2020). Historically, differences in absolute and relative sizes of the brain have been related to behavioral diversity and cognitive abilities (Bennett and Harvey 1985; Lefebvre et al. 2004; Benson-Amram et al. 2016). There is evidence that taxa with relative larger brains have a greater ability to respond to new challenges (Gossette 1968; Lefebvre et al. 2004) and, in birds and mammals, cognitive performance is positively correlated with relative brain size (MacLean et al. 2014; Benson-Amram et al. 2016; Street et al. 2017).

The idea that larger brains (in absolute or relative sizes) enable more complex behaviour is associated with the "principle of proper mass" (Jerison 1973). This theory suggests that the amount of neural tissue committed to a certain function is directly correlated with the amount of processing required for that function. Thus, according to this theory, a relatively large brain region is expected to have better or faster processing of information than a relatively small brain region (Jerison 1973). An example of this difference is the organization of the cerebral cortex of the naked mole-rat (*Heterocephalus glaber*). The extreme sensory specializations of this rodent are reflected in major rearrangements in the brain when compared to other rodents (Catania and Remple 2002; Xiao et al. 2006). For example, naked mole-rats have enlarged, mobile incisors that are constantly used for digging and feeding, and in this species approximately one-third of the primary somatosensory cortex is devoted to process the upper and lower incisors (Catania and Remple 2002). Thus, the relative size of somatosensory regions reflects their processing capacities, supporting the principle of proper mass (Jerison 1973).

Although the naked mole-rat is an example of the principle of proper mass applied to sensory systems, the theory is often invoked in the context of cognition (Gutiérrez-Ibánez et al. 2013; Barton and Venditti 2014; Wylie et al. 2015; Benson-Amram et al. 2016; Fristoe et al. 2017). Associating brain mass with cognitive performance assumes that a larger brain yields greater processing power (Jerison 1973). This increased processing capacity was thought to be a consequence of a one-to-one relationship between mass and number of neurons (Williams and Herrup 1988). Thus, a 3-fold increase in brain mass would necessarily entail three times more neurons. However, recent studies in several orders of mammals and birds show no universal relationship between brain mass and number of neurons (see review Herculano-Houzel et al. 2015; Olkowicz et al. 2016). In rodents, for example, the mass of the brain grows faster than the addition of neurons (Herculano-Houzel et al. 2006) whereas primates (including humans) increase brain mass and neuron numbers at a rate close to 1 (Figure 1.1; Herculano-Houzel et al. 2014). As a result of these differences in neuron numbers relative to brain mass (see Figure 1.1), comparing relative brain size between a rodent and primate are not equivalent in terms of neuron numbers or information processing capacity.

Not only is brain size problematic as a measurement because of clade-specific variations in neuronal density, the brain is a heterogeneous structure, comprised of multiple regions each with distinct connections and functions. In birds, for example, the fraction occupied by the telencephalon in relation to the total mass of the brain can vary by approximately two times. The common raven (*Corvus corax*) and African grey parrot (*Psittacus erithacus*) have telencephala that occupy 80% of their total brain mass, while in the red junglefowl (*Gallus gallus*) and diamond dove (*Geopelia cuneata*) the telencephalon is only 53% and 45%, respectively, of their total brain mass (Portmann 1947; Boire and Baron 1994). Given that the telencephalon is comprised of regions related to cognition and complex behaviour (Rehkämper et al. 1991a; Mehlhorn et al. 2010), a relatively large telencephalon may potentially enable species to perform complex abilities (Sol and Lefebvre 2000; Güntürkün 2012). For instance, corvid species are able to manufacture and use tools (Hunt 1996; Weir et al. 2002), and some parrots have an exceptional ability to communicate and understand numerical differences (Pepperberg 2002; Pepperberg and Gordon 2005). In contrast, there is little evidence that chicken-like birds and pigeons can perform similarly complex behaviour (Sol et al. 2002; Lefebvre et al. 2004). Thus, analyses that consider different brain regions and their roles in different functions will likely provide better insights into how the evolution of the brain is associated with processing capacity and cognition across species.

As mentioned above, brain size is only one metric, and other parameters of the brain could potentially change among species, and independently of changes in brain size. Although little attention has been paid to the variation of neuron size across vertebrate brains, plenty of evidence indicates that neuron size can reflect differences in brain physiology and behaviour (Bottjer et al. 1986; Thompson and Brenowitz 2005; Freas et al. 2013; Chang et al. 2020). In male zebra finches (*Taeniopygia guttata*), the size of neurons in the robust nucleus of the arcopallium (RA, a premotor brain region involved in vocal production) increases significantly during the period of song learning (Bottjer et al. 1986). This finding suggests that processing power of the brain is positively correlated with neuron size. In the same study, the HVC, another brain region involved in song processing, had the opposite correlation between cell size and song learning (Bottjer et al. 1986). Instead of having larger cells in adult individuals with consolidated stereotypical songs, HVC had more and smaller cells (Bottjer et al. 1986). In other species, like the canary (*Serinus canarius*), seasonal changes linked with vocal performance appear to explain variation in RA neuron size (Devoogd & Nottebohm, 1981a,b). During the breeding season, neuron soma size and dendritic trees become larger and are responsible, at least partially, for the expansion in size of the RA in this bird species (Devoogd & Nottebohm, 1981a,b).

Given that the relationships among brain size, number of neurons, and size of neurons vary greatly among clades and within brain regions (Devoogd & Nottebohm, 1981a; Bottjer et al. 1986; Herculano-Houzel et al. 2014; Olkowicz et al. 2016; Cunha et al. 2020), it is reasonable to expect that ‘allometric scaling rules’ (e.g., total number of neurons relative to brain mass) must also vary among different neuronal types. Most of the current quantitative data on the brain do not differentiate neuron types (Herculano-Houzel et al., 2014; Olkowicz et al., 2016; but see Cunha et al., 2020), and it remains unclear to what extent the relationship between brain size and neuron number/size is specific to neuron types. Investigating how these “allometric rules” vary would bring important insights into the evolution of the brain composition, connectivity, and function.

Not only might neuronal populations vary at different rates, but also brain regions. As stated above, larger brains are not necessarily scaled-up version of small brains (Barton and Harvey 2000; Iwaniuk et al. 2004; Smaers and Soligo 2013; Gutiérrez-Ibáñez et al. 2014), meaning that individual brain regions may change in size at different rates. The majority of the studies investigating the evolution of the brain, however, do not take into account the heterogeneity of the brain (Van Woerden et al. 2010; Navarrete et al. 2011; Van Schaik et al. 2012; DeCasien et al. 2017). Evolutionary patterns reported for overall brain size may not necessarily apply to all individual brain regions. Thus, evaluating how the interactions among the sizes of brain regions, traits and behaviour determine changes in the size of the brain would allow one to better infer evolutionary causes for brain size variation. For example, by assessing the potential direct and indirect relationships among the sizes of brain regions, behaviour, and traits, it is possible to better understand which variables affect changes in the size of a given brain region.

That said, an approach that considers not only the entire brain size but different brain regions and parameters within the brain (e.g., number and size of different neuronal populations) is wanting. This type of analysis, that includes as many different parameters as possible, would allow a more complete understanding of how the brain changes across species and ultimately what explains brain size variation. As stated above, variables within the brain are likely correlated to one another. Therefore, statistical analyses that take into account the potential interaction of these different parameters are indispensable if we wish to determine causal relationships among brain anatomy, function, and behaviour. In this thesis I provide detailed, quantitative data (brain size, neuron number, and neuron size) on different brain regions across a broad range of birds. By employing modern phylogenetic comparative methods, I determine what explains brain size variation across avian species.

An Integrative Approach to Testing the Principle of Proper Mass

As mentioned above, the principle of proper mass proposes that the size of a neural tissue involved in a particular function is directly associated to the amount of information processing to perform that function (Jerison 1973). This means that relatively larger brains are thought to have better processing capacity (Jerison 1973). The size of the brain, however, is the result of changes in many different parameters within the brain (e.g., neuron number). Therefore, the principle of proper mass applies to not only size of the brain but also other parameters. For example, across most vertebrates, increases in the size of the brain arise from increases in the numbers and sizes of neurons (Herculano-Houzel et al 2014; Olkowicz et al. 2016; Cunha et al. 2020). Both neuron sizes and neuron numbers have been suggested to positively correlate with processing capacity (DeVoogd and Nottebohm 1981; Herculano-Houzel 2017; Chang et al. 2020), but it remains unknown (1) how neuron number and neuron size change relative to one another and (2) which of these two parameters best explains brain size and function.

Even if we only consider brain size, individual brain regions may affect total brain size in different ways. As proposed by the Principle of Proper Mass, a particular function/behaviour is directly associated with the size of the brain region involved in that function (Jerison 1973). However, changes in a given brain region may also indirectly affect the sizes and anatomy of other brain regions. For instance, anatomical changes in the pallium are tightly correlated with changes in the anatomy of the cerebellum (Herculano-Houzel 2010; Barton and Venditti 2014). For that reason, the Principle of Proper Mass can be better understood if we first determine (1) what drives changes in the size of the brain across species, (2) how different behaviours affect the sizes of different brain regions, and (3) how brain regions vary in size relative to one another.

In this thesis, I test how number and size of neurons explain variation in the size of the brain, and how the size of the cerebellum varies relative to the sizes of the telencephalon and brain remainder and as a function of development and locomotory behaviours. I also test whether relative number and size of neurons are positively associated with processing capacity and behaviour. For each chapter, I raise three hypotheses, shown below.

Hypotheses

Hypothesis 1: Neuron number explains more variation in cerebellum size than neuron size (Chapter 2).

Hypothesis 2: Cerebellum size is positively associated with the evolution of complex motor behaviour (Chapter 3).

Hypothesis 3: The size of the oculomotor nuclei and numbers of neurons within them reflect the degree of eye movements of a species (Chapter 4).

To test these hypotheses, I collected data from the lab's large comparative brain collection using unbiased stereological methods. All data were then analyzed within a phylogenetic framework with an array of statistical tests including phylogenetic generalized least squares and analyses of covariance (Garamszegi 2014), and phylogenetic path analysis (von Hardenberg and Gonzalez-Voyer 2013; Gonzalez-Voyer and von Hardenberg 2014).

In Chapter 2, I test if neuron numbers explain more variation in cerebellum size than neuron size. The cerebellum is a multifunctional region involved in motor control, learning and cognitive processing (Ito 1984; Thach 1998; Rodriguez et al. 2005) and houses a large number of neurons (Herculano-Houzel et al, 2014; Olkowicz et al, 2016). In songbirds, the cerebellum comprises 50% of the total number of neurons in the entire brain (Olkowicz et al., 2016). The cerebellar neurons can be subdivided into different types and are found in different cell layers and connected to each other in different ways (Yopak et al 2017). As demonstrated for the whole brain size (Herculano-Houzel et al 2014, 2015), increases in the cerebellum size are positively associated with increases in the total number of cerebellar neurons. However, to what extent different neuron types within the cerebellum increase in number, relative to the size of the cerebellum, at similar rates remains unknown. For example, an increase in the total number of cerebellar neurons could arise from increases in the numbers of specific neuronal types, such as granule cells. To address this question, I provide quantitative data on the numbers and sizes of different cerebellar neurons (Purkinje cells, granule cells and cerebellar nuclei neurons) across 54 bird species to test whether (1) large cerebellum reflects more and/or larger neurons, and (2) different neuronal populations increase in number and size at similar rates. In this Chapter, I found that different neuronal populations can increase in number and size at different rates relative to brain size (e.g., cerebellum).

In Chapter 3, I test if a larger cerebellum is associated with flight maneuverability, a potential indicator of complex motor control, as well as several other covariates. Most comparative studies perform simple correlations between relative brain (or brain region) size and one given trait to investigate evolutionary causes for increases or decreases in size among species. However, multiple variables, and even other brain regions, may potentially explain variation in the size of a brain region (Whiting and Barton 2003; Barton and Venditti 2014; Jiménez-Ortega et al. 2020). By measuring and collating data on the volumes of the cerebellum, telencephalon, and brain remainder across nearly 300 species of birds, I tested alternative scenarios of evolutionary changes in the relative cerebellum size. The results in this chapter did not show a positive association between relative size of the cerebellum and flight maneuverability. Conversely, I found that the relationship between the sizes of the cerebellum and telencephalon is a function of migratory behaviour such that resident birds have larger telencephalon relative to the size of the cerebellum than migrant birds.

In Chapter 4, I tested my third hypothesis: the size of the oculomotor nuclei and numbers of neurons within them reflect the degree of eye movements across bird species. Although a large number of studies has focused on the relative sizes of sensory regions in vertebrate brains (Cunningham et al. 2013; Gutiérrez-Ibáñez et al. 2013; Wylie et al. 2015; Camilieri-Asch et al. 2020), relatively few studies have focused on motor nuclei. In sensory systems, acuity and/or sensitivity appears to be correlated with the size and number of neurons within sensory brain regions (DeVoogd and Nottebohm, 1981; Bottjer 1986; Herculano-Houzel et al. 2014, 2017; Iwaniuk and Wylie, 2020), but whether a similar pattern occurs between movement and the size of motor nuclei remains uncertain (but see Sherwood 2005). Here, I measured the volumes and neuron numbers of all four nuclei that control eye movements, including accommodation and pupillary reflex, in 67 bird species. Based on our somewhat limited knowledge of variation in eye movements in birds, I predicted that owls would have smaller oculomotor nuclei whereas predatory bifoveate birds would have larger oculomotor nuclei. As I expected, relative to brainstem volume, owls had smaller oculomotor nuclei than other birds, which reflects their low degrees of eye movements. Conversely, falcons, hawks, and vultures had relatively larger VI. The expansion of VI in these birds could reflect the need for extra degrees of eye movements (i.e., abduction) when hunting or scavenging. Last, volumetric shifts in the oculomotor nuclei among clades did not necessarily reflect changes in neuron numbers. I suggest that neuron size might better explain volumetric differences in brainstem motor nuclei than neuron number.

In my final chapter I provide a general discussion based on my results, and highlight the remaining questions still left to address. My results reveal that increases in brain size can reflect increases in both neuron numbers and neuron sizes. However, relative to brain size, neuron size and neuron number increase at different rates, and vary with each neuronal population. For the oculomotor nuclei, volumetric shifts were not necessarily associated with changes in the relative number of neurons. Thus, variation in brain size is explained by changes in many different parameters of the brain. Moreover, these changes are not uniform within the brain. For example, in sensory brain regions volumetric differences appears to be best explained by changes in neuron numbers, while in motor pathways of the brainstem (e.g., oculomotor nuclei) volumetric shifts are due to changes in neuron sizes rather neuron numbers. Taken together, I suggest that the principle of proper mass needs to be broadened to more than just brain volume. If we want to better understand how the brain size reflects processing power and behaviour, we need to determine, through an integrated approach that considers as many parameters as possible, what drives brain size variation across species.

References

Barton, R., A. Purvis, and P. Harvey. 1995. Evolutionary radiation of visual and olfactory brain systems in primates, bats and insectivores. Philosophical Transactions of the Royal Society of London. Series B: Biological Sciences 348:381-392.

Barton, R. A. and P. H. Harvey. 2000. Mosaic evolution of brain structure in mammals. Nature 405:1055-1058.

Barton, R. A. and C. Venditti. 2014. Rapid evolution of the cerebellum in humans and other great apes. Current Biology 24:2440-2444.

Bennett, P. M. and P. H. Harvey. 1985. Relative brain size and ecology in birds. Journal of Zoology 207:151-169.

Benson-Amram, S., B. Dantzer, G. Stricker, E. M. Swanson, and K. E. Holekamp. 2016. Brain size predicts problem-solving ability in mammalian carnivores. Proceedings of the National Academy of Sciences 113:2532-2537.

Boire, D. and G. Baron. 1994. Allometric comparison of brain and main brain subdivisions in birds. Journal of Brain Research 35:49-66.

Bottjer, S. W., E. A. Miesner, and A. P. Arnold. 1986. Changes in neuronal number, density and size account for increases in volume of song-control nuclei during song development in zebra finches. Neuroscience Letters 67:263-268.

Camilieri-Asch, V., K. E. Yopak, A. Rea, J. D. Mitchell, J. C. Partridge, and S. P. Collin. 2020. Convergence of olfactory inputs within the central nervous system of a cartilaginous and a bony fish: an anatomical indicator of olfactory sensitivity. Brain, Behavior and Evolution 95:139-161.

Catania, K. C. and M. S. Remple. 2002. Somatosensory cortex dominated by the representation of teeth in the naked mole-rat brain. Proceedings of the National Academy of Sciences 99:5692-5697.

Chang, W., A. Pedroni, V. Hohendorf, S. Giacomello, M. Hibi, R. W. Köster, and K. Ampatzis. 2020. Functionally distinct Purkinje cell types show temporal precision in encoding locomotion. Proceedings of the National Academy of Sciences 117:17330-17337.

Cunha, F., K. Racicot, J. Nahirney, C. Heuston, D. R. Wylie, and A. N. Iwaniuk. 2020. Allometric scaling rules of the cerebellum in galliform birds. Brain, Behavior and Evolution 95:78-92.

Cunningham, S. J., J. R. Corfield, A. N. Iwaniuk, I. Castro, M. R. Alley, T. R. Birkhead, and S. Parsons. 2013. The anatomy of the bill tip of kiwi and associated somatosensory regions of the brain: comparisons with shorebirds. PLoS One 8:e80036.

DeCasien, A. R., S. A. Williams, and J. P. Higham. 2017. Primate brain size is predicted by diet but not sociality. Nature Ecology & Evolution 1:1-7.

DeKosky, S. T. and S. W. Scheff. 1990. Synapse loss in frontal cortex biopsies in Alzheimer's disease: correlation with cognitive severity. Annals of Neurology 27:457-464.

DeVoogd, T. J. and F. Nottebohm. 1981a. Sex differences in dendritic morphology of a song control nucleus in the canary: a quantitative Golgi study. Journal of Comparative Neurology 196:309-316.

DeVoogd, T. and F. Nottebohm. 1981b. Gonadal hormones induce dendritic growth in the adult avian brain. Science, 214:202-204.

Dunbar, R. I. 1998. The social brain hypothesis. Evolutionary Anthropology 6:178-190.

Emery, N. J. 2000. The eyes have it: the neuroethology, function and evolution of social gaze. Neuroscience & Biobehavioral Reviews 24:581-604.

Fons, R., H. Stephan, and G. Baron. 1984. Brains of Soricidae: I. Encephalization and macromorphology, with special reference to *Suncus etruscus*. Journal of Zoological Systematics and Evolutionary Research 22:145-158.

Freas, C. A., T. C. Roth, L. D. LaDage, and V. V. Pravosudov. 2013. Hippocampal neuron soma size is associated with population differences in winter climate severity in food-caching chickadees. Functional Ecology 27:1341-1349.

Fristoe, T. S., A. N. Iwaniuk, and C. A. Botero. 2017. Big brains stabilize populations and facilitate colonization of variable habitats in birds. Nature Ecology & Evolution 1:1706-1715.

Garamszegi LZ (2014) Modern phylogenetic comparative methods and their application in evolutionary biology: concepts and practice. Springer, London.

Gonzalez-Voyer, A. and A. von Hardenberg. 2014. An introduction to phylogenetic path analysis. Pp. 201-229. In Garamszegi LZ (ed.): Modern phylogenetic comparative methods and their application in evolutionary biology. Springer, London.

Gossette, R. L. 1968. Examination of retention decrement explanation of comparative successive discrimination reversal learning by birds and mammals. Perceptual and Motor Skills 27:1147-1152.

Güntürkün, O. 2012. The convergent evolution of neural substrates for cognition. Psychological Research 76:212-219.

Gutiérrez-Ibáñez, C., A. N. Iwaniuk, T. J. Lisney, and D. R. Wylie. 2013. Comparative study of visual pathways in owls (Aves: Strigiformes). Brain, Behavior and Evolution 81:27-39.

Gutiérrez-Ibáñez, C., A. N. Iwaniuk, B. A. Moore, E. Fernández-Juricic, J. R. Corfield, J. M. Krilow, J. Kolominsky, and D. R. Wylie. 2014. Mosaic and concerted evolution in the visual system of birds. PLoS One 9:e90102.

Herculano-Houzel, S. 2010. Coordinated scaling of cortical and cerebellar numbers of neurons. Frontiers in neuroanatomy. 4:12.

Herculano-Houzel, S. 2017. Numbers of neurons as biological correlates of cognitive capability. Current Opinion in Behavioral Sciences 16:1-7.

Herculano-Houzel, S., K. Catania, P. R. Manger, and J. H. Kaas. 2015. Mammalian brains are made of these: a dataset of the numbers and densities of neuronal and nonneuronal cells in the brain of glires, primates, scandentia, eulipotyphlans, afrotherians and artiodactyls, and their relationship with body mass. Brain, Behavior and Evolution 86:145-163.

Herculano-Houzel, S., C. E. Collins, P. Wong, and J. H. Kaas. 2007. Cellular scaling rules for primate brains. Proceedings of the National Academy of Sciences 104:3562-3567.

Herculano-Houzel, S., P. R. Manger, and J. H. Kaas. 2014. Brain scaling in mammalian evolution as a consequence of concerted and mosaic changes in numbers of neurons and average neuronal cell size. Frontiers in Neuroanatomy 8:77.

Herculano-Houzel, S., B. Mota, and R. Lent. 2006. Cellular scaling rules for rodent brains. Proceedings of the National Academy of Sciences 103:12138-12143.

Hofman, M. A. 1985. Size and shape of the cerebral cortex in mammals (Part 1 of 2). Brain, Behavior and Evolution 27:28-40.

Hunt, G. R. 1996. Manufacture and use of hook-tools by New Caledonian crows. Nature 379:249-251.

Isler, K. and C. P. van Schaik. 2009. The expensive brain: a framework for explaining evolutionary changes in brain size. Journal of Human Evolution 57:392-400.

Ito, M. 1984. The cerebellum and neural control. Raven Press, New York.

Iwaniuk, A. N., K. M. Dean, and J. E. Nelson. 2004. A mosaic pattern characterizes the evolution of the avian brain. Proceedings of the Royal Society of London. Series B: Biological Sciences 271:S148-S151.

Iwaniuk, A. N., K. M. Dean, and J. E. Nelson. 2005. Interspecific allometry of the brain and brain regions in parrots (Psittaciformes): comparisons with other birds and primates. Brain, Behavior and Evolution 65:40-59.

Iwaniuk, A. N., L. Lefebvre, and D. R. Wylie. 2009. The comparative approach and brain–behaviour relationships: A tool for understanding tool use. Canadian Journal of Experimental Psychology 63:150.

Iwaniuk, A.N. and D. R. Wylie. 2020. Sensory systems in birds: What we have learned from studying sensory specialists. Journal of Comparative Neurology, 528(17):2902-2918.

Jerison, H. 1973. Evolution of the brain and intelligence. Academic Press, New York.

Jerison, H. 1977. The theory of encephalization. Annals of the New York Academy of Sciences 299:146-160.

Jiménez-Ortega, D., N. Kolm, S. Immler, A. A. Maklakov, and A. Gonzalez-Voyer. 2020. Long life evolves in large-brained bird lineages. Evolution 74:2617-2628.

Kaas, J. H. 1989. The evolution of complex sensory systems in mammals. Journal of Experimental Biology 146:165-176.

Kaas, J. H. 2013. The evolution of brains from early mammals to humans. Wiley Interdisciplinary Reviews: Cognitive Science 4:33-45.

Krubitzer, L. 2007. The magnificent compromise: cortical field evolution in mammals. Neuron 56:201-208.

Ksepka, D. T., A. M. Balanoff, N. A. Smith, G. S. Bever, B.-A. S. Bhullar, E. Bourdon, E. L. Braun, J. G. Burleigh, J. A. Clarke, and M. W. Colbert. 2020. Tempo and pattern of avian brain size evolution. Current Biology 30:2026-2036.

Lefebvre, L., S. M. Reader, and D. Sol. 2004. Brains, innovations and evolution in birds and primates. Brain, Behavior and Evolution 63:233-246.

MacLean, E. L., B. Hare, C. L. Nunn, E. Addessi, F. Amici, R. C. Anderson, F. Aureli, J. M. Baker, A. E. Bania, and A. M. Barnard. 2014. The evolution of self-control. Proceedings of the National Academy of Sciences 111:E2140-E2148.

Mehlhorn, J., G. R. Hunt, R. D. Gray, G. Rehkämper, and O. Güntürkün. 2010. Tool-making New Caledonian crows have large associative brain areas. Brain, Behavior and Evolution 75:63-70.

Michelsen, K. A., D. L. van den Hove, C. Schmitz, O. Segers, J. Prickaerts, and H. W. Steinbusch. 2007. Prenatal stress and subsequent exposure to chronic mild stress influence dendritic spine density and morphology in the rat medial prefrontal cortex. BMC Neuroscience 8:1-8.

Navarrete, A., C. P. van Schaik, and K. Isler. 2011. Energetics and the evolution of human brain size. Nature 480:91-93.

Olkowicz, S., M. Kocourek, R. K. Lučan, M. Porteš, W. T. Fitch, S. Herculano-Houzel, and P. Němec. 2016. Birds have primate-like numbers of neurons in the forebrain. Proceedings of the National Academy of Sciences 113:7255-7260.

Pearce, J. M. 2013. Animal learning and cognition: an introduction. Psychology Press. Hove (England).

Pepperberg, I. M. 2002. Cognitive and communicative abilities of grey parrots. Current Directions in Psychological Science 11:83-87.

Pepperberg, I. M. and J. D. Gordon. 2005. Number comprehension by a grey parrot (*Psittacus erithacus*), including a zero-like concept. Journal of Comparative Psychology 119:197.

Portmann, A. 1947. Etudes sur la cérébralisation des oiseaux. II. Les indices intra-cérébraux. Alauda 15:1-15.

Rehkämper, G., H. D. Frahm, and K. Zilles. 1991a. Quantitative development of brain and brain structures in birds (Galliformes and Passeriformes) compared to that in mammals (Insectivores and Primates)(Part 1 of 2). Brain, Behavior and Evolution 37:125-134.

Rehkämper, G., K.-L. Schuchmann, A. Schleicher, and K. Zilles. 1991b. Encephalization in hummingbirds (Trochilidae). Brain, Behavior and Evolution 37:85-91.

Rodriguez, F., E. Durán, A. Gómez, F. Ocana, E. Alvarez, F. Jiménez-Moya, C. Broglio, and C. Salas. 2005. Cognitive and emotional functions of the teleost fish cerebellum. Brain Research Bulletin 66:365-370.

Sherwood, C.C. 2005. Comparative anatomy of the facial motor nucleus in mammals, with an analysis of neuron numbers in primates. The Anatomical Record Part A: Discoveries in Molecular, Cellular, and Evolutionary Biology. 287(1):1067-1079.

Smaers, J. and C. Soligo. 2013. Brain reorganization, not relative brain size, primarily characterizes anthropoid brain evolution. Proceedings of the Royal Society B: Biological Sciences 280:20130269.

Sol, D. 2009. Revisiting the cognitive buffer hypothesis for the evolution of large brains. Biology Letters 5:130-133.

Sol, D. and L. Lefebvre. 2000. Behavioural flexibility predicts invasion success in birds introduced to New Zealand. Oikos 90:599-605.

Sol, D., S. Timmermans, and L. Lefebvre. 2002. Behavioural flexibility and invasion success in birds. Animal Behaviour 63:495-502.

Street, S. E., A. F. Navarrete, S. M. Reader, and K. N. Laland. 2017. Coevolution of cultural intelligence, extended life history, sociality, and brain size in primates. Proceedings of the National Academy of Sciences 114:7908-7914.

Thach, W. 1998. A role for the cerebellum in learning movement coordination. Neurobiology of Learning and Memory 70:177-188.

Thompson, C. K. and E. A. Brenowitz. 2005. Seasonal change in neuron size and spacing but not neuronal recruitment in a basal ganglia nucleus in the avian song control system. Journal of Comparative Neurology 481:276-283.

Van Schaik, C. P., K. Isler, and J. M. Burkart. 2012. Explaining brain size variation: from social to cultural brain. Trends in Cognitive Sciences 16:277-284.

Van Woerden, J. T., C. P. Van Schaik, and K. Isler. 2010. Effects of seasonality on brain size evolution: evidence from strepsirrhine primates. The American Naturalist 176:758-767.

van Woerden, J. T., E. P. Willems, C. P. van Schaik, and K. Isler. 2012. Large brains buffer energetic effects of seasonal habitats in catarrhine primates. Evolution 66:191-199.

von Hardenberg, A. and A. Gonzalez-Voyer. 2013. Disentangling evolutionary cause-effect relationships with phylogenetic confirmatory path analysis. Evolution 67:378-387.

Weir, A. A., J. Chappell, and A. Kacelnik. 2002. Shaping of hooks in New Caledonian crows. Science 297:981-981.

Whiting, B. and R. Barton. 2003. The evolution of the cortico-cerebellar complex in primates: anatomical connections predict patterns of correlated evolution. Journal of Human Evolution 44:3-10.

Williams, R. W. and K. Herrup. 1988. The control of neuron number. Annual Review of Neuroscience 11:423-453.

Wylie, D. R., C. Gutiérrez-Ibáñez, and A. Iwaniuk. 2015. Integrating brain, behavior, and phylogeny to understand the evolution of sensory systems in birds. Frontiers in Neuroscience 9:281.

Xiao, J., J. Levitt, and R. Buffenstein. 2006. A stereotaxic atlas of the brain of the naked mole-rat (*Heterocephalus glaber*). Neuroscience 141:1415-1435.

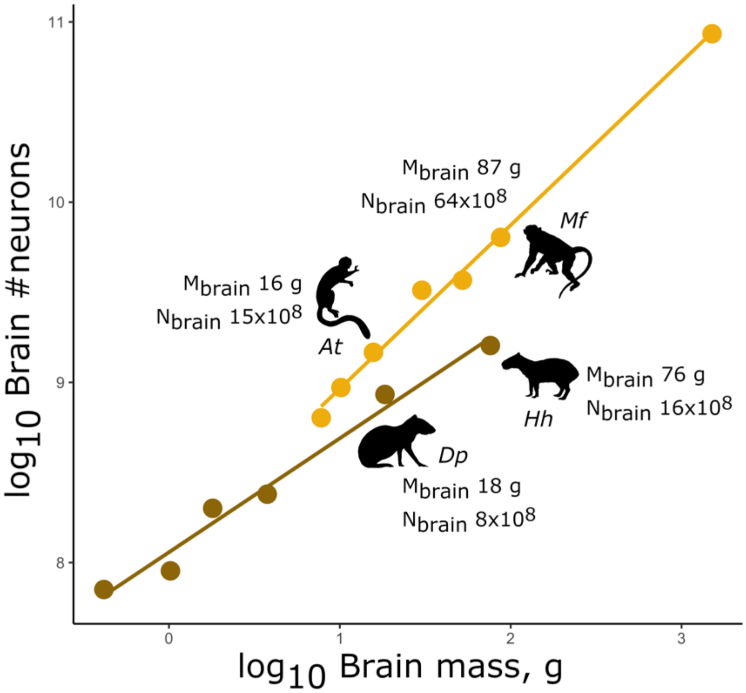

Figure 1.1. In rodents (brown), when the brain increases in size it does not gain as many neurons as a primate's brain (yellow). Species depicted are agouti (*Dasyprocta primnolopha; Dp*), capybara (*Hydrochoerus hydrochoeris; Hh*), owl monkey (*Aotus trivirgatus; At*), and crab-eating macaque (*Macaca fascicularis; Mf*). Data from Herculano-Houzel et al.(2006, 2007).

CHAPTER TWO: A QUANTITATIVE ANALYSIS OF CEREBELLAR ANATOMY IN BIRDS

Chapter published as: Cunha, F., C. Gutiérrez-Ibáñez, K. Racicot, D. R. Wylie, and A. N. Iwaniuk. 2021. A quantitative analysis of cerebellar anatomy in birds. Brain Structure and Function, 1-23. DOI 10.1007/s00429-021-02352-2

Abstract

The cerebellum is largely conserved in its circuitry, but varies greatly in size and shape across species. The extent to which differences in cerebellar morphology is driven by changes in neuron numbers, neuron sizes or both, remains largely unknown. To determine how species variation in cerebellum size and shape is reflective of neuron sizes and numbers requires the development of a suitable comparative data set and one that can effectively separate different neuronal populations. Here, we generated the largest comparative dataset to date on neuron numbers, sizes, volumes of cortical layers and surface area of the cerebellum across 54 bird species. Across different cerebellar sizes, the cortical layers maintained relatively constant proportions to one another and variation in cerebellum size was largely due to neuron numbers rather than neuron sizes. However, the rate at which neuron numbers increased with cerebellum size varied across Purkinje cells, granule cells, and cerebellar nuclei neurons. We also examined the relationship among neuron numbers, cerebellar surface area and cerebellar folding. Our estimate of cerebellar folding, the midsagittal foliation index, was a poor predictor of surface area and number of Purkinje cells, but surface area was the best predictor of Purkinje cell numbers. Overall, this represents the first comprehensive, quantitative analysis of cerebellar anatomy in a comparative context of any vertebrate. The extent to which these relationships occur in other vertebrates requires a similar approach and would determine whether the same scaling principles apply throughout the evolution of the cerebellum.

Introduction

The anatomy and circuitry of the cerebellum is largely conserved across jawed vertebrates (Voogd and Glickstein 1998), but cerebellar size and shape vary considerably across clades (Larsell 1967; Yopak et al. 2017). For example, while non-avian reptiles and amphibians have relatively small cerebella with few folds (i.e., low degree of foliation), mammals and birds have relatively large cerebella that are highly folded (Yopak et al. 2017). Even within vertebrate classes, such as birds, cerebellar morphology varies greatly across species (Iwaniuk et al. 2006, 2007; Sultan and Glickstein 2007). Some of this variation is thought to reflect differences in neuron number and/or neuron size (Herculano-Houzel et al., 2014), and thus neural processing related to, for example, cognitive processing (Hall et al. 2013; Iwaniuk et al. 2009; Smaers et al. 2018) and locomotion (Iwaniuk et al. 2007; Larsell 1967). However, the extent to which interspecific variation in cerebellum size and morphology arises from neuron sizes and numbers remains uncertain. Recent studies on total neuron numbers in the cerebellum indicate that the allometric relationship between the number of neurons and cerebellar mass is largely conserved across species (Herculano-Houzel et al. 2015a; Jardim-Messeder et al. 2017; Olkowicz et al. 2016), with only a couple of clades deviating from this general "scaling rule" (Herculano-Houzel et al. 2015a; Herculano-Houzel et al. 2014).

Of the mammal species studied thus far, two clades diverge from a general allometric relationship between cerebellar mass and total number of neurons such that they have higher neuronal densities in the cerebellum: primates and eulipotyphlans (shrews, moles and hedgehogs) (Herculano-Houzel et al. 2015a; Herculano-Houzel et al. 2014). This increased neuronal density accompanies a highly folded cerebellum and an expansion of the cerebellar hemispheres in primates (MacLeod et al. 2003; Smaers et al. 2018), but no comparable changes in eulipotyphlan cerebella. In birds, songbirds and parrots also have higher neuronal densities in the cerebellum compared with other avian clades (Olkowicz et al. 2016), but both songbirds and parrots also tend to have relatively smaller and more foliated cerebella (Iwaniuk et al. 2005; Iwaniuk et al. 2006). Thus, an increase in neuronal density in the cerebellum is associated with larger or smaller cerebella, a more folded cerebellar cortex or no discernible gross anatomical changes at all. These mixed results across mammals and birds means that the relationship between neuron numbers and cerebellar size and shape remains unclear.

All of the neuron-volume scaling relationships described above were obtained through the use of the isotropic fractionator (Herculano-Houzel and Lent 2005), which provides accurate estimates of total neuron numbers in dissectible brain regions (Herculano-Houzel et al. 2015c; Ngwenya et al. 2017), but does not yet allow for the separation of different neuronal populations within the cerebellum. Further, the isotropic fractionator method does not include Purkinje cells because they do not express NeuN (Apps and Hawkes 2009; Mullen et al. 1992). Like any larger brain region, the cerebellum is comprised of different types of neurons connected to each other in different ways (Yopak et al. 2017). For example, while granule cells receive input from mossy fibers and project to Purkinje cells through parallel fibers, Purkinje cells also receive input from climbing fibers and are the sole source of output to the cerebellar and vestibular nuclei (Apps and Hawkes, 2009). The numbers of these different neuronal populations could vary at a different rate relative to total cerebellar size. Determining whether different neuronal populations increase with cerebellum size at different rates would provide novel and more specific insights into the functional consequences of a relatively larger and/or more folded cerebellum. For example, if some clades or cerebellar morphologies have more Purkinje cells, this could indicate enhanced output processing from the cerebellar cortex.

Another caveat of the isotropic fractionator method is that neuron size is not measured directly, but rather is inferred as inversely proportional to neuronal density (Herculano-Houzel et al. 2014). This is because the method relies on rupturing cell membranes to stain nuclei. Scaling of neuron size with cerebellum size, or for that matter most brain regions, across species therefore remains largely unexplored (but see Stevens 1969; Teeter and Stevens 2011). Just as different neuronal populations might vary in neuron number-region volume relationships, the scaling of cell size could also vary among different types of neurons. This is especially true for the cerebellum, which contains both the largest neurons (Purkinje cells) and the smallest neurons (granule cells) in the brain (Lange 1982). In fact, across galliform birds (e.g., quail, partridge, pheasant), Purkinje cell size is positively correlated with the size of the cerebellum, while granule cell size is not (Cunha et al. 2020). Thus, instead of inferring the average size of total cerebellar neurons from neuronal density (Herculano-Houzel et al. 2014), actual measurements of neuron size are needed to determine to what extent species differences in cerebellum size are driven by neuron numbers and/or sizes.

As noted above, the cerebellum not only varies in overall size, but also morphology. More specifically, the degree of folding, referred to as foliation, varies greatly across and within clades (Cunha et al. 2020; Iwaniuk et al. 2006; Yopak et al. 2007). Such variation is thought to reflect behavioural differences across species. For example, fast-swimming sharks performing complex manoeuvres tend to have a more foliated cerebellum than slow-moving sharks (Yopak et al. 2007) and birds that build more complex nests (Hall et al. 2013) or use tools (Iwaniuk et al. 2009) have relatively more folded cerebella than other species. An assumption that underlies these studies is that a higher degree of foliation reflects an increase in the surface area of the cerebellum relative to cerebellar volume, therefore allowing more cells within a given volume and an increase in processing capacity (Hall et al. 2013; Iwaniuk et al. 2009). Within galliform birds, the degree of foliation is positively correlated with the number of cerebellar neurons, but neuronal populations differ in their allometric relationships with the degree of foliation (Cunha et al. 2020). Whether these same patterns can be generalized across other clades remains to be determined, but is critical to understand the functional implications of cerebellar foliation. For example, if a more foliated cerebellum has more Purkinje cells, that would reflect greater output from the cerebellar cortex to the cerebellar and vestibular nuclei. Thus, a detailed investigation on the cellular scaling of the cerebellum, combined with what is known of cerebellar circuitry, would provide novel insights into the functional consequences of species differences in not only cerebellar size, but also morphology.

To address these key issues in cerebellar evolution, we provide the most detailed quantitative analysis of cerebellar anatomy conducted in a comparative context so far. We quantified the volumes of different layers of the cerebellar cortex, surface area of the Purkinje cell layer, cerebellar foliation and the sizes and numbers of Purkinje cells, granule cells, and cerebellar nuclei neurons across 54 avian species. Using this data set, we calculated allometric relationships among all variables to test whether: (i) cerebellar layers increase in volume at a same rate across species; (ii) different neuronal populations scale with cerebellar size at the same rate; (iii) a higher degree of cerebellar foliation is associated with an increase in the surface area of the Purkinje cell layer and thus number of cerebellar neurons (e.g., Purkinje cells); and (iv) if there are quantitative differences in the cerebellar anatomy among clades.

Material and Methods

Specimens

We obtained measurements of the cerebella from 54 species representing 18 orders of birds (Fig. 2.1; Tables 2.1-3). With the exception of some galliform species (*Bonasa umbellus, Coturnix japonica,* and *Perdix perdix*; Cunha et al., 2020), a single individual was sampled per species. As described elsewhere, our brain collection is derived from specimens obtained from wildlife sanctuaries, veterinary clinics in Australia and hunters in Canada and New Zealand (Corfield et al. 2013; Corfield et al. 2015) and the methods of collection of the specimens adhered to the guidelines of the Canada Council for Animal Care. The heads of these specimens were immersion fixed in 4% buffered paraformaldehyde for at least two weeks. The brains were extracted, weighed and stored in paraformaldehyde. The brains then were place in 30% sucrose in 0.1 M phosphate buffer until they sank (for cryoprotection), embedded in gelatin, sectioned on a freezing stage microtome in the sagittal plane at a thickness of 40μm and every section collected in 0.1 M phosphate buffered saline. For some specimens, the cerebella were first dissected from the brain by cutting through the cerebellar peduncles and processed in the same way as the intact brains. For all species, every other section (1:2 series) was mounted onto gelatinized slides, stained with thionin acetate, dehydrated through a graded ethanol series, cleared in Hemo-De (Thermo Fisher Scientific, #HD-150) and coverslipped with Permount (Thermo Fisher Scientific, #SP15-150).

Volumetric measurements

We measured the volumes of molecular cell layer (ml), granule cell layer (gl), white matter layer including the cerebellar nuclei (wm+cn) and total cerebellum volume (cb) using the

Cavalieri method, as implemented in StereoInvestigator software (Microbrightfield Inc., VT, USA), with a 2.5x objective (n.a.= 0.075) on a Zeiss Axio Imager 2 microscope. The Cavalieri method consists of counting grid points that are inside a region of interest (e.g., molecular layer). Each point has a specific area, and the sum of those areas can be multiplied by the thickness of the tissue and sampling interval (i.e., inverse of the proportion of sections analyzed) to accurately estimate the volume of the entire region (Gundersen et al. 1999; Table S2.1). Each of the cerebellar layers measured are easily distinguishable from one another (Fig. 2.2), but the cerebellar nuclei were included with the white matter volume because of the indistinct borders of the cerebellar nuclei in sagittal sections. We therefore refer to this as the white matter plus cerebellar nuclei (wm+cn). The Purkinje cell layer is typically a thick, mono-cell layer with some discontinuous gaps between cells in sagittal sections. Hence, calculating the volume of this layer could lead to significant measurement errors. As an alternative, we measured the surface area of Purkinje cell layer, and size and number of Purkinje cells (see below) rather than the volume of the layer. Estimated volumes of all regions of interest are provided in Table 2.1. The distance between the grid points (grid size), and the sampling interval, varied according to overall cerebellum size (Table S2.1). The coefficients of error for all volumes ranged from 0.002 to 0.014.

Surface area of the Purkinje cell layer

The surface area of the Purkinje cell layer was calculated by measuring the total length of the Purkinje cell layer through the sagittal axis of the cerebellum, and multiplying it by the thickness of the sections (40 μm) and sampling interval (Table 2.1). The sampling interval was the same one used for the volumetric measurements (see Table S2.1).

Cerebellar Foliation Index (CFI)

We used the same approach as in Iwaniuk et al. (2006, 2009) to calculate the degree of foliation (i.e., folding) in the cerebellum (Table 2.1). First, we measured (a) the total length of the Purkinje cell layer of the mid-sagittal section and then (b) the length of the "envelope" enclosing the Purkinje cell layer (see Fig. 2.2a). The ratio (a/b) between these two measurements serves as a metric to calculate the degree of foliation, referred to as the cerebellar foliation index (CFI), and is comparable to gyrification indices calculated in mammals (Hofman 1985; Pillay and Manger 2007; Zilles et al. 1989). Thus, a higher number reflects a greater degree of foliation.

Cell counts

We estimated the number of three types of cerebellar neurons: Purkinje cells, granule cells and cerebellar nuclei neurons (Table 2.2; Fig. S2.1). Purkinje cells are found exclusively within the Purkinje cell layer and are readily identifiable from other cerebellar cell types based on size, shape and location. We only counted Purkinje cells with intact continuous cell membranes, typical "teardrop" shape and clearly visible nuclei. The numbers of Purkinje cells were estimated using the optical fractionator method implemented in StereoInvestigator software (Microbrightfield Inc., VT, USA), with a 20x objective (n.a.= 0.5) on a Zeiss Axio Imager 2 microscope. Frame size remained constant across all species, but grid size varied according to cerebellum size (Table S2.1). The coefficients of error (CE) of the Purkinje cell counts, defined as the standard error of the mean of repeated estimates divided by the mean (Microbrightfield

Inc., VT; USA), were all equal to or below 0.05, indicating that our measurements were precise (Gundersen et al. 1999).

Granule cells are densely packed within the granule cell layer and it is possible to distinguish them from other neuron types within this layer by cellular morphology and spatial distribution (Fig. S2.1). Granule cells, however, cannot be necessarily discerned from non-neuronal cells (e.g., glia) in Nissl stained tissue; thus, our granule cell counts likely represent an over-estimation of granule cell numbers (Cunha et al. 2020). The fact that specimens in our lab collection were fixed, prepared and mounted previously, at different times, prevented us from using NeuN as a neuron-specific marker in the cerebellum (Mullen et al. 1992). Still, given that specimens were processed consistently by the same method, neuronal counts likely yield comparable numbers across species within our study.

We counted granule cells with continuous, round shaped and intact cell membranes and darkly stained nuclei (Table 2.2), which distinguishes them from Lugaro, Golgi and unipolar brush cells. Lugaro cells are either globular or spindle-like in shape, are mostly clustered just below the Purkinje cell layer (Craciun et al. 2019; Fox 1959). Golgi cells have an irregular shape, are much larger than granule cells and typically have pale cytoplasmic staining (Andersen et al. 1992; Dieudonné 1998). Last, unipolar brush cells have circular-ovoid somata and are intermediate in size between granule cells and Golgi cells (Mugnaini and Floris 1994). Therefore, based on our morphological selection criteria, and given the low density of these other neuronal types, the potential inclusion of some is unlikely to affect our estimates of the total number of granule cells. The optical fractionator method was also used to quantify the numbers of granule cells under the same microscope with a 100x objective (n.a.=1.4). Frame size remained constant across species, but grid size varied (Table S2.1). Because granule cells are relatively small (< 20 μm^2) and densely packed (Fig. S2.1), they could be damaged or sectioned at the top and bottom surfaces of the tissue. Thus, guard zones of 4 -7 μm were used to protect against lost caps (Gardella et al. 2003). All granule cell counts had CEs that were equal to or below 0.07.

Cerebellar nuclei neurons are distributed in two paired nuclei within the white matter layer (Arends and Zeigler 1991). Here, we counted all of them as a single population (Table 2.2) because it was not possible to define clear anatomical borders between the cerebellar nuclei in sagittal sections (see also above). We only counted cerebellar nuclei neurons with intact cell membranes. The shape and size of the soma of cerebellar nuclei neurons was highly variable, ranging from globular to fusiform-like shape (Fig. S2.1). As with other cells, we used the optical fractionator probe with the same microscope, and a 40x objective (n.a.= 0.95), to estimate the numbers of cerebellar nuclei neurons. Frame size remained constant across species, but grid size varied (Table S2.1). To compensate and protect against lost caps, we used guard zones from 4 to 7 μm (Gardella et al. 2003). All cerebellar nuclei neuron counts had CEs that were equal to or below 0.07.

Cell sizes

We measured soma sizes of Purkinje cells, granule cells and cerebellar nuclei neurons. All cell sizes were measured using the nucleator probe (4 rays), implemented in StereoInvestigator (Microbrightfield Inc., VT, USA). The nucleator probe estimates the average cross-sectional area of randomly selected neurons. For the current study, at least 100 size measurements were made of each neuronal type for each specimen (Table 2.3). The measurements for each cell size followed a typical normal distribution (see Fig. 2.5). For all neuron types, cell membranes were intact, and morphologies followed the descriptions provided above.

Variation across orders

Due to common ancestry, closely related species are expected to have more traits in common (Garamszegi 2014). Therefore, to examine allometric relationships among all measurements, we performed phylogenetic generalized least squares (PGLS) of log-transformed data. The aim of PGLS is to test hypotheses about correlated evolution, assuming that the residuals from a linear model have a phylogenetic covariance. All statistical analyses were performed in R 4.0.3 (Team, 2020), using the pgls function in *caper* (Orme et al. 2013) and *nlme* (Pinheiro et al. 2006) with maximum likelihood estimations of Pagel's λ (Pagel 1999). We extracted 1,000 fully resolved trees from birdtree.org (Jetz et al. 2012), with Ericson et al. (2006) backbone phylogeny, and built a maximum clade credibility tree (consensus tree; Fig. 2.1) using *phangorn* (Schliep 2011). For all PGLS analyses, we used log-transformed data and the consensus phylogenetic tree. We ran phylogenetic analyses of covariance (pANCOVA) to test for significant differences across clades. We specifically tested for allometric differences across avian orders that have at least 5 species represented in our sample: Anseriformes (waterfowl), Galliformes (chicken-like birds), Passeriformes (songbirds) and Psittaciformes (parrots). Species from all other clades were lumped together as "other birds". Because Galliformes and Anseriformes form a monophyletic group ("Galloanserea") and Passeriformes and Psittaciformes form another monophyletic group ("Psittacopasserae") (Hackett et al. 2008; Jarvis et al. 2014; Prum et al. 2015), we also ran separate statistical analyses for both of these clades against "other birds". The percentage differences reported in the results (see below) are based on the differences between the intercepts and/or slopes for a given clade (e.g., Galliformes) and other birds.

Model selection and hypothesis testing

To test whether surface area of the Purkinje cell layer or cerebellar volume better explains the variation of the Purkinje cell number, we compared allometric models using Akaike information criterion (AIC) values to identify the most parsimonious model (Burnham and Anderson 2002, 2004).

Results

Allometric relationships of the cerebellum volume

The molecular, granule cell and white matter plus cerebellar nuclei (wm+cn) layers increased with the rest of the cerebellum with slopes that approximated isometry (Table S2.2; Fig. 2.3). The scaling of the molecular layer did not differ significantly across clades (Fig. 2.3a), but galliforms had relatively smaller granule cell layer (-38%; Fig. 2.3b; pANCOVA, $p=0.01$; no differences in slopes) and wm+cn volumes compared with other birds (-11%; Fig. 2.3c; pANCOVA, $p<0.01$; no differences in slopes). In contrast, parrots had significantly larger wm+cn volumes than other birds (+10%; Fig. 2.3c; pANCOVA, $p=0.04$; no differences in slopes). Note that despite these significant differences, there was quite a bit of overlap across clades (Fig. 2.3).

The number of Purkinje cells increased with cerebellar volume with a slope less than 1 (slope = 0.703 ± 0.035 (standard error); PGLS, $p<0.01$; Fig. 2.4a; Table S2.2). The only clade that differed significantly from this allometric relationship was Galliformes, which had relatively more Purkinje cells (+2.5%; Fig. 2.4a; pANCOVA, p=0.01; no differences in slopes). Waterfowl did not differ significantly from other groups and therefore the difference between Galliformes and other clades also drove a significant, but marginal, difference in relative Purkinje cell numbers between Galloanserae and other birds (+1.6%, Fig. 2.4a; pANCOVA, p=0.04; no differences in slopes). Granule cells increased in number with cerebellum volume with a steeper slope than that of Purkinje cells (0.867 ± 0.038, PGLS, p<0.01; Fig. 2.4b; Table S2.2). Across clades, galliforms had significantly fewer granule cells relative to cerebellar volume (-2.1%; Fig. 2.4b; pANCOVA, p<0.01; no differences in slopes) and songbirds have significantly more granule cells (+2.4%, Fig. 2.4b; pANCOVA, p<0.01). Last, the number of cerebellar nuclei neurons increases significantly with the cerebellum volume, but with the shallowest slope of the three neuron types (0.518 ± 0.027; Fig. 2.4c; PGLS, p<0.01; Table S2.2) and no significant differences were detected across clades.

As shown in Fig. 2.5, cell sizes varied greatly within species (coefficients of variation = 20-30%). Average cell sizes scaled at different slopes relative to total cerebellar volume (Table S2.2) and the slopes were much shallower than that for cell numbers (Fig. 2.4). Across clades, Galliformes have significantly larger Purkinje cells relative to cerebellar volume than other birds (+4.7%, Fig. 2.4d; pANCOVA, p<0.01; no differences in slopes). At the other end of the spectrum, songbirds have significantly smaller granule cells relative to cerebellum size than other birds, which also drove a significant difference between Psittacopasserae and other birds (-9%; Fig. 2.4e; pANCOVA, p=0.01; no slope differences). No significant differences were detected across orders or clades for the size of the cerebellar nuclei neurons relative to the volume of the cerebellum (Fig. 2.4f; Table S2.2).

Allometric relationships among neuronal populations

Among the three neuronal populations, allometric relationships varied in strength and slope. The number of granule cells increased with positive allometry relative to the number of Purkinje cells (1.125±0.064; Fig. 2.6a; PGLS, p<0.01; Table S2.2). Across clades, galliforms had significantly fewer granule cells relative to the number of Purkinje cells compared to other birds (-11%, Fig. 2.6a; pANCOVA, p<0.01) and drove a significant difference between Galloanserae and other birds (-7%, Fig. 2.6a; pANCOVA, p=0.01). Galliformes also had a steeper slope for the granule cell-Purkinje cell relationship compared to other birds (+36%, Fig. 2.6a; pANCOVA, p=0.03). The number of cerebellar nuclei neurons increased with the number of Purkinje cells with a much shallower slope than the number of granule cells (0.690± 0.037; Fig. 2.6b; PGLS, p<0.01; Table S2.2), and no significant differences were detected among clades. The number of cerebellar nuclei neurons increased with the number of granule cells with the shallowest slope (0.534 ± 0.041; Fig. 2.6c; PGLS, p<0.01; Table S2.2). As shown in Fig. 2.6c, Galliformes had significantly more cerebellar nuclei neurons relative to granule cells than other birds (+41%; Fig. 2.6c; pANCOVA, p=0.01) and this also drove significant differences between Galloanserae and other birds (+28%; Fig. 2.6c; pANCOVA, p<0.01; no slope differences).

Allometric relationships among the sizes of the three neuronal populations also varied in strength and slope. The size of granule cells increased with the size of Purkinje cells with the shallowest slope (0.280 ± 0.073; Fig. 2.6d; PGLS, p<0.01; Table S2.2). The size of cerebellar nuclei neurons increased with the size of Purkinje cells with a much steeper slope (0.452 ± 0.065; Fig. 2.6e; PGLS, p<0.01; Table S2.2). Lastly, the size of cerebellar nuclei neurons increased significantly with the size of granule cells with a slope similar to that of the Purkinje cells (0.408 ± 0.116; Fig. 2.6f; PGLS, p<0.01; Table S2.2). The only difference detected among clades is that the Psittacopasserae had a higher slope (+64%) for the relationship between cerebellar nuclei and granule cell sizes (Fig. 2.6f; pANCOVA, $p=0.04$). This difference remains significant (pANCOVA, $p<0.05$) when excluding an outlier (the brown thornbill (*Acanthiza pusilla*); Fig. 2.6f).

When plotting the numbers of each neuronal population against neuron size, no significant differences were detected across clades (Fig. 2.7). The number of Purkinje cells increased with the size of Purkinje cells with a slope close to isometry (1.105 ± 0.246; Fig. 2.7a; PGLS, $p<0.01$; Table S2.2). Similarly, the number of cerebellar nuclei neurons increased with the size of cerebellar nuclei neurons with a slope close to 1 (0.983 ± 0.311; Fig. 2.7b; PGLS, $p<0.01$; Table S2.2). However, for both of these relationships, the coefficients of correlation were no higher than 0.265 (see Table S2.2). For granule cells, the relationship between neuron number and neuron size was not significant (PGLS, $p>0.05$; Fig. 2.7c; Table S2.2).

Allometry of cerebellar foliation and surface area

As demonstrated in previous studies (Cunha et al. 2020; Iwaniuk et al. 2005), the avian cerebellum increased in volume relative to the rest of the brain with isometry (slope = 0.934 ± 0.046, PGLS, $p<0.01$; Table S2.2; Fig. 2.8a), although parrots and songbirds (Psittacopasserae) had relatively smaller cerebella (-18%; Fig. 2.8a; pANCOVA, $p = 0.01$; no differences in slopes). However, Iwaniuk et al. (2006) noted that the cerebellum is more foliated in these groups, as measured by the CFI, and suggested that the surface area of the cerebellum and the number of Purkinje cells would be higher in relation to cerebellar volume. When we plotted the surface area of the Purkinje cell layer against the rest of brain size (0.752 ± 0.044; Fig. 2.8b; PGLS, $p<0.01$), and number of Purkinje cells against the rest of brain size (0.656 ± 0.048; Fig.

2.8c; PGLS, $p<0.01$; Table S2.2), parrots and songbirds did not differ from other clades (Fig. 2.8b,c). These data support the inferences of Iwaniuk et al. (2006): despite having a relatively smaller cerebellum, parrots and songbirds do not have a smaller surface area or number of Purkinje cells relative to the rest of the brain.

However, the same data plotted relative to cerebellar volume yielded contradictory evidence. First, as shown above in Fig. 2.4A, the number of Purkinje cells relative to cerebellar volume is not higher for parrots and songbirds. Second, when the surface area of the Purkinje cell layer is plotted against cerebellar volume (Fig. 2.9a, Table S2.2) most of the parrots and songbirds lie above the regression line, but there were no significant differences across clades detected. Nonetheless, when we ran multiple allometric models to determine whether cerebellar volume or surface area of the Purkinje cell layer best explained the number of Purkinje cells (Figs. 2.4a, 2.9b; Table S2.3), Purkinje cell layer surface area was the best predictor of the number of Purkinje cells (dAIC>2; Table S2.3).

We then plotted CFI against cerebellar volume (Fig. 2.9c), Purkinje cell layer surface area (Fig. 2.9d) and number of Purkinje cells (Fig. 2.9e). In all three plots, parrots and songbirds are shifted to the left, indicating significantly higher CFI values relative to all three scaling variables. This grade shift indicates that the CFI is a poor proxy, specifically an overestimate, for both measures of cerebellar surface area and Purkinje cell numbers in parrots and songbirds.

Discussion

As found previously within galliform birds (Cunha et al. 2020), the expansion of the cerebellum across bird species is due to coordinated changes in volume across cerebellar layers such that no one layer increases in size more than another. Despite conservation of the proportional volumes of the layers, the numbers and sizes of different neuronal populations have different allometric relationships with cerebellar volume, and several differences among clades were detected (see Table 2.4).

Despite these overall patterns, a few caveats should be considered in interpreting our data and analyses. First, some avian/clades are represented by more species than others. We therefore cannot negate the possibility that there are other differences among clades that we were unable to detect due to small sample sizes. Second, we sampled only one individual of most species. The morphology of the cerebellum can vary significantly within species (El-Andari et al. 2020; Escalona et al. 1991; Inouye and Oda 1980; Puzdrowski and Leonard 1992), but variation in brain or brain region size is usually higher across species than within species (Herculano-Houzel et al. 2015a; Herculano-Houzel et al. 2014; Herculano-Houzel et al. 2015b) and the intraspecific coefficients of variation for the measurements on galliform species are typically lower than 15% (see Cunha et al., 2020; El-Andari et al. 2020). Although the specific slopes and intercepts of the various allometric relationships described herein might shift with the addition of more individuals per species and/or more species overall, the general patterns are unlikely to change. We also stress that it remains unclear to what extent fixation affects cell density or cell size. Given that our specimens were processed following the same procedure, this potential artifact is unlikely to affect our main findings, but could still affect direct comparisons between our data and future studies using different histological procedures. Last, our granule cell counts likely include non-neuronal cells (e.g., glia) and therefore represent an overestimation of total granule cell numbers. Because of that, our data cannot be compared directly with that of isotropic fractionation studies (Olkowicz et al. 2016) and the allometric equations that include granule cell numbers should be interpreted with caution. For example, when comparing the number of cerebellar neurons in the six species (*Cacatua galerita*, *Columba livia*, *Dromaius novaehollandiae*, *Melopsittacus undulatus*, *Nymphicus hollandicus*, *Tyto alba*) examined in this study and Olkowicz et al (2016), our study reports on average two times more cerebellar neurons than Olkowicz et al (2016). We also note that the brain sizes for the six species mentioned above were on average 1.2 times larger in our study than in Olkowicz et al. (2016). Nevertheless, our data is the most comprehensive to date for a comparative study and provides some novel insights into cerebellar evolution.

Allometric scaling within the cerebellum

The cerebellum has an anatomical organization that is highly conserved across most species, including the connectivity patterns across neuronal populations (Voogd and Glickstein 1998; Yopak et al. 2017). This pattern of connectivity is not only preserved across vertebrate species, but also across different functional units within the cerebellum itself (Apps et al. 2018; Voogd and Glickstein 1998; Yopak et al. 2017). It is therefore unsurprising that all three cerebellar layers change in volume in a concerted fashion, with little deviation across clades. As shown in Fig. 2.3, there is little scatter around the allometric lines and the correlation coefficients (r^2's in Table S2.2) are all above 0.95, indicating that interspecific variation in the absolute and relative size of the whole cerebellum largely arises from coordinated, volumetric increases across cell layers.

In contrast to the strong, nearly isometric relationships among layer volumes, larger cerebella have lower neuronal densities, a pattern that is typical of most brain regions and clades, regardless of whether the data is acquired through stereology (Cunha et al. 2020; Haug 1987; Lange 1975; Sherwood et al. 2020) or isotropic fractionation (Olkowicz et al., 2016; Herculano-

Houzel et al. 2015a; Herculano-Houzel et al. 2014). There are, however, differences in the slope and strength of the neuron number-cerebellum volume relationship (i.e., r^2) among the three neuronal populations (see Table S2.2). Relative to cerebellar volume, the number of granule cells increases faster than the number of Purkinje cells, which increases faster than the number of cerebellar nuclei neurons (Fig. 2.4; Cunha et al., 2020). Thus, different types of neurons vary in their scaling relationship with brain region size and, by extension, a constant scaling pattern (or neuronal scaling "rule" *sensu* Herculano-Houzel et al., 2014) does not apply uniformly to cerebellar neurons and is unlikely to apply to other brain regions. In much the same way that volumetric measurements have moved away from large, multifunctional brain regions to functionally specific regions and/or circuits (Corfield et al. 2015; Gutiérrez-Ibáñez et al. 2013; Gutiérrez-Ibáñez et al. 2011; Moore and DeVoogd 2017; Smaers and Vanier 2019; Vanier et al. 2019), the quantification of neuron numbers should extend to different neuronal populations and the role they have in neural circuits, to better understand how the brain evolves.

In addition to neuron numbers, we also estimated neuron sizes by measuring soma areas. Relative to cerebellum volume, neuron sizes increase at a significantly slower rate (see Fig. 2.4), and with much lower correlation coefficients (r^2's = 0.08-0.37) than neuron numbers (r^2's = 0.87-0.90). Thus, our results suggest that neuron size, relative to cerebellum volume, is more likely to vary across species than relative neuron numbers. The fact that neuron sizes are highly variable within a single neuronal population (see Fig. 2.5) might also explain why neuron size is much more variable than neuron number across species. As shown with neuron numbers (see above), each neuron type also scaled at a different rate with cerebellar volume. Neuron size is not discussed as frequently as neuron numbers in comparative studies, but it is an important contributor to brain region volume and information processing capacity (Chang et al. 2020; de

Sousa and Proulx 2014; Smith et al. 1997). Although soma size is only one metric of neuron size, it is often associated with the physiological properties of a neuron (Chang et al. 2020; Cooper and Stanford 2000; Meitzen and Thompson 2008). For example, variation in soma size of Purkinje cells can reflect firing type and input resistance (Chang et al. 2020), and larger cells tend to have larger or more organelles, such as the endoplasmic reticulum and mitochondria (Reber and Goehring 2015), which would potentially enable higher energetic capacity (Marshall 2015; Reber and Goehring 2015). Relatively larger (or smaller) neurons within a clade therefore might reflect physiological differences that are relevant to behaviour. However, what those differences might be is entirely speculative as little is known about differences in motor control and coordination across bird species. Regardless of the functional correlates and implications of neuron size, our data indicates neuron size cannot be inferred accurately from neuron numbers due to differences in the allometric scaling of neuron size and numbers across neuronal populations (see Figs. 2.6, 2.7). Moreover, as shown in Fig. 2.5, neuron size is highly variable within a single neuronal population, and for that reason estimations of neuron size from neuronal density (see Herculano-Houzel et al., 2014) are likely inaccurate.

One of the few exceptions to the general patterns observed across species is the order Galliformes. Galliforms have smaller granule cell and white matter layer-cerebellar nuclei ("wm+cn") layers relative to the size of the rest of the cerebellum compared to other birds (Fig. 2.3), even though they do not have relatively small cerebella (Fig. 2.8a). The molecular layer in galliforms is not proportionally expanded (Fig. 2.3a), indicating that the relative decrease in the other layers is due to a change in Purkinje cells. Accurately measuring the volume of the Purkinje cell layer is not possible due to frequent gaps between Purkinje cells (see Methods), but galliforms do have more and larger Purkinje cells relative to the size of the cerebellum (Fig. 2.4), which would result in a larger Purkinje cell layer. Why galliforms differ from other clades in these scaling relationships is unclear, but some insights might be gleaned by examining the cerebella of behaviorally and ecologically similar clades, such as tinamous (Tinamiformes), bustards (Otidiformes) and/or buttonquail (Turnicidae).

Cerebellar volume, surface area of the Purkinje cell layer, and foliation

Parrots and songbirds have relatively smaller cerebellar volumes (Fig. 2.8a; Iwaniuk et al., 2006), but a greater degree of foliation, as measured by a higher midsagittal CFI (Figs. 2.9c-e). In previous studies, this measure was considered a proxy for surface area and Purkinje cell number (Hall et al. 2013; Iwaniuk et al. 2009). That is, parrots and songbirds may have a smaller cerebellum by volume, but an increase in the foliation provides a larger surface area and thus a greater processing capacity for the cerebellum. In the present study, we actually measured the surface area of the cerebellum and the number of Purkinje cells. On the one hand, we found that relative to the rest of the brain, the surface area of the cerebellum and the number of Purkinje cells is not reduced in parrots and songbirds despite smaller cerebellar volumes (see Fig. 2.8). This is further supported by the cerebellar surface area being a better predictor of Purkinje cell number than cerebellar volume (see Figs. 2.4a, 2.9b). Thus, the increase in cerebellar foliation in parrots and songbirds maintains the processing capacity of a smaller cerebellum, a functionality that might be required for their expanded telencephala (Boire and Baron 1994; Iwaniuk et al. 2005). On the other hand, parrots and songbirds did not significantly increase surface area or Purkinje cell number relative to cerebellar volume (see Figs. 2.4a, 2.9a). We must therefore conclude that any effects of foliation are weak and that the midsagittal CFI is not a good proxy for surface area or number of Purkinje cells. This is very apparent in Figs. 2.9d-e, where the CFI grossly overestimates the surface area and number of Purkinje cells in parrots and songbirds. Intuitively, this should not come as a surprise. In birds the cerebellum is folded only in the anterior-posterior dimension, which is not the case in sharks (Yopak et al. 2017; Yopak et al. 2007), the cerebellar hemispheres in mammals (Smaers et al. 2018; Voogd and Glickstein 1998) or the cerebral cortex in mammals (Pillay and Manger 2007; Zilles et al. 1989). Thus, in birds the CFI is maximal in the midsagittal section, and progressively approaches 1.0 as one moves laterally to the flocculus and lateral unfoliated cortex. The result is that the midsagittal CFI overestimates total foliation, and by extension also overestimates surface area and Purkinje cell number.

Conclusions

Our results show that cerebellar layers increase in size proportionally and the numbers of cerebellar neurons explain more variation in cerebellar volume than the sizes of cerebellar neurons. Thus, despite all the species differences in cerebellar size and shape (Cunha et al. 2020; Macrì et al. 2019; Smaers et al. 2018), the conserved pattern of cerebellar connectivity across species is reflected in proportional increases in size of the cerebellar layers. Within this general framework, we also found that different neuronal populations have different allometric scaling rules relative to the size of the cerebellum, thus indicating that measuring total neuron numbers within larger brain regions (Herculano-Houzel et al. 2014; Olkowicz et al. 2016) might not provide a complete picture of the relationship between neuron numbers and brain region sizes. Given that patterns of cerebellar connectivity are relatively uniform across vertebrate species (Yopak et al. 2017), we expect to find similar changes across the volumes of cerebellar layers in other vertebrate clades, but also varying allometric scaling patterns across neuronal populations in the cerebellum. Testing the extent to which these patterns are conserved in the cerebellum across all vertebrates would provide insights into the putative mechanisms responsible for clade differences in relative cerebellum size and morphology.

References

Andersen BB, Korbo L, Pakkenberg B (1992) A quantitative study of the human cerebellum with unbiased stereological techniques. Journal of Comparative Neurology 326 (4):549-560

Apps R, Hawkes R (2009) Cerebellar cortical organization: a one-map hypothesis. Nature Reviews Neuroscience 10 (9):670-681

Apps R, Hawkes R, Aoki S, Bengtsson F, Brown AM, Chen G, Ebner TJ, Isope P, Jörntell H, Lackey EP (2018) Cerebellar modules and their role as operational cerebellar processing units. The Cerebellum 17 (5):654-682

Arends J, Zeigler HP (1991) Organization of the cerebellum in the pigeon (Columba livia): II. Projections of the cerebellar nuclei. Journal of comparative neurology 306 (2):245-272

Boire D, Baron G (1994) Allometric comparison of brain and main brain subdivisions in birds. Journal of Brain Research 35 (1):49-66

Burnham KP, Anderson DR (2002) Model selection and multimodel inference. A practical information-theoretic approach, 2nd edn. Springer, New York.

Burnham KP, Anderson DR (2004) Multimodel inference: understanding AIC and BIC in model selection. Sociological Methods & Research 33 (2):261-304

Chang W, Pedroni A, Hohendorf V, Giacomello S, Hibi M, Köster RW, Ampatzis K (2020) Functionally distinct Purkinje cell types show temporal precision in encoding locomotion. Proceedings of the National Academy of Sciences 117 (29):17330-17337

Cooper A, Stanford I (2000) Electrophysiological and morphological characteristics of three subtypes of rat globus pallidus neurone in vitro. The Journal of physiology 527 (2):291-304

Corfield JR, Birkhead TR, Spottiswoode CN, Iwaniuk AN, Boogert NJ, Gutiérrez-Ibáñez C, Overington SE, Wylie DR, Lefebvre L (2013) Brain size and morphology of the brood-parasitic and cerophagous honeyguides (Aves: Piciformes). Brain, Behavior and Evolution 81 (3):170-186

Corfield JR, Price K, Iwaniuk AN, Gutiérrez-Ibáñez C, Birkhead T, Wylie DR (2015) Diversity in olfactory bulb size in birds reflects allometry, ecology, and phylogeny. Frontiers in Neuroanatomy 9:102

Craciun I, Gutierrez-Ibanez C, Chan AS, Luksch H, Wylie DR (2019) Secretagogin immunoreactivity reveals lugaro cells in the pigeon cerebellum. The Cerebellum 18 (3):544-555

Cunha F, Racicot K, Nahirney J, Heuston C, Wylie DR, Iwaniuk AN (2020) Allometric scaling rules of the cerebellum in galliform birds. Brain, Behavior and Evolution 95 (2):78-92

de Sousa AA, Proulx MJ (2014) What can volumes reveal about human brain evolution? A framework for bridging behavioral, histometric, and volumetric perspectives. Frontiers in Neuroanatomy 8:51

Dieudonné S (1998) Submillisecond kinetics and low efficacy of parallel fibre-Golgi cell synaptic currents in the rat cerebellum. The Journal of Physiology 510 (3):845-866

El-Andari R, Cunha F, Tschirren B, Iwaniuk AN (2020) Selection for divergent reproductive investment affects neuron size and foliation in the cerebellum. Brain, Behavior and Evolution 95 (2):69-77

Ericson PG, Anderson CL, Britton T, Elzanowski A, Johansson US, Källersjö M, Ohlson JI, Parsons TJ, Zuccon D, Mayr G (2006) Diversification of Neoaves: integration of molecular sequence data and fossils. Biology Letters 2 (4):543-547

Escalona P, McDonald W, Doraiswamy P, Boyko O, Husain M, Figiel G, Laskowitz D, Ellinwood E, Krishnan K (1991) In vivo stereological assessment of human cerebellar volume: effects of gender and age. American Journal of Neuroradiology 12 (5):927-929

Fox CA (1959) The intermediate cells of Lugaro in the cerebellar cortex of the monkey. Journal of Comparative Neurology 112 (1):39-53

Garamszegi LZ (2014) Modern phylogenetic comparative methods and their application in evolutionary biology: concepts and practice. Springer, London.

Gardella D, Hatton WJ, Rind HB, Rosen GD, von Bartheld CS (2003) Differential tissue shrinkage and compression in the z-axis: implications for optical disector counting in vibratome-, plastic-and cryosections. Journal of Neuroscience Methods 124 (1):45-59

Gundersen H, Jensen E, Kiêu K, Nielsen J (1999) The efficiency of systematic sampling in stereology—reconsidered. Journal of Microscopy 193 (3):199-211

Gutiérrez-Ibáñez C, Iwaniuk AN, Lisney TJ, Wylie DR (2013) Comparative study of visual pathways in owls (Aves: Strigiformes). Brain, Behavior and Evolution 81 (1):27-39

Gutiérrez-Ibáñez C, Iwaniuk AN, Wylie DR (2011) Relative size of auditory pathways in symmetrically and asymmetrically eared owls. Brain, Behavior and Evolution 78 (4):286-301

Hackett SJ, Kimball RT, Reddy S, Bowie RC, Braun EL, Braun MJ, Chojnowski JL, Cox WA, Han K-L, Harshman J (2008) A phylogenomic study of birds reveals their evolutionary history. Science 320 (5884):1763-1768

Hall ZJ, Street SE, Healy SD (2013) The evolution of cerebellum structure correlates with nest complexity. Biology Letters 9 (6):20130687

Haug H (1987) Brain sizes, surfaces, and neuronal sizes of the cortex cerebri: a stereological investigation of man and his variability and a comparison with some mammals (primates, whales, marsupials, insectivores, and one elephant). American Journal of Anatomy 180 (2):126-142

Herculano-Houzel S, Catania K, Manger PR, Kaas JH (2015a) Mammalian brains are made of these: a dataset of the numbers and densities of neuronal and nonneuronal cells in the brain of glires, primates, scandentia, eulipotyphlans, afrotherians and artiodactyls, and their relationship with body mass. Brain, Behavior and Evolution 86 (3-4):145-163

Herculano-Houzel S, Lent R (2005) Isotropic fractionator: a simple, rapid method for the quantification of total cell and neuron numbers in the brain. Journal of Neuroscience 25 (10):2518-2521

Herculano-Houzel S, Manger PR, Kaas JH (2014) Brain scaling in mammalian evolution as a consequence of concerted and mosaic changes in numbers of neurons and average neuronal cell size. Frontiers in Neuroanatomy 8:77

Herculano-Houzel S, Messeder DJ, Fonseca-Azevedo K, Pantoja NA (2015b) When larger brains do not have more neurons: increased numbers of cells are compensated by decreased average cell size across mouse individuals. Frontiers in neuroanatomy 9:64

Herculano-Houzel S, von Bartheld CS, Miller DJ, Kaas JH (2015c) How to count cells: the advantages and disadvantages of the isotropic fractionator compared with stereology. Cell and Tissue Research 360 (1):29-42

Hofman MA (1985) Size and shape of the cerebral cortex in mammals (Part 1 of 2). Brain, Behavior and Evolution 27 (1):28-40

Inouye M, Oda SI (1980) Strain-specific variations in the folial pattern of the mouse cerebellum. Journal of Comparative Neurology 190 (2):357-362

Iwaniuk AN, Dean KM, Nelson JE (2005) Interspecific allometry of the brain and brain regions in parrots (Psittaciformes): comparisons with other birds and primates. Brain, Behavior and Evolution 65 (1):40-59

Iwaniuk AN, Hurd PL, Wylie DR (2006) Comparative morphology of the avian cerebellum: I. Degree of foliation. Brain, Behavior and Evolution 68 (1):45-62

Iwaniuk AN, Hurd PL, Wylie DR (2007) Comparative morphology of the avian cerebellum: II. Size of folia. Brain, Behavior and Evolution 69 (3):196-219

Iwaniuk AN, Lefebvre L, Wylie DR (2009) The comparative approach and brain–behaviour relationships: A tool for understanding tool use. Canadian Journal of Experimental Psychology 63 (2):150

Jardim-Messeder D, Lambert K, Noctor S, Pestana FM, de Castro Leal ME, Bertelsen MF, Alagaili AN, Mohammad OB, Manger PR, Herculano-Houzel S (2017) Dogs have the most neurons, though not the largest brain: trade-off between body mass and number of neurons in the cerebral cortex of large carnivoran species. Frontiers in Neuroanatomy 11:118

Jarvis ED, Mirarab S, Aberer AJ, Li B, Houde P, Li C, Ho SY, Faircloth BC, Nabholz B, Howard JT (2014) Whole-genome analyses resolve early branches in the tree of life of modern birds. Science 346 (6215):1320-1331

Jetz W, Thomas GH, Joy JB, Hartmann K, Mooers AO (2012) The global diversity of birds in space and time. Nature 491 (7424):444-448

Lange W (1975) Cell number and cell density in the cerebellar cortex of man and some other mammals. Cell and tissue research 157 (1):115-124

Lange W (1982) Regional differences in the cytoarchitecture of the cerebellar cortex. In: Palay SL, Chan-Palay V (eds) The cerebellum. New vistas. Exp Brain Res Suppl 6. Springer, Berlin, Heidelberg, pp 93–107

Larsell O (1967) The cerebellum: from myxinoids through birds. Minneapolis: University of Minnesota Press.

MacLeod CE, Zilles K, Schleicher A, Rilling JK, Gibson KR (2003) Expansion of the neocerebellum in Hominoidea. Journal of human evolution 44 (4):401-429

Macrì S, Savriama Y, Khan I, Di-Poï N (2019) Comparative analysis of squamate brains unveils multi-level variation in cerebellar architecture associated with locomotor specialization. Nature Communications 10 (1):1-16

Marshall WF (2015) How cells measure length on subcellular scales. Trends in Cell Biology 25 (12):760-768

Meitzen J, Thompson CK (2008) Seasonal-like growth and regression of the avian song control system: neural and behavioral plasticity in adult male Gambel's white-crowned sparrows. General and comparative endocrinology 157 (3):259-265

Moore JM, DeVoogd TJ (2017) Concerted and mosaic evolution of functional modules in songbird brains. Proceedings of the Royal Society B: Biological Sciences 284 (1854):20170469

Mugnaini E, Floris A (1994) The unipolar brush cell: a neglected neuron of the mammalian cerebellar cortex. Journal of Comparative Neurology 339 (2):174-180

Mullen RJ, Buck CR, Smith AM (1992) NeuN, a neuronal specific nuclear protein in vertebrates. Development 116 (1):201-211

Ngwenya A, Nahirney J, Brinkman B, Williams L, Iwaniuk AN (2017) Comparison of estimates of neuronal number obtained using the isotropic fractionator method and unbiased stereology in day old chicks (Gallus domesticus). Journal of neuroscience methods 287:39-46

Olkowicz S, Kocourek M, Lučan RK, Porteš M, Fitch WT, Herculano-Houzel S, Němec P (2016) Birds have primate-like numbers of neurons in the forebrain. Proceedings of the National Academy of Sciences 113 (26):7255-7260

Orme D, Freckleton R, Thomas G, Petzoldt T, Fritz S, Isaac N, Pearse W (2013) The caper package: comparative analysis of phylogenetics and evolution in R. R package version 5 (2):1-36

Pagel M (1999) The maximum likelihood approach to reconstructing ancestral character states of discrete characters on phylogenies. Systematic Biology 48 (3):612-622

Pillay P, Manger PR (2007) Order-specific quantitative patterns of cortical gyrification. European Journal of Neuroscience 25 (9):2705-2712

Pinheiro J, Bates D, DebRoy S, Sarkar D, Team RC (2006) nlme: Linear and nonlinear mixed effects models. R package version 3 (4):109

Prum RO, Berv JS, Dornburg A, Field DJ, Townsend JP, Lemmon EM, Lemmon AR (2015) A comprehensive phylogeny of birds (Aves) using targeted next-generation DNA sequencing. Nature 526 (7574):569-573

Puzdrowski RL, Leonard RB (1992) Variations in cerebellar morphology of the Atlantic stingray, *Dasyatis sabina*. Neuroscience Letters 135 (2):196-200

Reber S, Goehring NW (2015) Intracellular scaling mechanisms. Cold Spring Harbor perspectives in biology 7 (12):a019067

Schliep KP (2011) phangorn: phylogenetic analysis in R. Bioinformatics 27 (4):592-593

Sherwood CC, Miller SB, Karl M, Stimpson CD, Phillips KA, Jacobs B, Hof PR, Raghanti MA, Smaers JB (2020) Invariant Synapse Density and Neuronal Connectivity Scaling in Primate Neocortical Evolution. Cerebral Cortex 30 (10):5604-5615

Smaers JB, Turner AH, Gómez-Robles A, Sherwood CC (2018) A cerebellar substrate for cognition evolved multiple times independently in mammals. Elife 7:e35696

Smaers JB, Vanier DR (2019) Brain size expansion in primates and humans is explained by a selective modular expansion of the cortico-cerebellar system. Cortex 118:292-305

Smith GT, Brenowitz EA, Beecher MD, Wingfield JC (1997) Seasonal changes in testosterone, neural attributes of song control nuclei, and song structure in wild songbirds. Journal of Neuroscience 17 (15):6001-6010

Stevens C (1969) Structure of cat frontal olfactory cortex. Journal of neurophysiology 32 (2):184-192

Sultan F, Glickstein M (2007) The cerebellum: comparative and animal studies. The cerebellum 6 (3):168-176

Teeter CM, Stevens CF (2011) A general principle of neural arbor branch density. Current Biology 21 (24):2105-2108

Vanier DR, Sherwood CC, Smaers JB (2019) Distinct patterns of hippocampal and neocortical evolution in primates. Brain, behavior and evolution 93 (4):171-181

Voogd J, Glickstein M (1998) The anatomy of the cerebellum. Trends in cognitive sciences 2 (9):307-313

Yopak KE, Pakan J, Wylie D (2017) The cerebellum of nonmammalian vertebrates. In: Evolutionary Neuroscience. Elsevier, pp 247-260

Yopak KE, Lisney TJ, Collin SP, Montgomery JC (2007) Variation in brain organization and cerebellar foliation in chondrichthyans: sharks and holocephalans. Brain, behavior and evolution 69 (4):280-300

Zilles K, Armstrong E, Moser KH, Schleicher A, Stephan H (1989) Gyrification in the cerebral cortex of primates. Brain, Behavior and Evolution 34 (3):143-150

Table 2.1. A list of the avian species analyzed and their respective brain volumes, cerebellum volumes, molecular layer volumes, granule cell layer volumes, white matter volumes, surface area of the Purkinje cell layer, and cerebellar foliation index (CFI).

Order	**Common name/ Species**	**Brain volume (mm^3)**	**Cerebellum volume (mm^3)**	**Molecular layer volume (mm^3)**	**Granule cell layer volume (mm^3)**	**White matter volume (mm^3)**	**Purkinje cell layer, surface area (µm^2)**	**Cerebellar Foliation Index**
Accipitriformes	Collared sparrowhawk (*Accipiter cirrocephalus*)	4875.483	749.476	331.006	224.770	181.966	1,054,295,727	4.40
	Wedge-tailed eagle (*Aquila audax*)	15997.104	1466.816	685.260	406.260	367.796	1,557,879,727	4.68
	White-bellied sea eagle (*Haliaeetus leucogaster)*	12540.540	1108.880	507.160	289.580	312.360	964,970,443	4.57
Anseriformes	American wigeon (*Anas americana)*	5245.173	549.587	271.366	157.114	104.845	756,665,832	3.72
	Northern shoveler (*Anas clypeata*)	3288.513	279.091	133.606	88.934	56.550	378,222,471	3.14
	Mallard (*Anas platyrhynchos*)	6216.255	560.058	286.351	151.064	109.660	910,208,725	3.45
	Gadwall (*Anas strepera*)	4324.324	510.189	223.622	154.310	120.928	684,181,960	3.37
	Lesser scaup (*Aythya affinis*)	4546.139	437.920	213.370	132.678	79.014	637,152,788	3.76
	Bufflehead (*Bucephala albeola)*	4440.154	559.080	271.490	173.534	102.730	621,147,084	3.60
	Common goldeneye (*Bucephala clangula*)	5961.390	685.382	356.603	203.059	125.518	942,512,966	4.11
	Red-breasted merganser (*Mergus serrator*)	4247.104	442.431	178.120	148.054	111.274	614,832,009	3.56
Caprimulgiformes	Spotted nightjar (*Eurostopodus argus*)	1012.548	137.935	61.280	43.535	30.265	212,361,215	3.01
	Tawny frogmouth (*Podargus strigoides*)	5943.050	442.086	226.194	134.145	69.455	460,317,436	3.35
Casuariiformes	Emu (*Dromaius novaehollandiae*)	27750	3352.930	1576.430	944.610	766.880	2,966,617,590	4.94
Charadriiformes	Silver gull (*Larus novaehollandiae*)	2941.120	325.830	168.384	92.404	65.768	404,151,167	4.02
	Short-billed dowitcher (*Limnodromus griseus*)	1338.031	102.960	51.696	31.601	18.101	176,856,625	3.38
Columbiformes	Rock dove (*Columba livia*)	2343.436	296.410	135.962	91.635	63.283	500,813,356	4.16
	Peaceful dove (*Geopelia placida*)	776.062	85.2732	40.034	28.0512	14.767	153,994,538	2.97

Coraciiformes	Laughing kookaburra (*Dacelo novaeguineae*)	3970.077	389.618	174.675	135.877	78.870	551,543,759	3.55
Falconiformes	Brown falcon (*Falco berigora*)	6031.853	638.496	323.704	189.022	115.819	680,062,357	3.87
Galliformes	Ruffed grouse (*Bonasa umbellus*)	2288.120	324.170	139.995	84.374	55.716	497,138,294	4.01
	Japanese quail (*Coturnix japonica*)	936.390	118.867	57.609	33.693	17.387	208,022,535	3.53
	Spruce grouse (*Dendragapus canadensis*)	1944.500	340.710	157.025	88.557	57.332	498,244,020	3.75
	Turkey (*Meleagris gallopavo*)	5905.975	945.435	408.138	248.492	186.467	1,309,051,327	5.29
	Indian peafowl (*Pavo cristatus*)	6070.785	749.080	329.097	187.214	129.592	947,227,067	4.29
	Grey partridge (*Perdix perdix*)	2027.027	182.530	88.141	51.173	30.472	325,485,310	3.73
	Ring-necked pheasant (*Phasianus colchicus*)	4060.039	397.133	184.581	101.074	71.064	541,238,255	4.01
Gruiformes	American coot (*Fulica americana*)	2718.919	242.208	119.614	74.498	42.710	390,131,670	3.43
	Dusky moorhen (*Gallinula tenebrosa*)	2726.544	308.984	152.184	87.475	69.678	371,087,600	3.21
Otidiformes	Australian bustard (*Ardeotis australis*)	10500.965	1257.190	592.004	349.836	304.556	1,351,531,180	4.69
Passeriformes	Brown thornbill (*Acanthiza pusilla*)	434.363	37.080	18.536	12.103	5.632	105,390,527	3.45
	Little raven (*Corvus mellori*)	9833.977	689.292	371.034	177.280	134.669	1,065,446,231	5.34
	Australian magpie (*Gymnorhina tibicen*)	5665.058	412.762	205.552	114.084	86.645	797,050,699	4.92
	Superb lyrebird (*Menura novaehollandiae*)	10163.127	819.282	405.340	240.878	163.150	931,334,099	4.29
	Field sparrow (*Spizella pusilla*)	579.150	46.866	19.112	18.035	9.691	114,769,622	3.49
Pelecaniformes	Cattle egret (*Bubulcus ibis*)	4025.096	383.994	194.863	113.376	70.776	513,045,821	4.26
	Australian pelican (*Pelecanus conspicillatus*)	22500	2173.060	1117.048	584.068	468.124	2,297,435,251	4.89
Piciformes	Scaly-throated honeyguide (*Indicator variegatus*)	800	109.910	57.620	37.125	12.780	216,155,679	3.57
	Yellow-bellied sapsucker (*Sphyrapicus varius*)	1442.761	125.878	49.392	46.447	27.032	294,672,035	3.81
Procellariiformes	Short-tailed shearwater (*Puffinus tenuirostris*)	4757.722	756.520	394.480	231.700	116.220	1,103,366,504	4.25
	Black-browed albatross	14129.344	2047.780	1020.916	574.374	424.960	2,811,851,152	5.51

	(*Thalassarche melanophris*)							
Psittaciformes	Australian king parrot (*Alisterus scapularis*)	4901.544	322.714	157.542	92.083	67.942	517,671,690	4.41
	Sulphur-crested cockatoo (*Cacatua galerita*)	13937.259	1048.852	501.600	297.350	222.378	1,453,018,054	5.56
	Galah (*Cacatua roseicapilla*)	7455.598	479.634	226.720	141.215	104.328	643,265,073	4.80
	Purple-crowned lorikeet (*Glossopsitta porphyrocephala*)	1855.212	137.923	62.165	43.819	31.334	235,961,485	3.78
	Budgerigar (*Melopsittacus undulatus*)	1486.486	156.575	68.840	40.730	42.585	283,101,554	3.90
	Cockatiel (*Nymphicus hollandicus*)	2161.197	220.004	105.120	60.530	49.687	381,440,513	4.17
	Crimson rosella (*Platycercus elegans*)	3628.378	225.094	100.210	69.516	50.213	369,803,274	4.14
	Red-rumped parrot (*Psephotus haematonotus*)	1798.262	135.238	62.086	41.098	29.066	277,353,038	3.79
	Rainbow lorikeet (*Trichoglossus haematodus*)	3333.977	190.924	97.187	54.919	35.133	395,266,155	4.30
Sphenisciformes	Little penguin (*Eudyptula minor*)	7583.977	1365.146	777.134	340.858	225.882	1,561,508,578	4.91
Strigiformes	Northern saw-whet owl (*Aegolius acadicus*)	2857.143	239.494	95.868	80.798	54.648	380,425,115	3.70
	Australian boobook (*Ninox boobook*)	6338.803	377.972	174.938	122.534	69.491	452,608,686	3.61
	Barn owl (*Tyto alba*)	7142.857	397.556	186.926	122.954	77.710	559,195,713	3.79

Table 2.2. Numbers (#) of Purkinje cells, granule cells and cerebellar nuclei neurons across species analyzed.

Order	Common name/Species	#Purkinje cells	#Granule cells	#Cerebellar nuclei neurons
Accipitriformes	Collared sparrowhawk (*Accipiter cirrocephalus)*	897,955	890,894,656	169,550
	Wedge-tailed eagle (*Aquila audax*)	1,267,441	1,149,562,112	242,359
	White-bellied sea eagle (*Haliaeetus leucogaster)*	1,005,487	923,455,360	172,132
Anseriformes	American wigeon (*Anas americana*)	624,585	442,898,400	116,930
	Northern shoveler (*Anas clypeata*)	457,616	285,671,744	114,034
	Mallard (*Anas platyrhynchos*)	907,034	635,422,912	112,362
	Gadwall (*Anas strepera*)	617,042	480,030,240	137,483
	Lesser scaup (*Aythya affinis*)	581,555	447,906,304	148,472
	Bufflehead (*Bucephala albeola)*	511,940	442,348,640	88,386
	Common goldeneye (*Bucephala clangula*)	1383070	606,733,632	145,463
	Red-breasted merganser (*Mergus serrator*)	593,958	457,814,016	98,760
Caprimulgiformes	Spotted nightjar (*Eurostopodus argus*)	169,574	150,813,568	44,861
	Tawny frogmouth (*Podargus strigoides*)	455,900	376,710,656	77,081
Casuariiformes	Emu (*Dromaius novaehollandiae*)	4,735,835	2,584,285,440	357,850
Charadriiformes	Silver gull (*Larus novaehollandiae*)	333,034	302,858,368	70,523
	Short-billed dowitcher (*Limnodromus griseus*)	167,844	78,940,320	57,750
Columbiformes	Rock dove (*Columba livia*)	523,856	346,092,704	81,118
	Peaceful dove (*Geopelia placida*)	175,798	91,912,584	45,343
Coraciiformes	Laughing kookaburra (*Dacelo novaeguineae*)	543,676	940,231,232	81,467
Falconiformes	Brown falcon (*Falco berigora*)	740,853	652,221,632	80,901
Galliformes	Ruffed grouse (*Bonasa umbellus*)	568,783	307,992,725	105,378
	Japanese quail (*Coturnix japonica*)	402,471	106,524,944	69,634
	Spruce grouse (*Dendragapus canadensis*)	577,257	222,194,016	78,799
	Turkey (*Meleagris gallopavo*)	1,261,079	896,211,904	190,878
	Indian peafowl (*Pavo cristatus*)	904,452	393,968,960	144,161
	Grey partridge (*Perdix perdix*)	451,406	120,762,048	73,693
	Ring-necked pheasant (*Phasianus colchicus*)	586,874	401,393,760	87,841
Gruiformes	American coot	379,303	319,894,080	76,381

	(*Fulica americana*)			
	Dusky moorhen (*Gallinula tenebrosa*)	379,368	258,506,304	96,273
Otidiformes	Australian bustard (*Ardeotis australis*)	954,555	916,399,552	161,511
Passeriformes	Brown thornbill (*Acanthiza pusilla*)	172,757	85,635,896	35,690
	Little raven (*Corvus mellori*)	892,424	780,922,368	120,485
	Australian magpie (*Gymnorhina tibicen*)	768,936	814,053,056	93,900
	Superb lyrebird (*Menura novaehollandiae*)	870,097	904,763,584	147,375
	Field sparrow (*Spizella pusilla*)	134,504	75,443,432	30,442
Pelecaniformes	Cattle egret (*Bubulcus ibis*)	429,449	349,358,112	93,184
	Australian pelican (*Pelecanus conspicillatus*)	1,588,855	1,291,263,872	264,139
Piciformes	Scaly-throated honeyguide (*Indicator variegatus*)	210,990	101,545,400	48,422
	Yellow-bellied sapsucker (*Sphyrapicus varius*)	305,975	180,678,592	63,559
Procellariiformes	Short-tailed shearwater (*Puffinus tenuirostris*)	770,170	908,588,288	99,623
	Black-browed albatross (*Thalassarche melanophris*)	2,300,728	1,621,144,960	291,537
Psittaciformes	Australian king parrot (*Alisterus scapularis*)	509,073	348,362,976	88,750
	Sulphur-crested cockatoo (*Cacatua galerita*)	1,254,155	1,022,579,776	168,471
	Galah (*Cacatua roseicapilla*)	617,875	574,456,000	100,342
	Purple-crowned lorikeet (*Glossopsitta porphyrocephala*)	241,327	175,971,680	61,182
	Budgerigar (*Melopsittacus undulatus*)	289,087	155,686,048	59,123
	Cockatiel (*Nymphicus hollandicus*)	376,777	240,051,504	85,989
	Crimson rosella (*Platycercus elegans*)	259,291	271,755,136	82,464
	Red-rumped parrot (*Psephotus haematonotus*)	268,572	180,058,576	48,783
	Rainbow lorikeet (*Trichoglossus haematodus*)	323,122	217,400,720	66,609
Sphenisciformes	Little penguin (*Eudyptula minor*)	1,242,661	970,026,304	155,915
Strigiformes	Northern saw-whet owl (*Aegolius acadicus*)	380,817	265,476,624	53,250
	Australian boobook (*Ninox boobook*)	609,521	436,894,720	139,601
	Barn owl (*Tyto alba*)	451,163	472,394,048	95,436

Table 2.3. Soma sizes (µm ^{2}) of Purkinje cells, granule cells and cerebellar nuclei neurons across species analyzed (±SD).

Order	Common name/Species	Purkinje cell size	Granule cell size	Cerebellar nuclei neuron size
Accipitriformes	Collared sparrowhawk (*Accipiter cirrocephalus)*	300.710 ± 61.251	8.797 ± 1.256	334.739 ± 71.562
	Wedge-tailed eagle (*Aquila audax*)	456.756 ± 83.102	14.002 ± 2.896	479.626 ± 153.855
	White-bellied sea eagle (*Haliaeetus leucogaster)*	469.149 ± 112.661	11.225 ± 1.448	462.654 ± 141.603
Anseriformes	American wigeon (*Anas americana*)	459.791 ± 95.990	9.172 ± 1.434	405.114 ± 119.114
	Northern shoveler (*Anas clypeata*)	317.128 ± 71.180	10.069 ± 1.160	442.122 ± 106.362
	Mallard (*Anas platyrhynchos*)	476.699 ± 190.757	9.630 ± 1.254	348.200 ± 92.530
	Gadwall (*Anas strepera*)	247.916 ± 55.068	8.819 ± 1.534	336.350 ± 89.451
	Lesser scaup (*Aythya affinis*)	433.919 ± 106.203	11.824 ± 1.737	437.387 ± 155.998
	Bufflehead (*Bucephala albeola)*	343.081 ± 60.692	11.195 ± 1.136	392.749 ± 100.220
	Common goldeneye (*Bucephala clangula*)	511.195 ± 184.240	13.167 ± 2.318	395.496 ± 135.575
	Red-breasted merganser (*Mergus serrator*)	222.020 ± 43.691	9.056 ± 1.086	299.579 ± 88.618
Caprimulgiformes	Spotted nightjar (*Eurostopodus argus*)	274.709 ± 67.539	9.621 ± 1.241	271.130 ± 67.376
	Tawny frogmouth (*Podargus strigoides*)	511.705 ± 122.552	15.668 ± 2.285	437.580 ± 132.350
Casuariiformes	Emu (*Dromaius novaehollandiae*)	578.392 ± 110.782	20.144 ± 3.951	372.085 ± 95.745
Charadriiformes	Silver gull (*Larus novaehollandiae*)	400.590 ± 63.807	12.356 ± 2.210	329.251 ± 98.496
	Short-billed dowitcher (*Limnodromus griseus*)	304.695 ± 66.178	10.727 ± 1.252	345.054 ± 90.268
Columbiformes	Rock dove (*Columba livia*)	328.607 ± 70.135	14.038 ± 1.999	369.342 ± 114.043
	Peaceful dove (*Geopelia placida*)	331.634 ± 63.452	11.986 ± 1.885	354.633 ± 130.276
Coraciiformes	Laughing kookaburra (*Dacelo novaeguineae*)	347.044 ± 79.126	11.157 ± 1.527	434.509 ± 128.607
Falconiformes	Brown falcon (*Falco berigora*)	377.064 ± 97.670	10.932 ± 1.358	292.18 ± 63.169
Galliformes	Ruffed grouse (*Bonasa umbellus*)	417.338 ± 24.792	11.861 ± 1.337	408.100 ± 115.922
	Japanese quail (*Coturnix japonica*)	366.541 ± 25.575	13.602 ± 0.135	323.366 ± 73.456
	Spruce grouse (*Dendragapus canadensis*)	412.334 ± 66.047	13.459 ± 0.039	392.945 ± 89.769
	Turkey (*Meleagris gallopavo*)	501.821 ± 11.098	10.989 ± 0.078	412.496 ± 113.538
	Indian peafowl (*Pavo cristatus*)	529.581 ± 43.140	12.699 ± 1.754	501.634 ± 159.881
	Grey partridge (*Perdix perdix*)	403.532 ± 60.218	14.817 ± 0.849	401.63 ± 119.885
	Ring-necked pheasant (*Phasianus colchicus*)	481.987 ± 13.865	11.930 ± 0.736	372.831 ± 91.257
Gruiformes	American coot	397.465 ± 84.706	10.315 ± 1.325	371.351 ± 84.818

	(*Fulica americana*)			
	Dusky moorhen (*Gallinula tenebrosa*)	322.775 ± 71.775	10.386 ± 1.363	385.486 ± 101.154
Otidiformes	Australian bustard (*Ardeotis australis*)	393.842 ± 106.024	10.666 ± 1.435	369.809 ± 98.759
Passeriformes	Brown thornbill (*Acanthiza pusilla*)	189.003 ± 34.175	6.306 ± 0.967	226.162 ± 49.399
	Little raven (*Corvus mellori*)	484.401 ± 115.573	9.369 ± 1.220	459.757 ± 130.644
	Australian magpie (*Gymnorhina tibicen*)	345.135 ± 66.720	9.555 ± 1.366	413.521 ± 112.178
	Superb lyrebird (*Menura novaehollandiae*)	280.407 ± 59.367	8.708 ± 1.000	357.912 ± 82.596
	Field sparrow (*Spizella pusilla*)	191.211 ± 44.279	9.904 ± 1.788	302.391 ± 79.363
Pelecaniformes	Cattle egret (*Bubulcus ibis*)	543.942 ± 130.684	10.780 ± 1.534	421.988 ± 129.709
	Australian pelican (*Pelecanus conspicillatus*)	492.731 ± 111.300	16.094 ± 2.686	457.406 ± 154.674
Piciformes	Scaly-throated honeyguide (*Indicator variegatus*)	292.638 ± 62.710	11.430 ± 1.963	310.044 ± 96.800
	Yellow-bellied sapsucker (*Sphyrapicus varius*)	166.29 ± 39.679	11.771 ± 1.916	252.462 ± 67.996
Procellariiformes	Short-tailed shearwater (*Puffinus tenuirostris*)	344.706 ± 107.151	10.537 ± 1.279	305.454 ± 80.332
	Black-browed albatross (*Thalassarche melanophris*)	343.577 ± 76.180	12.244 ± 1.518	362.104 ± 99.151
Psittaciformes	Alistralian king parrot (*Alisterus scapularis*)	404.644 ± 79.071	9.461 ± 1.071	359.630 ± 144.957
	Sulphur-crested cockatoo (*Cacatua galerita*)	423.260 ± 86.903	10.784 ± 1.412	488.317 ± 187.910
	Galah (*Cacatua roseicapilla*)	346.342 ± 67.906	9.531 ± 1.037	317.196 ± 69.466
	Purple-crowned lorikeet (*Glossopsitta porphyrocephala*)	315.535 ± 69.678	10.368 ± 1.121	451.154 ± 145.499
	Budgerigar (*Melopsittacus undulatus*)	317.18 ± 66.208	10.160 ± 1.309	383.317 ± 110.859
	Cockatiel (*Nymphicus hollandicus*)	384.595 ± 69.721	9.586 ± 1.287	403.847 ± 123.281
	Crimson rosella (*Platycercus elegans*)	349.493 ± 71.025	8.993 ± 1.317	327.510 ± 102.433
	Red-rumped parrot (*Psephotus haematonotus*)	307.785 ± 45.189	9.497 ± 1.434	337.123 ± 83.237
	Rainbow lorikeet (*Trichoglossus haematodus*)	377.526 ± 96.850	9.909 ± 1.065	294.431 ± 62.871
Sphenisciformes	Little penguin (*Eudyptula minor*)	512.358 ± 133.930	13.308 ± 1.924	383.633 ± 97.203
Strigiformes	Northern saw-whet owl (*Aegolius acadicus*)	305.544 ± 76.990	10.730 ± 1.191	319.019 ± 88.886
	Australian boobook (*Ninox boobook*)	269.488 ± 45.881	8.200 ± 1.258	235.656 ± 60.165
	Barn owl (*Tyto alba*)	385.962 ± 98.792	12.076 ± 1.682	356.918 ± 78.560

Table 2.4. Summary of the clade differences for the measurements examined relative to brain volume (vol.) or cerebellum volume. Down arrow indicates relative reduction, up arrow indicates relative increase, and hyphen indicates no difference between a given clade and other birds.

Measurements/Order	**Anseriformes**	**Galliformes**	**Passeriformes**	**Psittaciformes**
Cerebellum vol.	-	-	↓	↓
Molecular layer vol.	-	-	-	-
Granule layer vol.	-	↓	-	-
WM + Cb vol.	-	↓	-	↑
#Purkinje cells	-	↑	-	-
Purkinje cell size	-	↑	-	-
#Granule cells	-	↓	↑	-
Granule cell size	-	-	↓	-
#CbN neurons	-	-	-	-
#CbN neuron size	-	-	-	-
Purkinje surface area	-	-	-	-
CFI	-	-	↑	↑

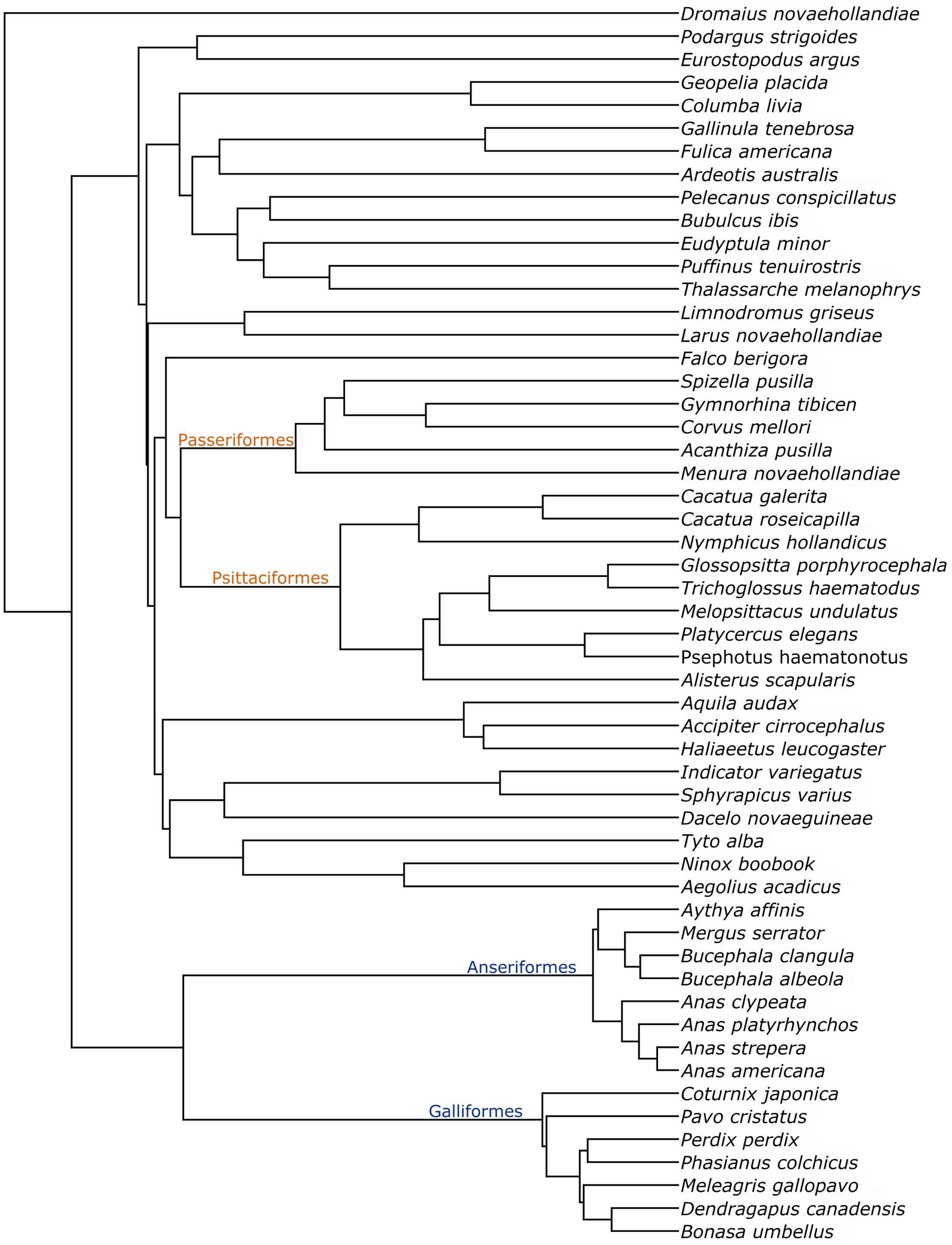

Figure 2.1. Phylogeny of the species analyzed in this study. The clades Passeriformes (songbirds), Psittaciformes (parrots), Anseriformes (waterfowls), and Galliformes (chicken-like birds) are indicated on the branches.

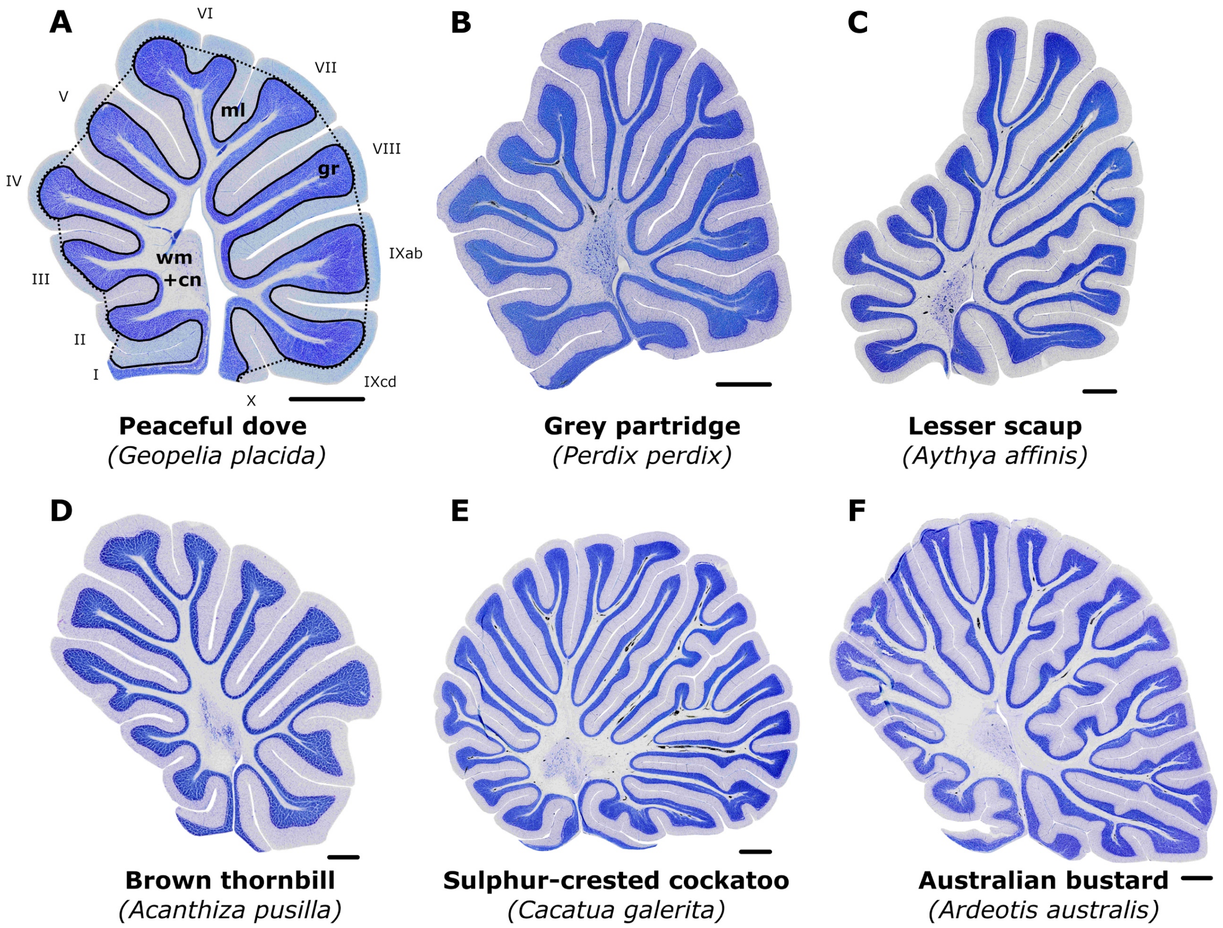

Figure 2.2. Midsagittal sections of Nissl-stained cerebella of: **A** peaceful dove (*Geopelia placida*), **B** grey partridge (*Perdix perdix*), **C** lesser scaup (*Aythya affinis*), **D** brown thornbill (*Acanthiza pusilla*), **E** sulphur-crested cockatoo (*Cacatua galerita*), and **F** Australian bustard (*Ardeotis australis*). Note the difference in cerebellar size and shape across avian species. For example, while the sulphur-crested cockatoo has a CFI of 5.56, the peaceful dove has a CFI of 2.97. For the peaceful dove (A), cerebellar folia are represented as roman numerals, from I (anterior) to X (posterior), as suggested by Larsell (1967). The black continuous line follows the Purkinje cell layer. The ratio between the length of the Purkinje cell layer (continuous black line) and the envelope length of this same layer (dotted black like) is referred to as the cerebellar foliation index (CFI). ml=molecular layer; gr = granule cell layer, and "wm+cn" = white matter layer and cerebellar nuclei. Scale-bars: A-C = 1mm, D = 0.5mm, E-F = 2mm.

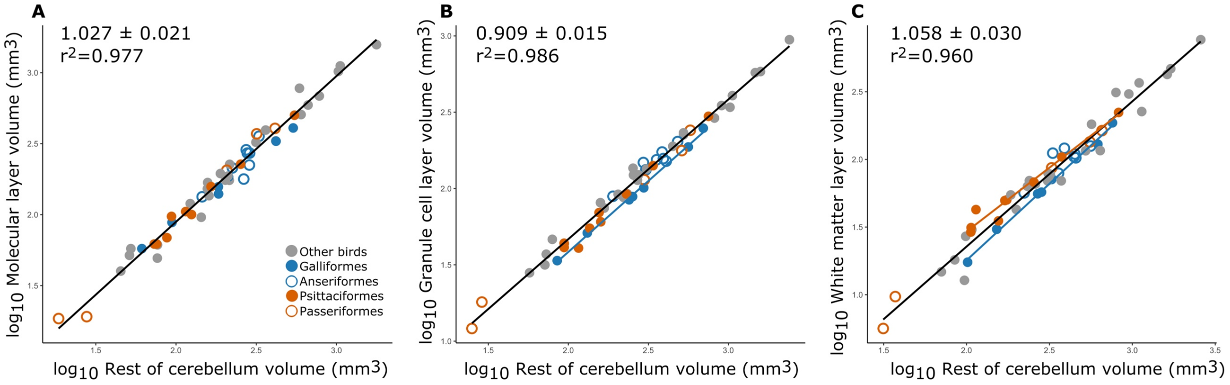

Figure 2.3. Scatterplots of the log-transformed volumes (mm^3) of: **A** molecular layer (mm^3) against rest of cerebellum and **B** granule cell layer against rest of the cerebellum, **C** white matter layer plus cerebellar nuclei neurons against rest of the cerebellum. Clades with significant differences from other birds are indicated in the graph. See allometric equations and statistical data in Table S2.2. The rest of the cerebellum refers to as total cerebellum size minus the size of the cerebellar layer in the y-axis.

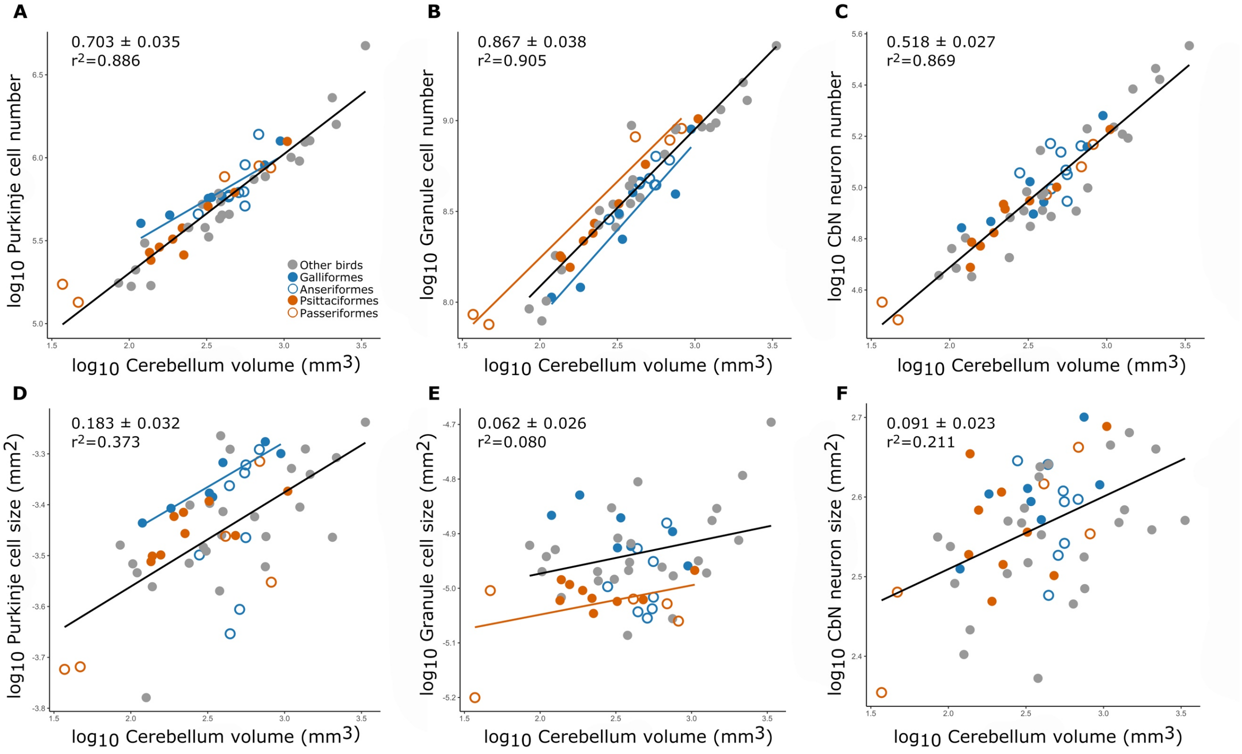

Figure 2.4. Scatterplots of the log-transformed of: **A** Purkinje cell number, **B** granule cell number, **C** cerebellar nuclei neuron number, **D** Purkinje cell size (mm^2), **E** granule cell size (mm^2), and **F** cerebellar nuclei neuron size (mm^2) against the log-transformed volume (mm^3) of the cerebellum. Clades with significant differences from other birds are indicated in the graph. See allometric equations and statistical data in Table S2.2. CbN=cerebellar nuclei.

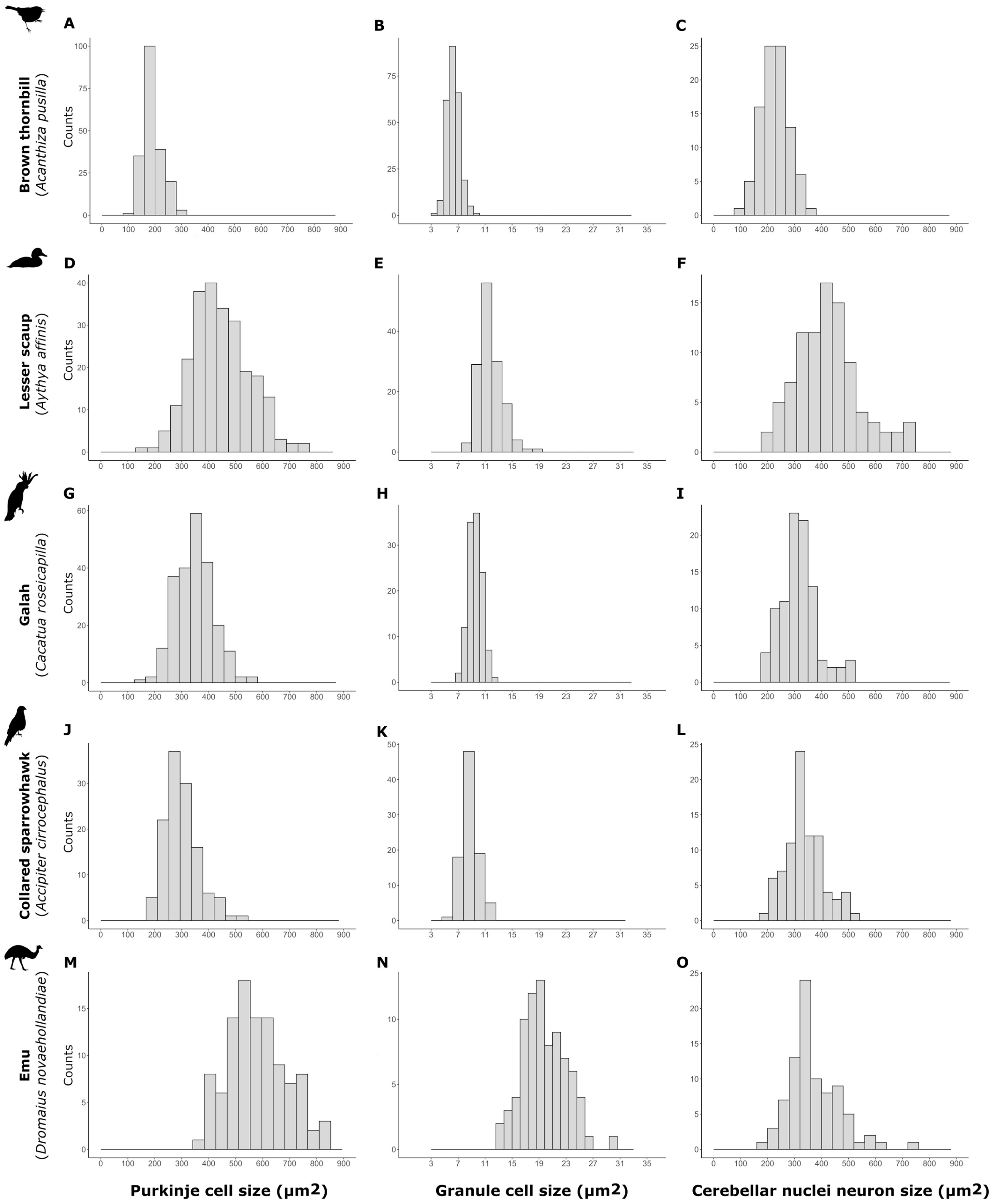

Figure 2.5. Distribution of cell soma sizes (µm^2) of Purkinje cells (A, D, G, J, M), granule cells (B, E, H, K, N) and cerebellar nuclei neurons (C, F, I, L, O) within the following specimens: brown thornbill (*Acanthiza pusilla,* A-C), lesser scaup (*Aythya affinis,* D-F), galah (*Cacatua roseicapilla*, G-I), collared sparrowhawk (*Accipiter cirrocephalus*, J-L) and emu (*Dromaius novaehollandiae*, M-O). The depicted bars represent the summed-up counts of cells within the

following ranges: 25-50 µm for Purkinje cells and cerebellar nuclei neurons, and 0.75-1.50 µm for granule cells. The distribution of cell soma sizes followed a normal distribution curve. Although the distribution of the granule cell sizes in the emu appears to be slightly different than a normal curve, most of the measurements were still restricted to a narrow range of sizes (e.g., 16-22 µm).

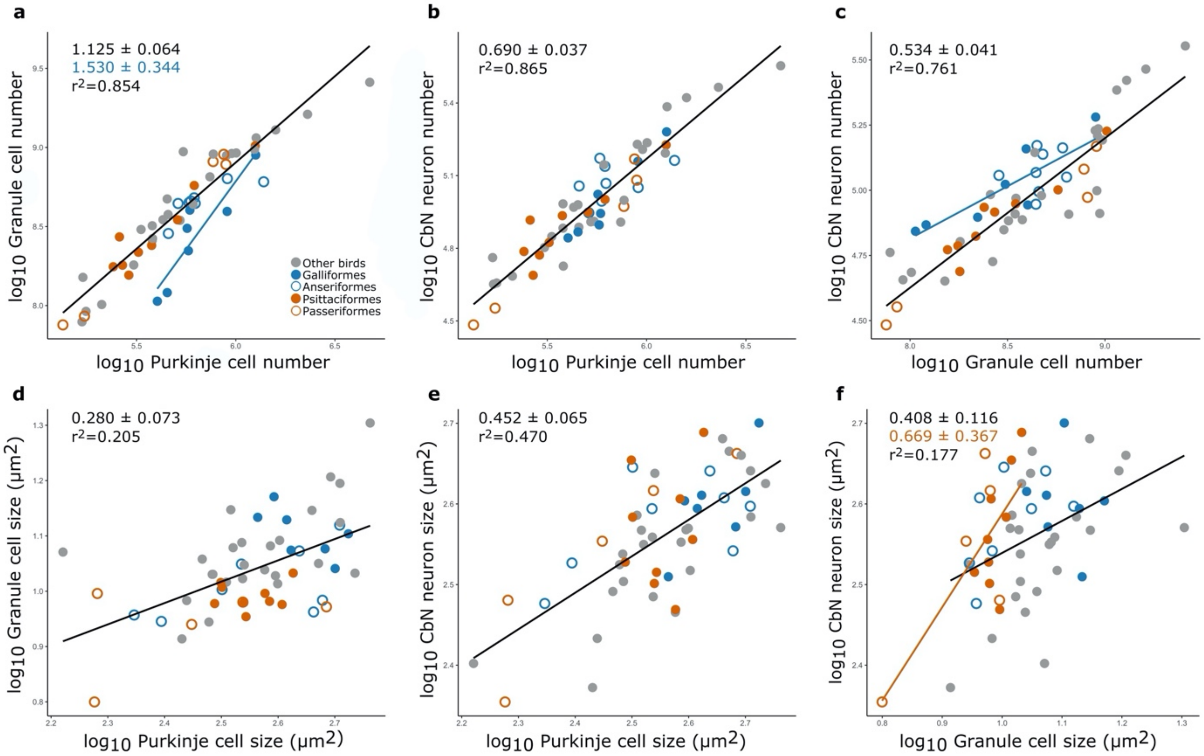

Figure 2.6. Scatterplots of the log-transformed of: **A** granule cell number against Purkinje cell number, **B** cerebellar nuclei neuron number against Purkinje cell number, **C** cerebellar nuclei neuron number against granule cell number, **D** granule cell size (μm^2) against Purkinje cell size (μm^2), **E** cerebellar nuclei neuron size (μm^2) against Purkinje cell size and **F** cerebellar nuclei neuron size against granule cell size. Clades with significant differences from other birds are indicated in the graph. See allometric equations and statistical data in Table S2.2. CbN=cerebellar nuclei.

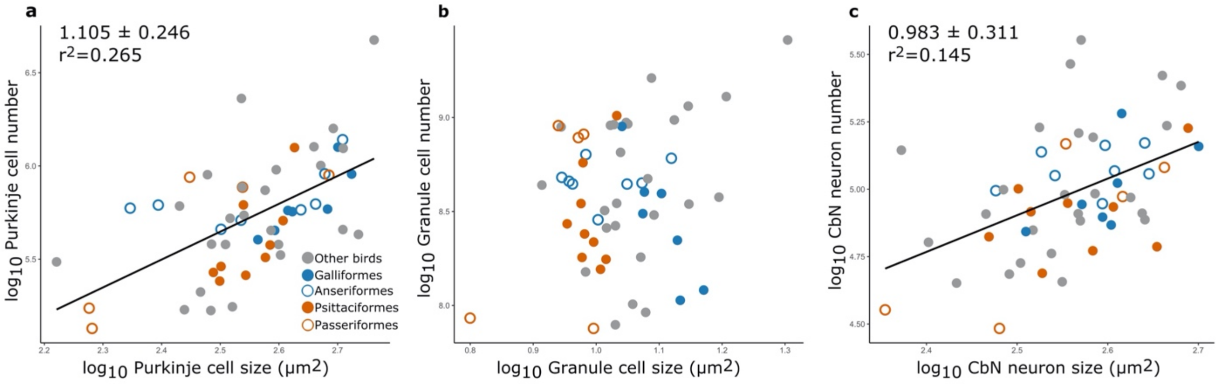

Figure 2.7. Scatterplots of the log-transformed of: **A** Purkinje cell number against Purkinje cell size (μm^2), **B** granule cell number against granule cell size (μm^2), and **C** cerebellar nuclei neuron number against cerebellar nuclei neuron size (μm^2). See allometric equations and statistical data in Table S2.2.

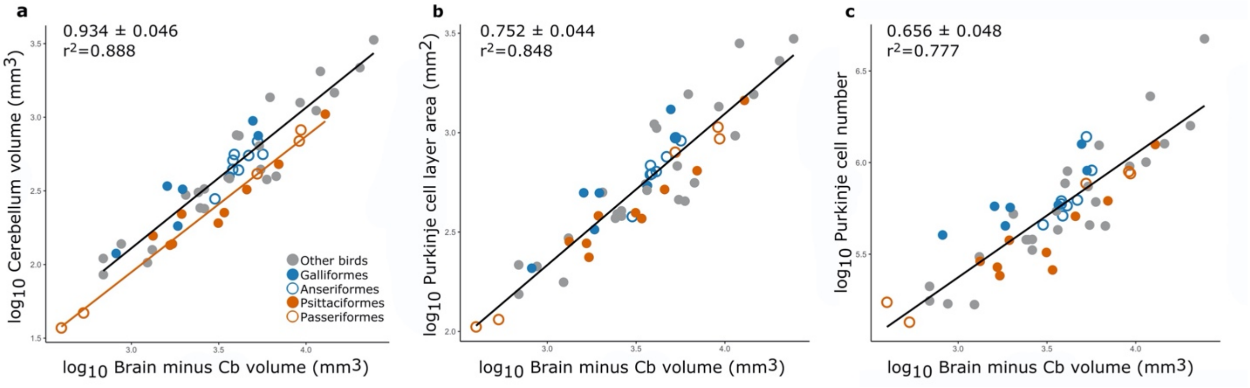

Figure 2.8. Scatterplots of the log-transformed of: **A** cerebellum volume (mm^3) against rest of the brain volume (mm^3), **B** surface area of Purkinje cell layer (mm^2) against rest of the brain volume, and **C** Purkinje cell number against rest of the brain volume. Clades with significant differences from other birds are indicated in the graph. See allometric equations and statistical data in Table S2.2.

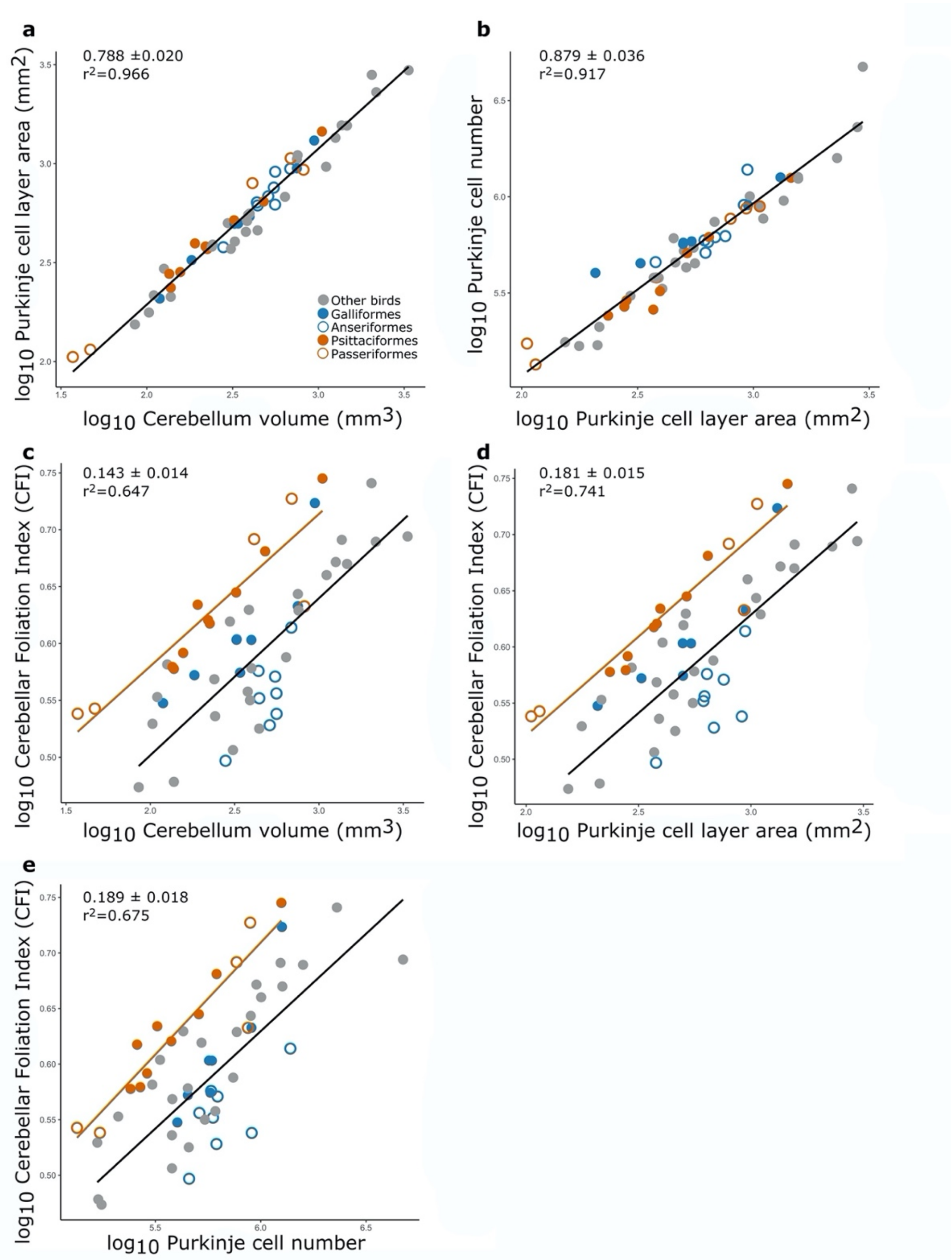

Figure 9. Scatterplots of the log-transformed of: **A** cerebellum volume (mm^3) against rest of the brain volume (mm^3), **B** surface area of Purkinje cell layer (mm^2) against rest of the brain volume, and **C** Purkinje cell number against rest of the brain volume. Clades with significant differences from other birds are indicated in the graph. See allometric equations and statistical data in Table S2.2.

CHAPTER THREE: EVOLUTION OF CEREBELLUM SIZE IN BIRDS: THE EFFECTS OF DEVELOPMENT, FLIGHT, MIGRATION AND TELENCEPHALON SIZE

Abstract

Many different hypotheses have been proposed to explain why brain and brain region sizes are larger in some species than others. Most studies restrict their analyses to the size of the brain or a single brain region and in doing so, overlook potential interactions among the sizes of different brain regions and the relationship between these interaction effects and other variables. Using phylogenetic generalized least squares and path analysis, we evaluate how the cerebella of 298 species of birds vary in size relative to the sizes of the telencephalon and rest of the brain, and test if these relationships are correlated with degree of aerial behaviour, manoeuverability, migration, and developmental mode. Across all species in our sample, cerebellum size increased at similar rates relative to both brain remainder and telencephalon sizes, although the cerebellum-telencephalon correlation was strongest. With respect to other variables, altricial species had relatively larger telencephala than precocial species, aerial birds had relatively smaller telencephala than non-aerial birds, and migratory species had larger cerebella relative to the telencephalon. Path analysis indicated that migration had the strongest effect on both cerebellum and telencephalon sizes. Overall then, our data indicate that migration is associated with a shift in the relationship between cerebellum and telencephalon size, which we interpret as support both the energetic and cognitive buffer hypotheses.

Introduction

Understanding how and why the brain expands among species is a major question in evolutionary neuroscience. A larger brain (in relative and absolute terms) is thought to provide more neurons and/or synapses (Cole 1985; Roth and Dicke 2012; Herculano-Houzel et al. 2014) and with that, improved cognitive abilities (Kotrschal et al. 2013; Benson-Amram et al. 2016). Accordingly, the evolution of larger brains within vertebrates has been associated with the emergence of several aspects of cognition, such as living in larger social groups (Dunbar 1998, 2009) and the ability to adapt to novel environmental conditions (Sol et al. 2007; Schuck-Paim et al. 2008; Sol 2009; van Woerden et al. 2012; Benson-Amram et al. 2016). Cognitive demands are not, however, the only variables thought to affect the relative size of the brain. The high energy costs of nervous tissue (Clarke and Sokoloff 1999; Raichle and Gusnard 2002) can pose constraints on brain evolution such that species living in harsh ecological conditions may not be able to grow and maintain a relatively larger brain (Isler and van Schaik 2009a; Navarrete et al. 2011; Kotrschal et al. 2013; Sayol et al. 2016; Luo et al. 2017). Thus, an increase in relative brain size likely evolves through a combination of selective pressures on cognition and metabolic constraints (Leigh 2004; Sol 2009; Jiménez-Ortega et al. 2020).

Studying overall brain size does reveal some aspects of brain evolution, but the brain is highly heterogeneous, comprised of multiple individual and functionally specific regions and circuits (Safi and Dechmann 2005; Healy and Rowe 2007; Barton 2012; Smaers and Soligo 2013; Wylie et al. 2015). Because the evolution of larger brains is driven by an array of selective forces acting differently on each brain region, simply correlating relative brain size with one trait/behaviour is therefore unlikely to provide a complete picture of how the brain evolves. This is supported by variation in the relative size of individual brain regions, which can occur independently from one brain region to the next (Krebs 1990; DeVoogd et al. 1993; Barton et al. 1995; Barton and Harvey 2000; Yopak et al. 2010). As a result of this variation among brain regions, patterns of evolutionary change observed for overall brain size do not necessarily apply to individual brain regions.

Of the many regions that comprise the vertebrate brain, the cerebellum stands out as being highly variable in relative size and shape across and within vertebrate classes (see review Yopak et al. 2017). Variation in cerebellar size is often associated with motor skill such that species with a relatively larger cerebellum execute more complex motor actions than those with smaller cerebella (Iwaniuk et al. 2007; Yopak et al. 2007; Montgomery et al. 2012). Indeed, several comparative studies indicate that the relative size of the cerebellum reflects differences in locomotion and/or motor learning (Larsell and Jansen 1967; Stephan and Pirlot 1970; Bennett and Harvey 1985; Boire and Baron 1994; Matano and Hirasaki 1997; Rilling and Insel 1998; Day et al. 2005; Iwaniuk et al. 2007; Yopak et al. 2007; Balanoff et al. 2016; Macrì et al. 2019). As the cerebellum plays a key role in motor control (Ito 1984), flight is often correlated with differences in size of the entire cerebellum or parts of the cerebellum within birds (Larsell 1948; Bennett and Harvey 1985; Boire and Baron 1994; Iwaniuk et al. 2007; Wylie et al. 2018; but see Walsh et al. 2013). For example, “strong fliers” (e.g., waterfowls) have expanded folia VI and VII (Iwaniuk et al. 2007), and relative cerebellum size is suggested to be associated with aspects of flight performance, such as maneuverability (Bennett and Harvey 1985; Boire and Baron 1994; Balanoff et al. 2016). Migratory behaviour is also associated with evolutionary changes in the brain; migrants have relatively smaller brains than non-migrants (Sol et al. 2010; McGuire and Ratcliffe 2011; Vincze et al. 2015; Sayol et al. 2016; Vincze 2016). While these studies support a negative association between migration and relative brain size, the question remains:

does the size of individual brain regions, including the cerebellum, differ between migrants and non-migrants (Vincze et al. 2015)?

Locomotion is not, however, the only variable that might be correlated with the relative size of the cerebellum in birds. Developmental mode in birds plays a major role in species differences in relative brain size such that altricial species have relatively larger brains as adults than precocial species (Portmann 1947; Bennett and Harvey 1985; Starck 1993; Starck and Ricklefs 1998; Iwaniuk and Nelson 2003). The relative size of brain regions, including the cerebellum, also appear to differ across developmental modes (Portmann 1947; Bennett and Harvey 1985), but the strength of this effect and how developmental mode interacts with other variables remains largely untested.

Changes in the size of a brain region can also be dependent on that of other brain regions (Finlay and Darlington 1995; Iwaniuk et al. 2004; Gutiérrez-Ibáñez et al. 2014; Smaers and Vanier 2019). Several studies indicate that cerebellar size and telencephalon size are evolutionarily correlated (Whiting and Barton 2003; Iwaniuk et al. 2004; Yopak et al. 2010; Smaers and Soligo 2013). More specifically, as total brain size increases, both the telencephalon and cerebellum increase in size in a coordinated fashion in relation to size, number of neurons, and connectivity (Whiting and Barton 2003; Ramnani 2006; Herculano-Houzel 2010; Barton 2012; Gutiérrez-Ibáñez et al. 2018; Smaers and Vanier 2019). Divergences in this coordinated evolution between the cerebellum and telencephalon are thought to play an important role in the evolution of complex cognitive behaviours (Barton and Venditti 2014; Gutiérrez-Ibáñez et al. 2018; Smaers and Vanier 2019). For example, the evolution of technological abilities (e.g., tool use) in apes is thought to be associated with a rapid increase in the size of the cerebellum relative to the size of the cerebral cortex (Barton and Venditti 2014). To what extent cerebellum size is correlated with telencephalon size in other clades and how the cerebellum-telencephalon relationship varies with locomotion, developmental mode or other variables remains unknown.

To understand how flight, migration, developmental mode, and telencephalon size are associated with variation in relative cerebellum size in birds, we adopted a two-pronged approach within a phylogenetic framework. First, we analyzed relative cerebellum size in relation to developmental mode, migration, flight style, and telencephalon size using the largest dataset compiled of cerebellum size in birds to date. Second, we used phylogenetic path analysis (von Hardenberg and Gonzalez-Voyer 2013; Gonzalez-Voyer and von Hardenberg 2014) to explore direct and indirect interactions among our variables in a multivariate framework. With this single multivariate model, we were able to assess how different variables influence the evolution of a larger or smaller cerebellum.

Material and Methods

Data collection

We compiled data for the sizes of the whole brain and cerebellum across 298 bird species from published studies and our own work (see Table 3.3). Among these 298 species, we also had telencephalon size data for 288 species. Data on brain size provided as weights were converted to volumes by dividing them into the density of fresh brain tissue (1.036 g/mL) (Ebinger 1995; Iwaniuk and Nelson 2001, 2002). The "brain remainder" was then calculated by subtracting the sizes of the cerebellum and telencephalon from the whole brain (see Table 3.3) and used as a scaling variable throughout our analyses.

As discussed above, developmental mode plays a major role in the evolution of relative brain size in birds (Iwaniuk and Nelson 2003). Species that hatch in an altricial, under-developed state (e.g., songbirds, parrots) tend to have relatively larger brains as adults whereas species that hatch in a precocial, more well-developed state (e.g., chickens, waterfowl) tend to have relatively smaller brains as adults (Bennett and Harvey 1985; Nealen and Ricklefs 2001; Iwaniuk and Nelson 2003). To determine if developmental mode explains differences in relative cerebellum size, we divided our species into altricial and precocial developmental modes, based upon Nice (1962) and Starck (1993) (Table 3.4).

In addition to developmental mode, we tested for differences in relative cerebellum size for variables related to locomotion. The first of these, migration, is often associated with relatively smaller brains (Sol et al. 2010; Vincze et al. 2015; Sayol et al. 2016; Vincze 2016). To test if migration is also associated with a change in relative cerebellum size, we categorized our species as migratory or non-migratory. Both migration distance (i.e., travelling distance) and migratory behaviour (e.g., migrants vs. residents) covary with brain size across species or within species (Cristol et al. 2003; Pravosudov et al. 2007; Sol et al. 2010; Vincze et al. 2015; Sayol et al. 2016; Vincze 2016). Migration distance, however, is likely to vary among individuals, populations, and subspecies (Cristol et al. 2003; Bearhop et al. 2005; Pravosudov et al. 2007; Maclean et al. 2008), and geometric means of wintering range may therefore be an inaccurate estimate of distance travelled, especially when the population that an individual is sampled from is unknown. To avoid this potential error in our large data set, we adopted a binary categorization of migration, dividing our species into migratory or non-migratory (residents). Similar to previous studies (Sayol et al. 2016; Dufour et al. 2020), both strict and partial migrants were categorized as migrants (Table 3.4).

The second locomotion related variable was differentiating species based on aerial activity. Postural control and motor requirements linked to aerial activity were suggested to be responsible for relatively larger cerebella in some species by Bennett and Harvey (1985). To test this in an expanded data set, we classified species as being aerial or non-aerial. Aerial species were defined as those species that spend the majority of their active periods in flight and are capable of feeding, drinking, sleeping, and/or mating on the wing (e.g., hummingbirds, swifts, nightjars, terns, swallows, and pelagic seabirds; Table 3.4). Cerebellar anatomy differs according to flight style in birds (Larsell 1948; Iwaniuk et al. 2007; Balanoff et al. 2016), but comparisons with relative cerebellum size are lacking. To test for differences in relative cerebellum size according to flight style we categorized species following Norberg (1990) ranking of manoeuvrability based on wing shape: (0) flightless; (1) slow, poorly manoeuvrable birds that soar; (2) fast, poorly manoeuvrable fliers; (3) slow manoeuvrable fliers; and (4) fast manoeuvrable fliers (Table 3.4). We note that species "flying" under water were also considered as fliers based on wing shape. For example, all of the penguins in our sample are categorized as "fast manoeuvrable fliers".

Statistical analyses

To examine allometric relationships among cerebellum size, telencephalon size, and brain remainder size across all our species, we performed phylogenetic generalized least squares (PGLS) of log-transformed data in R 4.0.3 (Team 2020) using the *pgls* function in *caper* (Orme et al. 2013) and *nlme* (Pinheiro et al. 2006) allowing the phylogenetic signal in the residuals, Pagel's lambda λ (Pagel 1999), to be optimized to its maximum likelihood (Table 3.1). We extracted 1,000 fully resolved trees from birdtree.org (Jetz et al. 2012) with Ericson et al. (2006) backbone phylogeny, and built a maximum credibility tree (consensus tree) using *phangorn* (Schliep 2011). For all PGLS analyses, we used log-transformed data and the consensus phylogenetic tree. We then ran phylogenetic analyses of covariance (pANCOVA) for all the relationships performed to test for significant differences across categories for each variable: developmental mode (altricial vs. precocial), migration (migrants vs. residents), and flight style (flight maneuverability, and aerial vs. non-aerial birds). Note that none of the variables were affected by multicollinearity effects across the allometric relationships performed (variance inflation factors, VIF<2).

Next, we tested hypothetical causal relationships among cerebellum, telencephalon, brain remainder and the other variables using phylogenetic path analysis (von Hardenberg and Gonzalez-Voyer 2013; Gonzalez-Voyer and von Hardenberg 2014). Path analysis is a combination of multiple regression models that determine the fit of alternative causal models (Schliep 2011; Gonzalez-Voyer and von Hardenberg 2014). Model selection is based on the minimal set of conditional independences that must all be true if the causal model is correct (von Hardenberg and Gonzalez-Voyer 2013). Testing the fit of the model is conducted with Fisher's C statistic, which estimates the goodness of fit of the model. Thus, a C statistic test with a p-value < 0.05 indicates that the model fits poorly (von Hardenberg and Gonzalez-Voyer 2013; Gonzalez-Voyer and von Hardenberg 2014). Different models can be compared by means of C statistic information criterium (CICc), which is analogous to the Akaike information criterion (AICc) (von Hardenberg and Gonzalez-Voyer 2013). As detailed below, we constructed models based on what variables were significant in our pANCOVAs. We then ran our models using *phylopath* (van der Bijl 2018), and selected the best-fitting model based on the C statistic (p > 0.05) and summed weights (w > 0.95) (Burnham and Anderson 2002).

Results

Cerebellar size increased at similar rates relative to both brain remainder and telencephalon sizes across species (Table 3.1). Telencephalon size also increased significantly with the brain remainder at a similar rate (Table 3.1). Despite sharing similar slopes, cerebellum size was more strongly correlated with telencephalon size than brain remainder size and had a higher λ value (Table 3.1).

Altricial and precocial species did not differ in cerebellum size relative to the brain remainder (pANCOVA, p=0.889; Fig. 3.1A). However, altricial species had larger telencephalic sizes relative to the brain remainder (+27%; pANCOVA, p=0.04; Fig 3.1B) and smaller cerebella relative to the telencephalon than precocial species (-23%; pANCOVA, p=0.02; Fig. 3.1C).

Neither cerebellum nor telencephalon size differed significantly between migratory and non-migratory species relative to the brain remainder (pANCOVA, p’s= 0.885; 0.105, respectively; Figs. 3.2A,B). However, migratory species had significantly larger cerebella relative to the telencephalon (+22%; pANCOVA, p=0.03; Fig. 3.2C). Thus, although cerebellum size was more strongly correlated with telencephalon size than brain remainder size (see Table 3.1), the relationship between telencephalon and cerebellum sizes differs between migratory and non-migratory species (Fig. 3.2C).

Relative to the brain remainder, cerebellum size did not differ between aerial and non-aerial species (pANCOVA, p=0.667; Fig. 3.3A), but the telencephalon was smaller in aerial than non-aerial species (-27%; pANCOVA, p<0.01; Fig. 3.3B). Relative to the telencephalon, the cerebellum was larger in aerial species (+35%; pANCOVA, p<0.01; Fig. 3.3C), likely due, at least in part, to the difference in relative telencephalon size (Fig. 3.3B).

In contrast to developmental mode, migration, and aerial behaviour, we detected no significant differences in relative cerebellum size, or telencephalon size among the five flight style categories (pANCOVA, $p>0.05$).

Path analysis

Our phylogenetic path analysis included the traits that were significant in our pANCOVAs of relative brain region sizes (see above): developmental mode (0=precocial, 1=altricial), migratory (0=non-migratory; 1=migratory) and aerial behaviour (0=non-aerial; 1=aerial). We constructed 10 models (Fig. 3.4) based on our predictor variables and the volumes of the cerebellum, telencephalon, and brain remainder. Model 10 received the strongest statistical support (Table 3.2) and is therefore the best-fitting model (Fig. 3.4). We note that this model did not include the category "aerial birds". For the models in which "aerial birds" were included (e.g., model 9), the path coefficients for aerial/non-aerial were statistically equal to zero and we therefore did not consider the inclusion of this variable in selecting the final model.

As expected, Model 10 supports direct relationships among the three brain regions (Fig. 3.4). In addition, an altricial mode of development is associated with a larger telencephalon, but a smaller cerebellum and rest of brain. However, the strongest relationships were with migration: migration is associated with a larger cerebellum and smaller telencephalon. These relationships contrasted starkly with brain remainder, which was not associated with migratory behaviour at all (Fig. 3.4).

Discussion

Overall, the size of the cerebellum relative to the brain remainder did not differ across any of our variables. In contrast, telencephalon size, relative to the brain remainder size, differed between altricial and precocial birds, and aerial and non-aerial birds. While altricial species had relatively larger telencephala than precocial species, aerial birds had relatively smaller telencephala than non-aerial birds. Both of these differences likely drove a change in cerebellum size relative to the telencephalon size in altricial and aerial birds. When partitioning species according to migration, the only significant difference detected was in the relationship between cerebellum size and telencephalon size, such that migratory species had relatively larger cerebella and smaller telencephala. As discussed below, the shift in the interrelationship cerebellum-telencephalon might reflect connectivity differences between these two brain regions, potentially enabling resident species to produce adaptive behavioural responses (e.g., food caching) against environmental challenges (e.g., low food availability). On the other hand, the smaller telencephalon relative to the cerebellum size in migratory birds may allow these species to energetically cope with the high metabolic costs associated with migration.

Altricial vs. Precocial Species

Although altricial and precocial species did not differ in cerebellum size relative to the brain remainder (Fig. 3.1A), altricial species did have larger telencephala (Fig. 3.1B) and this likely drove a difference in the relationship between the cerebellum and telencephalon (Fig. 3.1C). These findings are further corroborated in our path analysis: compared to changes in telencephalon size, cerebellum size is largely invariant between altricial and precocial species (Fig. 3.4). In fact, telencephalon size was the only brain region examined that had a direct and positive association with altriciality (Fig. 3.4).

In birds, differences in relative brain size between developmental modes appear to result from delays in postnatal neurogenesis (Striedter and Charvet 2008; Charvet and Striedter 2009a, b). While neurogenesis in precocial birds is largely complete before hatching, in altricial birds the neurogenesis continues well after hatching (Neff 1972; Striedter and Charvet 2008; Charvet and Striedter 2009b, 2011). This means that the expansion of relative brain size in altricial species (Portmann 1947; Bennett and Harvey 1985; Starck 1993; Starck and Ricklefs 1998; Iwaniuk and Nelson 2003) is mostly due to increases in the size of late-born brain regions, such as the telencephalon (Striedter and Charvet 2008; Charvet and Striedter 2009b). Accordingly, of the brain regions examined in this study, the telencephalon was the only brain region positively associated with altriciality (Fig. 3.4).

As suggested previously (Isler and Van Schaik 2009b; Charvet and Striedter 2011; Isler and van Schaik 2012), post-hatching delays in the maturation of the telencephalon may reflect the importance of processing new information and motor learning throughout the lifetime of altricial birds. Altricial hatchlings are relatively immobile, depend on their parents to feed and survive, and the prolonged neurogenesis of the telencephalon is thought to promote the evolution of specialized telencephalic circuits and with that, novel, flexible behaviours (Isler and Van Schaik 2009b; Charvet and Striedter 2011; Isler and van Schaik 2012). For example, delays in brain maturation of altricial species may have facilitated the evolution of innovative behaviours and motor skills, like tool use and vocal learning (Charvet and Striedter 2009b, 2011). Conversely, most precocial species are able to move and feed independently just after hatching and post-hatching development of the telencephalon may be less important than it is for altricial birds.

In contrast to the telencephalon, developmental mode does not drive significant changes in the relative size of the avian cerebellum (Fig. 3.1). While detailed studies comparing cerebellar neurogenesis between altricial and precocial species are still wanting, our results suggest that cerebellar neurogenesis may not vary significantly between altricial and precocial species. Most importantly, our data reveal that the relative expansion of the overall brain size in altricial birds (Portmann 1947; Bennett and Harvey 1985; Starck 1993; Starck and Ricklefs 1998; Iwaniuk and Nelson 2003) does not reflect relative increases in the sizes of all brain regions.

Flight behaviour and the cerebellum

Although the relative size of the cerebellum has been associated with aspects of flight behaviour in birds (Larsell 1948; Bennett and Harvey 1985; Iwaniuk et al. 2007; Balanoff et al. 2016) and other vertebrate classes (Stephan and Pirlot 1970; Matano and Hirasaki 1997; Rilling and Insel 1998; Macrì et al. 2019), we did not find any significant differences in relative cerebellum size among the flight maneuverability categories. In contrast, aerial species did differ from other species, but not in relative cerebellum size (Fig. 3.3A). Unexpectedly, aerial species tend to have smaller telencephalon relative to both the cerebellum and brain remainder sizes (Figs. 3.3B,C). It is difficult to interpret this result because the aerial/non-aerial variable was not included in the best-fitting model from our path analysis (Fig. 3.4). This might reflect an insufficiently strong effect size compared with the other variables and/or a relatively small sample size of aerial birds ($n = 13$). Regardless of the lack of inclusion in the path analysis, we propose that the difference detected in our ANCOVA likely arises from energetics. Many aerial species feed while flying, which could translate into greater energy expenditure on a daily basis compared to non-aerial birds. For example, to feed on a floral nectar while hovering, a hummingbird expends a large amount of energy (Powers and Nagy 1988; Suarez 1992). Swifts and swallows also execute most of their daily activities in mid-air (Lack 1951; Turner 2006;

Hedenström et al. 2016), and some of these species can even remain airborne for 10 months (Hedenström et al. 2016). Similarly, some seabirds can forage thousands of kilometers from their colonies, flying up to 11 hours continuously while foraging (Weimerskirch et al. 1997). Given the potential imbalance between flight costs and energy input, aerial birds may not have sufficient energy to grow and maintain a relatively larger telencephalon. This explanation is highly speculative, but could be tested through focused comparisons of energetic expenditure and quantitative measurements of the brain (i.e., neuron sizes and numbers within brain regions) between aerial and non-aerial species.

One issue that plagues comparisons of locomotion or motor skill among bird species is that coding locomotion or motor skill is likely an oversimplification and often based on assumptions (Iwaniuk and Whishaw 1999). For example, discretely categorizing flight maneuverability likely overlooks fine differences in motor skill and/or coordination across species. Soaring flight, may appear to be simple, but species that soar need to constantly detect wind speeds, air currents, and execute subtle changes in the position of the alula (Alvarez et al. 2001; Lee et al. 2015). Categorizing locomotion (e.g., flight performance) at a finer level is, however, problematic, and dependent on data that is unavailable in birds. In this study, we divided our large sample of birds based on available data on the wing loading and aspect ratios (Norberg 1990). Although these measurements might not reflect precise aspects of flight performance, they do describe flight efficiency and maneuverability among birds (Norberg and Rayner 1987; Norberg 1990). Thus, it is surprising that maneuverable fliers, which are expected to perform complex motor coordination, did not have relatively larger cerebella than other birds.

The lack of association between relative cerebellar size and flight maneuverability does not, however, negate the possibility that there are other differences in cerebellar anatomy that reflect species variation in flight performance. The cerebellum is highly compartmentalized in relation to connectivity and function (Oscarsson 1979; Witter and De Zeeuw 2015; Apps et al. 2018; Wylie et al. 2018), and differences in cerebellar anatomy according to motor skills could be confined to specific regions of the cerebellum. For example, based on immediate early gene expression, folium VI is activated during flight (Feenders et al. 2008) and folia VI-VIII receive visual information from the pretectum (Pakan and Wylie 2006) thought to be important for steering and other visually guided components of flight in birds (Wylie et al. 2018). These data, combined with the fact that folium VI is also enlarged in 'strong flier' birds (Iwaniuk et al. 2007), implicates folium VI specifically as important to flight. In this study, we were not able to collect folium specific data, but once measurements become available, we would be able to examine whether the size of each cerebellar folium covaries with flight maneuverability.

Migratory birds: a trade-off between the cerebellum and telencephalon

Here, we did not find any correlations between cerebellum size, relative to the brain remainder size, and migratory behaviour (Fig. 3.2A). Likewise, Vincze et al. (2015) did not find significant differences in the size of the cerebellum relative to body size according to migration distance. However, our larger sample size, together with the use of path analysis to investigate interactions between the sizes of the cerebellum and other brain regions, indicates a shift in the relationship between the cerebellum and telencephalon sizes as a function of migration. Migratory birds have larger cerebella relative to the telencephalon size than resident birds (Fig. 3.2C). Further, our path analysis confirms that migratory behaviour is correlated with the sizes of the cerebellum and telencephalon in opposite directions (Fig. 3.4).

While changes in cerebellar anatomy, including size, are often correlated with changes in the telencephalon (Whiting and Barton 2003; Iwaniuk et al. 2004; Herculano-Houzel 2010; Yopak et al. 2010; Smaers and Soligo 2013), divergences in this relationship occur in some clades (Barton and Venditti 2014; Gutiérrez-Ibáñez et al. 2018; Smaers and Vanier 2019) and appear to explain the evolution of certain aspects of cognition, such as the ability to learn complex motor skills and sensorimotor coordination (Barton and Venditti 2014; Gutiérrez-Ibáñez et al. 2018). In birds, parrots and songbirds increase the number of pallial neurons at a faster rate relative to cerebellar neurons than other birds (Olkowicz et al. 2016; Gutiérrez-Ibáñez et al. 2018). In parrots, this difference appears to correlate with increased connectivity between the telencephalon and cerebellum and is thought to at least partially explain the evolution of their cognitive abilities (e.g., tool use; Gutiérrez-Ibáñez et al., 2018). Likewise, the observed shift in the relationship between the sizes of the cerebellum and telencephalon as a function of migration might also indicate cognitive differences between migrants and residents (Sol et al. 2007; Sol 2009).

Birds that remain resident year-round typically experience more environmental variability (e.g., food availability) than migrants, which avoid harsh environmental conditions by moving to other places. The cognitive buffer hypothesis proposes that the evolution of larger brains facilitates behavioural responses to vagaries of the environment (Allman et al. 1993; Sol 2009). Indeed, birds inhabiting more variable environments tend to have relatively larger brains (Schuck-Paim et al. 2008; Sol et al. 2010; Sayol et al. 2016; Vincze 2016). The shift in the telencephalon-cerebellum relationship between migrants and residents (Fig. 3.2C) provides further support to the cognitive buffer hypothesis (Sol 2009; Sol et al. 2010; Sayol et al. 2016). As mentioned above, changes in the relationship telencephalon-cerebellum are suggested to reflect differences in connectivity and cognition across species (Barton and Venditti 2014; Gutiérrez-Ibáñez et al. 2018). Additionally, birds that have larger telencephala tend to perform more innovative and flexible behaviour, allowing them to respond more rapidly to changes in the environment (Lefebvre et al. 1997; Rosza et al. 1998; Sol and Lefebvre 2000). The larger telencephalon relative to the size of the cerebellum in resident birds might indicate increased connectivity between these two brain regions when compared to migratory birds. A stronger connection between the telencephalon and cerebellum could be important for the evolution of innovative behaviours. This could be further tested by comparing the brain anatomy and behaviour of species in which some individuals are migratory, and others are resident (e.g., dark-eyed junco, *Junco hyemalis*; Rabenold and Rabenold, 1985; Cristol et al., 2003).

An alternative explanation for the difference in the telencephalon-cerebellum relationship between migrants and residents is that it could also reflect energetics. Migration is highly energetic demanding (Ramenofsky 1990). This is reflected by several adaptations in migratory birds, such as dramatic increases in muscle mass and energetic storage in the form of lipids (Berthold 1975; Blem 1990; Weber 2009) often at the expense of other organs (Piersma and Lindström 1997; Piersma and Gill Jr 1998; Mathot et al. 2019). For example, prior to migration, birds may experience a reduction in the sizes of their digestive tract (e.g., gizzards), but at the same time a gain in muscle mass (Jehl Jr 1997; Piersma and Lindström 1997). Further, the metabolic costs of the pallium, which represents a large fraction of the telencephalon, are thought to be significantly higher than the costs of the cerebellum (Karbowski 2007; Herculano-Houzel 2011). As a result of the energetic expenses incurred by migration, the maintenance of a larger telencephalon relative to the cerebellum may not be energetically feasible in migratory birds. An evolutionary change in the relationship cerebellum-telencephalon sizes therefore might confer both adaptive cognitive skills (e.g., food caching) to resident birds, as well as reduction in the metabolic costs of the brain in migratory birds.

Conclusions

Overall, locomotion (flight manoeuverability or being aerial) does not appear to covary with the relative size of the cerebellum in birds. Despite this lack of association between flight and cerebellum size, migratory behaviour exerts a significant effect on the relationship between cerebellum and telencephalon size. We propose that this telencephalon-cerebellum shift between migrant and resident birds supports both the cognitive buffer hypothesis and energetic brain hypothesis (Isler and van Schaik 2009; Sol 2009). To what extent, however, these volumetric differences reflect other changes in the brain anatomy is still uncertain. For example, resident birds may have higher telencephalic neuronal densities but lower cerebellar neuronal densities when compared with migratory birds. A potential new avenue of research therefore is to explore the energetic and cognitive buffer hypotheses by comparing the anatomy of brain regions in migrants and residents at a finer level.

References

Allman, J., T. McLaughlin, and A. Hakeem. 1993. Brain weight and life-span in primate species. Proceedings of the National Academy of Sciences 90:118-122.

Alma, S. and N. Bee-de-Speroni. 1992. índices cerebrales y composición cuantitativa encefálica en *Athene cunicularia* y *Tyto alba* (Strigiformes: Strigidae y Tytonidae). Facena 9:19-37.

Alvarez, J., J. Meseguer, E. Meseguer, and A. Pérez. 2001. On the role of the alula in the steady flight of birds. Ardeola 48:161-173.

Apps, R., R. Hawkes, S. Aoki, F. Bengtsson, A. M. Brown, G. Chen, T. J. Ebner, P. Isope, H. Jörntell, and E. P. Lackey. 2018. Cerebellar modules and their role as operational cerebellar processing units. The Cerebellum 17:654-682.

Balanoff, A. M., J. B. Smaers, and A. H. Turner. 2016. Brain modularity across the theropod–bird transition: testing the influence of flight on neuroanatomical variation. Journal of Anatomy 229:204-214.

Barton, R., A. Purvis, and P. Harvey. 1995. Evolutionary radiation of visual and olfactory brain systems in primates, bats and insectivores. Philosophical Transactions of the Royal Society of London. Series B: Biological Sciences 348:381-392.

Barton, R. A. 2012. Embodied cognitive evolution and the cerebellum. Philosophical Transactions of the Royal Society B: Biological Sciences 367:2097-2107.

Barton, R. A. and P. H. Harvey. 2000. Mosaic evolution of brain structure in mammals. Nature 405:1055-1058.

Barton, R. A. and C. Venditti. 2014. Rapid evolution of the cerebellum in humans and other great apes. Current Biology 24:2440-2444.

Bearhop, S., W. Fiedler, R. W. Furness, S. C. Votier, S. Waldron, J. Newton, G. J. Bowen, P. Berthold, and K. Farnsworth. 2005. Assortative mating as a mechanism for rapid evolution of a migratory divide. Science 310:502-504.

Bennett, P. M. and P. H. Harvey. 1985. Brain size, development and metabolism in birds and mammals. Journal of Zoology 207:491-509.

Benson-Amram, S., B. Dantzer, G. Stricker, E. M. Swanson, and K. E. Holekamp. 2016. Brain size predicts problem-solving ability in mammalian carnivores. Proceedings of the National Academy of Sciences 113:2532-2537.

Berthold, P. 1975. Migration: Control and Metabolic Physiology. Avian Biology. 5:77-128.

Blem, C. 1990. Avian energy storage. Current Ornithology 7:59-113.

Boire, D. and G. Baron. 1994. Allometric comparison of brain and main brain subdivisions in birds. Journal of Brain Research 35:49-66.

Burnham KP, Anderson DR (2002) Model selection and multimodel inference. A practical information-theoretic approach, 2nd edn. Springer, New York.

Carezzano, F. and N. Bee-de-Speroni. 1995. Composición volumétrica encefálica e índices cerebrales en tres aves de ambiente acuático (Ardeidae, Podicipedide, Rallidae). Facena 11:75-83.

Charvet, C. J. and G. F. Striedter. 2009a. Developmental basis for telencephalon expansion in waterfowl: enlargement prior to neurogenesis. Proceedings of the Royal Society B: Biological Sciences 276:3421-3427.

Charvet, C. J. and G. F. Striedter. 2009b. Developmental origins of mosaic brain evolution: morphometric analysis of the developing zebra finch brain. Journal of Comparative Neurology 514:203-213.

Charvet, C. J. and G. F. Striedter. 2011. Developmental modes and developmental mechanisms can channel brain evolution. Frontiers in Neuroanatomy 5:4.

Clarke, D. D. and L. Sokoloff. 1999. Circulation and energy metabolism of the brain. Basic neurochemistry: Molecular, Cellular, and Medical Aspects (Siegel GJ, Agranoff BW, Albers RW, Fisher SK, Uhler MD, editors). (6th ed.). Philadelphia: Lippncott-Raven, p. 637– 669.

Cole, B. J. 1985. Size and behavior in ants: constraints on complexity. Proceedings of the National Academy of Sciences 82:8548-8551.

Corfield, J. R., H. L. Eisthen, A. N. Iwaniuk, and S. Parsons. 2014. Anatomical specializations for enhanced olfactory sensitivity in kiwi, *Apteryx mantelli*. Brain, Behavior and Evolution 84:214-226.

Corfield, J. R., A. C. Gsell, D. Brunton, C. P. Heesy, M. I. Hall, M. L. Acosta, and A. N. Iwaniuk. 2011. Anatomical specializations for nocturnality in a critically endangered parrot, the kakapo (*Strigops habroptilus*). PLoS One 6:e22945.

Corfield, J. R., K. Price, A. N. Iwaniuk, C. Gutiérrez-Ibáñez, T. Birkhead, and D. R. Wylie. 2015. Diversity in olfactory bulb size in birds reflects allometry, ecology, and phylogeny. Frontiers in Neuroanatomy 9:102.

Corfield, J. R., J. M. Wild, S. Parsons, and M. F. Kubke. 2012. Morphometric analysis of telencephalic structure in a variety of neognath and paleognath bird species reveals regional differences associated with specific behavioral traits. Brain, Behavior and Evolution 80:181-195.

Cristol, D. A., E. B. Reynolds, J. E. Leclerc, A. H. Donner, C. S. Farabaugh, and C. W. Ziegenfus. 2003. Migratory dark-eyed juncos, *Junco hyemalis*, have better spatial memory and denser hippocampal neurons than nonmigratory conspecifics. Animal Behaviour 66:317-328.

Cunha, F., K. Racicot, J. Nahirney, C. Heuston, D. R. Wylie, and A. N. Iwaniuk. 2020. Allometric scaling rules of the cerebellum in galliform birds. Brain, Behavior and Evolution 95:78-92.

Cunningham, S. J., J. R. Corfield, A. N. Iwaniuk, I. Castro, M. R. Alley, T. R. Birkhead, and S. Parsons. 2013. The anatomy of the bill tip of kiwi and associated somatosensory regions of the brain: comparisons with shorebirds. PLoS One 8:e80036.

Day, L. B., D. A. Westcott, and D. H. Olster. 2005. Evolution of bower complexity and cerebellum size in bowerbirds. Brain, Behavior and Evolution 66:62-72.

DeVoogd, T. J., J. R. Krebs, S. D. Healy, and A. Purvis. 1993. Relations between song repertoire size and the volume of brain nuclei related to song: comparative evolutionary analyses amongst oscine birds. Proceedings of the Royal Society of London. Series B: Biological Sciences 254:75-82.

Dufour, P., S. Descamps, S. Chantepie, J. Renaud, M. Guéguen, K. Schiffers, W. Thuiller, and S. Lavergne. 2020. Reconstructing the geographic and climatic origins of long-distance bird migrations. Journal of Biogeography 47:155-166.

Dunbar, R. I. 1998. The social brain hypothesis. Evolutionary Anthropology: Issues, News, and Reviews: Issues, News, and Reviews 6:178-190.

Dunbar, R. I. 2009. The social brain hypothesis and its implications for social evolution. Annals of Human Biology 36:562-572.

Ebinger, P. 1995. Domestication and plasticity of brain organization in mallards (*Anas platyrhynchos*). Brain, Behavior and Evolution 45:286-300.

Ericson, P. G., C. L. Anderson, T. Britton, A. Elzanowski, U. S. Johansson, M. Källersjö, J. I. Ohlson, T. J. Parsons, D. Zuccon, and G. Mayr. 2006. Diversification of Neoaves: integration of molecular sequence data and fossils. Biology Letters 2:543-547.

Feenders, G., M. Liedvogel, M. Rivas, M. Zapka, H. Horita, E. Hara, K. Wada, H. Mouritsen, and E. D. Jarvis. 2008. Molecular mapping of movement-associated areas in the avian brain: a motor theory for vocal learning origin. PLoS One 3:e1768.

Fernandez, P., F. Carezzano, and N. Bee-De-Speroni. 1997. Análisis cuantitativo encefálico e índices cerebrales en *Aratinga acuticaudata* y *Myiopsitta monachus* de Argentina (Aves: Psittacidae). Revista Chilena de Historia Natural 70:269-275.

Finlay, B. L. and R. B. Darlington. 1995. Linked regularities in the development and evolution of mammalian brains. Science 268:1578-1584.

Gonzalez-Voyer, A. and A. von Hardenberg. 2014. An introduction to phylogenetic path analysis. Pp. 201-229. Modern Phylogenetic Comparative Methods and Their Application in Evolutionary Biology. Springer, London.

Grigg, N. P., J. M. Krilow, C. Gutierrez-Ibanez, D. R. Wylie, G. R. Graves, and A. N. Iwaniuk. 2017. Anatomical evidence for scent guided foraging in the turkey vulture. Scientific Reports 7:1-10.

Gutiérrez-Ibáñez, C., A. N. Iwaniuk, B. A. Moore, E. Fernández-Juricic, J. R. Corfield, J. M. Krilow, J. Kolominsky, and D. R. Wylie. 2014. Mosaic and concerted evolution in the visual system of birds. PLoS One 9:e90102.

Gutiérrez-Ibáñez, C., A. N. Iwaniuk, and D. R. Wylie. 2018. Parrots have evolved a primate-like telencephalic-midbrain-cerebellar circuit. Scientific Reports 8:1-11.

Healy, S. D. and C. Rowe. 2007. A critique of comparative studies of brain size. Proceedings of the Royal Society B: Biological Sciences 274:453-464.

Hedenström, A., G. Norevik, K. Warfvinge, A. Andersson, J. Bäckman, and S. Åkesson. 2016. Annual 10-month aerial life phase in the common swift *Apus apus*. Current Biology 26:3066-3070.

Herculano-Houzel, S. 2010. Coordinated scaling of cortical and cerebellar numbers of neurons. Frontiers in Neuroanatomy 4:12.

Herculano-Houzel, S. 2011. Scaling of brain metabolism with a fixed energy budget per neuron: implications for neuronal activity, plasticity and evolution. PloS One 6:e17514.

Herculano-Houzel, S., P. R. Manger, and J. H. Kaas. 2014. Brain scaling in mammalian evolution as a consequence of concerted and mosaic changes in numbers of neurons and average neuronal cell size. Frontiers in Neuroanatomy 8:77.

Isler, K. and C. P. van Schaik. 2009a. The expensive brain: a framework for explaining evolutionary changes in brain size. Journal of Human Evolution 57:392-400.

Isler, K. and C. P. Van Schaik. 2009b. Why are there so few smart mammals (but so many smart birds)? Biology Letters 5:125-129.

Isler, K. and C. P. van Schaik. 2012. Allomaternal care, life history and brain size evolution in mammals. Journal of Human Evolution 63:52-63.

Ito, M. 1984. The cerebellum and neural control. Raven Press, New York.

Iwaniuk, A. N., K. M. Dean, and J. E. Nelson. 2004. A mosaic pattern characterizes the evolution of the avian brain. Proceedings of the Royal Society of London. Series B: Biological Sciences 271:S148-S151.

Iwaniuk, A. N., C. Gutierrez-Ibanez, J. M. Pakan, and D. R. Wylie. 2010. Allometric scaling of the tectofugal pathway in birds. Brain, Behavior and Evolution 75:122-137.

Iwaniuk, A. N., C. P. Heesy, M. I. Hall, and D. R. Wylie. 2008. Relative Wulst volume is correlated with orbit orientation and binocular visual field in birds. Journal of Comparative Physiology A 194:267-282.

Iwaniuk, A. N., P. L. Hurd, and D. R. Wylie. 2007. Comparative morphology of the avian cerebellum: II. Size of folia. Brain, Behavior and Evolution 69:196-219.

Iwaniuk, A. N. and J. E. Nelson. 2001. A comparative analysis of relative brain size in waterfowl (Anseriformes). Brain, Behavior and Evolution 57:87-97.

Iwaniuk, A. N. and J. E. Nelson. 2002. Can endocranial volume be used as an estimate of brain size in birds? Canadian Journal of Zoology 80:16-23.

Iwaniuk, A. N. and J. E. Nelson. 2003. Developmental differences are correlated with relative brain size in birds: a comparative analysis. Canadian Journal of Zoology 81:1913-1928.

Iwaniuk AN, and I. Q. Whishaw. 1999. How skilled are the skilled limb movements of the raccoon (*Procyon lotor*)? Behavioural brain research. 99:35-44.

Iwaniuk, A. N. and D. R. Wylie. 2006. The evolution of stereopsis and the Wulst in caprimulgiform birds: a comparative analysis. Journal of Comparative Physiology A 192:1313-1326.

Jehl Jr, J. R. 1997. Cyclical changes in body composition in the annual cycle and migration of the eared grebe *Podiceps nigricollis*. Journal of Avian Biology:132-142.

Jetz, W., G. H. Thomas, J. B. Joy, K. Hartmann, and A. O. Mooers. 2012. The global diversity of birds in space and time. Nature 491:444-448.

Jiménez-Ortega, D., N. Kolm, S. Immler, A. A. Maklakov, and A. Gonzalez-Voyer. 2020. Long life evolves in large-brained bird lineages. Evolution 74:2617-2628.

Kalisińska, E. 2005. Anseriform brain and its parts versus taxonomic and ecological categories. Brain, Behavior and Evolution 65:244-261.

Karbowski, J. 2007. Global and regional brain metabolic scaling and its functional consequences. BMC Biology 5:1-11.

Kotrschal, A., B. Rogell, A. Bundsen, B. Svensson, S. Zajitschek, I. Brännström, S. Immler, A. A. Maklakov, and N. Kolm. 2013. The benefit of evolving a larger brain: big-brained guppies perform better in a cognitive task. Animal Behaviour 86:e4.

Krebs, J. R. 1990. Food-storing birds: adaptive specialization in brain and behaviour? Philosophical Transactions of the Royal Society of London. Series B: Biological Sciences 329:153-160.

Lack, E. 1951. The breeding biology of the swift *Apus apus*. Ibis 93:501-546.

Larsell, O. 1948. The development and subdivisions of the cerebellum of birds. Journal of Comparative Neurology 89:123-189.

Larsell, O. and J. Jansen. 1967. The comparative anatomy and histology of the cerebellum, vol. 1: from myxinoids through birds. Minneapolis: University of Minnesota Press.

Lee, S., J. Kim, H. Park, P. G. Jabłoński, and H. Choi. 2015. The function of the alula in avian flight. Scientific Reports 5:1-5.

Lefebvre, L., P. Whittle, E. Lascaris, and A. Finkelstein. 1997. Feeding innovations and forebrain size in birds. Animal Behaviour 53:549-560.

Leigh, S. R. 2004. Brain growth, life history, and cognition in primate and human evolution. American Journal of Primatology 62:139-164.

Luo, Y., M. J. Zhong, Y. Huang, F. Li, W. B. Liao, and A. Kotrschal. 2017. Seasonality and brain size are negatively associated in frogs: evidence for the expensive brain framework. Scientific Reports 7:1-9.

Maclean, I. M., G. E. Austin, M. M. Rehfisch, J. Blew, O. Crowe, S. Delany, K. Devos, B. Deceuninck, K. Guenther, and K. Laursen. 2008. Climate change causes rapid changes in the distribution and site abundance of birds in winter. Global Change Biology 14:2489-2500.

Macrì, S., Y. Savriama, I. Khan, and N. Di-Poï. 2019. Comparative analysis of squamate brains unveils multi-level variation in cerebellar architecture associated with locomotor specialization. Nature Communications 10:1-16.

Matano, S. and E. Hirasaki. 1997. Volumetric comparisons in the cerebellar complex of anthropoids, with special reference to locomotor types. American Journal of Physical Anthropology 103:173-183.

Mathot, K. J., E. M. Kok, J. B. Burant, A. Dekinga, P. Manche, D. Saintonge, and T. Piersma. 2019. Evolutionary design of a flexible, seasonally migratory, avian phenotype: why trade gizzard mass against pectoral muscle mass? Proceedings of the Royal Society B 286:20190518.

McGuire, L. P. and J. M. Ratcliffe. 2011. Light enough to travel: migratory bats have smaller brains, but not larger hippocampi, than sedentary species. Biology Letters 7:233-236.

Mehlhorn, J., G. R. Hunt, R. D. Gray, G. Rehkämper, and O. Güntürkün. 2010. Tool-making New Caledonian crows have large associative brain areas. Brain, Behavior and Evolution 75:63-70.

Montgomery, J. C., D. Bodznick, and K. E. Yopak. 2012. The cerebellum and cerebellum-like structures of cartilaginous fishes. Brain, Behavior and Evolution 80:152-165.

Navarrete, A., C. P. van Schaik, and K. Isler. 2011. Energetics and the evolution of human brain size. Nature 480:91-93.

Nealen, P. M. and R. E. Ricklefs. 2001. Early diversification of the avian brain: body relationship. Journal of Zoology 253:391-404.

Neff, M. 1972. Untersuchungen über das embryonale und post-embryonale organwachstum bei vogelarten mit verschiedenem ontogenesemodus: mit 25 Tabellen. Kundig.

Nice, M. M. 1962. Development of behavior in precocial birds. New York:[Linnaean Society].

Norberg, U. M. 1990. Vertebrate flight: mechanics, physiology, morphology, ecology and evolution. Springer Science & Business Media, Berlin.

Norberg, U. M. and J. M. Rayner. 1987. Ecological morphology and flight in bats (Mammalia; Chiroptera): wing adaptations, flight performance, foraging strategy and echolocation. Philosophical Transactions of the Royal Society of London. B, Biological Sciences 316:335-427.

Olkowicz, S., M. Kocourek, R. K. Lučan, M. Porteš, W. T. Fitch, S. Herculano-Houzel, and P. Němec. 2016. Birds have primate-like numbers of neurons in the forebrain. Proceedings of the National Academy of Sciences 113:7255-7260.

Orme, D., R. Freckleton, G. Thomas, T. Petzoldt, S. Fritz, N. Isaac, and W. Pearse. 2013. The caper package: comparative analysis of phylogenetics and evolution in R. R Package Version 5:1-36.

Oscarsson, O. 1979. Functional units of the cerebellum-sagittal zones and microzones. Trends in Neurosciences 2:143-145.

Pagel, M. 1999. The maximum likelihood approach to reconstructing ancestral character states of discrete characters on phylogenies. Systematic Biology 48:612-622.

Pakan, J. M. and D. R. Wylie. 2006. Two optic flow pathways from the pretectal nucleus lentiformis mesencephali to the cerebellum in pigeons (*Columba livia*). Journal of Comparative Neurology 499:732-744.

Piersma, T. and R. E. Gill Jr. 1998. Guts don't fly: small digestive organs in obese bar-tailed godwits. The Auk 115:196-203.

Piersma, T. and Å. Lindström. 1997. Rapid reversible changes in organ size as a component of adaptive behaviour. Trends in Ecology & Evolution 12:134-138.

Pinheiro, J., D. Bates, S. DebRoy, D. Sarkar, and R. C. Team. 2006. Nlme: Linear and nonlinear mixed effects models. R Package Version 3:109.

Pistone, E., F. Carezzano, and N. Bee-De-Speroni. 2002. Tamano relativo encefalico e indices cerebrales en *Vanellus chilensis* (Aves: Charadriidae). Revista Chilena de Historia Natural 75:595-602.

Portmann, A. 1947. Etudes sur la cérébralisation des oiseaux. II. Les indices intra-cérébraux. Alauda 15:1-15.

Powers, D. R. and K. A. Nagy. 1988. Field metabolic rate and food consumption by free-living Anna's hummingbirds (*Calypte anna*). Physiological Zoology 61:500-506.

Pravosudov, V. V., K. Sanford, and T. P. Hahn. 2007. On the evolution of brain size in relation to migratory behaviour in birds. Animal Behaviour 73:535-539.

Rabenold, K. N. and P. P. Rabenold. 1985. Variation in altitudinal migration, winter segregation, and site tenacity in two subspecies of dark-eyed juncos in the southern Appalachians. The Auk 102:805-819.

Raichle, M. E. and D. A. Gusnard. 2002. Appraising the brain's energy budget. Proceedings of the National Academy of Sciences 99:10237-10239.

Ramenofsky, M. 1990. Fat storage and fat metabolism in relation to migration. Pp. 214-231. In Gwinner E (ed.): Bird Migration. Springer, Berlin

Ramnani, N. 2006. The primate cortico-cerebellar system: anatomy and function. Nature Reviews Neuroscience 7:511-522.

Rehkämper, G., H. D. Frahm, and K. Zilles. 1991. Quantitative development of brain and brain structures in birds (Galliformes and Passeriformes) compared to that in mammals (Insectivores and Primates)(Part 1 of 2). Brain, Behavior and Evolution 37:125-134.

Rilling, J. K. and T. R. Insel. 1998. Evolution of the cerebellum in primates: differences in relative volume among monkeys, apes and humans. Brain, Behavior and Evolution 52:308-314.

Rosza, L., A. Gaxiola, L. Lefebvre, S. Timmermans, S. Dawson, and P. Kabai. 1998. Feeding innovations and forebrain size in Australasian birds. Behaviour 135:1077-1097.

Roth, G. and U. Dicke. 2012. Evolution of the brain and intelligence in primates. Progress in Brain Research 195:413-430.

Safi, K. and D. K. Dechmann. 2005. Adaptation of brain regions to habitat complexity: a comparative analysis in bats (Chiroptera). Proceedings of the Royal Society B: Biological Sciences 272:179-186.

Sayol, F., J. Maspons, O. Lapiedra, A. N. Iwaniuk, T. Székely, and D. Sol. 2016. Environmental variation and the evolution of large brains in birds. Nature Communications 7:1-8.

Schliep, K. P. 2011. phangorn: phylogenetic analysis in R. Bioinformatics 27:592-593.

Schuck-Paim, C., W. J. Alonso, and E. B. Ottoni. 2008. Cognition in an ever-changing world: climatic variability is associated with brain size in neotropical parrots. Brain, Behavior and Evolution 71:200-215.

Smaers, J. and C. Soligo. 2013. Brain reorganization, not relative brain size, primarily characterizes anthropoid brain evolution. Proceedings of the Royal Society B: Biological Sciences 280:20130269.

Smaers, J. B. and D. R. Vanier. 2019. Brain size expansion in primates and humans is explained by a selective modular expansion of the cortico-cerebellar system. Cortex 118:292-305.

Sol, D. 2009. Revisiting the cognitive buffer hypothesis for the evolution of large brains. Biology Letters 5:130-133.

Sol, D., N. Garcia, A. Iwaniuk, K. Davis, A. Meade, W. A. Boyle, and T. Székely. 2010. Evolutionary divergence in brain size between migratory and resident birds. PLoS One 5:e9617.

Sol, D. and L. Lefebvre. 2000. Behavioural flexibility predicts invasion success in birds introduced to New Zealand. Oikos 90:599-605.

Sol, D., T. Székely, A. Liker, and L. Lefebvre. 2007. Big-brained birds survive better in nature. Proceedings of the Royal Society B: Biological Sciences 274:763-769.

Starck, J. 1993. Evolution of avian ontogenies. Pp. 275-366. Current Ornithology 10:277-366.

Starck, J. M. and R. E. Ricklefs. 1998. Avian growth and development: evolution within the altricial-precocial spectrum. Oxford University Press, New York.

Stephan, H. and P. Pirlot. 1970. Volumetric comparisons of brain structures in bats. Zeitschrift für zoologische Systematik und Evolutionsforschung 8:200-236.

Striedter, G. F. and C. J. Charvet. 2008. Developmental origins of species differences in telencephalon and tectum size: morphometric comparisons between a parakeet (*Melopsittacus undulatus*) and a quail (*Colinus virgianus*). Journal of Comparative Neurology 507:1663-1675.

Suarez, R. 1992. Hummingbird flight: sustaining the highest mass-specific metabolic rates among vertebrates. Experientia 48:565-570.

Team, R. C. 2020. R: A language and environment for statistical computing.

Turner, A. 2006. The barn swallow. Poyser, London.

van der Bijl, W. 2018. phylopath: Easy phylogenetic path analysis in R. PeerJ 6:e4718.

van Woerden, J. T., E. P. Willems, C. P. van Schaik, and K. Isler. 2012. Large brains buffer energetic effects of seasonal habitats in catarrhine primates. Evolution 66:191-199.

Vincze, O. 2016. Light enough to travel or wise enough to stay? Brain size evolution and migratory behavior in birds. Evolution 70:2123-2133.

Vincze, O., C. I. Vágási, P. L. Pap, G. Osváth, and A. P. Møller. 2015. Brain regions associated with visual cues are important for bird migration. Biology Letters 11:20150678.

von Hardenberg, A. and A. Gonzalez-Voyer. 2013. Disentangling evolutionary cause-effect relationships with phylogenetic confirmatory path analysis. Evolution 67:378-387.

Walsh, S. A., A. N. Iwaniuk, M. A. Knoll, E. Bourdon, P. M. Barrett, A. C. Milner, R. L. Nudds, R. L. Abel, and P. D. Sterpaio. 2013. Avian cerebellar floccular fossa size is not a proxy for flying ability in birds. PLoS One 8:e67176.

Weber, J.-M. 2009. The physiology of long-distance migration: extending the limits of endurance metabolism. Journal of Experimental Biology 212:593-597.

Weimerskirch, H., R. P. Wilson, and P. Lys. 1997. Activity pattern of foraging in the wandering albatross: a marine predator with two modes of prey searching. Marine Ecology Progress Series 151:245-254.

Whiting, B. and R. Barton. 2003. The evolution of the cortico-cerebellar complex in primates: anatomical connections predict patterns of correlated evolution. Journal of Human Evolution 44:3-10.

Witter, L. and C. I. De Zeeuw. 2015. Regional functionality of the cerebellum. Current Opinion in Neurobiology 33:150-155.

Wylie, D. R., C. Gutiérrez-Ibáñez, A. H. Gaede, D. L. Altshuler, and A. N. Iwaniuk. 2018. Visual-cerebellar pathways and their roles in the control of avian flight. Frontiers in Neuroscience 12:223.

Wylie, D. R., C. Gutiérrez-Ibáñez, and A. Iwaniuk. 2015. Integrating brain, behavior, and phylogeny to understand the evolution of sensory systems in birds. Frontiers in Neuroscience 9:281.

Yopak, K. E., T. J. Lisney, S. P. Collin, and J. C. Montgomery. 2007. Variation in brain organization and cerebellar foliation in chondrichthyans: sharks and holocephalans. Brain, Behavior and Evolution 69:280-300.

Yopak, K. E., T. J. Lisney, R. B. Darlington, S. P. Collin, J. C. Montgomery, and B. L. Finlay. 2010. A conserved pattern of brain scaling from sharks to primates. Proceedings of the National Academy of Sciences 107:12946-12951.

Yopak, K. E., J. Pakan, and D. Wylie. 2017. The cerebellum of nonmammalian vertebrates. In Kaas JH (ed): Evolution of Nervous Systems, 2nd ed. Oxford, Academic Press, pp. 373-386.

Table 3.1. Details of the allometric relationships between brain region sizes. Brain remainder corresponds to total brain size minus the volumes of the telencephalon and cerebellum. λ = Pagel's lambda; p = p-value; r^2 = coefficient of determination.

x-axis	y-axis	Intercept	F ratio	λ	p	r^2	slope	slope CI (± 95%)
Telencephalon size	cerebellum size	-0.117	1914	0.795	<0.01	0.869	0.835	0.816, 0.854
Brain remainder	cerebellum size	0.030	644	0.456	<0.01	0.691	0.879	0.844, 0.914
	telencephalon size	0.597	437	0.683	<0.01	0.602	0.916	0.872, 0.960

Table 3.2. Model comparison for our hypothesized causal relationships (see Fig. 3.4). We report: K, number of independence claims; q, number of parameters; C, Fisher's C statistics; p-values; CICc, C statistic information criterion corrected for small sample sizes; ΔCICc, difference in CICc from the best-fitting model; w, CICc weights.

Model	**K**	**q**	**C**	**p**	**CICc**	**ΔCICc**	**w**
1	8	13	40.6	<0.001	67.9	34.0	<0.01
2	7	14	14.8	0.391	44.3	10.5	**<0.01**
3	7	14	40.6	<0.001	70.1	36.2	<0.01
4	6	15	14.8	0.252	46.6	12.7	**<0.01**
5	8	13	34.1	0.005	61.4	27.6	<0.01
6	7	14	13.5	0.486	43.0	9.2	**0.01**
7	8	13	34.1	0.005	61.4	27.6	<0.01
8	7	14	13.5	0.486	43.0	9.2	**0.01**
9	6	15	4.3	0.977	36.1	2.2	**0.243**
10	7	14	4.3	0.993	33.9	0.0	**0.737**

Table 3.3. A list of the bird species analyzed and their respective orders, brain volumes (=brvol), telencephalon volumes (=telenvol), cerebellum volumes (=cbvol), and remaining brain structures volumes (=RBrvol), and sources from which data were extracted. Order abbreviations: Acc=Accipitriformes; Ans=Anseriformes; Apod=Apodiformes; Apt=Apterygiformes; Buce= Bucerotiformes; Capr=Caprimulgiformes; Casua=Casuariiformes; Cath=Cathartiformes; Cico=Ciconiiformes; Colum=Columbiformes; Cora=Coraciiformes; Cucu=Cuculiformes; Fal=Falconiformes; Galli=Galliformes; Gavi=Gaviiformes; Grui=Gruiformes; Otidi=Otidiformes; Passe=Passeriformes; Pelec=Pelecaniformes; Phoe=Phoenicopteriformes; Pici=Piciformes; Podic= Podicipediformes; Proce=Procellariiformes; Psi=Psittaciformes; Rhei=Rheiformes; Sphen=Sphenisciformes; Stri=Strigiformes; Strut=Struthioniformes; Suli=Suliformes; Tin=Tinamiformes.

Species	Common name	Order	brvol	telenvol	cbvol	RBrvol	Source
Accipiter cirrocephalus	Collared sparrowhawk	Acc	4,875	2,217	749	1,909	This study
Accipiter fasciatus	Brown goshawk	Acc	5,010	2,713	768	1,528	Iwaniuk et al., 2004
Accipiter gentilis	Northern goshawk	Acc	7,407	4,456	1050	1,900	Portmann, 1947
Accipiter nisus	Eurasian sparrowhawk	Acc	2,974	1,538	481	955	Portmann, 1947
Accipiter striatus	Sharp-shinned hawk	Acc	4,179	2,703	532	945	This study
Aegypius monachus	Cinereous vulture	Acc	23,946	17,313	2714	3,919	Portmann, 1947
Aquila audax	Wedge-tailed eagle	Acc	15,997	-	1467	-	This study
Aquila chrysaetos	Golden eagle	Acc	18,041	11,926	1891	4,224	Portmann, 1947
Buteo buteo	Common buzzard	Acc	8,452	5,343	1169	1,939	Portmann, 1947
Buteo swainsoni	Swainson's hawk	Acc	8,099	4,270	1048	2,782	This study; Grigg et al., 2017 (telen.)
Haliaeetus leucogaster	White-bellied sea eagle	Acc	12,541	7,456	1109	3,976	This study; Corfield et al., 2015 (telen.)
Pandion haliaetus	Osprey	Acc	11,005	6,929	1345	2,732	Portmann, 1947
Anas americana	American wigeon	Ans	5,245	2,345	550	2,351	This study
Anas castanea	Chestnut teal	Ans	4,367	2,889	369	1,108	This study; Corfield et al., 2015 (telen.)
Anas clypeata	Northern shoveler	Ans	3,289	2,196	279	814	This study; Corfield et al., 2015 (telen.)
Anas crecca	Eurasian teal	Ans	2,693	1,708	319	666	Kalisinska, 2005
Anas penelope	Eurasian wigeon	Ans	3,909	2,557	439	913	Portmann, 1947
Anas platyrhynchos	Mallard	Ans	5,738	3,720	560	1,457	This study; Iwaniuk et al., 2008 (telen.)
Anas querquedula	Garganey	Ans	2,635	1,757	280	598	Kalisinska, 2005
Anas strepera	Gadwall	Ans	4,324	2,017	510	1,797	This study; Grigg et al., 2017 (telen.)
Anser albifrons	Greater white-fronted goose	Ans	8,861	6,042	1120	1,699	Kalisinska, 2005
Anser anser	Greylag goose	Ans	11,873	8,571	1361	1,940	Kalisinska, 2005
Anser fabalis	Bean goose	Ans	11,322	7,944	1332	2,046	Kalisinska, 2005
Aythya affinis	Lesser scaup	Ans	4,725	3,095	438	1,192	This study; Corfield et al., 2015 (telen.)
Aythya ferina	Common pochard	Ans	6,139	4,228	695	1,216	Kalisinska, 2005
Aythya fuligula	Tufted duck	Ans	4,730	3,272	502	956	Kalisinska, 2005
Aythya marila	Greater scaup	Ans	5,608	3,793	618	1,197	Kalisinska, 2005
Bucephala albeola	Bufflehead	Ans	4,440	2,393	559	1,488	This study; Corfield et al., 2015 (telen.)
Bucephala clangula	Common goldeneye	Ans	5,961	3,718	685	1,558	This study; Corfield et al., 2015 (telen.)
Clangula hyemalis	Long-tailed duck	Ans	5,058	3,292	656	1,110	Kalisinska, 2005
Cygnus olor	Mute swan	Ans	14,624	9,826	2046	2,751	Kalisinska, 2005
Dendrocygna eytoni	Plumed whistling duck	Ans	4,850	3,186	581	1,083	Iwaniuk et al., 2004
Melanitta fusca	Velvet scoter	Ans	7,770	5,521	888	1,361	Kalisinska, 2005

Melanitta nigra	Common scoter	Ans	5,869	4,025	676	1,168	Kalisinska, 2005
Mergus merganser	Common merganser	Ans	6,959	4,614	907	1,438	Kalisinska, 2005
Mergus serrator	Red-breasted merganser	Ans	4,247	3,245	442	560	This study; Corfield et al., 2015 (telen.)
Somateria mollissima	Common eider	Ans	6,216	3,764	994	1,458	Kalisinska, 2005
Tadorna variegata	Paradise shelduck	Ans	4,157	2,690	615	852	Corfield et al., 2015; Corfield, unpubl. data (cb.)
Amazilia tzacatl	Rufous-tailed hummingbird	Apod	154	84	18	52	This study
Apus apus	Common swift	Apod	642	358	106	178	Portmann, 1947
Calypte anna	Anna's hummingbird	Apod	184	90	31	62	This study
Chaetura pelagica	Chimney swift	Apod	343	160	66	117	Boire and Baron, 1994
Chlorostilbon mellisugus	Blue-tailed emerald	Apod	119	56	23	39	Boire and Baron, 1994
Phaethornis superciliosus	Long-tailed hermit	Apod	209	99	38	72	This study
Selasphorus rufus	Rufous hummingbird	Apod	152	78	23	51	This study
Tachymarptis melba	Alpine swift	Apod	1,068	599	170	300	Portmann, 1947
Apteryx mantelli	North Island brown kiwi	Apt	5,299	4,268	575	456	Corfield et al., 2014
Upupa epops	Eurasian hoopoe	Buce	1,191	793	162	236	Portmann, 1947
Caprimulgus europaeus	European nightjar	Capr	743	331	131	280	Portmann, 1947
Eurostopodus argus	Spotted nightjar	Capr	1,013	427	138	448	This study; Iwaniuk and Wylie, 2006 (telen.)
Podargus strigoides	Tawny frogmouth	Capr	5,311	3,827	389	1,095	Iwaniuk et al., 2004
Dromaius novaehollandiae	Emu	Casua	27,750	13,696	3353	10,701	This study; Corfield et al., 2015 (telen.)
Cathartes aura	Turkey vulture	Cath	9,212	6,154	1191	1,867	Grigg et al., 2017; Iwaniuk, unpubl. data
Coragyps atratus	Black vulture	Cath	11,579	8,113	1721	1,745	Grigg et al., 2017; Iwaniuk, unpubl. data
Actitis hypoleucos	Common sandpiper	Char	746	381	99	266	Portmann, 1947
Burhinus oedicnemus	Eurasian stone-curlew	Char	3,417	2,009	462	946	Portmann, 1947
Calidris minutilla	Least sandpiper	Char	472	256	63	154	Boire and Baron, 1994
Charadrius vociferus	Killdeer	Char	1,073	524	146	404	Boire and Baron, 1994
Fratercula arctica	Atlantic puffin	Char	4,278	2,448	802	1,028	Portmann, 1947
Gallinago gallinago	Common snipe	Char	1,220	705	130	385	Portmann, 1947
Haematopus ostralegus	Eurasian oystercatcher	Char	3,477	2,188	371	917	Portmann, 1947
Himantopus himantopus	Black-winged stilt	Char	1,678	999	254	425	Cunningham et al., 2013; Corfield, unpubl. data
Larus argentatus	European herring gull	Char	4,312	2,488	664	1,160	Portmann, 1947
Larus marinus	Great black-backed gull	Char	7,505	4,621	1221	1,662	Portmann, (1947)
Larus novaehollandiae	Silver gull	Char	2,941	720	326	1,895	This study; Corfield et al., 2015 (telen.)
Larus philadelphia	Bonaparte's gull	Char	2,513	1,021	405	1,087	This study
Larus ridibundus	Black-headed gull	Char	2,714	1,495	474	745	Portmann, 1947
Limnodromus griseus	Short-billed dowitcher	Char	1,338	725	103	510	This study; Iwaniuk et al., 2004 (telen)
Limosa lapponica	Bar-tailed godwit	Char	2,417	1,563	313	541	Corfield et al., 2015 (telen.); Corfield, unpubl. data
Lymnocryptes minimus	Jack snipe	Char	898	483	106	309	Portmann, 1947
Numenius arquata	Eurasian curlew	Char	3,945	2,357	616	973	Portmann, 1947
Philomachus pugnax	Ruff	Char	1,590	923	231	436	Portmann, 1947
Scolopax rusticola	Eurasian woodcock	Char	2,503	1,572	313	617	Portmann, 1947
Sterna albifrons	Little tern	Char	919	423	203	294	Portmann, 1947
Sterna hirundo	Common tern	Char	1,434	757	274	403	Portmann, 1947
Vanellus chilensis	Southern Lapwing	Char	2,461	1,687	286	489	Pistone et al., 2002
Vanellus miles	Masked lapwing	Char	2,686	1,573	368	745	Iwaniuk et al., 2004
Vanellus vanellus	Northern lapwing	Char	2,131	1,173	313	645	Portmann, 1947
Ciconia ciconia	White stork	Cico	14,166	8,857	2150	3,160	Portmann, 1947
Leptoptilos crumeniferus	Marabou stork	Cico	30,231	21,275	4249	4,707	Portmann, 1947

Columba leucomela	White-headed pigeon	Colum	2,355	1,056	216	1,083	This study; Iwaniuk et al., 2010 (telen.)
Columba livia	Rock dove	Colum	2,343	902	296	1,145	This study
Columba palumbus	Common wood pigeon	Colum	2,315	1,263	338	715	Portmann, 1947
Ducula spilorrhoa	Torresian imperial pigeon	Colum	2,698	-	281	-	This study
Geopelia cuneata	Diamond dove	Colum	466	212	68	186	Portmann, 1947
Geopelia humeralis	Bar-shouldered dove	Colum	1,106	547	133	427	This study
Geopelia placida	Peaceful dove	Colum	776	414	85	277	This study; Iwaniuk et al., 2010 (telen.)
Goura cristata	Western crowned pigeon	Colum	5,097	2,885	791	1,421	Portmann, 1947
Patagioenas leucocephala	White-crowned pigeon	Colum	2,206	1,056	331	818	Iwaniuk et al. 2004
Phaps elegans	Brush bronzewing	Colum	1,756	873	273	610	Iwaniuk et al. 2004
Ptilinopus superbus	Superb fruit dove	Colum	1,052	588	153	311	This study
Stigmatopelia chinensis	Spotted dove	Colum	1,431	717	160	553	This study
Streptopelia decaocto	Barbary dove	Colum	1,141	631	137	373	Boire and Baron, 1994
Zenaida macroura	Mourning dove	Colum	983	428	123	432	This study
Alcedo atthis	Common kingfisher	Cora	878	488	113	277	Portmann, 1947
Dacelo novaeguineae	Laughing kookaburra	Cora	3,970	2,452	390	1,129	This study; Iwaniuk et al., 2010 (telen.)
Merops apiaster	European bee-eater	Cora	848	401	149	298	Portmann, 1947
Todiramphus sanctus	Sacred kingfisher	Cora	967	578	119	270	Iwaniuk et al. 2004
Cuculus canorus	Common cuckoo	Cucu	1,412	797	171	444	Portmann, 1947
Falco berigora	Brown falcon	Fal	6,032	3,647	638	1,747	This study; Iwaniuk et al., 2004 (telen.)
Falco cenchroides	Australian kestrel	Fal	3,211	1,848	452	911	Iwaniuk et al., 2004
Falco columbarius	Merlin	Fal	3,510	1,848	418	1,244	This study; Grigg et al., 2017 (telen.)
Falco longipennis	Australian hobby	Fal	3,462	1,729	575	1,159	Iwaniuk et al., 2004
Falco peregrinus	Peregrine falcon	Fal	6,187	3,371	1184	1,633	Iwaniuk et al., 2004
Falco sparverius	American kestrel	Fal	2,368	572	182	1,614	This study
Falco tinnunculus	Common kestrel	Fal	3,543	2,195	445	903	Portmann, 1947
Bonasa umbellus	Ruffed grouse	Galli	3,136	1,900	324	912	Cunha et al., 2020; Iwaniuk et al., 2010 (telen.)
Callipepla californica	California quail	Galli	990	544	121	325	Cunningham et al., 2013; Corfield, unpubl. data
Chrysolophus pictus	Golden pheasant	Galli	3,083	1,729	401	953	Portmann, 1947
Coturnix chinensis	King quail	Galli	434	235	48	151	Portmann, 1947
Coturnix coturnix	Common quail	Galli	756	387	89	280	Portmann, 1947
Coturnix japonica	Japanese quail	Galli	827	386	119	322	Cunha et al., 2020; This study (telen.)
Dendragapus canadensis	Spruce grouse	Galli	2,151	1,159	341	652	Cunha et al., 2020; This study (telen.)
Dendragapus obscurus	Dusky grouse	Galli	3,469	1,228	315	1,926	This study
Gallus gallus	Red junglefowl	Galli	2,583	1,379	326	877	Portmann, 1947
Lophura nycthemera	Silver pheasant	Galli	4,514	2,648	497	1,369	Portmann, 1947
Meleagris gallopavo	Wild turkey	Galli	5,906	3,374	945	1,587	Cunha et al., 2020; This study (telen.)
Numida meleagris	Helmeted guineafowl	Galli	3,951	2,223	548	1,180	Boire and Baron, 1994
Ortalis canicollis	Chaco chachalaca	Galli	3,374	1,830	526	1,018	Boire and Baron, 1994
Pavo cristatus	Indian peafowl	Galli	6,071	3,540	749	1,782	Cunha et al., 2020; This study (telen.)
Perdix perdix	Grey partridge	Galli	2,027	973	183	871	This study
Phasianus colchicus	Ring-necked Pheasant	Galli	3,252	1,757	397	1,098	Cunha et al., 2020; This study (telen.)
Tetrao tetrix	Black grouse	Galli	3,755	1,979	589	1,187	Portmann, 1947
Tetrao urogallus	Western capercaillie	Galli	5,500	2,994	828	1,678	Portmann, 1947
Tympanuchus cupido	Greater prairie chicken	Galli	3,336	1,299	317	1,720	This study

Tympanuchus pallidicinctus	Lesser prairie chicken	Galli	3,051	1,241	326	1,484	This study
Tympanuchus phasianellus	Sharp-tailed grouse	Galli	2,205	1,303	363	539	This study
Gavia stellata	Red-throated loon	Gavi	4,687	2,347	1037	1,303	Portmann, 1947
Balearica pavonina	Black crowned crane	Grui	13,913	9,429	1886	2,598	Portmann, 1947
Crex crex	Corn crake	Grui	1,260	724	155	380	Portmann, 1947
Fulica americana	American coot	Grui	2,719	1,843	242	634	This study; Iwaniuk et al., 2010 (telen.)
Fulica armillata	Red-gartered coot	Grui	4,015	2,738	400	877	Carezzano and Bee De Speroni, 1995
Fulica atra	Eurasian coot	Grui	3,211	2,016	395	800	Portmann, 1947
Gallinula chloropus	Common moorhen	Grui	1,990	1,164	269	557	Portmann, 1947
Gallinula tenebrosa	Dusky moorhen	Grui	2,727	1,653	309	765	This study
Grus antigone	Sarus crane	Grui	19,328	13,716	1783	3,829	Portmann, 1947
Grus virgo	Demoiselle crane	Grui	9,670	5,989	1497	2,184	Portmann, 1947
Porphyrio porphyrio	Western swamphen	Grui	4,953	3,156	657	1,140	Portmann, 1947
Porzana porzana	Spotted crake	Grui	1,118	595	146	377	Portmann, 1947
Rallus aquaticus	Water rail	Grui	1,702	1,023	238	441	Portmann, 1947
Ardeotis australis	Australian bustard	Otidi	10,501	6,378	1257	2,866	This study; Corfield et al., 2015 (telen.)
Acanthiza pusilla	Brown thornbill	Passe	434	233	37	164	This study; Iwaniuk et al., 2010 (telen.)
Acanthorhynchus tenuirostris	Eastern spinebill	Passe	489	294	39	155	This study
Acrocephalus scirpaceus	Eurasian reed warbler	Passe	466	272	64	130	Portmann, 1947
Aegithalos caudatus	Long-tailed tit	Passe	441	273	34	134	Portmann, 1947
Agelaius phoeniceus	Red-winged blackbird	Passe	1,615	697	111	807	This study
Ailuroedus crassirostris	Green catbird	Passe	1,259	938	101	220	Day et al., 2005
Alauda arvensis	Eurasian skylark	Passe	1,136	835	84	217	Portmann, 1947
Baeolophus bicolor	Tufted titmouse	Passe	920	534	85	301	This study; Corfield et al., 2015 (telen.)
Bombycilla cedrorum	Cedar waxwing	Passe	777	299	57	421	This study
Bombycilla garrulus	Bohemian waxwing	Passe	1,102	685	140	276	Portmann, 1947
Carduelis cannabina	Common linnet	Passe	614	414	63	137	Portmann, 1947
Carduelis carduelis	European goldfinch	Passe	597	406	67	124	Portmann, 1947
Carduelis spinus	Eurasian siskin	Passe	527	342	67	119	Portmann, 1947
Carpodacus mexicanus	House finch	Passe	1,059	551	82	426	This study
Certhia familiaris	Eurasian treecreeper	Passe	432	267	48	117	Portmann, 1947
Chlamydera nuchalis	Great bowerbird	Passe	1,858	1,449	132	277	Day et al., 2005
Cinclus cinclus	White-throated dipper	Passe	1,403	873	188	343	Portmann, 1947
Coccothraustes coccothraustes	Hawfinch	Passe	1,569	1,076	154	338	Portmann, 1947
Cormobates leucophaea	White-throated treecreeper	Passe	782	560	113	109	This study
Corvus corax	Common raven	Passe	14,648	11,802	1113	1,733	Portmann, 1947
Corvus corone	Carrion crow	Passe	9,574	7,167	768	1,638	Mehlhorn et al., 2010
Corvus frugilegus	Rook	Passe	7,520	5,797	617	1,105	Portmann, 1947
Corvus mellori	Little raven	Passe	9,834	-	689	-	This study
Corvus monedula	Western jackdaw	Passe	4,593	3,468	382	743	Portmann, 1947
Corvus moneduloides	New Caledonian crow	Passe	7,295	5,559	593	1,144	Mehlhorn et al., 2010
Delichon urbicum	Common house martin	Passe	426	273	44	110	Portmann, 1947
Dumetella carolinensis	Gray catbird	Passe	883	552	122	210	This study
Emblema pictum	Painted finch	Passe	367	-	42	-	This study
Entomyzon cyanotis	Blue-faced honeyeater	Passe	2,227	1,580	228	419	Iwaniuk et al., 2004
Eopsaltria australis	Eastern yellow robin	Passe	839	513	105	221	Iwaniuk unpubl. data
Euphagus cyanocephalus	Brewer's blackbird	Passe	1,535	-	153	-	Iwaniuk unpubl. data
Fringilla coelebs	Common chaffinch	Passe	706	450	76	179	Portmann, 1947
Garrulus glandarius	Eurasian jay	Passe	3,735	2,545	332	859	Mehlhorn et al., 2010
Grallina cyanoleuca	Magpie-lark	Passe	3,732	1,021	178	2,533	This study

Gymnorhina tibicen	Australian magpie	Passe	5,665	2,922	413	2,330	This study
Hirundo rustica	Barn swallow	Passe	531	330	79	122	Portmann, 1947
Lichenostomus penicillatus	White-plumed honeyeater	Passe	917	604	107	206	This study
Loxia curvirostra	Red crossbill	Passe	1,341	932	145	264	Portmann, 1947
Manorina melanocephala	Noisy miner	Passe	2,279	1,548	241	491	This study
Melanocorypha calandra	Calandra lark	Passe	1,314	908	137	269	Portmann, 1947
Melospiza melodia	Song sparrow	Passe	909	492	72	345	This study
Menura novaehollandiae	Superb lyrebird	Passe	10,163	-	819	-	This study
Molothrus ater	Brown-headed cowbird	Passe	952	671	107	175	This study
Montifringilla nivalis	White-winged snowfinch	Passe	1,055	680	115	260	Portmann, 1947
Neochmia temporalis	Red-browed finch	Passe	490	-	81	-	This study
Pardalotus punctatus	Spotted pardalote	Passe	448	191	52	205	This study; Iwaniuk et al., 2010 (telen.)
Parus atricapillus	Black-capped chickadee	Passe	814	565	79	171	This study
Parus carolinensis	Carolina chickadee	Passe	605	310	50	246	This study
Parus gambeli	Mountain chickadee	Passe	625	419	79	127	Iwaniuk unpubl. data
Passer domesticus	House sparrow	Passe	955	638	93	224	Mehlhorn et al., 2010
Passerina cyanea	Indigo bunting	Passe	619	360	64	195	This study
Pica pica	Eurasian magpie	Passe	5,387	4,120	425	842	Portmann, 1947
Prionodura newtoniana	Golden bowerbird	Passe	843	619	75	149	Day et al., 2005
Prunella modularis	Dunnock	Passe	700	424	78	198	Portmann, 1947
Ptilonorhynchus violaceus	Satin bowerbird	Passe	1,786	1,429	119	238	Day et al., 2005
Pyrrhocorax pyrrhocorax	Red-billed chough	Passe	6,263	4,890	472	901	Portmann, 1947
Pyrrhula pyrrhula	Eurasian bullfinch	Passe	900	519	79	302	This study; Corfield et al., 2015 (telen.)
Quiscalus quiscula	Common grackle	Passe	1,183	736	152	296	This study
Regulus regulus	Goldcrest	Passe	345	217	41	87	Portmann, 1947
Scenopoeetes dentirostris	Tooth-billed bowerbird	Passe	1,194	904	94	197	Day et al., 2005
Serinus canaria	Atlantic canary	Passe	436	276	53	107	Portmann, 1947
Sitta carolinensis	White-breasted nuthatch	Passe	1,000	613	96	291	This study; Corfield et al., 2015 (telen.)
Sitta europaea	Eurasian nuthatch	Passe	1,023	701	120	202	Portmann, 1947
Spizella passerina	Chipping sparrow	Passe	654	236	46	372	This study
Spizella pusilla	Field sparrow	Passe	579	248	47	284	This study
Stagonopleura guttata	Diamond firetail	Passe	720	376	57	288	This study; Corfield et al., 2015
Strepera versicolor	Grey currawong	Passe	5,425	3,984	506	935	Iwaniuk et al., 2004
Sturnus roseus	Rosy starling	Passe	1,425	927	164	334	Portmann, 1947
Sturnus vulgaris	European starling	Passe	1,725	1,178	179	368	Portmann, 1947
Sylvia borin	Garden warbler	Passe	565	340	67	158	Portmann, 1947
Taeniopygia bichenovii	Double-barred finch	Passe	409	222	50	137	This study
Taeniopygia guttata	Zebra finch	Passe	371	231	34	105	This study
Troglodytes aedon	House wren	Passe	614	306	55	253	This study
Troglodytes troglodytes	Eurasian wren	Passe	487	295	53	140	Portmann, 1947
Turdus merula	Common blackbird	Passe	1,745	1,120	187	438	Portmann, 1947
Turdus philomelos	Song thrush	Passe	1,408	864	163	381	Portmann, 1947
Zonotrichia albicollis	White-throated sparrow	Passe	1,220	564	92	565	This study; Corfield et al., 2015 (telen.)
Ardea cinerea	Grey heron	Pelec	7,594	4,794	962	1,838	Portmann, 1947
Botaurus stellaris	Eurasian bittern	Pelec	5,068	3,180	699	1,189	Portmann, 1947
Bubulcus ibis	Cattle egret	Pelec	4,025	1,835	384	1,807	This study
Casmerodius albus	Great egret	Pelec	5,114	3,081	741	1,292	Portmann, 1947
Egretta garzetta	Little egret	Pelec	3,348	2,000	462	886	Portmann, 1947

Egretta thula	Snowy egret	Pelec	3,612	1,973	610	1,029	Carezzano and Bee De Speroni, 1995
Ixobrychus minutus	Little bittern	Pelec	1,559	916	219	424	Portmann, 1947
Nycticorax caledonicus	Nankeen night heron	Pelec	3,360	1,922	439	1,000	Iwaniuk et al., 2004
Pelecanus conspicillatus	Australian pelican	Pelec	22,500	-	2173	-	This study
Pelecanus onocrotalus	Great white pelican	Pelec	30,373	22,020	4014	4,340	Portmann, 1947
Phoenicopterus ruber	American flamingo	Phoe	10,674	7,115	1766	1,793	Portmann, 1947
Dendrocopos major	Great spotted woodpecker	Pici	2,609	1,895	270	444	Portmann, 1947
Dendrocopos medius	Middle spotted woodpecker	Pici	1,990	1,439	212	339	Portmann, 1947
Dryocopus martius	Black woodpecker	Pici	7,701	5,939	614	1,148	Portmann, 1947
Indicator variegatus	Scaly-throated honeyguide	Pici	800	290	110	400	This study
Jynx torquilla	Eurasian wryneck	Pici	776	478	89	210	Portmann, 1947
Picus canus	Grey-headed woodpecker	Pici	3,344	2,480	338	526	Portmann, 1947
Picus viridis	Eurasian green woodpecker	Pici	4,232	3,108	404	719	Portmann, 1947
Sphyrapicus varius	Yellow-bellied sapsucker	Pici	1,443	697	126	620	This study; Corfield et al., 2015 (telen.)
Podiceps cristatus	Great crested grebe	Podic	3,633	2,051	658	925	Portmann, 1947
Rollandia rolland	White-tufted grebe	Podic	2,059	1,184	288	587	Carezzano and Bee De Speroni, 1995
Tachybaptus ruficollis	Little grebe	Podic	1,656	917	261	477	Portmann, 1947
Puffinus tenuirostris	Short-tailed shearwater	Proce	4,758	2,334	757	1,667	This study; Iwaniuk et al., 2010 (telen.)
Thalassarche melanophrys	Black-browed Albatross	Proce	14,129	7,553	2048	4,529	This study
Agapornis fischeri	Fischer's lovebird	Psi	1,928	1,440	117	371	Portmann, 1947
Agapornis personatus	Yellow-collared lovebird	Psi	2,786	2,070	243	474	Iwaniuk et al., 2004
Agapornis roseicollis	Rosy-faced lovebird	Psi	2,008	1,455	171	383	Iwaniuk et al., 2004
Alisterus scapularis	Australian king parrot	Psi	4,902	3,271	323	1,307	This study; Iwaniuk et al., 2010 (telen.)
Amazona aestiva	Turquoise-fronted parrot	Psi	7,903	5,672	621	1,609	Iwaniuk et al., 2004
Amazona versicolor	St. Lucia parrot	Psi	7,546	5,750	600	1,196	Portmann, 1947
Ara ararauna	Blue-and-yellow macaw	Psi	18,139	14,944	1261	1,934	Portmann, 1947
Ara chloropterus	Red-and-green macaw	Psi	23,497	19,188	1856	2,453	Portmann, 1947
Aratinga acuticaudata	Blue-crowned parakeet	Psi	5,410	4,326	315	769	Fernandez et al., 1997
Cacatua galerita	Sulphur-crested cockatoo	Psi	13,937	11,292	1049	1,596	This study; Iwaniuk et al., 2010 (telen.)
Cacatua roseicapilla	Galah	Psi	6,653	4,909	638	1,106	Iwaniuk et al., 2004
Cacatua sulphurea	Yellow-crested cockatoo	Psi	8,417	6,652	309	1,457	Portmann, 1947
Cacatua tenuirostris	Long-billed corella	Psi	11,778	9,753	668	1,357	This study
Calyptorhynchus funereus	Yellow-tailed black-cockatoo	Psi	16,078	12,824	1155	2,100	Iwaniuk et al., 2004
Eclectus roratus	Eclectus parrot	Psi	6,248	4,583	474	1,191	Iwaniuk et al., 2004
Glossopsitta concinna	Glossopsitta concinna	Psi	3,150	2,280	300	570	Iwaniuk et al., 2004
Glossopsitta porphyrocephala	Purple-crowned lorikeet	Psi	1,855	-	138	-	This study
Melopsittacus undulatus	Budgerigar	Psi	1,486	825	157	505	This study; Iwaniuk et al., 2010 (telen.)
Myiopsitta monachus	Monk parakeet	Psi	3,830	2,733	291	806	Fernandez et al., 1997
Neopsephotus bourkii	Neopsephotus bourkii	Psi	1,207	834	113	261	Iwaniuk et al., 2004
Nymphicus hollandicus	Cockatiel	Psi	2,161	1,309	220	632	This study
Pionus menstruus	Blue-headed parrot	Psi	5,283	3,852	383	1,048	Boire and Baron, 1994

Platycercus elegans	Crimson rosella	Psi	3,628	2,688	225	716	This study; Iwaniuk et al., 2010 (telen.)
Platycercus eximius	Eastern rosella	Psi	3,246	2,326	292	628	Iwaniuk et al., 2004
Polytelis swainsonii	Superb parrot	Psi	3,149	2,153	298	698	Iwaniuk et al., 2004
Psephotus haematonotus	Red-rumped parrot	Psi	1,914	1,403	173	338	Iwaniuk et al., 2004
Psittacula eupatria	Alexandrine parakeet	Psi	6,327	4,942	489	896	Iwaniuk et al., 2004
Psittacula krameri	Rose-ringed parakeet	Psi	4,239	3,270	296	674	Iwaniuk et al., 2004
Psittacus erithacus	Grey parrot	Psi	6,392	4,727	602	1,062	Iwaniuk et al., 2004
Pyrrhura molinae	Green-cheeked parakeet	Psi	4,656	3,124	505	1,028	Iwaniuk et al., 2004
Strigops habroptila	Kakapo	Psi	14,768	12,421	774	1,573	Corfield et al., 2011
Trichoglossus haematodus	Rainbow lorikeet	Psi	3,726	2,727	354	645	Iwaniuk et al., 2004
Rhea americana	Greater rhea	Rhei	19,228	10,281	2974	5,973	Boire and Baron, 1994
Eudyptula minor	Little penguin	Sphen	7,584	4,338	1365	1,880	This study; Corfield et al., 2015 (telen.)
Spheniscus demersus	African penguin	Sphen	13,948	9,076	1891	2,980	Portmann, 1947
Spheniscus magellanicus	Magellanic penguin	Sphen	16,757	10,890	2626	3,240	Boire and Baron, 1994
Aegolius acadicus	Northern saw-whet owl	Stri	2,857	2,010	239	608	This study; Iwaniuk et al., 2010 (telen.)
Asio flammeus	Short-eared owl	Stri	5,300	2,457	181	2,662	This study
Asio otus	Long-eared owl	Stri	5,321	3,967	421	933	Portmann, 1947
Athene cunicularia	Burrowing owl	Stri	6,090	4,814	413	864	Alma and Bee De Speroni, 1992
Athene noctua	Little owl	Stri	3,786	2,914	289	583	Portmann, 1947
Bubo bubo	Eurasian eagle-owl	Stri	16,307	12,481	1317	2,509	Portmann, 1947
Bubo scandiaca	Snowy owl	Stri	18,127	13,922	-	-	Corfield et al., 2015
Bubo virginianus	Great horned owl	Stri	14,730	8,704	847	5,178	This study
Ninox boobook	Australian boobook	Stri	6,339	5,525	378	436	This study
Otus scops	Eurasian scops-owl	Stri	2,132	1,395	231	506	Portmann, 1947
Strix aluco	Tawny owl	Stri	8,513	6,465	666	1,382	Portmann, 1947
Strix nebulosa	Great grey owl	Stri	13,433	8,095	607	4,731	This study
Strix varia	Barred owl	Stri	12,727	5,669	529	6,529	This study
Surnia ulula	Northern hawk-owl	Stri	7,480	6,004	509	967	This study
Tyto alba	Barn owl	Stri	7,143	4,109	398	2,637	This study; Iwaniuk and Wylie, 2006
Struthio camelus	Common ostrich	Strut	39,631	26,131	5844	7,656	Portmann, 1947
Phalacrocorax auritus	Double-crested Cormorant	Suli	7,323	4,342	1138	1,844	Boire and Baron, 1994
Phalacrocorax carbo	Great cormorant	Suli	9,529	6,116	1425	1,987	Portmann, 1947
Nothura darwinii	Darwin's nothura	Tin	1,482	809	163	510	Corfield, unpub. data; Corfield et al., 2014 (telen.)
Rhynchotus rufescens	Red-winged tinamou	Tin	3,014	1,705	382	927	Cunningham et al., 2013
Tinamus major	Great tinamou	Tin	2,242	1,222	294	726	Cunningham et al., 2013

Table 3.4. List of the species analyzed and their respective behaviours. Dev.=developmental mode; Altr.=altricial; prec.=precocial; Y=yes; N=no. For flight, rank is based on Norberg's (2012) as: 0 = flightless, 1 = slow, poor manoeuvrable birds that soar, 2 = fast, poorly manoeuvrable fliers, 3 = slow manoeuvrable fliers, 4 = fast manoeuvrable fliers. Order abbreviations: Acc=Accipitriformes; Ans=Anseriformes; Apod=Apodiformes; Apt=Apterygiformes; Buce= Bucerotiformes; Capr=Caprimulgiformes; Casua=Casuariiformes; Cath=Cathartiformes; Cico=Ciconiiformes; Colum=Columbiformes; Cora=Coraciiformes; Cucu=Cuculiformes; Fal=Falconiformes; Galli=Galliformes; Gavi=Gaviiformes; Grui=Gruiformes; Otidi=Otidiformes; Passe=Passeriformes; Pelec=Pelecaniformes; Phoe=Phoenicopteriformes; Pici=Piciformes; Podic= Podicipediformes; Proce=Procellariiformes; Psi=Psittaciformes; Rhei=Rheiformes; Sphen=Sphenisciformes; Stri=Strigiformes; Strut=Struthioniformes; Suli=Suliformes; Tin=Tinamiformes.

Species	**Common name**	**Order**	**Dev.**	**Migration**	**Aerial**	***Flight***
Accipiter cirrocephalus	Collared sparrowhawk	Acc	altr	N	N	3
Accipiter fasciatus	Brown goshawk	Acc	altr	N	N	3
Accipiter striatus	Sharp-shinned hawk	Acc	altr	Y	N	3
Accipiter gentilis	Northern goshawk	Acc	altr	Y	N	3
Accipiter nisus	Eurasian sparrowhawk	Acc	altr	Y	N	3
Aegypius monachus	Cinereous vulture	Acc	altr	Y	N	1
Aquila audax	Wedge-tailed eagle	Acc	altr	N	N	1
Aquila chrysaetos	Golden eagle	Acc	altr	Y	N	1
Buteo buteo	Common buzzard	Acc	altr	Y	N	1
Buteo swainsoni	Swainson's hawk	Acc	altr	Y	N	1
Haliaeetus leucogaster	White-bellied sea eagle	Acc	altr	N	N	1
Pandion haliaetus	Osprey	Acc	altr	Y	N	3
Anas castanea	Chestnut teal	Ans	prec	N	N	2
Anas clypeata	Northern shoveler	Ans	prec	Y	N	2
Anas crecca	Eurasian teal	Ans	prec	Y	N	2
Anas penelope	Eurasian wigeon	Ans	prec	Y	N	2
Anas platyrhynchos	Mallard	Ans	prec	Y	N	2
Anas querquedula	Garganey	Ans	prec	Y	N	2
Anas americana	American wigeon	Ans	prec	Y	N	2
Anas_strepera	Gadwall	Ans	prec	Y	N	2
Anser albifrons	Greater white-fronted goose	Ans	prec	Y	N	2
Anser anser	Greylag goose	Ans	prec	Y	N	2
Anser fabalis	Bean goose	Ans	prec	Y	N	2
Aythya affinis	Lesser scaup	Ans	prec	Y	N	2
Aythya ferina	Common pochard	Ans	prec	Y	N	2
Aythya_fuligula	Tufted duck	Ans	prec	Y	N	2
Aythya_marila	Greater scaup	Ans	prec	Y	N	2
Bucephala albeola	Bufflehead	Ans	prec	Y	N	2
Bucephala clangula	Common goldeneye	Ans	prec	Y	N	2
Clangula hyemalis	Long-tailed duck	Ans	prec	Y	N	2
Cygnus olor	Mute swan	Ans	prec	Y	N	2
Dendrocygna eytoni	Plumed whistling duck	Ans	prec	N	N	2
Melanitta fusca	Velvet scoter	Ans	prec	Y	N	2
Melanitta nigra	Common scoter	Ans	prec	Y	N	2
Mergus merganser	Common merganser	Ans	prec	Y	N	2
Mergus serrator	Red-breasted merganser	Ans	prec	Y	N	2
Somateria mollissima	Common eider	Ans	prec	Y	N	2
Tadorna variegata	Paradise shelduck	Ans	prec	N	N	2
Amazilia tzacatl	Rufous-tailed hummingbird	Apod	altr	N	Y	4
Apus apus	Common swift	Apod	altr	Y	Y	3
Calypte anna	Anna's hummingbird	Apod	altr	Y	Y	4
Chaetura pelagica	Chimney swift	Apod	altr	Y	Y	3

Chlorostilbon mellisugus	Blue-tailed emerald	Apod	altr	N	Y	4
Phaethornis superciliosus	Long-tailed hermit	Apod	altr	N	Y	4
Selasphorus rufus	Rufous hummingbird	Apod	altr	Y	Y	4
Tachymarptis melba	Alpine swift	Apod	altr	Y	Y	3
Apteryx mantelli	North Island brown kiwi	Apt	prec	N	N	0
Upupa epops	Eurasian hoopoe	Buce	altr	Y	N	3
Caprimulgus europaeus	European nightjar	Capr	prec	Y	Y	3
Eurostopodus argus	Spotted nightjar	Capr	prec	N	Y	3
Podargus strigoides	Tawny frogmouth	Capr	altr	N	N	3
Dromaius novaehollandiae	Emu	Casua	prec	N	N	0
Cathartes aura	Turkey vulture	Cath	altr	Y	N	1
Coragyps atratus	Black vulture	Cath	altr	N	N	1
Actitis hypoleucos	Common sandpiper	Char	prec	Y	N	2
Burhinus oedicnemus	Eurasian stone-curlew	Char	prec	Y	N	2
Calidris minutilla	Least sandpiper	Char	prec	Y	N	2
Charadrius vociferus	Killdeer	Char	prec	Y	N	2
Fratercula arctica	Atlantic puffin	Char	prec	Y	N	2
Gallinago gallinago	Common snipe	Char	prec	Y	N	2
Haematopus ostralegus	Eurasian oystercatcher	Char	prec	Y	N	2
Himantopus himantopus	Black-winged stilt	Char	prec	Y	N	2
Larus argentatus	European herring gull	Char	prec	Y	N	1
Larus marinus	Great black-backed gull	Char	prec	Y	N	1
Larus novaehollandiae	Silver gull	Char	prec	Y	N	1
Larus philadelphia	Bonaparte's gull	Char	prec	Y	N	1
Larus ridibundus	Black-headed gull	Char	prec	Y	N	1
Limnodromus griseus	Short-billed dowitcher	Char	prec	Y	N	2
Limosa lapponica	Bar-tailed godwit	Char	prec	Y	N	2
Lymnocryptes minimus	Jack snipe	Char	prec	Y	N	2
Numenius arquata	Eurasian curlew	Char	prec	Y	N	2
Philomachus pugnax	Ruff	Char	prec	Y	N	2
Scolopax rusticola	Eurasian woodcock	Char	prec	Y	N	2
Sterna albifrons	Little tern	Char	prec	Y	N	1
Sterna hirundo	Common tern	Char	prec	Y	N	1
Vanellus chilensis	Southern Lapwing	Char	prec	N	N	2
Vanellus miles	Masked lapwing	Char	prec	N	N	2
Vanellus vanellus	Northern lapwing	Char	prec	Y	N	2
Ciconia ciconia	White stork	Cico	altr	Y	N	1
Leptoptilos crumeniferus	Marabou stork	Cico	altr	N	N	1
Columba leucomela	White-headed pigeon	Colum	altr	N	N	3
Columba livia	Rock dove	Colum	altr	N	N	3
Columba palumbus	Common wood pigeon	Colum	altr	Y	N	3
Ducula spilorrhoa	Torresian imperial pigeon	Colum	altr	Y	N	3
Geopelia cuneata	Diamond dove	Colum	altr	N	N	3
Geopelia humeralis	Bar-shouldered dove	Colum	altr	N	N	3
Geopelia placida	Peaceful dove	Colum	altr	N	N	3
Goura cristata	Western crowned pigeon	Colum	altr	N	N	3
Patagioenas leucocephala	White-crowned pigeon	Colum	altr	N	N	3
Phaps elegans	Brush bronzewing	Colum	altr	N	N	3
Ptilinopus superbus	Superb fruit dove	Colum	altr	N	N	3
Stigmatopelia chinensis	Spotted dove	Colum	altr	N	N	3
Streptopelia decaocto	Barbary dove	Colum	altr	N	N	3
Zenaida macroura	Mourning dove	Colum	altr	Y	N	3
Alcedo atthis	Common kingfisher	Cora	altr	Y	N	3
Dacelo novaeguineae	Laughing kookaburra	Cora	altr	N	N	3
Merops apiaster	European bee-eater	Cora	altr	Y	N	3
Todiramphus sanctus	Sacred kingfisher	Cora	altr	Y	N	3
Cuculus canorus	Common cuckoo	Cucu	altr	Y	N	3
Falco berigora	Brown falcon	Fal	altr	N	N	3
Falco cenchroides	Australian kestrel	Fal	altr	N	N	3
Falco columbarius	Merlin	Fal	altr	Y	N	3
Falco longipennis	Australian hobby	Fal	altr	N	N	3

Falco peregrinus	Peregrine falcon	Fal	altr	Y	N	3
Falco sparverius	American kestrel	Fal	altr	Y	N	3
Falco tinnunculus	Common kestrel	Fal	altr	Y	N	3
Bonasa umbellus	Ruffed grouse	Galli	prec	N	N	2
Callipepla californica	California quail	Galli	prec	N	N	2
Chrysolophus pictus	Golden pheasant	Galli	prec	N	N	2
Coturnix chinensis	King quail	Galli	prec	N	N	2
Coturnix coturnix	Common quail	Galli	prec	Y	N	2
Coturnix japonica	Japanese quail	Galli	prec	Y	N	2
Dendragapus canadensis	Spruce grouse	Galli	prec	N	N	2
Dendragapus obscurus	Dusky grouse	Galli	prec	N	N	2
Gallus gallus	Red junglefowl	Galli	prec	N	N	2
Lophura nycthemera	Silver pheasant	Galli	prec	N	N	2
Meleagris gallopavo	Wild turkey	Galli	prec	N	N	2
Numida meleagris	Helmeted guineafowl	Galli	prec	N	N	2
Ortalis canicollis	Chaco chachalaca	Galli	prec	N	N	2
Pavo cristatus	Indian peafowl	Galli	prec	N	N	2
Perdix perdix	Grey partridge	Galli	prec	N	N	2
Phasianus colchicus	Ring-necked Pheasant	Galli	prec	N	N	2
Tetrao tetrix	Black grouse	Galli	prec	N	N	2
Tetrao urogallus	Western capercaillie	Galli	prec	N	N	2
Tympanuchus cupido	Greater prairie chicken	Galli	prec	N	N	2
Tympanuchus pallidicinctus	Lesser prairie chicken	Galli	prec	N	N	2
Tympanuchus phasianellus	Sharp-tailed grouse	Galli	prec	N	N	2
Gavia stellata	Red-throated loon	Gavi	prec	Y	N	2
Balearica pavonina	Black crowned crane	Grui	prec	N	N	1
Crex crex	Corn crake	Grui	prec	Y	N	1
Fulica americana	American coot	Grui	prec	Y	N	1
Fulica armillata	Red-gartered coot	Grui	prec	N	N	1
Fulica atra	Eurasian coot	Grui	prec	Y	N	1
Gallinula chloropus	Common moorhen	Grui	prec	Y	N	1
Gallinula tenebrosa	Dusky moorhen	Grui	prec	N	N	1
Grus antigone	Sarus crane	Grui	prec	Y	N	1
Grus virgo	Demoiselle crane	Grui	prec	Y	N	1
Porphyrio porphyrio	Western swamphen	Grui	prec	N	N	1
Porzana porzana	Spotted crake	Grui	prec	Y	N	1
Rallus aquaticus	Water rail	Grui	prec	Y	N	1
Ardeotis australis	Australian bustard	Otidi	prec	N	N	2
Acanthiza pusilla	Brown thornbill	Passe	altr	N	N	3
Acanthorhynchus tenuirostris	Eastern spinebill	Passe	altr	N	N	3
Acrocephalus scirpaceus	Eurasian reed warbler	Passe	altr	Y	N	3
Aegithalos caudatus	Long-tailed tit	Passe	altr	N	N	3
Agelaius phoeniceus	Red-winged blackbird	Passe	altr	Y	N	3
Ailuroedus crassirostris	Green catbird	Passe	altr	N	N	3
Alauda arvensis	Eurasian skylark	Passe	altr	Y	N	3
Baeolophus bicolor	Tufted titmouse	Passe	altr	N	N	3
Bombycilla cedrorum	Cedar waxwing	Passe	altr	Y	N	3
Bombycilla garrulus	Bohemian waxwing	Passe	altr	Y	N	3
Carduelis cannabina	Common linnet	Passe	altr	Y	N	3
Carduelis carduelis	European goldfinch	Passe	altr	Y	N	3
Carduelis spinus	Eurasian siskin	Passe	altr	Y	N	3
Carpodacus mexicanus	House finch	Passe	altr	N	N	3
Certhia familiaris	Eurasian treecreeper	Passe	altr	N	N	3
Chlamydera nuchalis	Great bowerbird	Passe	altr	N	N	3
Cinclus cinclus	White-throated dipper	Passe	altr	Y	N	3
Coccothraustes coccothraustes	Hawfinch	Passe	altr	Y	N	3
Cormobates leucophaea	White-throated treecreeper	Passe	altr	N	N	3
Corvus corax	Common raven	Passe	altr	N	N	1
Corvus corone	Carrion crow	Passe	altr	Y	N	1
Corvus frugilegus	Rook	Passe	altr	Y	N	1
Corvus mellori	Little raven	Passe	altr	N	N	1

Corvus monedula	Western jackdaw	Passe	altr	Y	N	1
Corvus moneduloides	New Caledonian crow	Passe	altr	N	N	1
Delichon urbicum	Common house martin	Passe	altr	Y	N	3
Dumetella carolinensis	Gray catbird	Passe	altr	Y	N	3
Emblema pictum	Painted finch	Passe	altr	N	N	3
Entomyzon cyanotis	Blue-faced honeyeater	Passe	altr	N	N	3
Eopsaltria australis	Eastern yellow robin	Passe	altr	N	N	3
Euphagus cyanocephalus	Brewer's blackbird	Passe	altr	N	N	3
Fringilla coelebs	Common chaffinch	Passe	altr	Y	N	3
Garrulus glandarius	Eurasian jay	Passe	altr	N	N	3
Grallina cyanoleuca	Magpie-lark	Passe	altr	N	N	1
Gymnorhina tibicen	Australian magpie	Passe	altr	N	N	1
Hirundo rustica	Barn swallow	Passe	altr	Y	Y	3
Lichenostomus penicillatus	White-plumed honeyeater	Passe	altr	N	N	3
Loxia curvirostra	Red crossbill	Passe	altr	Y	N	3
Manorina melanocephala	Noisy miner	Passe	altr	N	N	3
Melanocorypha calandra	Calandra lark	Passe	altr	Y	N	3
Melospiza melodia	Song sparrow	Passe	altr	Y	N	1
Menura novaehollandiae	Superb lyrebird	Passe	altr	N	N	1
Molothrus ater	Brown-headed cowbird	Passe	altr	Y	N	3
Montifringilla nivalis	White-winged snowfinch	Passe	altr	N	N	3
Neochmia temporalis	Red-browed finch	Passe	altr	N	N	3
Pardalotus punctatus	Spotted pardalote	Passe	altr	N	N	3
Parus atricapillus	Black-capped chickadee	Passe	altr	N	N	3
Parus carolinensis	Carolina chickadee	Passe	altr	N	N	3
Parus gambeli	Mountain chickadee	Passe	altr	N	N	3
Passer domesticus	House sparrow	Passe	altr	N	N	1
Passerina cyanea	Indigo bunting	Passe	altr	Y	N	1
Pica pica	Eurasian magpie	Passe	altr	N	N	1
Prionodura newtoniana	Golden bowerbird	Passe	altr	N	N	3
Prunella modularis	Dunnock	Passe	altr	Y	N	3
Ptilonorhynchus violaceus	Satin bowerbird	Passe	altr	N	N	3
Pyrrhocorax pyrrhocorax	Red-billed chough	Passe	altr	N	N	3
Pyrrhula pyrrhula	Eurasian bullfinch	Passe	altr	Y	N	3
Quiscalus quiscula	Common grackle	Passe	altr	Y	N	3
Regulus regulus	Goldcrest	Passe	altr	Y	N	3
Scenopoeetes dentirostris	Tooth-billed bowerbird	Passe	altr	N	N	3
Serinus canaria	Atlantic canary	Passe	altr	N	N	3
Sitta carolinensis	White-breasted nuthatch	Passe	altr	N	N	3
Sitta europaea	Eurasian nuthatch	Passe	altr	N	N	3
Spizella passerina	Chipping sparrow	Passe	altr	Y	N	3
Spizella pusilla	Field sparrow	Passe	altr	Y	N	3
Stagonopleura guttata	Diamond firetail	Passe	altr	N	N	3
Strepera versicolor	Grey currawong	Passe	altr	N	N	3
Sturnus roseus	Rosy starling	Passe	altr	Y	N	1
Sturnus vulgaris	European starling	Passe	altr	Y	N	1
Sylvia borin	Garden warbler	Passe	altr	Y	N	3
Taeniopygia bichenovii	Double-barred finch	Passe	altr	N	N	3
Taeniopygia guttata	Zebra finch	Passe	altr	N	N	3
Troglodytes aedon	House wren	Passe	altr	Y	N	3
Troglodytes troglodytes	Eurasian wren	Passe	altr	N	N	3
Turdus merula	Common blackbird	Passe	altr	Y	N	1
Turdus philomelos	Song thrush	Passe	altr	Y	N	1
Zonotrichia albicollis	White-throated sparrow	Passe	altr	Y	N	1
Ardea cinerea	Grey heron	Pelec	altr	Y	N	1
Botaurus stellaris	Eurasian bittern	Pelec	altr	Y	N	1
Bubulcus ibis	Cattle egret	Pelec	altr	Y	N	1
Casmerodius albus	Great egret	Pelec	altr	Y	N	1
Egretta garzetta	Little egret	Pelec	altr	Y	N	1
Egretta thula	Snowy egret	Pelec	altr	Y	N	1
Ixobrychus minutus	Little bittern	Pelec	altr	Y	N	1

Nycticorax caledonicus	Nankeen night heron	Pelec	altr	N	N	1
Pelecanus conspicillatus	Australian pelican	Pelec	altr	N	N	1
Pelecanus onocrotalus	Great white pelican	Pelec	altr	Y	N	1
Phoenicopterus ruber	American flamingo	Phoe	altr	N	N	1
Dendrocopos major	Great spotted woodpecker	Pici	altr	N	N	3
Dendrocopos medius	Middle spotted woodpecker	Pici	altr	N	N	3
Dryocopus martius	Black woodpecker	Pici	altr	N	N	3
Indicator variegatus	Scaly-throated honeyguide	Pici	altr	N	N	3
Jynx torquilla	Eurasian wryneck	Pici	altr	Y	N	3
Picus canus	Grey-headed woodpecker	Pici	altr	N	N	3
Picus viridis	Eurasian Green woodpecker	Pici	altr	N	N	3
Sphyrapicus varius	Yellow-bellied sapsucker	Pici	altr	Y	N	3
Podiceps cristatus	Great crested grebe	Podic	prec	Y	N	2
Rollandia rolland	White-tufted grebe	Podic	prec	N	N	2
Tachybaptus ruficollis	Little grebe	Podic	prec	Y	N	2
Puffinus tenuirostris	Short-tailed shearwater	Proce	prec	Y	Y	1
Thalassarche melanophrys	Black-browed Albatross	Proce	prec	Y	Y	1
Agapornis fischeri	Fischer's lovebird	Psi	altr	N	N	1
Agapornis personatus	Yellow-collared lovebird	Psi	altr	N	N	1
Agapornis roseicollis	Rosy-faced lovebird	Psi	altr	N	N	1
Alisterus scapularis	Australian king parrot	Psi	altr	N	N	1
Amazona aestiva	Turquoise-fronted parrot	Psi	altr	N	N	1
Amazona versicolor	St. Lucia parrot	Psi	altr	N	N	1
Ara ararauna	Blue-and-yellow macaw	Psi	altr	N	N	1
Ara chloropterus	Red-and-green macaw	Psi	altr	N	N	1
Aratinga acuticaudata	Blue-crowned parakeet	Psi	altr	N	N	1
Cacatua galerita	Sulphur-crested cockatoo	Psi	altr	N	N	1
Cacatua roseicapilla	Galah	Psi	altr	N	N	1
Cacatua sulphurea	Yellow-crested cockatoo	Psi	altr	N	N	1
Cacatua tenuirostris	Long-billed corella	Psi	altr	N	N	1
Calyptorhynchus funereus	Yellow-tailed black-cockatoo	Psi	altr	N	N	1
Eclectus roratus	Eclectus parrot	Psi	altr	N	N	1
Glossopsitta concinna	Musk lorikeet	Psi	altr	N	N	1
Glossopsitta porphyrocephala	Purple-crowned lorikeet	Psi	altr	N	N	1
Melopsittacus undulatus	Budgerigar	Psi	altr	N	N	1
Myiopsitta monachus	Monk parakeet	Psi	altr	N	N	1
Neopsephotus bourkii	Bourke’s parrot	Psi	altr	N	N	1
Nymphicus hollandicus	Cockatiel	Psi	altr	N	N	1
Pionus menstruus	Blue-headed parrot	Psi	altr	N	N	1
Platycercus elegans	Crimson rosella	Psi	altr	N	N	1
Platycercus eximius	Eastern rosella	Psi	altr	N	N	1
Polytelis swainsonii	Superb parrot	Psi	altr	N	N	1
Psephotus haematonotus	Red-rumped parrot	Psi	altr	N	N	1
Psittacula eupatria	Alexandrine parakeet	Psi	altr	N	N	1
Psittacula krameri	Rose-ringed parakeet	Psi	altr	N	N	1
Psittacus erithacus	Grey parrot	Psi	altr	N	N	1
Pyrrhura molinae	Green-cheeked parakeet	Psi	altr	N	N	1
Strigops habroptila	Kakapo	Psi	altr	N	N	1
Trichoglossus haematodus	Rainbow lorikeet	Psi	altr	N	N	1
Rhea americana	Greater rhea	Rhei	prec	N	N	0
Eudyptula minor	Little penguin	Sphen	altr	N	N	4
Spheniscus demersus	African penguin	Sphen	altr	N	N	4
Spheniscus magellanicus	Magellanic penguin	Sphen	altr	Y	N	4
Aegolius acadicus	Northern saw-whet owl	Stri	altr	Y	N	1
Asio flammeus	Short-eared owl	Stri	altr	Y	N	1
Asio otus	Long-eared owl	Stri	altr	Y	N	1
Athene cunicularia	Burrowing owl	Stri	altr	Y	N	1
Athene noctua	Little owl	Stri	altr	N	N	1
Bubo bubo	Eurasian eagle-owl	Stri	altr	N	N	1
Bubo scandiaca	Snowy owl	Stri	altr	Y	N	1
Bubo virginianus	Great horned owl	Stri	altr	N	N	1

Ninox boobook	Australian boobook	Stri	altr	N	N	1
Otus scops	Eurasian scops owl	Stri	altr	Y	N	1
Strix aluco	Tawny owl	Stri	altr	N	N	1
Strix nebulosa	Great grey owl	Stri	altr	N	N	1
Strix varia	Barred owl	Stri	altr	N	N	1
Surnia ulula	Northern hawk-owl	Stri	altr	N	N	1
Tyto alba	Barn owl	Stri	altr	N	N	1
Struthio camelus	Common ostrich	Strut	prec	N	N	0
Phalacrocorax auritus	Double-crested cormorant	Suli	altr	Y	N	2
Phalacrocorax carbo	Great cormorant	Suli	altr	Y	N	2
Nothura darwinii	Darwin's nothura	Tin	prec	N	N	2
Rhynchotus rufescens	Red-winged tinamou	Tin	prec	N	N	2
Tinamus major	Great tinamou	Tin	prec	N	N	2

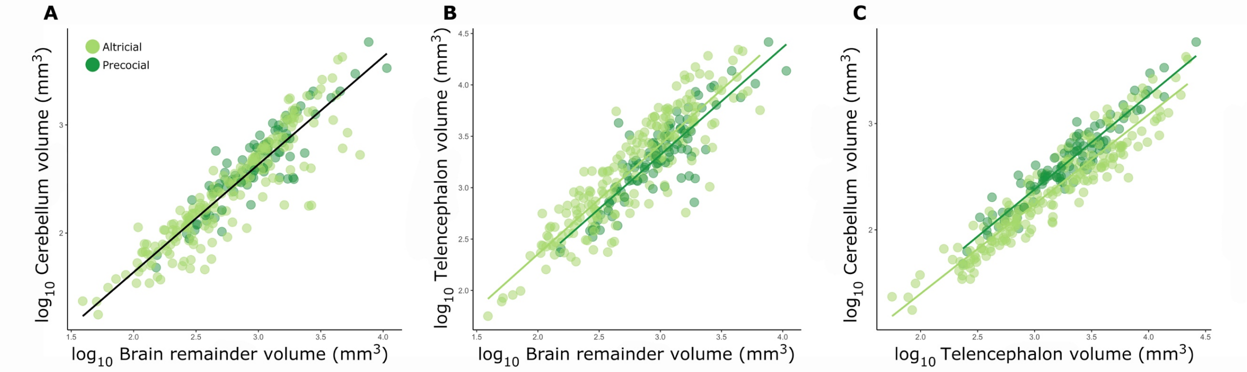

Figure 3.1. Scatterplots of log-transformed volumes (mm^3) of: **A.** cerebellum against brain remainder, **B.** telencephalon against brain remainder, and **C**. cerebellum against telencephalon. Altricial and precocial species are depicted in different colors, as shown in the legend. The brain remainder refers to brain size minus the sizes of the telencephalon and cerebellum.

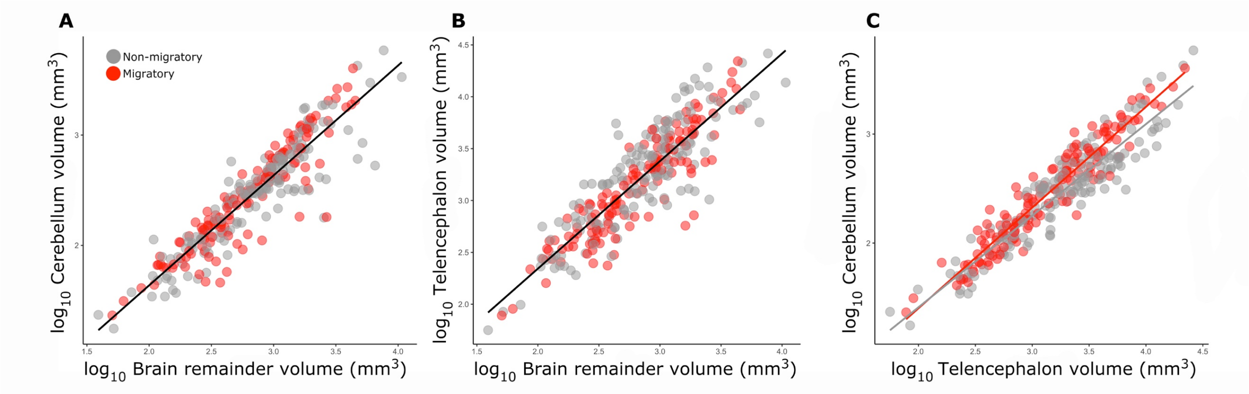

Figure 3.2. Scatterplots of log-transformed volumes (mm^3) of: **A.** cerebellum against brain remainder, **B.** telencephalon against brain remainder, and **C.** cerebellum against telencephalon. Migratory (red) and non-migratory (gray) species are depicted in different colors, as shown in the legend. The brain remainder refers to brain size minus the sizes of the telencephalon and cerebellum.

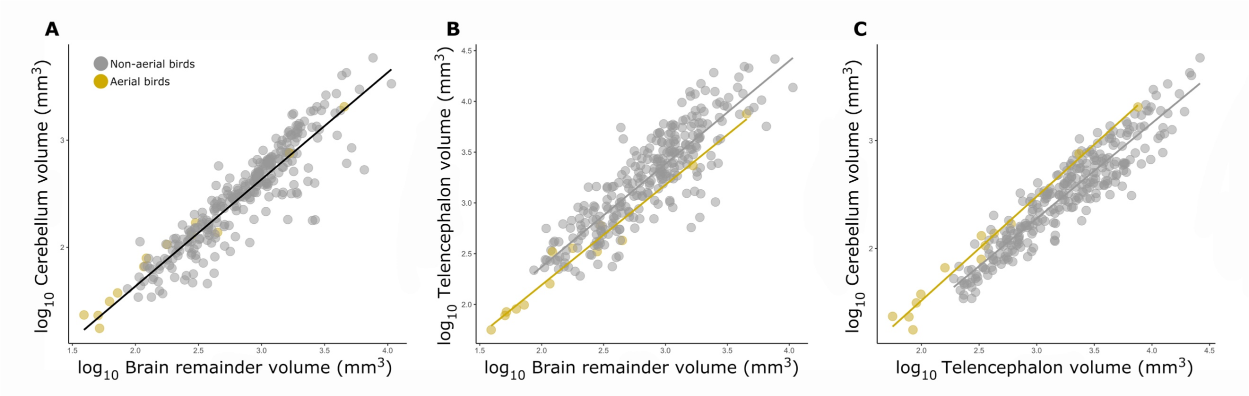

Figure 3.3. Scatterplots of log-transformed volumes (mm^3) of: **A.** cerebellum against brain remainder, **B.** telencephalon against brain remainder, and **C.** cerebellum against telencephalon. Aerial (yellow) and non-aerial (gray) species are depicted in different colors, as shown in the legend. The brain remainder refers to brain size minus the sizes of the telencephalon and cerebellum.

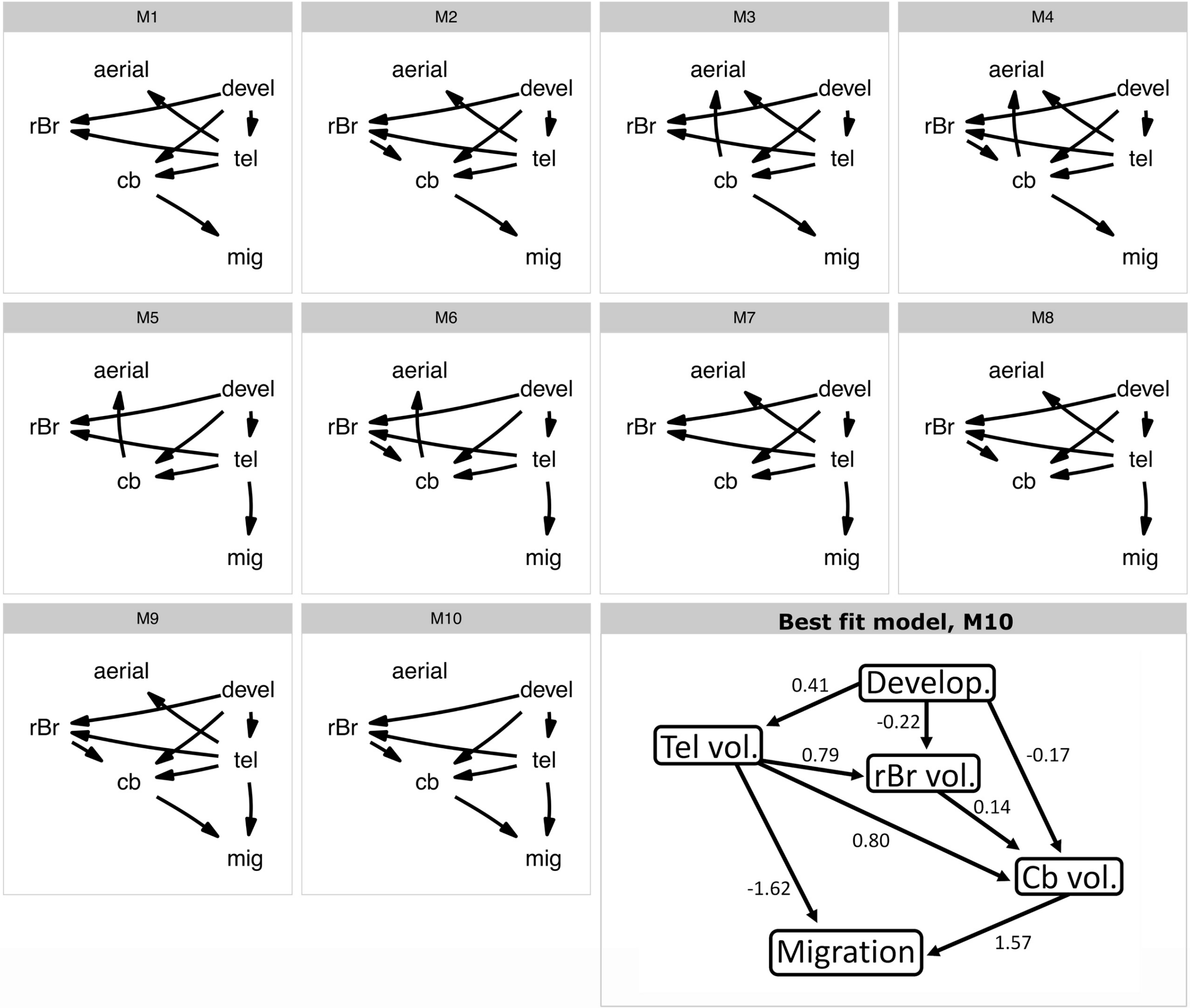

Figure 3.4. Hypothetical models (M1-M10) based on our trait predictors, and brain region sizes. The best-fitting model ('Best fit model, M10') is depicted in the figure. Arrows represent hypothetical causal links, and values represent the standardized average coefficients of the causal links from the best-fitting model.

CHAPTER FOUR: VARIATION IN THE VOLUME AND NUMBER OF NEURONS OF THE OCULOMOTOR NUCLEI ACROSS BIRD SPECIES

Abstract

Eye movements are a critical component of visually guided behaviors, allowing organisms to scan the environment and bring stimuli of interest to regions of high receptor density in the retina. Although the control and modulation of eye movements by cranial nerve nuclei are highly conserved within vertebrates, species variation in visually guided behavior and eye morphology could lead to variation in the size of oculomotor nuclei. Here, we test for differences in the size and neuron numbers of the oculomotor nuclei among bird clades that vary in behavior and eye morphology. Using unbiased stereology, we measured the volumes and numbers of neurons of the oculomotor (III), trochlear (IV), abducens (VI), and Edinger-Westphal (EW) nuclei in 67 bird species that vary, or are predicted to vary, in their degree of eye movements. Relative to brainstem volume, owls had smaller III, IV, VI and EW nuclei than other birds, which reflects their limited degrees of eye movements, and lack of observable accommodation and pupillary reflexes. In contrast, VI was relatively larger in falcons, hawks, and vultures. The expansion of VI in these predatory or scavenging species might be related to shifting focus between the nasal and temporal foveae during different stages of foraging and prey capture. However, unlike comparisons of neuron numbers in most other brain regions, grade shifts in the size of III, IV, VI or EW nuclei were rarely reflected changes in neuron numbers. The lack of a clear association between volumetric changes in the oculomotor nuclei and number of neurons suggests that at least some brainstem nuclei evolve differences in relative size through other mechanisms, such as neuron size or neuropil volume.

Introduction

Eye movements are important for a wide range of behaviours, including detection of predators and food items, visual communication, and movement through the environment. Mobile eyes enable organisms to scan the environment and bring stimuli of interest to regions of high receptor density on the retina (Moore et al. 2017). Convergent eye movements permit binocular visual field overlap and stereoscopic vision (Pettigrew 1986; Martin 2009), which can be critical for prey capture (Fox et al. 1977; Wallman and Pettigrew 1985; Moroney and Pettigrew 1987; Iwaniuk and Wylie 2020). Divergent eye movements reduce the size of blind areas in the visual field (Land et al. 1999; Martin 2007; Land 2015; Land 2019) enabling a broader overall view that can be important for predator detection (Wallman and Pettigrew 1985). Finally, moving through the environment (i.e., self-motion) often requires compensatory eye movements that stabilize the image on the retina (Collewijn et al. 1983; Wylie and Frost 1996). Not only do eye movements vary in size, magnitude, and direction across these different functions, they also vary among species. For example, chameleons move both eyes at high degrees (up to 180°), whereas frogs and toads lack spontaneous eye movements (Walls 1962; Gioanni et al. 1993; Pettigrew et al. 1999; Land 2015; Land 2019).

Within birds, eye movements also vary in magnitude (Martin 2007); some songbirds have eye movements greater than 60° whereas owls have little to no eye movement (Table 4.1) (Steinbach and Money 1972; Steinbach et al. 1974; Martin 2007; Moore et al. 2013; Moore et al. 2015). The degree of eye movement present is thought to be associated with the dimensions of the visual field and retinal topography in birds (Martin 2009; Moore et al. 2017). The visual field is the three-dimensional space around the head in which an animal can see and depends on the position of the eyes in the skull and eye movements (Martin 2017). In owls, a broad binocular visual field (Martin 1984; Wylie et al. 1994; Martin 2009) is associated with frontally oriented eyes that are largely immobile (Walls 1942; Steinbach and Money 1972; Hughes 1979; Hall and Ross 2007; Lisney et al. 2012a) and a retina with a single, temporal, high density region of retinal ganglion cells (Wood 1917; Wathey and Pettigrew 1989; Lisney et al. 2012a). In many bird species, eye movements play an important role in changing the visual fields from monocular to binocular (Martin 2007). For example, the tawny frogmouth (*Podargus strigoides*) can diverge its eyes to enable broad, lateral vision and then converge its eyes to create greater binocular overlap, allowing better depth perception for prey capture (Wallman and Pettigrew 1985). Eye movements can also be important for shifting focus between regions of high retinal ganglion cell density, such as bifoveate species (Wallman and Pettigrew 1985; Moroney and Pettigrew 1987). Thus, extraocular movements are important for changing the dimensions of visual field and dynamically bringing visual stimuli into, and even between, specialized regions of the retina.

The degree of pupillary constriction and lens/corneal accommodation varies among bird species as well (Walls 1942; Murphy and Howland 1983; Sivak et al. 1985; Wagner and Schaeffel 1991; Glasser and Howland 1996; Glasser et al. 1997; Martin 1999). The change in pupillary constriction is important for the control of retinal image brightness and depth of field, ensuring that sensitivity and/or resolution are maximized according to light levels (De Groot and Gebhard 1952; Martin and Katzir 1994b; Glasser and Howland 1996; Jonson et al. 1997; Martin 1999). Diving birds, for example, have pupils that vary more in size than other species, which is thought to reflect differences in light levels experienced during underwater foraging compared to the surface (Sivak et al. 1985; Martin 1999). Just like pupillary constriction, the range of lens accommodation also varies greatly across species from low in owls and kiwi to high in diving ducks and cormorants (Murphy and Howland 1983; Sivak et al. 1985; Glasser et al. 1997; Katzir and Howland 2003; Machovsky-Capuska et al. 2012). This interspecific variation reflects different foraging strategies, such as the need to compensate the loss of corneal refractive power in species that engage in underwater pursuit of prey (Walls 1942; Sivak 1980; Ott 2006). Thus, just as extraocular eye movements reflect behaviour, so do the movements generated by the intraocular muscles.

Extraocular eye movements, pupillary constriction and lens/corneal accommodation are controlled and modulated by the oculomotor, trochlear, and abducens nerves and their associated brainstem nuclei (Büttner-Ennever 2006). Despite the aforementioned interspecific variation in eye movements, quantitative data among species on the size and number of neurons within the brainstem nuclei responsible for eye movements are lacking. If the principle of proper mass (Jerison 1973) applies to eye movements in the same way as sensory systems (Wylie et al. 2015), then the size of the nuclei, and number of neurons within them, will vary with the magnitude of eye movements, pupillary constriction, and accommodation reflex across species. Here, we measured the four brainstem nuclei that control eye movements, the oculomotor, abducens, trochlear, and Edinger-Westphal nuclei, in 67 bird species to test this hypothesis. Based on the interspecific variations in eye movements, visual field, and retinal topography, we had several specific predictions. First, predatory species with two regions of retinal specialization, such as falcons, hawks, and kingfishers (Walls 1942; Fite and Rosenfield-Wessels 1975; Wallman and Pettigrew 1985; Moore et al. 2017; Potier et al. 2020), will have relatively large nuclei with more neurons than other species in order to shift focus between lateral and frontal vision. Second, owls will have relatively small nuclei with few neurons because their eye movements are limited (Steinbach and Money 1972; Steinbach et al. 1974; Glasser and Howland 1996; Glasser et al. 1997) and they lack accommodative power (Howland et al. 1991; Glasser and Howland 1996;

Glasser et al. 1997). Last, species with high accommodative power, such as pursuit divers (Sivak 1980; Katzir and Howland 2003; Machovsky-Capuska et al. 2012), will have an enlarged Edinger-Westphal nucleus, the brainstem nucleus responsible for accommodation (Marwitt et al. 1971; Pilar and Tuttle 1982; Gamlin and Reiner 1991).

Material and Methods

Specimens

We measured brain regions in 67 avian species representing a total of 15 orders (Table 4.2). Following the guidelines of the Canada Council for Animal Care, our specimens were donated from wildlife sanctuaries, veterinary clinics in Australia, or hunters in Canada and New Zealand. The heads of these specimens were immersion fixed in 4% buffered paraformaldehyde for at least two weeks. The brains were extracted, weighed and stored in paraformaldehyde until being processed. For histology, brains were cryoprotected in 30% sucrose in 0.1 M phosphate buffer until they sank, embedded in gelatin and sectioned on a freezing stage microtome in the sagittal plane at a thickness of 40 mm and every section collected in 0.1 M phosphate buffered saline. Every other section, or every fourth section (1:2 series, or 1:4 series) depending on the species (see below), was mounted onto gelatinized slides, stained with thionin acetate, dehydrated through a graded ethanol series, cleared in Hemo-De (Thermo Fisher Scientific, #HD-150) and coverslipped with Permount (Thermo Fisher Scientific, #SP15-150).

For each specimen, we measured all four of the brainstem nuclei that control and modulate the intra- and extra-ocular muscles: the Edinger-Westphal nucleus (EW), oculomotor nucleus (III), trochlear nucleus (IV), and abducens nucleus (VI) (Figure 4.1). In contrast to the mammalian EW (Kozicz et al. 2011), the avian EW is dorsolateral to the III (Figure 4.2) and contains only pre-ganglionic neurons (Gamlin and Reiner 1991; Reiner et al. 1991). The neurons within EW innervate the ciliary ganglion, which controls the lens, cornea, pupil and choroidal blood vessels (Marwitt et al. 1971; Pilar and Tuttle 1982; Fitzgerald et al. 1990; Gamlin and Reiner 1991; Reiner et al. 1991). The oculomotor nucleus (III) consists of three distinct subregions (ventral, dorsomedial, dorsolateral; see Figure 4.1), each of which innervates different extraocular muscle(s). The dorsolateral sub-nucleus projects ipsilaterally to the inferior rectus, whereas the dorsomedial sub-nucleus projects ipsilaterally to the medial rectus (Heaton and Wayne 1983). The ventral sub-nucleus sends ipsilateral projections to the inferior oblique and contralateral projections to the superior rectus (Heaton and Wayne 1983). Finally, the trochlear nucleus (IV) projects contralaterally to the superior oblique muscle (Sohal and Holt 1978), while the abducens nucleus (VI) projects ipsilaterally to the lateral rectus muscle (Labandeira-Garcia et al. 1987).

The extraocular eye muscles share a similar three-dimensional reference frame as the semicircular canals (Wylie and Frost 1996; Voogd and Wylie 2004). More specifically, horizontal recti eye muscles are aligned with the horizontal canal, vertical recti are aligned with the anterior canal, and oblique muscles are aligned with the posterior canal (Wylie and Frost 1996). This means that the action of eye muscles is best described according to the axes of the semicircular canals (Wylie and Frost 1996). Although every eye movement involves the action of all extraocular muscles, the contraction of the inferior rectus (dorsolateral III) and superior rectus (ventral III) mainly causes depression and elevation, respectively; the contraction of the medial rectus (dorsomedial III) causes adduction with little vertical displacement, and contraction of the lateral rectus (VI) causes abduction and depression (Walls 1942; Wylie and

Frost 1996). The contraction of the superior (IV) and inferior (ventral III) oblique muscles mainly causes elevation, depression, and torsional eye movements (Walls 1942; Walls 1962).

Stereological measurements

We measured the volumes of the whole brain, brainstem, and all four brainstem nuclei (III, IV, VI, and EW), as well as the three subregions of III (see above), using the Cavalieri method, as implemented in StereoInvestigator software (Microbrightfield Inc., VT, USA), with a 10x objective (n.a.= 0.05) on a Zeiss Axio Imager 2 microscope (Table 4.2). We measured every second section (1:2 series) of all species, except for the Swainson's hawk (*Buteo swainsonii*) and the larger owls, which were mounted in a 1:4 series, and the vulture species, which were mounted in a 1:10 series. EW could not be identified in all owl species (see Results) and due to brainstem damage VI could not be measured in the Canada goose (*Branta canadensis*). Otherwise, the four nuclei were identified and quantified. Finally, as a scaling variable, we measured the brainstem, which was defined as the combined volumes of the diencephalon, tegmentum, pons and medulla (*sensu* Iwaniuk and Hurd 2005; Corfield et al. 2016).

In addition to region volumes, we also estimated neuron numbers within all four nuclei and the subregions of III: dorsolateral III, dorsomedial III, ventral III, EW, IV, and VI. Only cells with intact, continuous cell membranes and clearly visible nuclei were counted. Neuron numbers were estimated using the optical fractionator method implemented in StereoInvestigator software (Microbrightfield Inc., VT, USA), with a 40x objective (n.a.=0.95) on a Zeiss Axio Imager 2 microscope. The sampling interval was the same as that for the volumetric measurements (see above) and frame size (40x40 μm) and grid size (50x50 μm) remained constant for all species. To account for lost caps (Gardella et al. 2003), we used guard zones of 7 μm. The coefficients of error (CE) of neuronal counts (Gundersen et al. 1999), defined as the standard error of the mean of repeated estimates divided by the mean (Microbrightfield Inc., VT; USA), were all equal to or below 0.10.

Retinal topography

Given that species with two foveae are thought to have higher degrees of eye movement (Moore et al. 2017), we tested whether relative volume and number of neurons of the oculomotor nuclei differed among different types of retinal topographies. Data on retinal topography were collated from the literature (see Table 4.5) and species were categorized as having a retina of one of seven types: (1) area centralis, (2) area temporalis, (3) central fovea, (4) temporal fovea, (5) area centralis and area nasalis, (6) central fovea and area temporalis or (7) two foveae. Although descriptions of retinal topography were not available for all of the falcons and hawks included in our study, we assumed that they were all bifoveate based on description of congeners (Walls 1942; Potier et al. 2018; Potier et al. 2020; see Table 4.5). We tested for differences among the aforementioned categories as well as the following groups of categories: species with one specialized region *vs*. species with two specialized regions in the retina; afoveate *vs*. foveate species; and bifoveate *vs*. all other species.

Data analyses

Because of common ancestry, closely related species are expected to have more traits in common (Garamszegi 2014). We therefore used a phylogenetic generalized least squares (PGLS) approach for all of our analyses. All quantitative volumetric data and neuron numbers were log-transformed; statistical analyses were performed in R 4.0.3 (R Team 2020) by using the pgls function in *caper* (Orme et al. 2013) and *nlme* (Pinheiro et al. 2006) and obtaining maximum likelihood estimations of Pagel's λ (Pagel 1999). We extracted 1,000 fully resolved trees from birdtree.org (Jetz et al. 2012), using an Ericson et al. (2006) backbone phylogeny, and built a maximum clade credibility tree using *phangorn* (Schliep 2011). The consensus phylogenetic tree was used for all PGLS analyses, and phylogenetic analyses of covariance (pANCOVA) were performed to test for significant differences in nucleus volume and neuron numbers among clades and retinal topography categories.

Results

Cytoarchitecture of the oculomotor nuclei

The morphology of nuclei III, IV and VI was relatively similar across clades. For every species examined, we were able to subdivide III into three recognizable, different groups of cells: dorsomedial III, dorsolateral III and ventral III (Figs. 4.1, 4.2). The EW was located dorsolaterally to nucleus III in all species (Fig. 4.2) and the neurons were typically smaller than those in III, IV and VI. Of the eight owl species examined, EW could only be identified in the three largest species: great horned owl (*Bubo virginianus*), snowy owl (*Bubo scandiaca*), and great grey owl (*Strix nebulosa*) (Table 4.2; Fig. 4.2). For the other owl species, we were not able to identify in Nissl stained sections any structure as EW (Fig. 4.2E). This is not to say that EW neurons do not exist in these species, but rather that a distinct EW nucleus, as defined in other species, was not recognizable.

Oculomotor nucleus (nIII)

The different subregions of the oculomotor nucleus (III) varied in size with negative allometry relative to the rest of the brainstem (slopes range: 0.909-0.929; Table 4.4; Fig. 4.3). The numbers of neurons in the nIII subregions increased with brainstem size with a lower slope than that of the volumes (slopes range: 0.378-0.432) and had lower correlation coefficients (<0.639; Table 4.4; Fig. 4.4). As expected, volumes and neuron numbers were significantly correlated with one another, with neuron numbers explaining 79-88% of the variation in volume (Table 4.4; Fig. 4.5).

Across avian orders, owls had significantly smaller nIII volumes, with fewer neurons, relative to brainstem volume, for all of the subregions of III (pANCOVA, all $p<0.02$; no slope differences; Fig. 4.3, 4.4). At the other end of the spectrum, falcons had more neurons in both dorsomedial and dorsolateral regions of III relative to brainstem volume (pANCOVA, all $p< 0.01$, Table 4.4, Fig. 4.4A-D). Similarly, the two falcons in our sample also had more neurons in the dorsomedial and dorsolateral of III relative to the volumes of each subregion (pANCOVA, all $p=0.04$; no slope differences; Fig. 4.5A-D). We did not, however, detect any significant differences in relative nucleus size or neuron numbers among retinal topography categories, regardless of which statistical comparisons were made.

Trochlear nucleus (nIV)

In a similar fashion to III, the size and number of neurons of the trochlear nucleus (IV) varied with negative allometry relative to brainstem size, but the slope for neuron numbers (0.428) was much lower than that of IV volume (0.902; Table 4.4; Fig. 4.6A-D). The number of neurons explained 73% of the variation in the volume of IV (Table 4.4, Fig. 4.6E-F).

Across orders, owls had smaller IV volumes (pANCOVA, p<0.01; no slope differences; Fig. 4.6A-B) than other birds, relative to brainstem volume. However, we did not detect any significant differences among orders for the number of neurons of IV relative to the brainstem volume (Fig. 4.6C-D). Differently from what we expected from the volume of IV, owls have more neurons relative to IV volume than other birds (pANCOVA, p<0.01; no slope differences; Fig. 4.6E-F). Last, we found no significant differences according to retinal categories, regardless of which comparisons were made.

Abducens (VI)

The abducens nucleus (VI) repeats the same general pattern of allometric scaling found in both III and IV: its volume and number of neurons scaled with negative allometry relative to brainstem volume with a lower slope for neuron numbers (Table 4.4; Fig. 4.7A-D). The number of neurons in VI explained approximately 69% of the variation in volume (Table 4.4, Fig. 4.7E-F).

Across orders, owls had overall smaller VI relative to the size of the brainstem than other birds (pANCOVA, p=0.01; Fig. 4.7A-B). Conversely, hawks, falcons, and vultures had relatively larger VI volumes than other birds (pANCOVA, p=0.04, p=0.04, p=0.02, respectively; no slope differences; Fig. 4.7A-B). Although there were no significant differences among orders in neuron numbers of VI relative to brainstem volume (Fig. 4.7C-D), songbirds differed in the number of neurons relative to the volume of VI. That is, songbirds had relatively more neurons in VI than other birds (pANCOVA, p=0.02; no slope differences; Fig. 4.7E-F). Last, there was no significant differences in any measurements of VI among retinal topography categories, regardless of which comparisons were made.

Edinger-Westphal (EW)

The volume of the Edinger-Westphal nucleus (EW) scaled with brainstem volume with a similar slope to III, IV, and VI, but had a lower correlation coefficient (Table 4.4; Fig. 4.8A-B). This was also true for the number of neurons relative to brainstem volume, which had an even lower correlation coefficient (Table 4.4; Fig. 4.8C-D). The number of neurons in EW explained 75% of the variation in volume (Table 4.4, Fig. 4.8E-F).

As discussed above, the majority of owl species lack a recognizable EW nucleus and we could only quantify EW in the three largest species: great horned owl, snowy owl, and great grey owl. For these three species, relative to the size of the brainstem, EW volume was significantly smaller than other bird orders (pANCOVA, $p<0.01$; no slope differences; Fig. 4.8A-B), but no significant differences were detected between owls and others birds for the number of neurons (pANCOVA, $p>0.05$; Fig. 4.8C-D). Apart from owls, songbirds also differed significantly from other birds in the relative volume and/or number of neurons of EW. Songbirds have relatively larger EW volumes (pANCOVA, $p<0.01$; no slope differences; Fig. 4.8A-B) as well as relatively more neurons compared with brainstem volume (pANCOVA, $p<0.01$; no slope differences; Fig. 4.8C-D) and EW volume (pANCOVA, $p<0.01$; Fig. 4.8E-F). Overall, waterfowl did not differ significantly from other birds, but once restricting our comparisons only to waterfowl, the red-breasted merganser (*Mergus serrator*) stood out as having a considerably larger EW, with more neurons, relative to the size of the brainstem (Fig. 4.9). Last, there were no significant differences in relative EW volume or neuron numbers among the retinal topography categories.

Discussion

Overall, our results yielded several differences in the relative volume and number of neurons of the oculomotor nuclei among clades, some of which supported our predictions. For example, relative to the size of the brainstem, owls had relatively small III, IV, VI, and EW volumes, and hawks, falcons, and vultures had relatively larger VI volumes than other birds. However, differences in relative volumes were not always supported by differences in neuron numbers, and retinal topography was unrelated to interspecific variation in volumes or neuron numbers. Given the dearth of information on eye movements and degrees of pupillary constriction and accommodation across species, some of these clade differences are difficult to intepret, but likely reflect oculomotor strategies (e.g., eye movements or head movements) and foraging behaviour, as discussed below.

Nucleus VI and EW in Songbirds

Songbirds had unexpectedly higher neuronal densities in nucleus VI (Figs. 4.7E-F) as well as a larger EW, with more neurons relative to the size of the brainstem and EW volume, than other clades (Fig. 4.8). Assuming that the principle of proper mass (Jerison 1973) applies to the neural control of eye movements, these results suggest that songbirds may be capable of faster, more precise, and/or broader range of eye movements mediated by VI (i.e., abduction) as well as a broader pupillary reflex range and/or higher accommodative power (both controlled by EW). Based on the ophthalmoscope technique, many songbird species have saccadic eye movements of greater magnitude than other clades, with some species exceeding 50° (Table 4.1). VI is responsible for horizontal saccades (Fuchs and Luschei 1970; Baker and Spencer 1981; Delgado-Garcia et al. 1986; Donaldson and Knox 1991), which could at least partially explain why songbirds have an enlarged VI. There is also some evidence that songbirds have relatively high accommodative power (Martin 1986; Glaeser and Paulus 2015). To bring an object into focus at a starling's (*Sturnus vulgaris*) bill tip, an accommodation power of 29 diopters (D) is required (Martin 1986), a magnitude considerably higher than that calculated in most other avian species (Levy and Sivak 1980; Glasser et al. 1997). Thus, the need to alter focus from the surrounding environment to the bill tip, could place greater demands on EW in at least some songbirds. Why songbirds would require this accomodative power, or broader saccades, than other pecking species, like pigeons or galliforms, is unclear and highlights the need for more detailed information on eye movements and accommodation reflexes across bird species.

It is worth noting that although songbirds had enlarged and/or more neurons in VI and EW nuclei on average, songbirds were also more variable in these measurements than other clades (Figs. 4.7-4.8). Our songbird data set is sparse compared to the diversity of extant songbirds, but nevertheless includes a range of species that vary in diet, foraging behaviour, and habitat, any or all of which could be associated with species differences in eye movements and/or brain anatomy. As an example of this diversity, our largest species, the Australian magpie (*Gymnorhina tibicen*), forages primarily on the ground and preys upon invertebrates and small vertebrates in addition to carrion and fruit as part of its ominivorous diet (Brown and Veltman 1987; Barker and Vestjens 1990). The Australian magpie is therefore likely using different oculomotor strategies than other songbird species, like chickadees (*Poecile* spp.), which forage in trees and shrubs for small invertebrates and seeds (Morse 1970; Otter 2007). How EW anatomy and function might relate to this kind of variation in behaviour and ecology is unknown, but songbirds might be an appropriate group to investigate this further given the variation in EW size and neuron numbers we found (Fig. 4.8).

Pursuit diving

Many diving birds that actively pursue prey underwater have greater accommodative power than that of other species. For example, while cormorants have an accommodative range of 50-65 D (Glasser and Howland 1996; Katzir and Howland 2003; Strod et al. 2004), non-diving birds tend to have accommodative ranges of no more than 10 D (Sivak et al. 1985; Glasser and Howland 1996; Glasser et al. 1997). In fact, the highest accommodative range reported thus far occurs in some diving ducks (Sivak et al. 1985). Thus, based on species differences in accommodative range, we predicted that pursuit diving species would have an enlarged EW. In our data set, we only had a single pursuit diving species, the red-breasted merganser (*Mergus serrator*). Although waterfowl overall did not differ from other clades in terms of EW volume or neuron numbers, the merganser was an outlier relative to other waterfowl (Fig. 4.9). Sivak et al. (1985) reports that the closely related hooded merganser (*Lophodytes cucullatus*) dramatically increases the refractive power of its eyes through powerful accommodative changes in the lens of up to 90 D. Given that the red-breasted merganser is also a pursuit diver (Nilsson 1970; Johnsgard 2010), it probably has high accommodative power and this is associated with an enlarged EW. We therefore predict a similar enlargement of EW in other pursuit divers with high accommodative power, such as cormorants and gannets (Katzir and Howland 2003; Strod et al. 2004; Machovsky-Capuska et al. 2012), but suitable neuroanatomical material for this species is currently wanting.

Smaller oculomotor nuclei in owls

Owls have lower degrees of eye movements, accommodation, and pupillary change than other birds (Walls 1942; Rochon-Duvigneaud 1943; Duke-Elder 1958; Steinbach and Money 1972; Hughes 1979; Glasser et al. 1997; Lind et al. 2008), which likely stems from the unique tubular shape of their eyes and the shape and orientation of the orbits (Walls 1942; Steinbach and Money 1972; Hughes 1979; Martin 1984). In fact, several owl species appear to lack accommodation (Glasser et al. 1997), including two of the species examined in this study: the short-eared owl (*Asio flammeus*) and snowy owl (*Bubo scandiaca*). Based on the general lack of eye movements and poor accomodative and pupillary reflexes, we predicted that owls would have relatively smaller III, IV, VI and EW nuclei and our data support this prediction.

EW was not only small in owls, it was impossible to identify in the smaller owl species we sampled (Table 4.2; Fig. 4.2). We emphasize, however, that the apparent absence of EW in some of our owl species does not necessarily mean that this nucleus is entirely missing. On the contrary, degrees of accommodation, and pupillary constriction, even if minimal, must occur in owls (Howland et al. 1991; Wagner and Schaeffel 1991; Schaeffel and Wagner 1992; Glasser et al. 1997; Lind et al. 2008), and therefore putative EW neurons are present, they just cannot be identified by Nissl-staining as an organized EW nucleus. Similar observations were made of the isthmo-optic nucleus of some seabirds, which lack a recognizable isthmo-optic nucleus in Nissl stained tissue (Gutiérrez-Ibáñez et al. 2012). Just as it is unlikely that these seabirds lack an isthmo-optic nucleus, the smaller owls have EW neurons that are involved in accommodation and pupillary reflexes, they are simply not organized in a discrete nucleus that can be identified in our tissue samples.

Although the volumes of nuclei III, IV, and VI were relatively small in owls, the number of neurons, relative to brainstem size, did not differ from other birds for nuclei IV and VI (Figs. 4.6, 4.7). This is unexpected because species differences in brain region volumes are typically due to changes in neuron numbers (Herculano-Houzel et al. 2014; Corfield et al. 2016; Cunha et al. 2020). Although we were not able to measure neuron soma size accurately within these nuclei, owls had higher neuronal densities in IV than other birds (Figs. 4.6E,F). Our results therefore suggest that the reduction in IV and VI in owls is due to smaller neurons and/or neuropil and not fewer neurons. These results are congruent with quantitative studies on other brainstem nuclei (e.g., facial nucleus) suggesting that motoneuron size directly reflects recruitment of motor units (Binder et al. 1983; Welt and Abbs 1990; Sherwood 2005) such that larger motoneurons supply faster, well-developed muscles (Welt and Abbs 1990). For example, primate species that execute complex facial expressions have larger nuclei, but do not have proportionally more neurons (Sherwood 2005; Sherwood et al. 2005). Our results represent another example of brainstem nuclei directly projecting to muscles in which grade shifts in volume are not driven by neuron numbers. Together, our results and those of Sherwood (2005), suggest that the expansion of some brainstem regions reflects neuron size more than neuron numbers, as discussed further below.

Larger VI in falcon, hawks and vultures

We predicted that bifoveate predatory birds would have enlarged III, IV, VI and EW nuclei, with more neurons, as these birds are expected to have larger degrees of eye movements (Moore et al. 2017) and often need to focus dynamically on moving prey (Potier et al. 2018; Potier et al. 2020). Contrary to our prediction, not all predatory species had enlarged nuclei and the two clades that did, hawks and falcons, only have an enlarged VI. Despite not being predatory and bifoveate, vultures also appeared to have an enlarged VI, just as we observed in hawks and falcons.

One potential reason for the lack of enlarged nuclei in some predatory, bifoveate species is that different species use different strategies to shift focus between specialized regions of the retina (Moroney and Pettigrew 1987; O'Rourke et al. 2010a; O'Rourke et al. 2010b). Supporting evidence for this explanation is provided by variation in both the position of the temporal fovea relative to the central fovea and the degree of eye movements observed across species (Wallman and Pettigrew 1985; Moroney and Pettigrew 1987). For example, the temporal foveae of kingfishers are frontally aligned with the beak axis such that binocular vision can be accomplished with eye movements of low amplitude (Moroney and Pettigrew 1987). In contrast, the temporal foveae of hawks and related species are not frontally directed or aligned with the beak, resulting in larger eye movements to align the foveae (Moroney and Pettigrew 1987). In addition to this variation in the amplitude of eye movement across bifoveate species, neck and/or head movements can be more effective in shifting visual stimuli to different regions of the retina than moving both eyes in some species (Knudsen and Konishi 1979; Knudsen and Knudsen 1985; Wallman and Pettigrew 1985; Moroney and Pettigrew 1987; O'Rourke et al. 2010a; O'Rourke et al. 2010b). Thus, simply having more than one specialized area in the retina does not necessarily mean higher degrees of eye movements (Moroney and Pettigrew 1987) and similarly being a bifoveate, predatory species is not always associated with larger oculomotor nuclei.

Despite the lack of a general pattern for all bifoveate, predatory species, it was clear that hawks and falcons have a larger oculomotor nucleus (III). Hawks and falcons were at the upper end of the distribution for the relative volume of all three subdivisions of III (Figure 4.4), but did not differ significantly from other clades. Although not shown in the results, this was also apparent when we considered the entire oculomotor nucleus rather than the individual subregions (Fig. 4.10). Because diurnal raptor species are represented in our study by relatively few species, we can not negate the possibility that III is significantly larger in hawks and falcons. Somewhat unexpectedly, falcons did have significantly more neurons in the dorsomedial and lateral subdivisions (Figure 4.5). The lack of sufficient data on eye movements and visual abilities in diurnal raptors (Potier et al. 2020) makes it difficult to determine why falcons and hawks are different in neuron numbers. Moroney and Pettigrew (1987) suggest that falcons rely more on head and neck movements than eagles, but one would then predict smaller nuclei in falcons rather than more neurons. Nevertheless, the fact that we found some differences in the relative size and neuron numbers of the oculomotor nuclei among or within hawks and falcons reinforces the idea that predatory birds are highly variable in their ecology, hunting behaviour, and visual requirements, as recently observed by Potier et al. (2020). Regardless of the potential functional consequences of more neurons, treating all diurnal predatory birds as a homogenous, uniform clade is unlikely to be appropriate to examining sensory system anatomy and function and there is clearly a need to better understand vision and eye movements in raptors.

Hawks, falcons, and vultures had systematically enlarged VI, relative to the size of the brainstem, which could reflect the need for extra degrees of eye movements when foraging or scavenging (e.g., detecting prey; Wallman and Pettigrew 1985; Moroney and Pettigrew 1987; O'Rourke et al. 2010a). Abduction of the eyes would assist in projecting the image onto the central fovea, typically the region with the highest visual acuity (Fite and Rosenfield-Wessels 1975; Reymond 1985; Bringmann 2019). Further, a larger VI could facilitate quicker and/or a broader amplitude of eye movement enabling hawks and falcons to shift between divergent and convergent eye positions during different phases of foraging and prey capture. Although New World vultures are not bifoveate in a strict sense, they do have two areas of retinal specialization: a central fovea and an area temporalis (Inzunza et al. 1991; Lisney et al. 2013a). They too might need to switch between these regions when foraging for carrion, requiring similar types of eye movements to falcons and hawks and therefore also sharing an enlarged VI.

The enlargement of VI in hawks, falcons, and vultures did not, however, reflect changes in the relative number of neurons (Figs. 4.7A-D). Thus, the relatively small nuclei of owls is not due to proportionally fewer neurons (Figs. 4.7C-D) and the enlargement of EW in the merganser (Fig. 4.9) and VI in falcons, hawks, and vultures (Figs. 4.7A-B) are not due to proportionally more neurons. Combined with the data from Sherwood (2005), this suggests that changes in neuron size (or neuropil) are responsible for evolutionary differences in the relative size of brainstem motor nuclei and that adding neurons is not the only way to increase the relative size of a brain region. As discussed above, larger neurons potentially enable faster and/or larger muscles (Welt and Abbs 1990) and this could be a general pattern common to brainstem motor nuclei.

Conclusions

Based on our analyses, some of the volumetric changes in the oculomotor nuclei examined yielded the principle of proper mass, such as the relatively small nuclei of owls and enlarged VI in falcons and hawks. Although retinal configuration was not associated with changes in the oculomotor nuclei anatomy, variation in the relative sizes of the oculomotor nuclei within avian clades (e.g., waterfowls) suggests that species ecological differences related somehow to visually guided behaviour do reflect changes in oculomotor nuclei sizes. However, as emphasized above, there is a dire need for more information on visual strategies and eye movements in birds, including accommodation and pupillary reflex. With more detailed, complete data on the visual system of birds, particularly predatory bifoveate species, it will be possible to determine how visually guided behaviours shape the anatomy of the oculomotor nuclei. Last, grade shifts in the relative size of the oculomotor nuclei were not necessarily driven by the numbers of neurons. Our results therefore suggest that neuron size/neuropil play an important role in volumetric changes of brainstem nuclei as well as function.

References

Baker, R. and R. Spencer. 1981. Synthesis of horizontal conjugate eye movement signals in the abducens nucleus. Jap. J. EEG & EMG Suppl. 7,49-59.

Barker, R. D. and W. J. M. Vestjens. 1990. The food of Australian birds 2. Passerines. CSIRO Publishing, Clayton.

Binder, M. D., P. Bawa, P. Ruenzel, and E. Henneman. 1983. Does orderly recruitment of motoneurons depend on the existence of different types of motor units? Neuroscience Letters 36:55-58.

Binggeli, R. L. and W. Paule. 1969. The pigeon retina: quantitative aspects of the optic nerve and ganglion cell layer. Journal of Comparative Neurology 137:1-18.

Bischof, H.-J. 1988. The visual field and visually guided behavior in the zebra finch (*Taeniopygia guttata*). Journal of Comparative Physiology A 163:329-337.

Bloch, S., S. Rivaud, and C. Martinoya. 1984. Comparing frontal and lateral viewing in the pigeon. III. Different patterns of eye movements for binocular and monocular fixation. Behavioural Brain Research 13:173-182.

Bringmann, A. 2019. Structure and function of the bird fovea. Anatomia, Histologia, Embryologia 48:177-200.

Brown, E. D. and C. J. Veltman. 1987. Ethogram of the Australian magpie (*Gymnorhina tibicen*) in comparison to other Cracticidae and Corvus species. Ethology 76:309-333.

Büttner-Ennever, J. A. 2006. The extraocular motor nuclei: organization and functional neuroanatomy. Progress in Brain Research 151:95-125.

Cantlay, J. C., S. J. Portugal, and G. R. Martin. 2019. Visual fields and foraging ecology of Blacksmith Lapwings *Vanellus armatus*. Ibis 161:895-900.

Coimbra, J. P., S. P. Collin, and N. S. Hart. 2014. Topographic specializations in the retinal ganglion cell layer correlate with lateralized visual behavior, ecology, and evolution in cockatoos. Journal of Comparative Neurology 522:3363-3385.

Collewijn, H., A. Martins, and R. Steinman. 1983. Compensatory eye movements during active and passive head movements: fast adaptation to changes in visual magnification. The Journal of Physiology 340:259-286.

Corfield, J. R., B. Long, J. M. Krilow, D. R. Wylie, and A. N. Iwaniuk. 2016. A unique cellular scaling rule in the avian auditory system. Brain Structure and Function 221:2675-2693.

Cunha, F., K. Racicot, J. Nahirney, C. Heuston, D. R. Wylie, and A. N. Iwaniuk. 2020. Allometric scaling rules of the cerebellum in galliform birds. Brain, Behavior and Evolution 95:78-92.

De Groot, S. and J. Gebhard. 1952. Pupil size as determined by adapting luminance. JOSA 42:492-495.

Delgado-Garcia, J., F. Del Pozo, and R. Baker. 1986. Behavior of neurons in the abducens nucleus of the alert cat—I. Motoneurons. Neuroscience 17:929-952.

Demery, Z. P., J. Chappell, and G. R. Martin. 2011. Vision, touch and object manipulation in Senegal parrots *Poicephalus senegalus*. Proceedings of the Royal Society B: Biological Sciences 278:3687-3693.

Dolan, T. and E. Fernández-Juricic. 2010. Retinal ganglion cell topography of five species of ground-foraging birds. Brain, Behavior and Evolution 75:111-121.

Donaldson, I. and P. C. Knox. 1991. Afferent signals from pigeon extraocular muscles modify the vestibular responses of units in the abducens nucleus. Proceedings of the Royal Society of London. Series B: Biological Sciences 244:233-239.

Duke-Elder, S. 1958. System of Ophthalmology Vol. 1 The Eye in Evolution: Henry Kimpton.

Ericson, P. G., C. L. Anderson, T. Britton, A. Elzanowski, U. S. Johansson, M. Källersjö, J. I. Ohlson, T. J. Parsons, D. Zuccon, and G. Mayr. 2006. Diversification of Neoaves: integration of molecular sequence data and fossils. Biology Letters 2:543-547.

Fernández-Juricic, E., P. E. Baumhardt, L. P. Tyrrell, A. Elmore, S. T. DeLiberto, and S. J. Werner. 2019. Vision in an abundant North American bird: the red-winged blackbird. The Auk 136:ukz039.

Fernández-Juricic, E., M. D. Gall, T. Dolan, C. O'Rourke, S. Thomas, and J. R. Lynch. 2011. Visual systems and vigilance behaviour of two ground-foraging avian prey species: white-crowned sparrows and California towhees. Animal Behaviour 81:705-713.

Fernández-Juricic, E., M. D. Gall, T. Dolan, V. Tisdale, and G. R. Martin. 2008. The visual fields of two ground-foraging birds, house finches and house sparrows, allow for simultaneous foraging and anti-predator vigilance. Ibis 150:779-787.

Fernández-Juricic, E., C. O'Rourke, and T. Pitlik. 2010. Visual coverage and scanning behavior in two corvid species: American crow and western scrub jay. Journal of Comparative Physiology A 196:879-888.

Fite, K. V. and S. Rosenfield-Wessels. 1975. A comparative study of deep avian foveas. Brain, Behavior and Evolution 12:97-115.

Fitzgerald, M., B. A. Vana, and A. Reiner. 1990. Control of choroidal blood flow by the nucleus of Edinger-Westphal in pigeons: a laser Doppler study. Investigative Ophthalmology & Visual Science 31:2483-2492.

Fox, R., S. W. Lehmkuhle, and R. C. Bush. 1977. Stereopsis in the falcon. Science 197:79-81.

Fuchs, A. and E. Luschei. 1970. Firing patterns of abducens neurons of alert monkeys in relationship to horizontal eye movement. Journal of Neurophysiology 33:382-392.

Gaffney, M. F. and W. Hodos. 2003. The visual acuity and refractive state of the American kestrel (*Falco sparverius*). Vision Research 43:2053-2059.

Gall, M. D. and E. Fernández-Juricic. 2010. Visual fields, eye movements, and scanning behavior of a sit-and-wait predator, the black phoebe (*Sayornis nigricans*). Journal of Comparative Physiology A 196:15.

Gamlin, P. D. and A. Reiner. 1991. The Edinger-Westphal nucleus: sources of input influencing accommodation, pupilloconstriction, and choroidal blood flow. Journal of Comparative Neurology 306:425-438.

Garamszegi, L. Z. 2014. Modern Phylogenetic Comparative methods and Their Application in Evolutionary Biology: Concepts and Practice. Springer, London.

Gardella, D., W. J. Hatton, H. B. Rind, G. D. Rosen, and C. S. von Bartheld. 2003. Differential tissue shrinkage and compression in the z-axis: implications for optical disector counting in vibratome-, plastic-and cryosections. Journal of Neuroscience Methods 124:45-59.

Gioanni, H. 1988. Stabilizing gaze reflexes in the pigeon (*Columba livia*). Experimental Brain Research 69:567-582.

Gioanni, H., M. Bennis, and A. Sansonetti. 1993. Visual and vestibular reflexes that stabilize gaze in the chameleon. Visual Neuroscience 10:947-956.

Glaeser, G. and H. F. Paulus. 2015. The Evolution of The Eye. Springer, Berlin.

Glasser, A. and H. C. Howland. 1996. A history of studies of visual accommodation in birds. The Quarterly Review of Biology 71:475-509.

Glasser, A., M. T. Pardue, M. E. Andison, and J. G. Sivak. 1997. A behavioral study of refraction, corneal curvature, and accommodation in raptor eyes. Canadian Journal of Zoology 75:2010-2020.

Guillemain, M., G. Martin, and H. Fritz. 2002. Feeding methods, visual fields and vigilance in dabbling ducks (Anatidae). Functional Ecology 16:522-529.

Gundersen, H., E. Jensen, K. Kiêu, and J. Nielsen. 1999. The efficiency of systematic sampling in stereology—reconsidered. Journal of Microscopy 193:199-211.

Gutiérrez-Ibáñez, C., A. N. Iwaniuk, T. J. Lisney, M. Faunes, G. J. Marín, and D. R. Wylie. 2012. Functional implications of species differences in the size and morphology of the isthmo optic nucleus (ION) in birds. PloS One 7:e37816.

Hall, M. and C. Ross. 2007. Eye shape and activity pattern in birds. Journal of Zoology 271:437-444.

Heaton, M. B. and D. B. Wayne. 1983. Patterns of extraocular innervation by the oculomotor complex in the chick. Journal of Comparative Neurology 216:245-252.

Herculano-Houzel, S. 2017. Numbers of neurons as biological correlates of cognitive capability. Current Opinion in Behavioral Sciences 16:1-7.

Herculano-Houzel, S., P. R. Manger, and J. H. Kaas. 2014. Brain scaling in mammalian evolution as a consequence of concerted and mosaic changes in numbers of neurons and average neuronal cell size. Frontiers in Neuroanatomy 8:77.

Howland, H. C., M. Rowland, K. Schmid, and J. D. Pettigrew. 1991. Restricted range of ocular accommodation in barn owls (Aves: Tytonidae). Journal of Comparative Physiology A 168:299-303.

Hughes, A. 1979. A schematic eye for the rat. Vision Research 19:569-588.

Inzunza, O., H. Bravo, R. L. Smith, and M. Angel. 1991. Topography and morphology of retinal ganglion cells in Falconiforms: A study on predatory and carrion-eating birds. The Anatomical Record 229:271-277.

Iwaniuk, A. N. and P. L. Hurd. 2005. The evolution of cerebrotypes in birds. Brain, Behavior and Evolution 65:215-230.

Iwaniuk, A. N. and D. R. Wylie. 2020. Sensory systems in birds: What we have learned from studying sensory specialists. Journal of Comparative Neurology 528:2902-2918.

Jerison, H. 1973. Evolution of the brain and intelligence. Academic Press, New York.

Jetz, W., G. H. Thomas, J. B. Joy, K. Hartmann, and A. O. Mooers. 2012. The global diversity of birds in space and time. Nature 491:444-448.

Johnsgard, P. A. 2010. Ducks, Geese, and Swans of the World. University of Nebraska Press, Lincoln.

Jonson, A. J., M. Land, D. Osorio, and D.-E. Nilsson. 1997. Relationships between pupil working range and habitat luminance in flies and butterflies. Journal of Comparative Physiology A 182:1-9.

Katzir, G. and H. C. Howland. 2003. Corneal power and underwater accommodation in great cormorants (*Phalacrocorax carbo sinensis*). Journal of Experimental Biology 206:833-841.

Knudsen, E. I. 1982. Auditory and visual maps of space in the optic tectum of the owl. Journal of Neuroscience 2:1177-1194.

Knudsen, E. I. and P. F. Knudsen. 1985. Vision guides the adjustment of auditory localization in young barn owls. Science 230:545-548.

Knudsen, E. I. and M. Konishi. 1979. Mechanisms of sound localization in the barn owl (*Tyto alba*). Journal of Comparative Physiology 133:13-21.

Kozicz, T., J. C. Bittencourt, P. J. May, A. Reiner, P. D. Gamlin, M. Palkovits, A. K. Horn, C. A. Toledo, and A. E. Ryabinin. 2011. The Edinger-Westphal nucleus: A historical, structural, and functional perspective on a dichotomous terminology. Journal of Comparative Neurology 519:1413-1434.

Labandeira-Garcia, J., M. Guerra-Seijas, L. Segade, and J. Suarez-Nuñez. 1987. Identification of abducens motoneurons, accessory abducens motoneurons, and abducens internuclear neurons in the chick by retrograde transport of horseradish peroxidase. Journal of Comparative Neurology 259:140-149.

Land, M. 2019. Eye movements in man and other animals. Vision Research 162:1-7.

Land, M., N. Mennie, and J. Rusted. 1999. The roles of vision and eye movements in the control of activities of daily living. Perception 28:1311-1328.

Land, M. F. 2015. Eye movements of vertebrates and their relation to eye form and function. Journal of Comparative Physiology A 201:195-214.

Levy, B. and J. Sivak. 1980. Mechanisms of accommodation in the bird eye. Journal of Comparative Physiology 137:267-272.

Lind, O. E., A. Kelber, and R. H. Kröger. 2008. Multifocal optical systems and pupil dynamics in birds. Journal of Experimental Biology 211:2752-2758.

Lisney, T. J., A. N. Iwaniuk, M. V. Bandet, and D. R. Wylie. 2012a. Eye shape and retinal topography in owls (Aves: Strigiformes). Brain, Behavior and Evolution 79:218-236.

Lisney, T. J., A. N. Iwaniuk, J. Kolominsky, M. V. Bandet, J. R. Corfield, and D. R. Wylie. 2012b. Interspecifc variation in eye shape and retinal topography in seven species of galliform bird (Aves: Galliformes: Phasianidae). Journal of Comparative Physiology A 198:717-731.

Lisney, T. J., K. Stecyk, J. Kolominsky, G. R. Graves, D. R. Wylie, and A. N. Iwaniuk. 2013a. Comparison of eye morphology and retinal topography in two species of New World vultures (Aves: Cathartidae). The Anatomical Record 296:1954-1970.

Lisney, T. J., K. Stecyk, J. Kolominsky, B. K. Schmidt, J. R. Corfield, A. N. Iwaniuk, and D. R. Wylie. 2013b. Ecomorphology of eye shape and retinal topography in waterfowl (Aves: Anseriformes: Anatidae) with different foraging modes. Journal of Comparative Physiology A 199:385-402.

Lisney, T. J., D. R. Wylie, J. Kolominsky, and A. N. Iwaniuk. 2015. Eye morphology and retinal topography in hummingbirds (Trochilidae: Aves). Brain, Behavior and Evolution 86:176-190.

Machovsky-Capuska, G. E., H. C. Howland, D. Raubenheimer, R. Vaughn-Hirshorn, B. Würsig, M. E. Hauber, and G. Katzir. 2012. Visual accommodation and active pursuit of prey underwater in a plunge-diving bird: the Australasian gannet. Proceedings of the Royal Society B: Biological Sciences 279:4118-4125.

Marhounová, L., A. Kotrschal, K. Kverková, N. Kolm, and P. Němec. 2019. Artificial selection on brain size leads to matching changes in overall number of neurons. Evolution 73:2003-2012.

Martin, G. 1994. Visual fields in woodcocks *Scolopax rusticola* (Scolopacidae; Charadriiformes). Journal of Comparative Physiology A 174:787-793.

Martin, G. 1999. Optical structure and visual fields in birds: their relationship with foraging behaviour and ecology. Pp. 485-508. Adaptive Mechanisms in The Ecology of Vision. Springer.

Martin, G., L. Rojas, Y. R. Figueroa, and R. McNeil. 2004. Binocular vision and nocturnal activity in Oilbirds (*Steatornis caripensis*) and Pauraques (*Nyctidromus albicollis*): Caprimulgiformes. Ornitologia Neotropical 15:233-242.

Martin, G. R. 1984. The visual fields of the tawny owl, *Strix aluco* L. Vision Research 24:1739-1751.

Martin, G. R. 1986. The eye of a passeriform bird, the European starling (*Sturnus vulgaris*): eye movement amplitude, visual fields and schematic optics. Journal of Comparative Physiology A 159:545-557.

Martin, G. R. 1998. Eye structure and amphibious foraging in albatrosses. Proceedings of the Royal Society of London. Series B: Biological Sciences 265:665-671.

Martin, G. R. 2007. Visual fields and their functions in birds. Journal of Ornithology 148:547-562.

Martin, G. R. 2009. What is binocular vision for? A birds' eye view. Journal of Vision 9:14-14.

Martin, G. R. 2017. The sensory ecology of birds. Oxford University Press, New York.

Martin, G. R. and H. C. Coetzee. 2004. Visual fields in hornbills: precision-grasping and sunshades. Ibis 146:18-26.

Martin, G. R. and C. Katzir. 1994a. Visual fields in the Stone-curlew *Burhinus oedicnemus*. Ibis 136:448-453.

Martin, G. R. and G. Katzir. 1994b. Visual fields and eye movements in herons (Ardeidae). Brain, Behavior and Evolution 44:74-85.

Martin, G. R. and G. Katzir. 1999. Visual fields in short-toed eagles, *Circaetus gallicus* (Accipitridae), and the function of binocularity in birds. Brain, Behavior and Evolution 53:55-66.

Martin, G. R. and T. Piersma. 2009. Vision and touch in relation to foraging and predator detection: insightful contrasts between a plover and a sandpiper. Proceedings of the Royal Society B: Biological Sciences 276:437-445.

Martin, G. R. and S. J. Portugal. 2011. Differences in foraging ecology determine variation in visual fields in ibises and spoonbills (Threskiornithidae). Ibis 153:662-671.

Martin, G. R., S. J. Portugal, and C. P. Murn. 2012. Visual fields, foraging and collision vulnerability in Gyps vultures. Ibis 154:626-631.

Martin, G. R. and P. A. Prince. 2001. Visual fields and foraging in procellariiform seabirds: sensory aspects of dietary segregation. Brain, Behavior and Evolution 57:33-38.

Martin, G. R. and S. Wanless. 2015. The visual fields of common guillemots *Uria aalge* and atlantic puffins *Fratercula arctica*: foraging, vigilance and collision vulnerability. Ibis 157:798-807.

Martin, G. R., C. R. White, and P. J. Butler. 2008. Vision and the foraging technique of great cormorants *Phalacrocorax carbo*: pursuit or close-quarter foraging? Ibis 150:485-494.

Martinoya, C., J. Le Houezec, and S. Bloch. 1982. Vergence eye movements during feeding in free moving pigeons. Neuroscience Letters 10:318.

Martinoya, C., J. Le Houezec, and S. Bloch. 1984. Pigeon's eyes converge during feeding: evidence for frontal binocular fixation in a lateral-eyed bird. Neuroscience Letters 45:335-339.

Marwitt, R., G. Pilar, and J. Weakly. 1971. Characterization of two ganglion cell populations in avian ciliary ganglia. Brain Research 25:317-334.

Mitkus, M., S. Chaib, O. Lind, and A. Kelber. 2014. Retinal ganglion cell topography and spatial resolution of two parrot species: budgerigar (*Melopsittacus undulatus*) and Bourke's parrot (*Neopsephotus bourkii*). Journal of Comparative Physiology A 200:371-384.

Moore, B. A., M. Doppler, J. E. Young, and E. Fernández-Juricic. 2013. Interspecific differences in the visual system and scanning behavior of three forest passerines that form heterospecific flocks. Journal of Comparative Physiology A 199:263-277.

Moore, B. A., D. Pita, L. P. Tyrrell, and E. Fernández-Juricic. 2015. Vision in avian emberizid foragers: maximizing both binocular vision and fronto-lateral visual acuity. Journal of Experimental Biology 218:1347-1358.

Moore, B. A., L. P. Tyrrell, D. Pita, O. R. Bininda-Emonds, and E. Fernández-Juricic. 2017. Does retinal configuration make the head and eyes of foveate birds move? Scientific Reports 7:1-7.

Moroney, M. K. and J. D. Pettigrew. 1987. Some observations on the visual optics of kingfishers (Aves, Coraciformes, Alcedinidae). Journal of Comparative Physiology A 160:137-149.

Morse, D. H. 1970. Ecological aspects of some mixed-species foraging flocks of birds. Ecological Monographs 40:119-168.

Murphy, C. and H. Howland. 1983. Owl eyes: accommodation, corneal curvature and refractive state. Journal of Comparative Physiology 151:277-284.

Němec, P. and P. Osten. 2020. The evolution of brain structure captured in stereotyped cell count and cell type distributions. Current Opinion in Neurobiology 60:176-183.

Nilsson, L. 1970. Food-seeking activity of south Swedish diving ducks in the non-breeding season. Oikos 1:145-154.

Nye, P. W. 1969. The monocular eye movements of the pigeon. Vision Research 9:133-144.

O'Rourke, C. T., M. I. Hall, T. Pitlik, and E. Fernández-Juricic. 2010a. Hawk eyes I: diurnal raptors differ in visual fields and degree of eye movement. PloS One 5:e12802.

O'Rourke, C. T., T. Pitlik, M. Hoover, and E. Fernández-Juricic. 2010b. Hawk eyes II: diurnal raptors differ in head movement strategies when scanning from perches. PLoS One 5:e12169.

Orme, D., R. Freckleton, G. Thomas, T. Petzoldt, S. Fritz, N. Isaac, and W. Pearse. 2013. The caper package: comparative analysis of phylogenetics and evolution in R. R Package Version 5:1-36.

Ott, M. 2006. Visual accommodation in vertebrates: mechanisms, physiological response and stimuli. Journal of Comparative Physiology A 192:97.

Otter, K. A. 2007. Ecology and behavior of chickadees and titmice: an integrated approach. Oxford University Press on Demand.

Pagel, M. 1999. The maximum likelihood approach to reconstructing ancestral character states of discrete characters on phylogenies. Systematic Biology 48:612-622.

Pettigrew, J. D. 1986. The evolution of binocular vision. In Visual Neuroscience, J.D. Pettigrew, K.J. Sanderson, and W.R. Levick, eds. Cambridge University Press, Cambridge, pp. 208-222.

Pettigrew, J. D., S. P. Collin, and M. Ott. 1999. Convergence of specialised behaviour, eye movements and visual optics in the sandlance (Teleostei) and the chameleon (Reptilia). Current Biology 9:421-424.

Pilar, G. and J. Tuttle. 1982. A simple neuronal system with a range of uses: the avian ciliary ganglion. Progress in Cholinergic Biology: Model Cholinergic Synapses 1:213-247.

Pinheiro, J., D. Bates, S. DebRoy, D. Sarkar, and R. C. Team. 2006. nlme: Linear and nonlinear mixed effects models. R Package Version 3:109.

Potier, S., O. Duriez, G. B. Cunningham, V. Bonhomme, C. O'Rourke, E. Fernández-Juricic, and F. Bonadonna. 2018. Visual field shape and foraging ecology in diurnal raptors. Journal of Experimental Biology 221(14).

Potier, S., M. Mitkus, and A. Kelber. 2020. Visual adaptations of diurnal and nocturnal raptors. Seminars in Cell & Developmental Biology. Elsevier, Amsterdam.

Pratt, D. W. 1982. Saccadic eye movements are coordinated with head movements in walking chickens. Journal of Experimental Biology 97:217-223.

Reiner, A., J. T. Erichsen, J. B. Cabot, C. Evinger, M. E. Fitzgerald, and H. J. Karten. 1991. Neurotransmitter organization of the nucleus of Edinger-Westphal and its projection to the avian ciliary ganglion. Visual Neuroscience 6:451-472.

Reymond, L. 1985. Spatial visual acuity of the eagle *Aquila audax*: a behavioural, optical and anatomical investigation. Vision Research 25:1477-1491.

Rochon-Duvigneaud, A. 1943. Les yeux et la vision des vertébrés. Masson Paris.

Schaeffel, F. and H. Wagner. 1992. Barn owls have symmetrical accommodation in both eyes, but independent pupillary responses to light. Vision Research 32:1149-1155.

Schliep, K. P. 2011. phangorn: phylogenetic analysis in R. Bioinformatics 27:592-593.

Sherwood, C. C. 2005. Comparative anatomy of the facial motor nucleus in mammals, with an analysis of neuron numbers in primates. The Anatomical Record Part A: Discoveries in Molecular, Cellular, and Evolutionary Biology: An Official Publication of the American Association of Anatomists 287:1067-1079.

Sherwood, C. C., P. R. Hof, R. L. Holloway, K. Semendeferi, P. J. Gannon, H. D. Frahm, and K. Zilles. 2005. Evolution of the brainstem orofacial motor system in primates: a comparative study of trigeminal, facial, and hypoglossal nuclei. Journal of Human Evolution 48:45-84.

Sivak, J., T. Hildebrand, and C. Lebert. 1985. Magnitude and rate of accommodation in diving and nondiving birds. Vision Research 25:925-933.

Sivak, J. G. 1980. Avian mechanisms for vision in air and water. Trends in Neurosciences 3:314-317.

Sohal, G. and R. Holt. 1978. Identification of the trochlear motoneurons by retrograde transport of horseradish peroxidase. Experimental Neurology 59:509-514.

Steinbach, M. J., R. G. Angus, and K. Money. 1974. Torsional eye movements of the owl. Vision Research 14:745-746.

Steinbach, M. J. and K. Money. 1972. Eye movements of the owl. Defence and Civil Inst of Environmental Medicine Downsview (Ontario).

Strod, T., Z. Arad, I. Izhaki, and G. Katzir. 2004. Cormorants keep their power: visual resolution in a pursuit-diving bird under amphibious and turbid conditions. Current Biology 14:R376-R377.

Troscianko, J., A. M. Von Bayern, J. Chappell, C. Rutz, and G. R. Martin. 2012. Extreme binocular vision and a straight bill facilitate tool use in New Caledonian crows. Nature Communications 3:1-7.

Tyrrell, L. P., S. R. Butler, and E. Fernández-Juricic. 2015. Oculomotor strategy of an avian ground forager: tilted and weakly yoked eye saccades. Journal of Experimental Biology 218:2651-2657.

Tyrrell, L. P. and E. Fernández-Juricic. 2017. The hawk-eyed songbird: retinal morphology, eye shape, and visual fields of an aerial insectivore. The American Naturalist 189:709-717.

Tyrrell, L. P., B. Goller, B. A. Moore, D. L. Altshuler, and E. Fernández-Juricic. 2018. The orientation of visual space from the perspective of hummingbirds. Frontiers in Neuroscience 12:16.

Voogd, J. and D. R. Wylie. 2004. Functional and anatomical organization of floccular zones: a preserved feature in vertebrates. Journal of Comparative Neurology 470:107-112.

Voss, J. and H.-J. Bischof. 2009. Eye movements of laterally eyed birds are not independent. Journal of Experimental Biology 212:1568-1575.

Wagner, H. and F. Schaeffel. 1991. Barn owls (*Tyto alba*) use accommodation as a distance cue. Journal of Comparative Physiology A 169:515-521.

Wallman, J. and J. D. Pettigrew. 1985. Conjugate and disjunctive saccades in two avian species with contrasting oculomotor strategies. Journal of Neuroscience 5:1418-1428.

Walls, G. 1962. The evolutionary history of eye movements. Vision Research 2:69-80.

Walls, G. L. 1942. The vertebrate eye. Cranbrook Institute of Science, Michigan.

Wathey, J. C. and J. D. Pettigrew. 1989. Quantitative analysis of the retinal ganglion cell layer and optic nerve of the barn owl Tyto alba. Brain, Behavior and Evolution 33:279-292.

Welt, C. and J. H. Abbs. 1990. Musculotopic organization of the facial motor nucleus in *Macaca fascicularis*: a morphometric and retrograde tracing study with cholera toxin B-HRP. Journal of Comparative Neurology 291:621-636.

Wood, C. A. 1917. The fundus oculi of birds: especially as viewed by the ophthalmoscope; a study in the comparative anatomy and physiology. Lakeside Press, Chicago.

Wylie, D. R. and B. J. Frost. 1996. The pigeon optokinetic system: visual input in extraocular muscle coordinates. Visual Neuroscience 13:945-954.

Wylie, D. R., C. Gutiérrez-Ibáñez, and A. Iwaniuk. 2015. Integrating brain, behavior, and phylogeny to understand the evolution of sensory systems in birds. Frontiers in Neuroscience 9:281.

Wylie, D. R., S. W. Shaver, and B. J. Frost. 1994. The visual response properties of neurons in the nucleus of the basal optic root of the northern saw-whet owl (*Aegolius acadicus*). Brain, Behavior and Evolution 43:15-25.

Table 4.1. Published data on eye movements. EOG=electro-oculogram; N/D=not detected; NR=values not reported. Notes: [1]=anectodal observation; [2]=animal's head was immbolized; [3]=technique cannot detect small amplitude of eye movements.

Order	***Species***	***Source***	***Method***	***Type of eye movement studied***	***Amplitude of eye movement***	***Notes***
Accipitriformes	Little eagle (*Hieraaetus morphnoides*)	Wallman and Pettigrew 1985	Magnetic coil technique	Saccades, VOR and OKN	Up to 24°	[2]
	Short-toed eagle (*Circaetus gallicus*)	Martin and Katzir 1999	Ophthalmoscope	Saccades	N/D	[2], [3]
	Red-tailed hawk (*Buteo jamaicensis*)	O'Rourke et al. 2010a	Ophthalmoscope	Saccades	5°	[2]. [3]
	Cooper's hawk (*Accipiter cooperi*)	O'Rourke et al. 2010a	Ophthalmoscope	Saccades	8°	[2]. [3]
Anseriformes	Northern shoveler (*Anas clypeata*)	Guilleman et al. 2002	Ophthalmoscope	Saccades	N/D	[2], [3]
	Eurasian wigeon (*Anas penelope*)	Guilleman et al. 2002	Ophthalmoscope	Saccades	N/D	[2], [3]
Apodiformes	Anna's hummingbird (*Calypte anna*)	Tyrrell et al. 2018	Ophthalmoscope	Saccades	9°	[2], [3]
	Rufous hummingbird (*Selasphorus rufus*)	Tyrrell et al. 2018	Ophthalmoscope	Saccades	12°	[2], [3]
Bucerotiformes	Southern ground hornbill (*Bucorvus leadbeateri*)	Martin and Coetzee 2004	Ophthalmoscope	Saccades	30° to 40°	[2], [3]
	Southern yellow-billed hornbill (*Tockus leucomelas*)	Martin and Coetzee 2004	Ophthalmoscope	Saccades	30° to 40°	[2], [3]
Caprimulgiformes	Tawny frogmouth (*Podargus strigoides*)	Wallman and Pettigrew 1985	Magnetic coil technique	Saccades, VOR and OKN	Up to ~20°	[2]
	Oilbird (*Steatornis caripensis*)	Martin et al. 2004	Ophthalmoscope	Saccades	N/D	[2], [3]
	Pauraque (*Nyctidromus albicollis*)	Martin et al. 2004	Ophthalmoscope	Saccades	N/D	[2], [3]
Cathartiformes	Eurasian griffon vulture (*Gyps fulvus*)	Martin et al. 2012	Ophthalmoscope	Saccades	NR	[1], [2], [3]
	African white-backed vulture (*Gyps africanus*)	Martin et al. 2012	Ophthalmoscope	Saccades	NR	[1], [2], [3]
Charadriiformes	Eurasian stone-curlew (*Burhinus oedicnemus*)	Martin and Katzir 1994a	Ophthalmoscope	Saccades	N/D	[2], [3]
	Eurasian woodcock (*Scolopax rusticola*)	Martin 1994	Ophthalmoscope	Saccades	N/D	[2], [3]
	Red knot (*Calidris canutus*)	Martin and Piersma 2009	Ophthalmoscope	Saccades	N/D	[2], [3]
	Golden plover (*Pluvialis apricaria*)	Martin and Piersma 2009	Ophthalmoscope	Saccades	N/D	[2], [3]
	Blacksmith lapwing (*Vanellus armatus*)	Cantlay et al. 2019	Ophthalmoscope	Saccades	N/D	[2], [3]
	Common guillemot (*Uria aalge*)	Martin and Wanless 2015	Ophthalmoscope	Saccades	20°	[1], [2], [3]
	Atlantic puffin (*Fratercula arctica*)	Martin and Wanless 2015	Ophthalmoscope	Saccades	20°	[1], [2], [3]
Columbiformes	Pigeon (*Columba livia*)	Nye 1969	Mirror attachments	Oscillations	3° to 5°	[2]
		Bloch et al. 1984	EOG	Saccades	~14°	[2]
		Martinoya et al. 1982, 1984	EOG	Saccades	~17°	-
		Gioanni 1988	Magnetic coil technique	OKN	Horizontal: 6-7° Vertical: 3-4°	-

Coraciiformes	Kingfishers	Moroney and Pettigrew 1987	NR	Saccades	NR; infrequent	[1], [2]
Falconiformes	American Kestrel (*Falco sparverius*)	O'Rourke et al. 2010	Ophthalmoscope	Saccades	<1°	[2], [3]
Galliformes	Chicken (*Gallus domesticus*)	Pratt 1982	Photography	Saccades	NR	-
Passeriformes	European starling (*Sturnus vulgaris*)	Martin 1986	Opthalmoscope	Saccades	Up to 32°	[2], [3]
	European starling (*Sturnus vulgaris*)	Tyrrell et al. 2015	Infra-red sensitive cameras	Saccades	~13°	[2]
	Zebra finch (*Taeniopygia guttata)*	Bischof 1988	NR	NR	10° to 15°	[1]
		Voss and Bischof 2009	CCD cameras	Saccades	Up to 21°	[2]
	House finch (*Carpodacus mexicanus*)	Fernández-Juricic et al. 2008	Ophthalmoscope	Saccades	11°	[2], [3]
	House sparrow (*Passer domesticus*)	Fernández-Juricic et al. 2008	Ophthalmoscope	Saccades	16°	[2], [3]
	American crow (*Corvus brachyrhynchos*)	Fernández-Juricic et al. 2010	Ophthalmoscope	Saccades	16°	[2], [3]
	Western scrub jay (*Aphelocoma californica*)	Fernández-Juricic et al. 2010	Ophthalmoscope	Saccades	7°	[2], [3]
	Black phoebe (*Sayornis nigricans*)	Gall and Fernández-Juricic 2009	Ophthalmoscope	Saccades	Up to 18°	[2], [3]
	White-crowned sparrow (*Zonotrichia leucophrys*)	Fernández-Juricic et al. 2011	Ophthalmoscope	Saccades	12°	[2], [3]
	California towhee (*Pipilo crissalis*)	Fernández-Juricic et al. 2011	Ophthalmoscope	Saccades	~11°	[2], [3]
	Carolina chickadee (*Parus carolinensis*)	Moore et al. 2013	Ophthalmoscope	Saccades	71°	[2], [3]
	Tufted titmice (*Baeolophus bicolor*)	Moore et al. 2013	Ophthalmoscope	Saccades	76°	[2], [3]
	White-breasted nuthatch (*Sitta carolinensis*)	Moore et al. 2013	Ophthalmoscope	Saccades	61°	[2], [3]
	New-Caledonian crow (*Corvus menuloides*)	Troscianko et al. 2015	Infra-red Ophthalmoscope	Saccades	~40°	[2]
	Carrion crow (*Corvus corone*)	Troscianko et al. 2015	Infra-red Ophthalmoscope	Saccades	27°	[2]
	Jackdaw (*Corvus monedula*)	Troscianko et al. 2015	Infra-red Ophthalmoscope	Saccades	26°	[2]
	Pied crow (*Corvus albus*)	Troscianko et al. 2015	Infra-red Ophthalmoscope	Saccades	32°	[2]
	Raven (*Corvus corax*)	Troscianko et al. 2015	Infra-red Ophthalmoscope	Saccades	22°	[2]
	Rook (*Corvus frugilegus*)	Troscianko et al. 2015	Infra-red Ophthalmoscope	Saccades	29°	[2]
	American tree sparrow (*Spizella arborea*)	Moore et al. 2015	Ophthalmoscope	Saccades	22°	[2], [3]
	Chipping sparrow (*Spizella passerina*)	Moore et al. 2015	Ophthalmoscope	Saccades	31°	[2], [3]
	Dark-eyed junco (*Junco hyemalis*)	Moore et al. 2015	Ophthalmoscope	Saccades	33°	[2], [3]
	Eastern towhee (*Pipilo erythrophthalmus*)	Moore et al. 2015	Ophthalmoscope	Saccades	35°	[2], [3]
	Field sparrow (*Spizella pusilla*)	Moore et al. 2015	Ophthalmoscope	Saccades	36°	[2], [3]
	Song sparrow (*Melospiza melodia*)	Moore et al. 2015	Ophthalmoscope	Saccades	33°	[2], [3]
	White-throated sparrow (*Zonotrichia albicollis*)	Moore et al. 2015	Ophthalmoscope	Saccades	31°	[2], [3]
	Tree swallow (*Tachycineta bicolor*)	Tyrrell and Fernández-Juricic 2017	Ophthalmoscope	Saccades	19.5°	[2], [3]
	Acadian flycatcher (*Empidonax virescens*)	Tyrrell and Fernández-Juricic 2017	Ophthalmoscope	Saccades	18.6°	[2], [3]

	Least flycatcher (Empidonax minimus)	Tyrrell and Fernández-Juricic 2017	Ophthalmoscope	Saccades	18.6°	[2], [3]
Pelecaniformes	Cattle egret (*Bubulcus ibis*)	Martin and Katzir 1994b	Ophthalmoscope	Saccades	Up to 18°	[2], [3]
	Squacco heron *(Ardeola ralloides)*	Martin and Katzir 1994b	Ophthalmoscope	Saccades	~13°	[2], [3]
	Reef heron (*Egretta gularis schistaceae*)	Martin and Katzir 1994b	Ophthalmoscope	Saccades	~13°	[2], [3]
	Black-browed albatross (*Thalassarche melanophris*)	Martin 1998	Ophthalmoscope	Saccades	20° to 25°	[2], [3]
	Grey-headed albatross (*Thalassarche chrysostoma*)	Martin 1998	Ophthalmoscope	Saccades	20° to 25°	[2], [3]
	Puna ibis (*Plegadis ridgwayi*)	Martin and Portugal 2011	Ophthalmoscope	Saccades	14°	[2], [3]
	Northern bald ibis (*Geronticus eremita*)	Martin and Portugal 2011	Ophthalmoscope	Saccades	14°	[2], [3]
	African spoonbill (*Platalea alba*)	Martin and Portugal 2011	Ophthalmoscope	Saccades	14°	[2], [3]
	Eurasian spoonbill (*Platalea leucorodia*)	Martin and Portugal 2011	Ophthalmoscope	Saccades	14°	[2], [3]
Procellariiformes	White-chinned petrel (*Procellaria aequinoctialis*)	Martin and Prince 2001	Ophthalmoscope	Saccades	17° to 20°	[2], [3]
	Antarctic prion (*Procellaria desolata*)	Martin and Prince 2001	Ophthalmoscope	Saccades	N/D	[2], [3]
Psittaciformes	Senegal parrot (*Poicephalus senegalus*)	Demery et al. 2011	Ophthalmoscope	Saccades	24°	[2], [3]
Strigiformes	Barn owl (*Tyto alba*)	Knudsen 1982	Ophthalmoscope	Saccades	1-2°	[2]
	Great horned owl (*Bubo virginianus*)	Steinbach and Money 1972	Mirror attachments	Slow drifts, rapid flicks and oscillations	<1.5°	[2]
	Great horned owl (*Bubo virginianus*)	Steinbach and Money 1974	Photography	Counter-torsion	<3.5°	[2]
Suliformes	Great cormorant (*Phalacrocorax carbo*)	Martin et al. 2008	Ophthalmoscope	Saccades	14-15°	[2], [3]

Table 4.2. Volumes of the brain, brainstem, abducens (VI), trochlear (IV), III-dorsolateral, III-dorsomedial, III-dorsoventral, and Edinger-Westphal nuclei for the species analysed. Grid sizes varied between 20 - 50 µm.

Order	Common name/ Species	Brain volume (mm^3)	Brainstem volume (mm^3)	Abducens (VI) nucleus volume (mm^3)	Trochlear (IV) nucleus volume (mm^3)	III-dorsolateral nucleus volume (mm^3)	III-dorsomedial nucleus volume (mm^3)	III-ventral nucleus volume (mm^3)	Edinger-Westphal (EW) volume (mm^3)
Accipitriformes	Collared sparrowhawk (*Accipiter cirrocephalus*)	4875	781	0.894	0.532	0.570	0.423	0.927	0.276
	Sharp-shinned hawk (*Accipiter striatus*)	4,179	607	0.550	0.401	0.272	0.362	0.826	0.166
	Swainson's hawk (*Buteo swainsoni)*	8,099	921	0.996	0.539	0.810	0.806	1.242	0.321
Anseriformes	American wigeon (*Anas americana)*	3,950	478	0.189	0.318	0.199	0.205	0.420	0.086
	Chestnut teal (*Anas castanea)*	3,425	463	0.269	0.280	0.125	0.200	0.311	0.094
	Northern shoveler (*Anas clypeata*)	3,288	452	0.260	0.307	0.193	0.208	0.436	0.073
	Blue-winged teal (*Anas discors*)	2,896	452	0.229	0.308	0.127	0.175	0.317	0.055
	Mallard (*Anas platyrhynchos)*	6,216	769	0.276	0.707	0.317	0.345	0.715	0.094
	Lesser scaup (*Aythya affinis*)	4,546	586	0.220	0.370	0.182	0.242	0.444	0.101
	Canada goose (*Branta canadensis*)	11,347	1,227	-	1.106	0.389	0.408	0.852	0.265
	Common goldeneye (*Bucephala clangula*)	5,961	763	0.346	0.553	0.323	0.348	0.565	0.177
	Red-breasted merganser (*Mergus serrator*)	4,247	554	0.462	0.552	0.255	0.292	0.571	0.250
Apodiformes	Rufous-tailed hummingbird (*Amazilia tzacatl*)	176	30	0.027	0.036	0.017	0.020	0.055	0.008
	Long-tailed hermit (*Phaetornis superciliosus*)	193	36	0.041	0.041	0.021	0.019	0.066	0.007
	Rufous hummingbird (*Selasphorus rufus*)	152	28	0.032	0.050	0.016	0.028	0.078	0.005
Caprimulgiformes	Tawny frogmouth (*Podargus strigoides*)	5,943	561	0.449	0.250	0.241	0.316	0.516	0.064
Cathartiformes	Turkey vulture (*Cathartes aura*)	10,467	1,145	1.145	0.830	0.556	0.551	1.271	0.326
	Black vulture (*Coragyps atratus*)	13,299	1,206	1.469	0.831	0.499	0.610	1.443	0.276
Charadriiformes	Bonaparte's gull (*Larus philadelphia*)	2,512	364	0.284	0.421	0.281	0.296	0.410	0.121
	Eurasian woodcock								

	(*Scolopax rusticola*)	2,594	358	0.236	0.449	0.119	0.137	0.368	0.038
Columbiformes	White-headed pigeon (*Columba leucomela*)	2,355	375	0.317	0.375	0.221	0.259	0.448	0.207
	Rock dove (*Columba livia*)	2,343	430	0.301	0.264	0.204	0.255	0.401	0.143
	Bar-shouldered dove (*Geopelia humeralis*)	1,106	209	0.173	0.223	0.125	0.104	0.261	0.078
	Spotted dove (*Stigmatopelia chinensis*)	1,430	223	0.157	0.204	0.121	0.106	0.257	0.095
	Mourning dove (*Zenaida macroura*)	983	171	0.104	0.139	0.074	0.080	0.195	0.059
Coraciiformes	Laughing kookaburra (*Dacelo novaeguineae*)	3,970	444	0.379	0.419	0.247	0.225	0.316	0.072
Falconiformes	Merlin (*Falco columbarius*)	3,510	294	0.420	0.228	0.196	0.209	0.428	0.097
	American kestrel (*Falco sparverius*)	2,368	331	0.339	0.275	0.323	0.333	0.495	0.165
Galliformes	Chukar (*Alectoris chukar*)	2,285	377	0.268	0.190	0.127	0.238	0.349	0.110
	Ruffed grouse (*Bonasa umbellus*)	2,288	508	0.535	0.465	0.283	0.321	0.708	0.200
	Japanese quail (*Coturnix japonica*)	936	203	0.123	0.200	0.119	0.134	0.224	0.099
	Spruce grouse (*Dendragapus canadensis*)	2,949	472	0.205	0.476	0.266	0.388	0.632	0.228
	Grey partridge (*Perdix perdix*)	2,027	339	0.146	0.234	0.169	0.190	0.267	0.099
	Common pheasant (*Phasianus colchicus*)	3,722	403	0.280	0.322	0.204	0.192	0.421	0.177
	Lesser prairie chicken (*Tympanuchus pallidicinctus*)	3,051	454	0.363	0.398	0.264	0.320	0.665	0.144
	Sharp-tailed grouse (*Tympanuchus phasianellus*)	3,023	502	0.430	0.493	0.313	0.364	0.658	0.250
Gruiformes	American coot (*Fulica americana*)	2,719	375	0.168	0.209	0.138	0.130	0.225	0.118
Passeriformes	Red-winged blackbird (*Agelaius phoeniceus*)	1,615	158	0.091	0.096	0.055	0.083	0.190	0.074
	Tufted titmouse (*Baeolophus bicolor*)	784	94	0.077	0.062	0.069	0.080	0.120	0.078
	House finch (*Carpodacus mexicanus*)	1,059	102	0.099	0.102	0.081	0.086	0.180	0.100
	Gray catbird (*Dumetella carolinensis*)	883	117	0.085	0.086	0.073	0.085	0.152	0.108
	Australian magpie (*Gymnorhina tibicen*)	4,017	352	0.219	0.316	0.219	0.227	0.641	0.288

	Dark-eyed junco (*Junco hyemalis*)	835	103	0.086	0.065	0.050	0.080	0.120	0.081
	Song sparrow (*Melospiza melodia*)	909	105	0.131	0.060	0.060	0.084	0.137	0.088
	Brown-headed cowbird (*Molothrus ater*)	1,313	176	0.110	0.150	0.097	0.097	0.256	0.106
	Carolina chickadee (*Parus carolinensis*)	565	62	0.078	0.042	0.029	0.045	0.067	0.059
	Chipping sparrow (*Spizella passerina*)	654	56	0.064	0.037	0.038	0.030	0.061	0.041
	Field sparrow (*Spizella pusilla*)	579	72	0.067	0.060	0.034	0.042	0.102	0.038
	Double-barred finch (*Taeniopygia bichenovii*)	409	58	0.067	0.064	0.034	0.036	0.109	0.020
	Zebra finch (*Taeniopygia guttata*)	475	45	0.032	0.028	0.021	0.024	0.051	0.016
	House wren (*Troglodytes aedon*)	614	77	0.063	0.040	0.034	0.047	0.079	0.050
	White-throated sparrow (*Zonotrichia albicollis*)	937	119	0.109	0.070	0.074	0.071	0.153	0.070
Pelecaniformes	Nankeen night heron (*Nycticorax caledonicus*)	3,360	465	0.490	0.346	0.225	0.334	0.435	0.161
Psittaciformes	Australian king parrot (*Alisterus scapularis*)	4,901	474	0.212	0.418	0.201	0.253	0.623	0.093
	Galah (*Cacatua roseicapilla*)	7,455	420	0.252	0.372	0.174	0.195	0.489	0.076
	Long-billed corella (*Cacatua tenuirostris*)	11,778	642	0.340	0.372	0.199	0.293	0.672	0.098
	Budgerigar (*Melopsittacus undulatus*)	1,486	117	0.122	0.090	0.068	0.078	0.227	0.031
	Cockatiel (*Nymphicus hollandicus*)	2,161	205	0.192	0.218	0.126	0.158	0.356	0.052
Strigiformes	Northern saw-whet owl (*Aegolius acadicus*)	2,857	367	0.143	0.148	0.101	0.116	0.135	-
	Short-eared owl (*Asio flammeus*)	6,221	528	0.371	0.168	0.125	0.142	0.219	-
	Snowy owl (*Bubo scandiaca*)	18,127	970	0.595	0.444	0.272	0.287	0.952	0.096
	Great horned owl (*Bubo virginianus*)	17,994	991	0.504	0.341	0.188	0.199	0.536	0.060
	Great grey owl (*Strix nebulosa*)	13,433	797	0.364	0.303	0.171	0.204	0.637	0.075
	Barred owl (*Strix varia*)	12,727	800	0.360	0.262	0.118	0.128	0.387	-
	Northern hawk-owl (*Surnia ulula*)	9,408	701	0.521	0.311	0.237	0.294	0.792	-

Barn owl (*Tyto alba*)	5,850	489	0.157	0.116	0.099	0.101	0.121	-

Table 4.3. Numbers of neurons (*n*) of the abducens, trochlear, III-dorsolateral, III-dorsomedial, III-ventral, and Edinger-Westphal nuclei for the species analysed. For every species, grid size was 50 µm and frame size was 40 µm.

Order	Common name/ Species	Abducens (VI) nucleus, n	Trochlear (IV) nucleus, n	III-dorsolateral nucleus, n	III-dorsomedial nucleus, n	III-ventral nucleus, n	Edinger-Westphal (EW), n
Accipitriformes	Collared sparrowhawk (*Accipiter cirrocephalus*)	9,225	6,291	8,126	7,164	11,249	8,274
	Sharp-shinned hawk (*Accipiter striatus*)	8,098	6,513	6,123	6,568	9,986	6,483
	Swainson's hawk (*Buteo swainsoni)*	12,580	7,152	13,497	9,971	15,564	10,153
Anseriformes	American wigeon (*Anas americana)*	3,306	5,897	5,897	4,647	8,914	5,242
	Chestnut teal (*Anas castanea)*	5,556	7,076	4,799	4,451	7,671	5,251
	Northern shoveler (*Anas clypeata*)	4,596	5,225	5,470	4,734	8,521	4,524
	Blue-winged teal (*Anas discors*)	3,103	7,586	4,388	3,315	7,050	4,466
	Mallard (*Anas platyrhynchos)*	4,071	10,838	6,760	6,356	12,564	5,960
	Lesser scaup (*Aythya affinis*)	4,749	4,831	4,385	4,549	7,448	5,381
	Canada goose (*Branta canadensis*)	-	12,120	6,919	5,879	9,271	12,256
	Common goldeneye (*Bucephala clangula*)	5,721	8,596	6,660	6,428	9,525	7,899
	Red-breasted merganser (*Mergus serrator*)	9,637	8,616	7,366	6,250	9,687	9,598
Apodiformes	Rufous-tailed hummingbird (*Amazilia tzacatl*)	1,663	2,044	1,638	1,525	2,922	1,576
	Long-tailed hermit (*Phaetornis superciliosus*)	1,479	1,877	1,761	1,679	3,045	1,339
	Rufous hummingbird (*Selasphorus rufus*)	2,302	3,386	2,005	2,104	4,536	1,200
Caprimulgiformes	Tawny frogmouth (*Podargus strigoides*)	9,083	5,665	7,278	6,569	12,212	5,088
Cathartiformes	Turkey vulture (*Cathartes aura*)	13,236	9,050	8,152	7,928	15,632	8,377
	Black vulture (*Coragyps atratus*)	10,308	8,261	10,025	9,143	15,318	10,827
Charadriiformes	Bonaparte's gull (*Larus philadelphia*)	4,579	8,000	6,845	6,973	9,155	4,791
	Eurasian woodcock (*Scolopax rusticola*)	5,864	8,534	4,932	5,152	11,498	4,241
Columbiformes	White-headed pigeon (*Columba leucomela*)	7,992	8,189	7,732	6,575	9,968	10.515
	Rock dove (*Columba livia*)	7,753	6,203	6,167	6,095	9,053	8,656
	Bar-shouldered dove (*Geopelia humeralis*)	4,607	7,954	5,772	4,247	9,151	4,927
	Spotted dove (*Stigmatopelia chinensis*)	4,425	5,443	4,138	3,486	6,564	6,503
	Mourning dove (*Zenaida macroura*)	3,895	5,564	4,352	3,970	7,206	4,081
Coraciiformes	Laughing kookaburra (*Dacelo novaeguineae*)	6,535	6,724	6,035	4,822	6,124	5,976
Falconiformes	Merlin (*Falco columbarius*)	5,858	7,815	7,986	7,766	11,760	10,531
	American kestrel (*Falco sparverius*)	6,405	7,098	8,607	7,290	9,925	8,520
Galliformes	Chukar						

	(*Alectoris chukar*)	5,326	4,532	4,916	5,185	8,796	5,603
	Ruffed grouse (*Bonasa umbellus*)	5,125	5,873	5,917	6,196	10,586	8,178
	Japanese quail (*Coturnix japonica*)	2,403	4,340	4,551	4,642	7,204	5,516
	Spruce grouse (*Dendragapus canadensis*)	3,739	10,269	6,138	6,871	9,376	8,734
	Grey partridge (*Perdix perdix*)	2,508	3,780	6,003	6,063	9,244	4,604
	Common pheasant (*Phasianus colchicus*)	8,018	6,767	6,162	4,898	10,397	9,670
	Lesser prairie chicken (*Tympanuchus pallidicinctus*)	5,502	6,504	6,923	6,023	10,897	7,234
	Sharp-tailed grouse (*Tympanuchus phasianellus*)	6,713	10,266	7,460	7,394	12,489	11,757
Gruiformes	American coot (*Fulica americana*)	4,196	5,524	5,110	3,683	7,159	7,738
Passeriformes	Red-winged blackbird (*Agelaius phoeniceus*)	5,465	4,095	3,276	4,138	6,681	6,552
	Tufted titmouse (*Baeolophus bicolor*)	3,604	2,356	3,669	3,498	4,783	6,524
	House finch (*Carpodacus mexicanus*)	3,371	3,638	4,269	3,751	5,401	6,387
	Gray catbird (*Dumetella carolinensis*)	5,025	4,085	4,085	4,220	6,623	7,899
	Australian magpie (*Gymnorhina tibicen*)	5,140	6,180	5,857	6,051	16,147	13,267
	Dark-eyed junco (*Junco hyemalis*)	5,575	4,278	4,243	5,084	7,241	10,591
	Song sparrow (*Melospiza melodia*)	6,739	3,614	4,150	4,487	6,279	9,113
	Brown-headed cowbird (*Molothrus ater*)	3,397	4,448	3,678	3,144	6,162	6,523
	Carolina chickadee (*Parus carolinensis*)	4,413	3,605	2,845	3,621	5,803	7,436
	Chipping sparrow (*Spizella passerina*)	2,306	1,761	1,871	2,021	3,207	2,971
	Field sparrow (*Spizella pusilla*)	4,361	3,937	3,149	3,543	6,829	5,799
	Double-barred finch (*Taeniopygia bichenovii*)	2,656	2,251	2,341	2,131	4,636	2,951
	Zebra finch (*Taeniopygia guttata*)	2,249	1,836	1,527	2,666	2,603	3,910
	House wren (*Troglodytes aedon*)	4,868	2,965	3,325	3,460	6,470	7,249
	White-throated sparrow (*Zonotrichia albicollis*)	4,621	2,163	4,278	4,167	7,205	6,298
Pelecaniformes	Nankeen night heron (*Nycticorax caledonicus*)	9,300	9,912	8,397	7,244	12,052	10,735
Psittaciformes	Australian king parrot (*Alisterus scapularis*)	4,629	7,647	6,060	5,870	11,137	6,124
	Galah (*Cacatua roseicapilla*)	6,727	6,843	6,166	4,399	10,903	4,420
	Long-billed corella (*Cacatua tenuirostris*)	6,299	7,322	6,206	6,132	10,879	3,854
	Budgerigar (*Melopsittacus undulatus*)	4,450	3,221	3,145	3,183	7,540	3,483
	Cockatiel (*Nymphicus hollandicus*)	6,053	6,135	5,602	4,088	8,421	3,391
Strigiformes	Northern saw-whet owl (*Aegolius acadicus*)	4,298	5,628	4,174	4,793	5,411	-
	Short-eared owl (*Asio flammeus*)	10,105	7,442	5,159	5,337	6,197	-
	Snowy owl (*Bubo scandiaca*)	7,918	8,982	7,427	5,903	11,934	4,888

Great horned owl (*Bubo virginianus*)	10,688	10,168	4,614	4,346	11,760	3,456
Great grey owl (*Strix nebulosa*)	6,338	8,508	6,221	5,280	11,636	5,885
Barred owl (*Strix varia*)	6,247	8,285	5,135	4,820	6,521	-
Northern hawk-owl (*Surnia ulula*)	10,349	8,187	7,750	5,889	14,780	-
Barn owl (*Tyto alba*)	5,101	4,241	4,488	4,395	4,953	-

Table 4.4. Details of the allometric relationships among the variables from the oculomotor nuclei examined. λ = Pagel's lambda; p = p-value; r^2 = coefficient of determination; CI = confidence interval.

x-axis	y-axis	Intercept	F ratio	λ	p	r^2	slope	slope CI (± 95%)
brainstem volume (-y)	dorsomedial III volume	-3.096	214.7	0.965	<0.01	0.767	0.929	0.866, 0.992
	dorsomedial III #neurons	2.745	93.1	0.535	<0.01	0.586	0.378	0.339, 0.417
	dorsolateral III volume	-3.115	216.0	0.747	<0.01	0.768	0.915	0.853, 0.977
	dorsolateral III #neurons	2.641	115.9	0.517	<0.01	0.639	0.432	0.390, 0.472
	ventral III volume	-2.757	162.4	0.839	<0.01	0.713	0.909	0.838, 0.980
	ventral III #neurons	2.954	75.1	0.461	<0.01	0.533	0.388	0.343, 0.433
	IV volume	-2.890	209.4	0.802	<0.01	0.762	0.902	0.840, 0.964
	IV #neurons	2.688	182.0	0	<0.01	0.736	0.428	0.396, 0.460
	VI volume	-2.838	210.4	0.521	<0.01	0.766	0.880	0.819, 0.941
	VI #neurons	2.675	67.1	0.252	<0.01	0.508	0.418	0.367, 0.469
	EW volume	-3.208	82.4	0.849	<0.01	0.578	0.862	0.767, 0.957
	EW #neurons	2.694	33.2	0.808	<0.01	0.349	0.428	0.354, 0.502
nucleus volume (from y-axis)	dorsomedial III #neurons	4.028	293.4	0.271	<0.01	0.818	0.438	0.412, 0.464
	dorsolateral III #neurons	4.112	465.2	0.040	<0.01	0.877	0.472	0.450, 0.494
	ventral III #neurons	4.137	247.5	0.101	<0.01	0.791	0.451	0.422, 0.480
	IV #neurons	4.068	179.0	0.204	<0.01	0.732	0.481	0.445, 0.517
	VI #neurons	4.041	141.6	0.265	<0.01	0.687	0.500	0.458, 0.542
	EW #neurons	4.318	180.9	0.481	<0.01	0.750	0.528	0.489, 0.567

Table 4.5. Data collated in the literature on retinal topography for the species in our sample. Notes: for species highlighted with "1", data on retinal topography was assumed based on available data of congeners; for species highlighted with "2", data is still insufficient, another area or fovea could be present (see Lisney et al., 2015).

Order	Common name/ Species	Retinal topography	Source
Accipitriformes	Collared sparrowhawk (*Accipiter cirrocephalus*)	Two foveae[1]	-
	Sharp-shinned hawk (*Accipiter striatus*)	Two foveae[1]	-
	Swainson's hawk (*Buteo swainsoni)*	Two foveae[1]	-
Anseriformes	American wigeon (*Anas americana)*	Area centralis	Lisney et al. 2013b
	Chestnut teal (*Anas castanea)*	Area centralis[1]	-
	Northern shoveler (*Anas clypeata*)	Area centralis	Lisney et al. 2013b
	Blue-winged teal (*Anas discors*)	Area centralis	Lisney et al. 2013b
	Mallard (*Anas platyrhynchos)*	Area centralis	Lisney et al. 2013b
	Lesser scaup (*Aythya affinis*)	Area centralis	Lisney et al. 2013b
	Canada goose (*Branta canadensis*)	Area centralis	Lisney et al. 2013b
	Common goldeneye (*Bucephala clangula*)	Area centralis[1]	-
	Red-breasted merganser (*Mergus serrator*)	Area centralis	Lisney et al. 2013b
Apodiformes	Rufous-tailed hummingbird (*Amazilia tzacatl*)	Central fovea[1], area temporalis	Lisney et al. 2015
	Long-tailed hermit (*Phaetornis superciliosus*)	Central fovea[1,2]	Lisney et al. 2015
	Rufous hummingbird (*Selasphorus rufus*)	N/A	-
Caprimulgiformes	Tawny frogmouth (*Podargus strigoides*)	Temporal fovea	Wallman and Pettigrew 1985
Cathartiformes	Turkey vulture (*Cathartes aura*)	Central fovea, area temporalis	Lisney et al. 2013
	Black vulture (*Cathartes atratus*)	Central fovea, area temporalis	Lisney et al. 2013
Charadriiformes	Bonaparte's gull (*Larus philadelphia*)	N/A	-
	Eurasian woodcock (*Scolopax rusticola*)	N/A	-
Columbiformes	White-headed pigeon (*Columba leucomela*)	N/A	-
	Rock dove (*Columba livia*)	Central fovea, area temporalis	Binggeli and Paule 1969
	Bar-shouldered dove (*Geopelia humeralis*)	N/A	-
	Spotted dove (*Stigmatopelia chinensis*)	N/A	-
	Mourning dove (*Zenaida macroura*)	Area centralis	Dolan and Fernández-Juricic 2010

Coraciiformes	Laughing kookaburra (*Dacelo novaeguineae*)	Two foveae	Moroney and Pettigrew 1987
Falconiformes	Merlin (*Falco columbarius*)	Two foveae[1]	-
	American kestrel (*Falco sparverius*)	Two foveae	Gaffney and Hodos 2003
Galliformes	Chukar (*Alectoris chukar*)	Area centralis	Lisney et al. 2012b
	Ruffed grouse (*Bonasa umbellus*)	Area centralis	Lisney et al. 2012b
	Japanese quail (*Coturnix japonica*)	Area centralis	Lisney et al. 2012b
	Spruce grouse (*Dendragapus canadensis*)	Area centralis	Lisney et al. 2012b
	Grey partridge (*Perdix perdix*)	Area centralis	Lisney et al. 2012b
	Common pheasant (*Phasianus colchicus*)	Area centralis	Lisney et al. 2012b
	Lesser prairie chicken (*Tympanuchus pallidicinctus*)	Area centralis[1]	-
	Sharp-tailed grouse (*Tympanuchus phasianellus*)	Area centralis	Lisney et al. 2012b
Gruiformes	American coot (*Fulica americana*)	Central fovea	Walls 1942
Passeriformes	Red-winged blackbird (*Agelaius phoeniceus*)	Central fovea	Fernández-Juricic et al. 2019
	Tufted titmouse (*Baeolophus bicolor*)	Central fovea	Moore et al. 2013
	House finch (*Carpodacus mexicanus*)	Area centralis	Dolan and Fernandez-Juricic 2010
	Gray catbird (*Dumetella carolinensis*)	N/A	-
	Australian magpie (*Gymnorhina tibicen*)	N/A	-
	Dark-eyed junco (*Junco hyemalis*)	Central fovea	Moore et al. 2015
	Song sparrow (*Melospiza melodia*)	Central fovea	Moore et al. 2015
	Brown-headed cowbird (*Molothrus ater*)	Area centralis	Dolan and Fernandez-Juricic 2010
	Carolina chickadee (*Parus carolinensis*)	Central fovea	Moore et al. 2013
	Chipping sparrow (*Spizella passerina*)	Central fovea	Moore et al. 2015
	Field sparrow (*Spizella pusilla*)	Central fovea	Moore et al. 2015
	Double-barred finch (*Taeniopygia bichenovii*)	Central fovea[1]	-
	Zebra finch (*Taeniopygia guttata*)	Central fovea	Bischof 1988
	House wren (*Troglodytes aedon*)	N/A	-
	White-throated sparrow (*Zonotrichia albicollis*)	Central fovea	Moore et al. 2015
Pelecaniformes	Nankeen night heron (*Nycticorax caledonicus*)	Area centralis	Walls 1942
Psittaciformes	Australian king parrot (*Alisterus scapularis*)	N/A	-

	Galah (*Cacatua roseicapilla*)	Central fovea, area temporalis	Coimbra et al. 2014
	Long-billed corella (*Cacatua tenuirostris*)	Central fovea, area temporalis	Coimbra et al. 2014
	Budgerigar (*Melopsittacus undulatus*)	Area centralis, area nasalis	Mitkus et al. 2014
	Cockatiel (*Nymphicus hollandicus*)	Central fovea	Coimbra et al. 2014
Strigiformes	Northern saw-whet owl (*Aegolius acadicus*)	Temporal fovea	Lisney et al. 2012
	Short-eared owl (*Asio flammeus*)	Temporal fovea	Lisney et al. 2012
	Snowy owl (*Bubo scandiaca*)	Temporal fovea	Lisney et al. 2012
	Great horned owl (*Bubo virginianus*)	Temporal fovea	Lisney et al. 2012
	Great grey owl (*Strix nebulosa*)	Temporal fovea	Lisney et al. 2012
	Barred owl (*Strix varia*)	Temporal fovea	Lisney et al. 2012
	Northern hawk-owl (*Surnia ulula*)	Temporal fovea	Lisney et al. 2012
	Barn owl (*Tyto alba*)	Area temporalis	Lisney et al. 2012

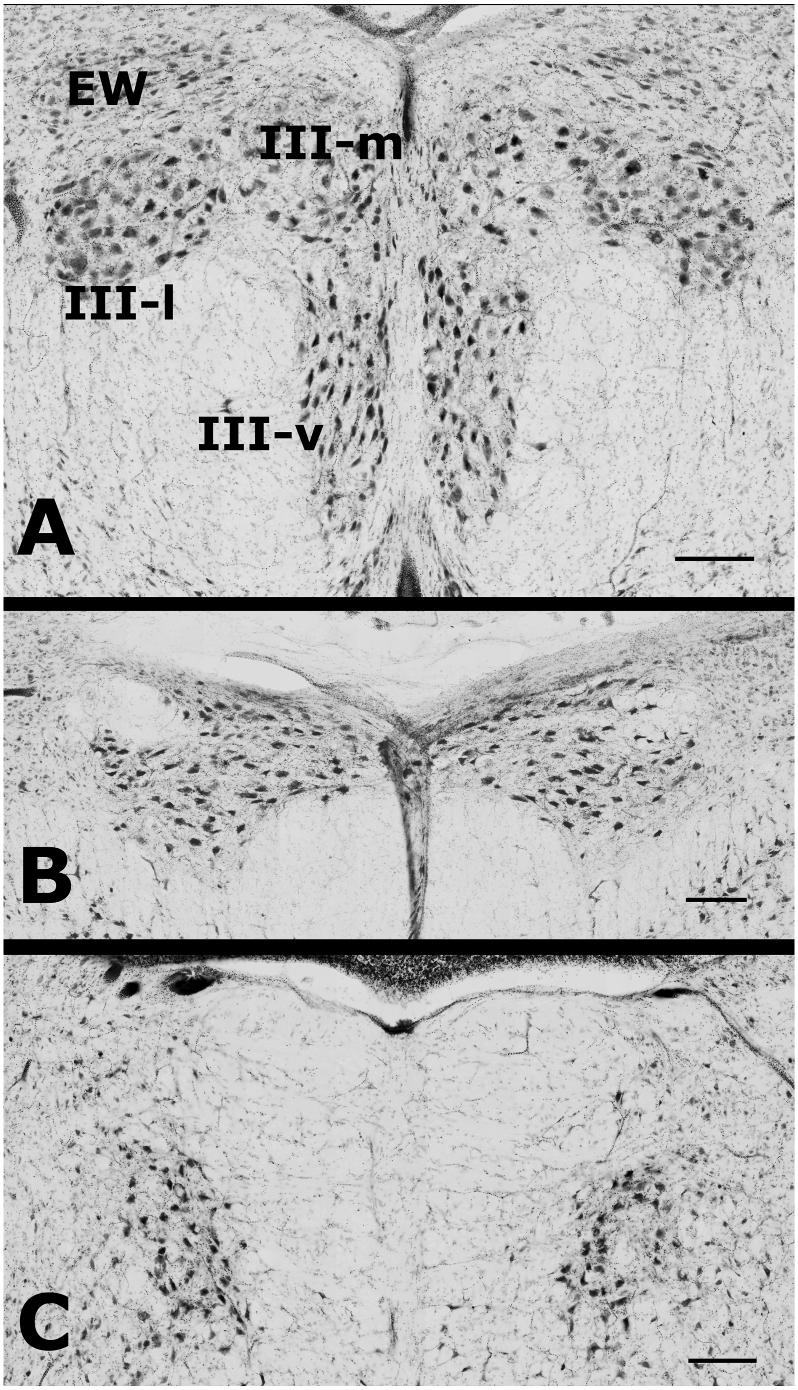

Figure 4.1. A. Oculomotor (III) and Edinger-Westphal (EW), **B.** trochlear (IV), and **C.** abducens (VI) nuclei of a ring-necked pheasant (*Phasianus colchicus*). Subnuclei of nIII are depicted in **A.**, III-m = dorsomedial III, III-l = dorsolateral III, III-v = ventral III. Scale-bar = 200 μm.

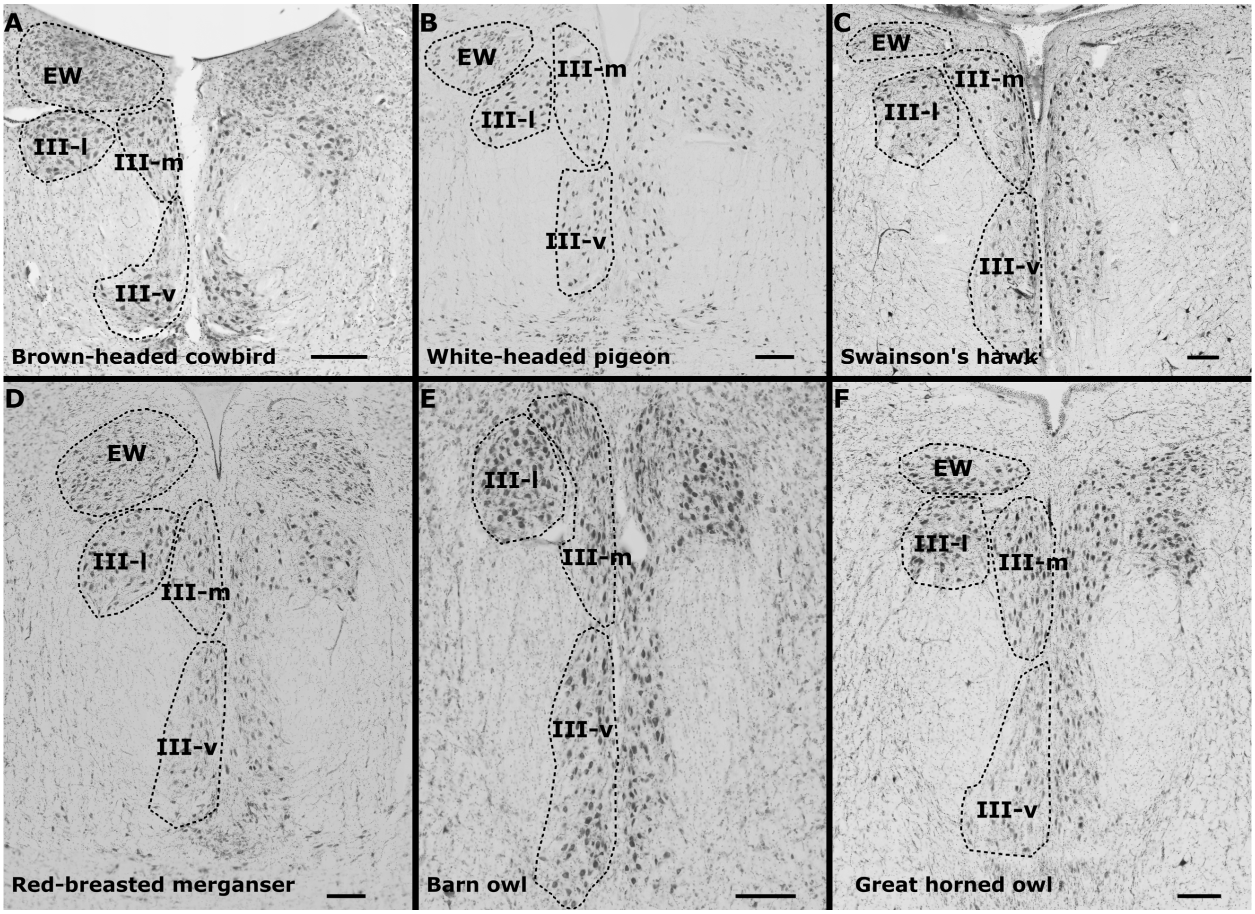

Figure 4.2. Oculomotor and Edinger-Westphal nuclei of: **A.** brown-headed cowbird (*Molothrus ater*), **B.** white-headed pigeon (*Columba leucomela*), **C.** Swainson's hawk (*Buteo swainsoni*), **D.** red-breasted merganser (*Mergus serrator*), **E.** barn owl (*Tyto alba*), and **F.** great horned owl (*Bubo virginianus*). EW = Edinger-Westphal; III-m = dorsomedial III; III-l = dorsolateral III; III-v = ventral III. Scale-bar = 200 μm.

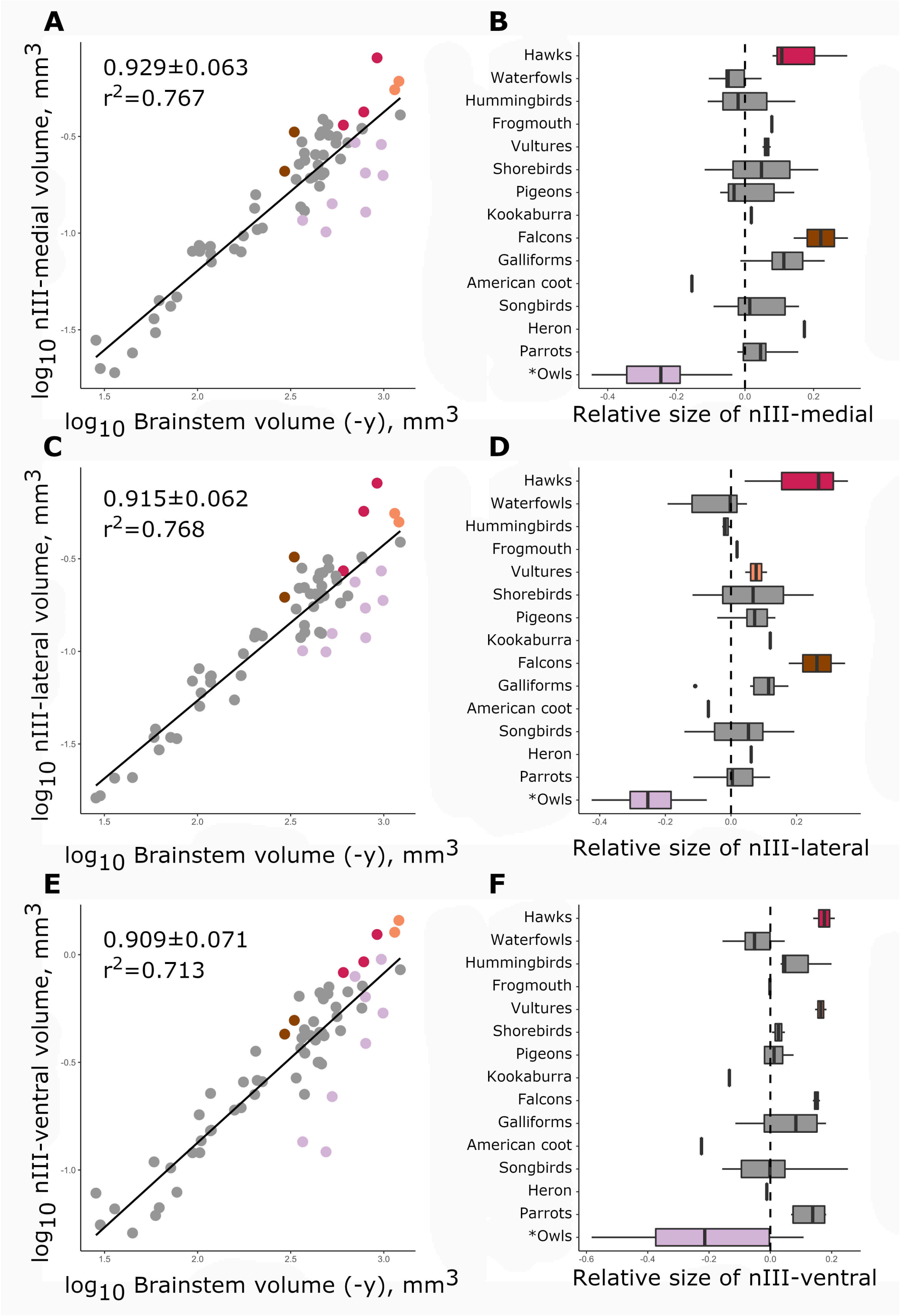

Figure 4.3. Scatterplots of log-transformed volumes (mm^3) of: **A.** dorsomedial III against brainstem, **C.** dorsolateral III against brainstem, and **E.** ventral III against brainstem. Residuals distribution across avian orders from each scatterplot performed are shown for: **B.** relative size of dorsomedial III, **D.** relative size of dorsolateral III, and **F.** relative size of ventral III. Significant differences found among bird orders by pANCOVAs are shown with an asterisk (*). Residuals boxplots are only a visual depiction of the differences found in graphs **A**, **C**, and **E**. III = oculomotor nucleus.

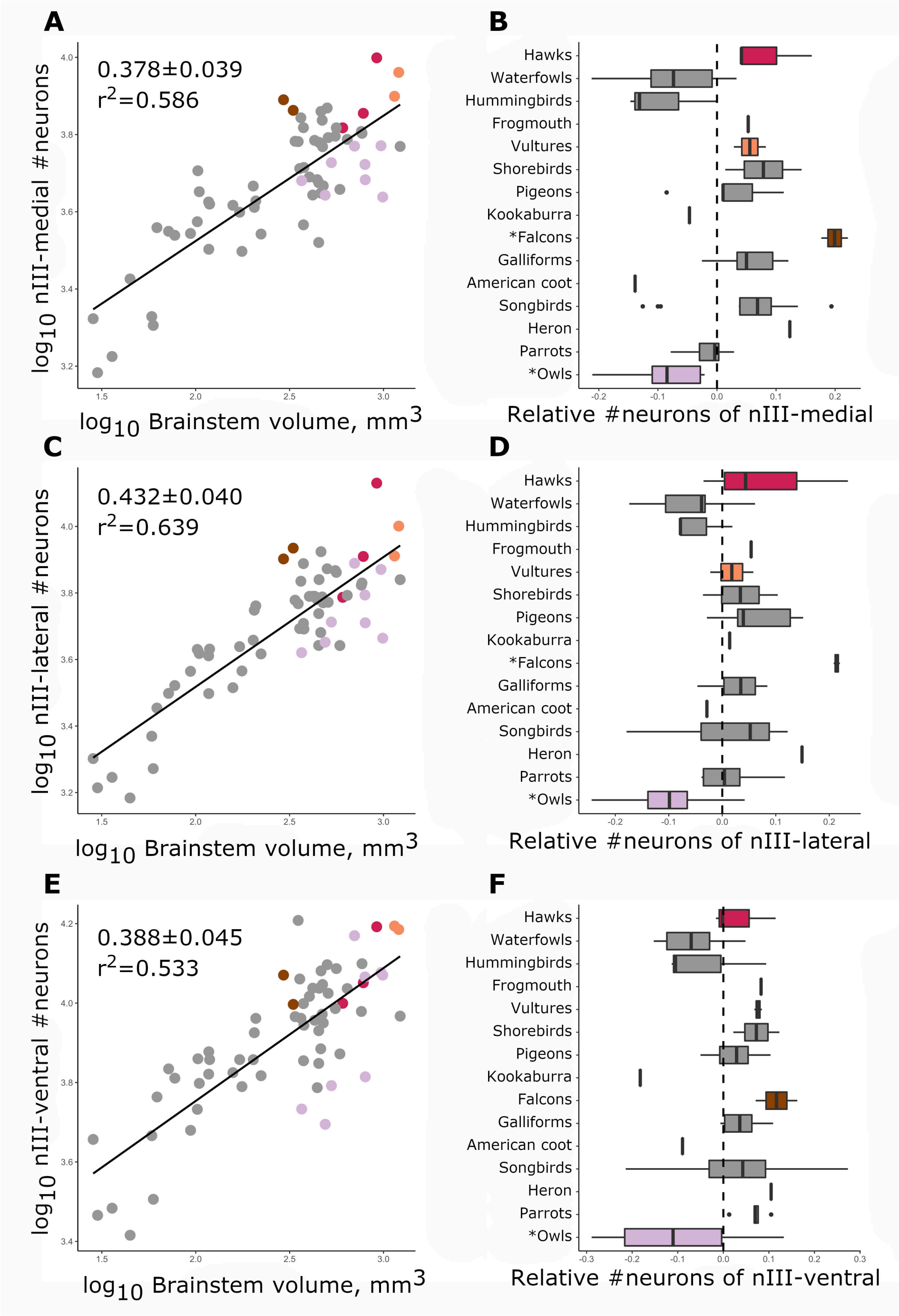

Figure 4.4. Scatterplots of log-transformed of: **A.** number of neurons of dorsomedial III against brainstem volume (mm^3), **C.** number of neurons of dorsolateral III against brainstem volume, and **E.** number of neurons of ventral III against brainstem volume. Residuals distribution across avian orders from each scatterplot performed are shown for: **B.** relative number of neurons of dorsomedial III, **D.** relative number of neurons of dorsolateral III, and **F.** relative number of neurons of ventral III. Significant differences found among bird orders by pANCOVAs are shown with an asterisk (*). Residuals boxplots are only a visual depiction of the differences found in graphs **A**, **C**, and **E**. III = oculomotor nucleus.

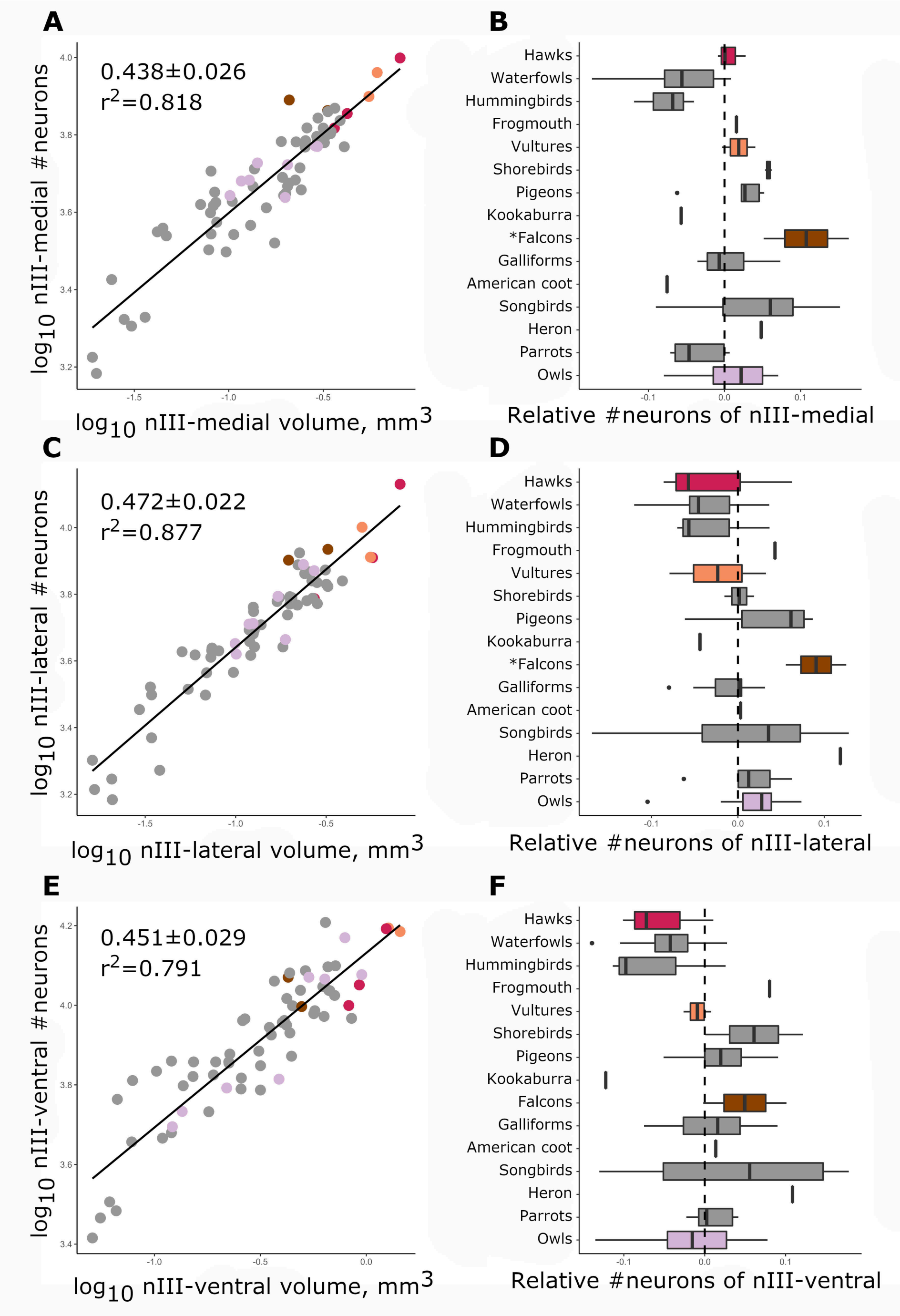

Figure 4.5. Scatterplots of log-transformed of: **A.** number of neurons of dorsomedial III against dorsomedial III volume (mm^3), **C.** number of neurons of dorsolateral III against dorsolateral III volume (mm^3), and **E.** number of neurons of ventral III against ventral III volume (mm^3). Residuals distribution across avian orders from each scatterplot performed are shown for: **B.** relative number of neurons of dorsomedial III, **D.** relative number of neurons of dorsolateral III, and **F.** relative number of neurons of ventral III. Significant differences found among bird orders by pANCOVAs are shown with an asterisk (*). Residuals boxplots are only a visual depiction of the differences found in graphs **A**, **C**, and **E**. III = oculomotor nucleus.

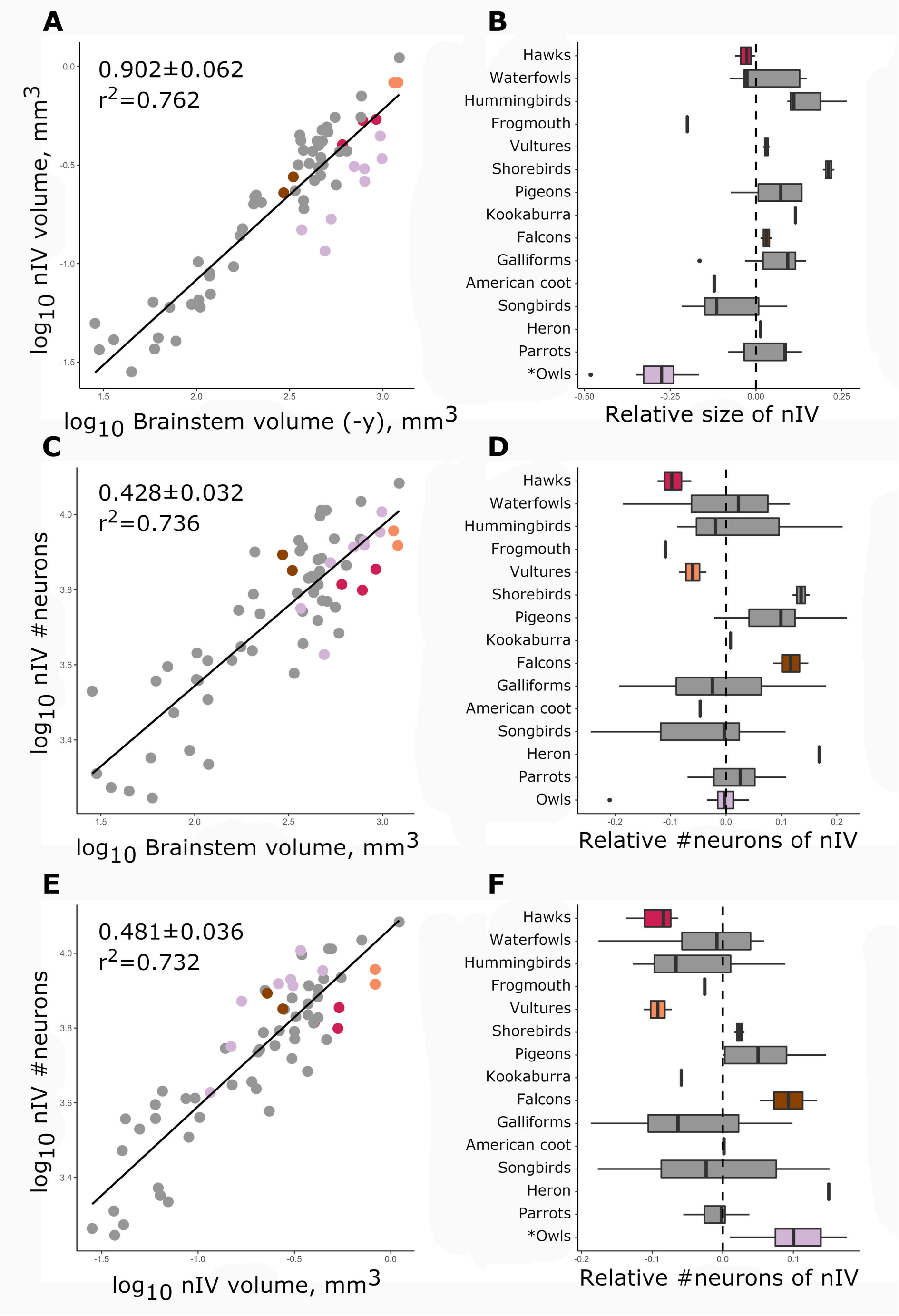

Figure 4.6. Scatterplots of log-transformed of: **A.** IV volume (mm^3) against brainstem volume (mm^3), **C.** number of neurons of IV against brainstem volume, and **E.** number of neurons of IV against IV volume. Residuals distribution across avian orders from each scatterplot performed are shown for: **B.** relative volume of IV, **D.** number of neurons of IV relative to brainstem size, and **F.** number of neurons of IV relative to IV volume. Significant differences found among bird orders by pANCOVAs are shown with an asterisk (*). Residuals boxplots are only a visual depiction of the differences found in graphs **A**, **C**, and **E**. IV = trochlear nucleus.

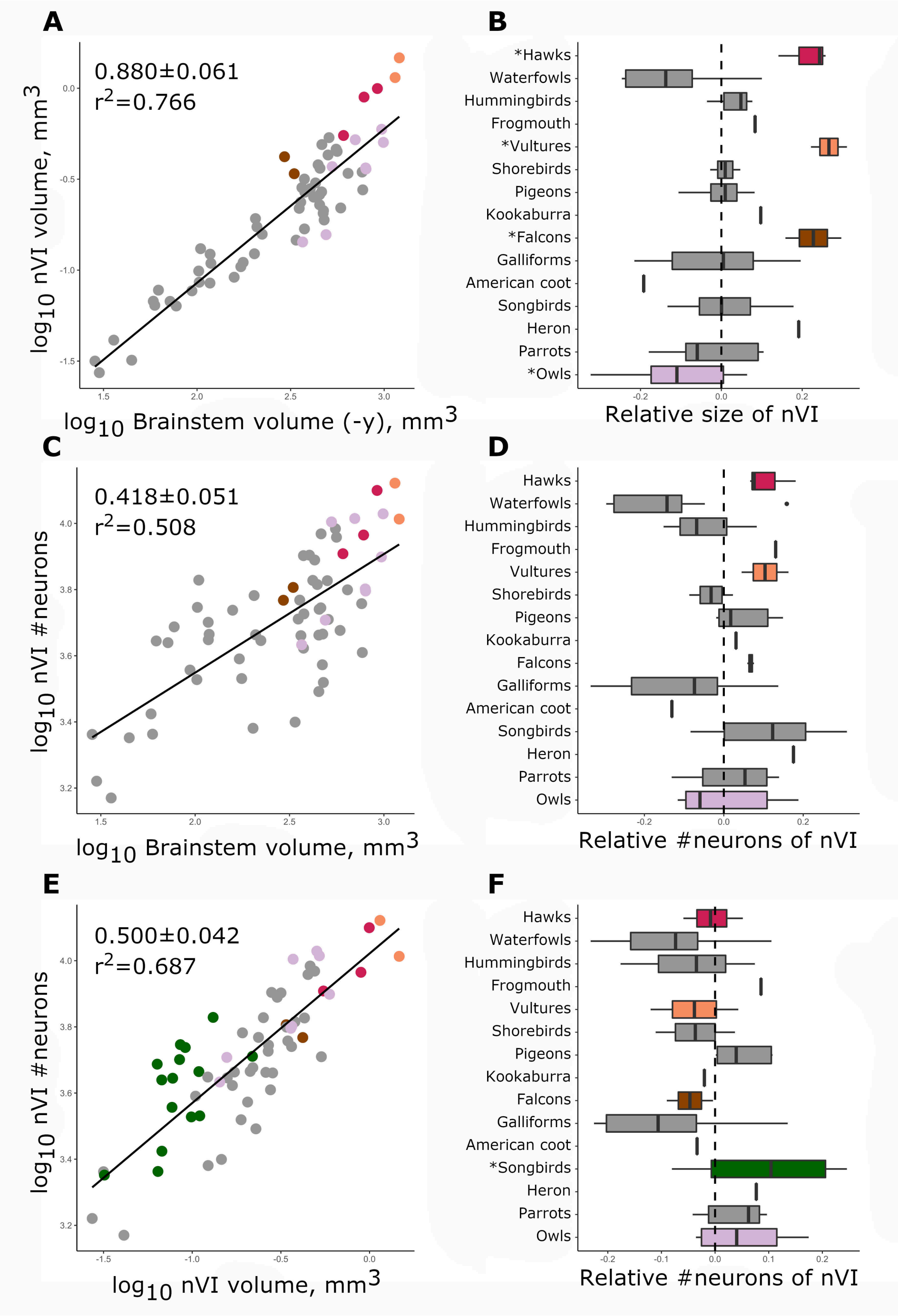

Figure 4.7. Scatterplots of log-transformed of: **A.** VI volume (mm^3) against brainstem volume (mm^3), **C.** number of neurons of VI against brainstem volume, and **E.** number of neurons of VI against VI volume. Residuals distribution across avian orders from each scatterplot performed are shown for: **B.** relative volume of VI, **D.** number of neurons of VI relative to brainstem size, and **F.** number of neurons of VI relative to VI volume. Significant differences found among bird orders by pANCOVAs are shown with an asterisk (*). Residuals boxplots are only a visual depiction of the differences found in graphs **A**, **C**, and **E**. VI = abducens nucleus.

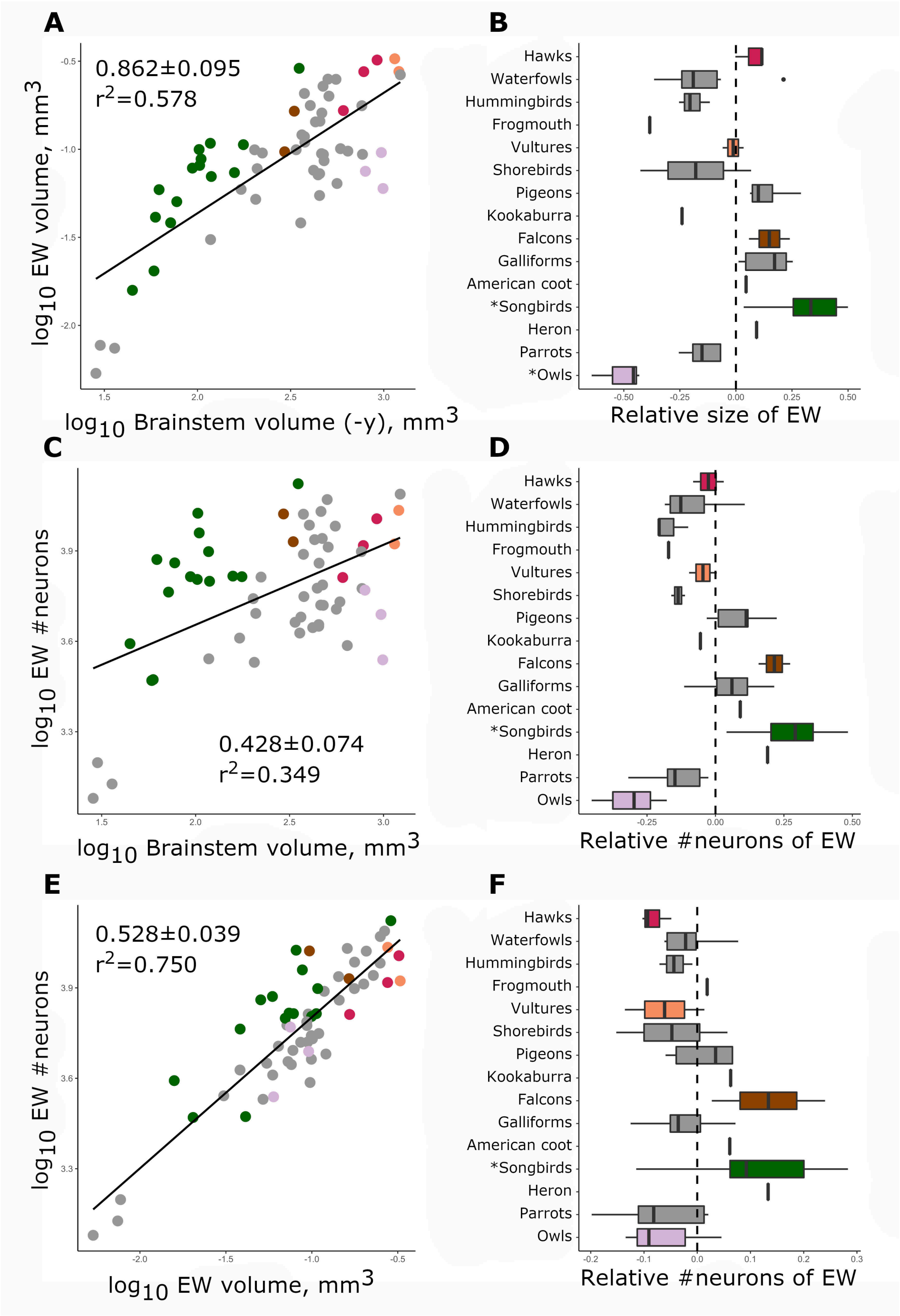

Figure 4.8. Scatterplots of log-transformed of: **A.** EW volume (mm^3) against brainstem volume (mm^3), **C.** number of neurons of EW against brainstem volume, and **E.** number of neurons of EW against EW volume. Residuals distribution across avian orders from each scatterplot performed are shown for: **B.** relative volume of EW, **D.** number of neurons of EW relative to brainstem size, and **F.** number of neurons of EW relative to EW volume. Significant differences found among bird orders by pANCOVAs are shown with an asterisk (*). Residuals boxplots are only a visual depiction of the differences found in graphs **A**, **C**, and **E**. EW = Edinger-Westphal.

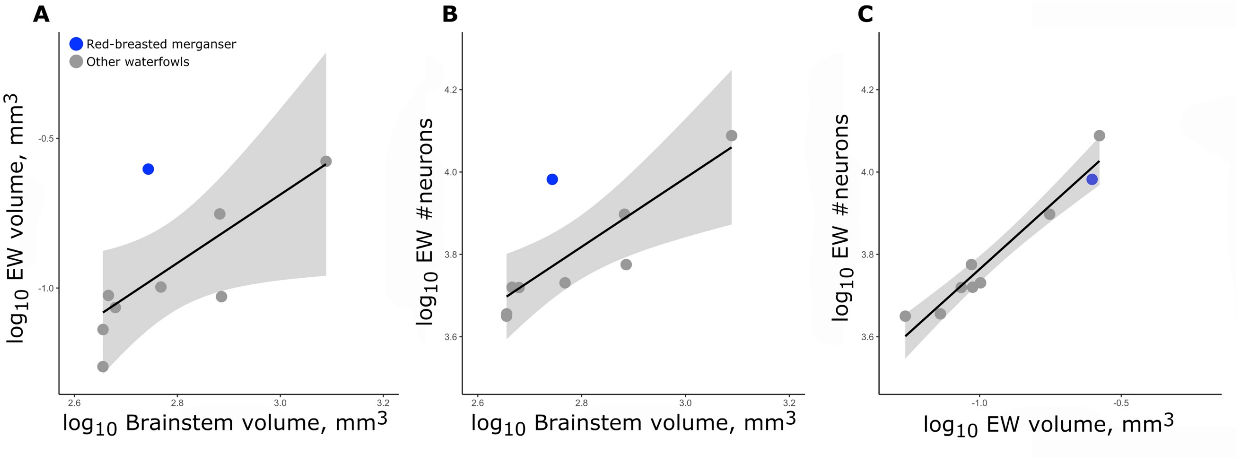

Figure 4.9. Scatterplots of log-transformed of: **A.** EW volume (mm^3) against brainstem volume (mm^3), **B.** number of neurons of EW against brainstem volume, and **C.** number of neurons of EW against EW volume across waterfowls. The red-breasted merganser (*Mergus serrator*) is highlighted in blue. Confidence intervals (95%) of the allometric regressions are indicated as gray shades in the graphs.

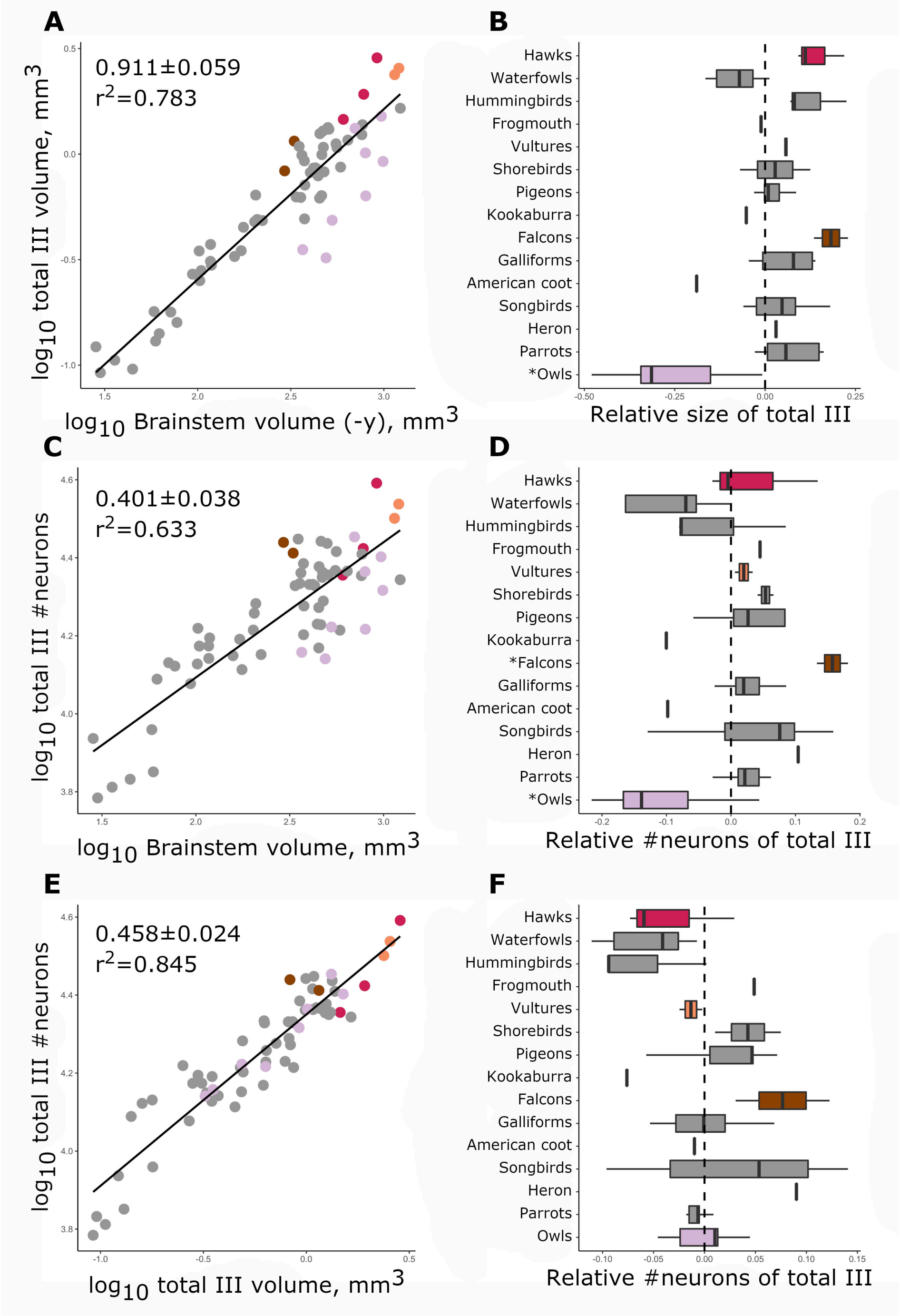

Figure 4.10. Scatterplots of log-transformed of: **A.** total III volume (mm^3) against brainstem volume (mm^3), **C.** number of neurons of total III against brainstem volume, and **E.** number of neurons of total III against total III volume. Residuals distribution across avian orders from each scatterplot performed are shown for: **B.** relative volume of total III, **D.** number of neurons of total III relative to brainstem volume, and **F.** number of neurons of total III relative to total III volume. Residuals boxplots are only a visual depiction of the differences found in graphs **A**, **C**, and **E.**

CHAPTER FIVE: GENERAL DISCUSSION

Recapitulation

Overall, the findings in this thesis shed light on the evolution of the avian brain by investigating species differences on the sizes of different brain regions as well as their neuronal composition. Thus far, most of what we know regarding cellular composition of the brain across different species is based on analyses of total neuron numbers, without distinguishing neuron types (Tramontin et al. 1998; Herculano-Houzel et al. 2014; Gabi et al. 2016; Olkowicz et al. 2016; Marhounová et al. 2019). In Chapter 2, by investigating how different neuronal types of the cerebellum vary in number among species, I demonstrated that the allometric relationships between brain size (e.g., cerebellum) and number of neurons may change with neuron types (Fig. 2.4). I also investigated in Chapter 2 how neuron size varies among species. By directly measuring neuron soma sizes, I found that allometric scaling rules between neuron size and cerebellum size can also vary among neuronal types, just as we found for the neuron numbers (Fig. 2.4). Next, in Chapter 3, by extracting the volumes of the cerebellum, telencephalon, and brain remainder across almost 300 species of birds, I explored how the interactions among brain region sizes, locomotory behaviours, and developmental mode affect the evolution of larger or smaller cerebella in birds (Fig. 3.4). For example, while altriciality in birds was weakly associated with the relative size of the cerebellum (Fig. 3.1), migration was positively associated with the size of the cerebellum relative to telencephalon size (Fig. 3.2). Lastly, in Chapter 4, I investigated how volume and number of neurons of the oculomotor nuclei change among birds; the results indicate that the sizes of the oculomotor nuclei, relative to brainstem size, vary greatly across bird species. Even though visually guided behaviours (e.g., predatory birds) and retinal configuration (e.g., bifoveate species) were not necessarily linked to a relative increase in the size and number of neurons of the oculomotor nuclei, owls did have overall relatively smaller oculomotor nuclei than other birds (Figs. 4.3, 4.6-4.8). Because owls have large immobile eyes (Walls 1942; Steinbach and Money 1972), I suggest that the relative reduction in size of the oculomotor nuclei across owls might reflect their low degrees of eye movements. In Chapter 4, I also found that volumetric shifts in the oculomotor nuclei among species were not necessarily driven by changes in the relative number of neurons. The results from Chapter 4 suggest that volumetric changes in the oculomotor nuclei are primarily driven by increases or decreases in neuron size.

With these results in mind, in the next sections I will develop a general discussion based on my main findings and the implications they have for understanding of the evolution of the brain. I will also stress the limitations of this current dissertation, further emphasizing several questions still left to answer, and future directions.

Brain size and neuron numbers: more complex than what we think

The principle of proper mass proposes that relative brain size reflects processing power (Jerison 1973). An increase in brain size is thought to arise from several anatomical changes, like numbers and sizes of neurons (Olkowicz et al. 2016; Cunha et al., 2020). Thus far, the most common belief is that increases in brain size are mainly governed by increases in neuron numbers, which would explain the improvement in processing power of the brain with increasing size (Herculano-Houzel et al 2014, 2017; Olkowicz et al 2016). For the last few decades, extensive quantitative data on neuron numbers were provided across a wide range of vertebrates (Herculano-Houzel et al. 2014; Olkowicz et al. 2016; Aicardi et al. 2020; Cunha et al. 2020;

Storks et al. 2020), and invertebrates (Polilov 2012; Makarova and Polilov 2013; Godfrey et al. 2021). A great part of these data became available by using a recent developed neuronal counting technique, the isotropic fractionator (Herculano-Houzel and Lent 2005). Although these studies confirmed that larger brains generally have more neurons, they also showed that 'allometric scaling rules' between brain size and number of neurons can vary greatly among clades (Herculano-Houzel et al. 2014; Olkowicz et al. 2016; Godfrey et al. 2021). For example, in primate species, the brain increases in mass close to the same rate as the increase in neuron numbers (Herculano-Houzel et al. 2007), whereas in rodents the brain mass increases at a faster rate than the addition of neurons (Herculano-Houzel et al. 2006). Taking a more extreme example, some birds, such as parrots, can reach similar or higher neuronal densities as mid-size primates, even though their brains are much smaller (Olkowicz et al. 2016). Therefore, a universal allometric scaling that explains the relationship between number of neurons and brain size does not exist across all species.

Despite these novel insights into of how brains are constructed among clades (Herculano-Houzel et al. 2014; Olkowicz et al. 2016), and how differences in the allometric scaling of the brain are related to phylogeny and cognition (Roth and Dicke 2005; Herculano-Houzel 2017; Marhounová et al. 2019), several other important questions remained unanswered. For example, most of the studies making use of the isotropic fractionator method do not distinguish neuronal types in their counting sample (Herculano-Houzel et al. 2014; Olkowicz et al. 2016; Godfrey et al. 2021). By immunostaining neurons with the antibody NeuN (Mullen et al. 1992), brain cells can only be categorized as neurons or non-neuronal cells (Herculano-Houzel and Lent 2005; Herculano-Houzel et al. 2014). However, just as allometric relationships for total neuron numbers may vary among clades or brain regions (Herculano-Houzel et al. 2014; Olkowicz et al.

2016), the allometric scaling for each type of neuron (e.g., Purkinje cells) or non-neuronal cell (e.g., astrocytes) could also vary within the brain (Cunha et al. 2020). Thus, an analysis that considers not only brain regions, but also different neuronal types was required to investigate whether 'allometric scaling rules' varied with neuron types, and if so, how it relates to phylogeny and function.

My first hypothesis, species differences in cerebellum size are primarily due to neuron numbers, was supported by the results in Chapter 2. As shown in Figure 2.4, neuron number is more strongly correlated with cerebellum size and increases at a faster rate than neuron size. However, Chapter 2 also clearly shows that relationships between neuron number and cerebellum size differ among neuronal populations. For example, relative to cerebellar volume, the number of granule cells increases at a significantly faster rate than the number of cerebellar nuclei neurons (Fig. 2.4). In the same way that total neuronal density may vary among clades (Herculano-Houzel et al. 2014; Olkowicz et al. 2016), the 'allometric scaling rules' between neuron numbers and brain size can also vary within the brain, depending on which neuronal type is being considered. This means that quantitative studies should not only consider regions of interest in the brain, but also their different neuronal types, either by morphological, molecular and/or circuitry criteria. A more detailed, quantitative data set on the neuronal composition of the brain will be critical to determine how differences in neuron numbers reflect cognition based on brain circuitry.

In addition to neuron numbers, the variation in neuron size among species has also been discussed to a lesser extent in the literature (DeVoogd and Nottebohm 1981; Born and Rubel 1985; Flood and Coleman 1988; Meitzen et al. 2011). There is evidence that neuron size (e.g., soma size) correlates with brain physiology (DeVoogd and Nottebohm 1981; Chang et al. 2020), and as such, might explain inter- and intraspecies differences in behaviour and ecology (DeVoogd and Nottebohm 1981). Nevertheless, data on neuron sizes across species are still largely scarce, and so is the understanding of the role of neuron size on brain evolution. In fact, most of what we know thus far about species variation in neuron size comes from indirect measurements of estimates done through the isotropic fractionator method (Herculano-Houzel et al. 2014). In these studies, the inverse of total neuronal density is adopted as an index to estimate neuron size rather measuring neuron size (e.g., soma size) directly (see review Herculano-Houzel et al., 2014). Neuron size can, however, vary independently of neuronal density, rendering this estimation technique inaccurate. Accordingly, when directly measuring soma sizes for different neuronal populations in the cerebellum (Chapter 2), I show that neuron size, relative to the cerebellum volume, does not vary at the same rate as the changes in neuron number (Figure 2.4). Moreover, the "allometric scaling rules" relative to neuron size can also vary among neuron types (Fig. 2.4). This stresses the importance of actual neuron size measurements in the study of brain allometry and indicates that more detailed approaches are needed than what is typical of isotropic fractionation or volumetric studies.

Chapter 4 reinforces the notion that counting neurons provides an incomplete picture of evolutionary differences in brain anatomy. In this chapter, I tested the hypothesis that both nucleus volume and neuron number covaried with eye movements. Accordingly, grade shifts in the volume of the oculomotor nuclei appear to be associated with eye movements across species. Owls, for example, have extremely limited degrees of eye movements and had relatively smaller oculomotor nuclei than other birds (Figs. 4.3, 4.6-4.8). These volumetric shifts, however, did not necessarily reflect similar changes in the numbers of neurons. This means that neuron number does not appear to always explain volumetric differences in the oculomotor nuclei. Instead, the results indicate that volumetric differences in these brainstem nuclei are better explained by neuron sizes rather than neuron numbers.

Altogether, the results from Chapter 2 and 4 cast new light on the biological meaning of neuron numbers in the evolution of the brain. Specifically, they call into question the assumption that total number of neurons is the most important variable driving volumetric changes (Roth and Dicke 2005; Herculano-Houzel et al. 2014; Herculano-Houzel 2017; Marhounová et al. 2019) and that the principle of proper mass needs to be expanded to parameters beyond brain size or neuron numbers. Here, I suggest that brain size variation must occur through a combination of changes in multiple, different variables: neuron numbers, neuron sizes, neuropil, number of synapses and dendritic spines, etc. For instance, the number of neurons could be a major driver for volumetric increases in sensory regions of the brain, whereas the size of neurons may be an important driver for volumetric changes in motor regions. Likewise, the correlation between brain variables (e.g., neuron number or neuron size) and neural processing capacity is likely to vary among different regions of the brain. Thus, neuron number might reflect processing power in some brain regions, but in other brain regions, neuron size may better predict processing power. The solution therefore is to accept the idea that within the brain, there are different possible ways to increase brain size. As a result, when trying to understand what determines the evolution of the brain, serious efforts should be made to include the maximum number of parameters that could potentially explain the expansion of the brain.

Are there "allometric scaling rules" in the brain?

Many different studies have attempted to determine the "allometric scaling *rules*" of the brain for different vertebrate species (Herculano-Houzel et al. 2014, 2015; Olkowicz et al. 2016;

Burger et al. 2019; Cunha et al. 2020; Aicardi et al. 2020; Storks et al. 2020). Most of these studies report several different "scaling rules" depending on the level of analyses (Herculano-Houzel et al. 2014; Olkowicz et al. 2016; Cunha et al. 2020). For example, although primates appear to share an 'allometric scaling rule' for the relationship between the total number of neurons and whole brain size (Herculano-Houzel et al. 2007, 2014), this relationship is broken down into different "scaling rules" when different brain regions (e.g., cerebral cortex and cerebellum) are considered separately in the analysis (Herculano-Houzel et al. 2014).

As shown in Chapter 2, there is no single, universal allometric *rule* within the brain. For this reason, I suggest avoiding the concept of "allometric scaling *rules*". As revealed here, allometric relationships will always depend and vary according to the species and variables sampled. This limitation therefore should prevent us from calling allometric relationships in the brain as "scaling *rules"*. The emphasis should therefore be on the slopes and intercepts of interspecific allometry and that these allometric relationships can be modifed over evolutionary time, as revealed by several recent comparative studies (Tsuboi et al. 2018; Ksepka et al. 2020 Smaers et al. 2021).

2-in-1: concerted and mosaic brain hypotheses

Not only does whole brain size varies enormously (in relative and absolute terms) within vertebrate species, but also the sizes of individual brain regions (Striedter 2005). The evolutionary mechanisms underlying this variation are still a matter of debate. Currently, two main theories have attempted to explain the evolutionary patterns observed in the variation of the brain size of vertebrates. The "mosaic brain evolution hypothesis" posits that evolutionary changes in the sizes of brain regions may occur independently from one another (Barton and

Harvey 2000). In contrast, the “hypothesis of concerted brain evolution” presumes that regions of the brain are intricately connected by physiology and/or development, and therefore evolutionary changes in the brain involve all parts of the tissue (Finlay and Darlington 1995). These hypotheses, however, are not mutually exclusive. In fact, several studies indicate that brain evolution generally operates through a combination of both models (Gutiérrez-Ibáñez et al. 2014; Herculano-Houzel et al. 2014; Noreikiene et al. 2015; Hoops et al. 2017; Moore and DeVoogd 2017).

In my thesis I could test both hypotheses by not only analyzing variation in the sizes of different brain regions across species (Chapters 3, 4), but also investigating how different compartments belonging to one brain region, the cerebellum, vary in size relative to one another (Chapter 2). Overall, the results in this dissertation confirm what it has been suggested by recent studies (Gutiérrez-Ibáñez et al. 2014; Noreikiene et al. 2015; Hoops et al. 2017; Moore and DeVoogd 2017): depending on the level of investigation, or which variables are incorporated into the analysis, one hypothesis will be more supported than the other, yet this does not mean one excludes the other. The results from Chapter 2 and 4 help illustrate this phenomenon. In Chapter 2, for example, I found that the three cerebellar layers increase in size, relative to one another, through a tight, concerted fashion across bird species. In contrast, in Chapter 4, although hawks had a relatively larger nucleus VI, the other oculomotor nuclei examined were not significantly enlarged in this avian clade. This highlights that the evolution of larger brain regions arises from both concerted and mosaic patterns of change.

Further evidence in support of both hypotheses playing a role in the evolution of larger or smaller brains is provided in Chapter 3. In that chapter, my analyses reveal that sizes of the cerebellum and telencephalon evolve in a concerted fashion in birds (Fig. 3.4), such that larger cerebella correlate with larger telencephala. In contrast, when evaluating how these two brain regions vary in size as a function of developmental mode in birds, altricial species had relatively larger telencephala than precocial species, but no relative changes in the size of the cerebellum (Fig. 3.1). Again, these findings confirm that changes in the size of the brain arise from both concerted and mosaic evolutionary influences and explaining brain size variation through one single evolutionary hypothesis (Finlay and Darlington 1995; Barton and Harvey 2000; Finlay et al. 2001; Yopak et al. 2010) clearly does not take into account the many different possibilities in which the brain evolves across species (see Avin et al. 2021).

I therefore endorse the view that the two hypotheses of brain evolution, 'mosaic' and 'concerted', are not in dispute. So, does it still matter understanding how brain regions vary relative to one another? Yes, it still does. By determining how brain components change in size relative to one another or body size, we can further speculate on reasons for why the brain expands as a function of connectivity, development and/or behaviour. For instance, the isometric, coordinated changes among the volumes of cerebellar layers (Fig. 2.3) appear to be associated with the fact that patterns of connectivity and organization among these layers are highly uniform across different species. That is, the concerted changes among the cerebellar compartments provide clues about the evolution of the cerebellum in relation to its connectivity across avian clades, and even vertebrates in general. Conversely, the finding that nucleus VI was the only oculomotor nucleus relatively enlarged in hawks indicates that even brain regions involved in similar functions (e.g., eye movement) can change in size independently from one another. Thus, investigating how individual brain regions vary in size relative to one another still gives valuable insights into how the brain evolves in relation to connectivity, development, and function.

In addition to having implications for the mosaic vs. concerted "debate", the comparative results from this thesis only partially support the principle of proper mass. Species executing lower degrees of eye movements, such as owls, had relatively smaller oculomotor nuclei than other birds. Conversely, hawks, falcons, and vultures had relatively larger abducens nucleus, which might reflect the need for extra degrees of eye movements when these birds are hunting or scavenging. These findings mentioned above support my third hypothesis: size of the oculomotor nuclei and numbers of neurons within them reflect the degree of eye movements. In contrast, I did not find any significant associations between cerebellum size and flight manoeuverability (Chapter 3). Although these results argue against my second hypothesis, the analysis of the cerebellum as a whole could have masked potential correlations between cerebellum size and the evolution of complex motor behaviour (see below). Similarly, our understanding of motor control/coordination among bird species is poor and there are often issues when assuming a particular behaviour is more "complex" than another (Healy and Rowe 2007). The relationship between brain region size and behaviour therefore continues to be ambiguous and not universal, but as discussed above, this is likely a product of focusing on volumetric measurements in testing the principle of proper mass. More effective tests will be enabled by the development of comparative data sets that include additional measurements, such as neuron numbers, neuron size, differentiation of neuronal populations, and even synapse numbers.

Future directions

Based on the analyses I completed in my thesis, several other interesting questions remain to be answered that are crucial to understanding brain evolution. For Chapter 2, similar examination of the cerebellar morphology in mammalian species would offer great insights into whether the allometric patterns among the volumes of the cerebellar layers in birds also apply to other vertebrate classes. Given that the cerebellum is uniformly organized in most vertebrate species (Yopak et al. 2017), different cerebellar layers might also increase in a concerted fashion, relative to one another, in other vertebrates. If the concerted relationships among the volumes of cerebellar layers hold true for mammals and other vertebrates, we can infer that isometric volumetric changes within the cerebellum are a conserved pattern across vertebrates in general.

Although the entire cerebellum is uniformly organized in relation to its anatomy and internal connectivity (Yopak et al. 2017; Apps et al. 2018), different folia of the cerebellum are involved in different functions (Oscarsson 1979; Apps et al. 2018; Wylie et al. 2018). Folium VI, for example, receives visual input from several sources and is therefore suggested to play an important role in visual motion processing in flying birds (Wylie et al. 2018). Combined with the fact that strong flier birds have folium VI and VII enlarged (Iwaniuk et al. 2007), anatomical differences in the cerebellum as a function of behaviour (e.g., flight maneuverability) are likely restricted to specific folia or functional zones. Maneuverable or strong flying birds, for instance, could have relatively more (or larger) neurons in folium VI than other birds or even proportionally more neurons of a specific type (e.g., Purkinje cells). A question for future research is to investigate how the relative number of neurons in each folium varies according to different behaviours in birds, like flight performance.

Related to Chapter 2, a logical extension of the path analyses in Chapter 3 would be to include neuron numbers. Because neuronal density can vary across clades (Herculano-Houzel et al. 2014; Olkowicz et al. 2016; Cunha et al. 2020), the inclusion of this variable into evolutionary path analysis or other models would enable one to assess the interaction effects of neuron numbers in the evolution of the brain. By including neuron numbers in the path analysis, it will be possible to test whether evolutionary patterns found for the volumes of brain regions also apply to numbers of neurons.

In Chapter 3, I also suggest that shifts in the relationship between cerebellum and telencephalon sizes, as a function of migration, support both the energetic and cognitive buffer hypotheses. As a result, an interesting continuation of this chapter would be to further explore the two hypotheses by comparing finer aspects of the brain anatomy between migratory and resident birds. For example, does the shift in the relationship between telencephalon size and cerebellum size in residents and migrants reflect other differences in the brain? The inclusion of number of neurons in this analysis would permit a test of whether residents have higher neuron numbers in the telencephalon, relative to the neuron numbers in the cerebellum, than migratory birds. Another interesting way to test the energetic and cognitive buffer hypotheses as a function of migration would be to analyze species in which some populations are migratory, and others are resident. For example, subspecies of dark-eyed juncos (*Junco hyemalis*) can either be resident or migratory (Rabenold and Rabenold 1985; Cristol et al. 2003). By analyzing individuals with different migratory behaviour, it will be possible to effectively answer questions such as: do we still find shifts in the interrelationship telencephalon-cerebellum between migratory and resident populations, and do resident populations show better performance in cognitive tests than migratory populations?

Finally, in chapter 4, the inclusion of more bifoveate predatory birds into our sample will be critical to confirm some of the patterns observed. As mentioned in Chapter 4, predatory birds are highly diverse in relation to visually guided behaviour (Potier 2020), but detailed studies investigating differences in the visual aspects in these species are still wanting. The inclusion of quantitative data on the oculomotor nuclei across a wide range of predatory birds, combined with a more comprehensive knowledge on their visually-guided behaviours, will bring important clues on the evolution of the oculomotor complex. More specifically, it will be of great value to include Old World vultures in the analysis. This group of birds is actually more closely related to hawks and eagles than New World vultures (Lerner and Mindell 2005). However, most Old World vultures are scavengers just like New World vultures (Buechley and Sekercioglu 2016). Thus, by including more species of hawks, eagles, and vultures in the analysis, it will be possible to effectively test whether the allometric relationships of the oculomotor nuclei differ among vultures (Old and New World vultures), hawks, and eagles. For example, if both Old and New World vultures differ from hawks and eagles, I can infer that scavenging behaviour might reflect differences in the anatomy of the oculomotor nuclei.

In conclusion, the results in this thesis reveal that within the brain there are multiple explanations for changes in brain and brain region size. Differently from what it would have been expected from previous results (Herculano-Houzel et al 2014, 2015; Olkowicz et al. 2016), grade shifts in the relative size of the brain do not always reflect changes in the numbers of neurons. As shown in my results, differences in brain size can arise through changes in other parameters beyond neuron numbers, like neuron sizes. Therefore, the idea of the principle of proper mass that relatively larger brains provide more and/or better processing capacity can be explained by several, different parameters in the brain. In addition to that, different parameters within the brain (e.g., neuron size and neuron number) are likely correlated to one another, which means that brain size is the result of an intricate interaction among all of these parameters as well as behaviour. Quantifying many different parameters within the brain (neuron number, neuron size, dendritic arborization, number of synapses, vasculature, etc) will be crucial to understand how they vary (1) across species, (2) within the brain, and (3) relative to one another. Although this will require herculean efforts to collect all of the required data, it will get us much closer to determining how and why brain anatomy varies across species and the relationship between brain anatomy and behaviour.

References

Aicardi, S., A. Amaroli, L. Gallus, D. Di Blasi, L. Ghigliotti, F. Betti, M. Vacchi, and S. Ferrando. 2020. Quantification of neurons in the olfactory bulb of the catsharks *Scyliorhinus canicula* (Linnaeus, 1758) and *Galeus melastomus* (Rafinesque, 1810). Zoology 141:125796.

Apps, R., R. Hawkes, S. Aoki, F. Bengtsson, A. M. Brown, G. Chen, T. J. Ebner, P. Isope, H. Jörntell, and E. P. Lackey. 2018. Cerebellar modules and their role as operational cerebellar processing units. The Cerebellum 17:654-682.

Avin, S., A. Currie, and S. H. Montgomery. 2021. An agent-based model clarifies the importance of functional and developmental integration in shaping brain evolution. BMC Biology 19:1-18.

Barton, R. A. and P. H. Harvey. 2000. Mosaic evolution of brain structure in mammals. Nature 405:1055-1058.

Born, D. E. and E. W. Rubel. 1985. Afferent influences on brain stem auditory nuclei of the chicken: neuron number and size following cochlea removal. Journal of Comparative Neurology 231:435-445.

Brown, W. M. 2001. Natural selection of mammalian brain components. Trends in Ecology & Evolution 16:471-473.

Buechley, E. R. and C. H. Sekercioglu. 2016. Vultures. Current Biology 26:R560-R561.

Burger, J. R., M. A. George Jr., C. Leadbetter, and F. Shaikh. 2019. The allometry of brain size in mammals. Journal of Mammalogy 100:276–283.

Chang, W., A. Pedroni, V. Hohendorf, S. Giacomello, M. Hibi, R. W. Köster, and K. Ampatzis. 2020. Functionally distinct Purkinje cell types show temporal precision in encoding locomotion. Proceedings of the National Academy of Sciences 117:17330-17337.

Cristol, D. A., E. B. Reynolds, J. E. Leclerc, A. H. Donner, C. S. Farabaugh, and C. W. Ziegenfus. 2003. Migratory dark-eyed juncos, *Junco hyemalis*, have better spatial memory and denser hippocampal neurons than nonmigratory conspecifics. Animal Behaviour 66:317-328.

Cunha, F., K. Racicot, J. Nahirney, C. Heuston, D. R. Wylie, and A. N. Iwaniuk. 2020. Allometric scaling rules of the cerebellum in galliform birds. Brain, Behavior and Evolution 95:78-92.

DeKosky, S. T. and S. W. Scheff. 1990. Synapse loss in frontal cortex biopsies in Alzheimer's disease: correlation with cognitive severity. Annals of Neurology 27:457-464.

DeVoogd, T. and F. Nottebohm. 1981. Gonadal hormones induce dendritic growth in the adult avian brain. Science 214:202-204.

Dicke, U. and G. Roth. 2016. Neuronal factors determining high intelligence. Philosophical Transactions of the Royal Society B: Biological Sciences 371:20150180.

Finlay, B. L. and R. B. Darlington. 1995. Linked regularities in the development and evolution of mammalian brains. Science 268:1578-1584.

Finlay, B. L., R. B. Darlington, and N. Nicastro. 2001. Developmental structure in brain evolution. Behavioral and Brain Sciences 24:263-278.

Flood, D. G. and P. D. Coleman. 1988. Neuron numbers and sizes in aging brain: comparisons of human, monkey, and rodent data. Neurobiology of Aging 9:453-463.

Gabi, M., K. Neves, C. Masseron, P. F. Ribeiro, L. Ventura-Antunes, L. Torres, B. Mota, J. H. Kaas, and S. Herculano-Houzel. 2016. No relative expansion of the number of prefrontal neurons in primate and human evolution. Proceedings of the National Academy of Sciences 113:9617-9622.

Godfrey, R. K., M. Swartzlander, and W. Gronenberg. 2021. Allometric analysis of brain cell number in Hymenoptera suggests ant brains diverge from general trends. Proceedings of the Royal Society B 288:20210199.

Gutiérrez-Ibáñez, C., A. N. Iwaniuk, B. A. Moore, E. Fernández-Juricic, J. R. Corfield, J. M. Krilow, J. Kolominsky, and D. R. Wylie. 2014. Mosaic and concerted evolution in the visual system of birds. PLoS One 9:e90102.

Healy, S. D. and C. Rowe. 2007. A critique of comparative studies of brain size. Proceedings of the Royal Society B: Biological Sciences 274:453-464.

Herculano-Houzel, S. 2017. Numbers of neurons as biological correlates of cognitive capability. Current Opinion in Behavioral Sciences 16:1-7.

Herculano-Houzel, S., C. E. Collins, P. Wong, and J. H. Kaas. 2007. Cellular scaling rules for primate brains. Proceedings of the National Academy of Sciences 104:3562-3567.

Herculano-Houzel, S. and R. Lent. 2005. Isotropic fractionator: a simple, rapid method for the quantification of total cell and neuron numbers in the brain. Journal of Neuroscience 25:2518-2521.

Herculano-Houzel, S., P. R. Manger, and J. H. Kaas. 2014. Brain scaling in mammalian evolution as a consequence of concerted and mosaic changes in numbers of neurons and average neuronal cell size. Frontiers in Neuroanatomy 8:77.

Herculano-Houzel, S., B. Mota, and R. Lent. 2006. Cellular scaling rules for rodent brains. Proceedings of the National Academy of Sciences 103:12138-12143.

Hoops, D., M. Vidal-García, J. F. Ullmann, A. L. Janke, T. Stait-Gardner, D. A. Duchêne, W. S. Price, M. J. Whiting, and J. S. Keogh. 2017. Evidence for concerted and mosaic brain evolution in dragon lizards. Brain, Behavior and Evolution 90:211-223.

Iwaniuk, A. N., P. L. Hurd, and D. R. Wylie. 2007. Comparative morphology of the avian cerebellum: II. Size of folia. Brain, Behavior and Evolution 69:196-219.

Jerison, H. 1973. Evolution of the brain and intelligence. Academic Press, New York.

Ksepka, D. T., A. M. Balanoff, N. A. Smith, G. S. Bever, B.-A. S. Bhullar, E. Bourdon, E. L. Braun, J. G. Burleigh, J. A. Clarke, and M. W. Colbert. 2020. Tempo and pattern of avian brain size evolution. Current Biology 30:2026-2036.

Lerner, H. R. and D. P. Mindell. 2005. Phylogeny of eagles, Old World vultures, and other Accipitridae based on nuclear and mitochondrial DNA. Molecular Phylogenetics and Evolution 37:327-346.

Makarova, A. and A. Polilov. 2013. Peculiarities of the brain organization and fine structure in small insects related to miniaturization. The smallest Hymenoptera (Mymaridae, Trichogrammatidae). Entomological Review 93:714-724.

Marhounová, L., A. Kotrschal, K. Kverková, N. Kolm, and P. Němec. 2019. Artificial selection on brain size leads to matching changes in overall number of neurons. Evolution 73:2003-2012.

Meitzen, J., K. R. Pflepsen, C. M. Stern, R. L. Meisel, and P. G. Mermelstein. 2011. Measurements of neuron soma size and density in rat dorsal striatum, nucleus accumbens core and nucleus accumbens shell: differences between striatal region and brain hemisphere, but not sex. Neuroscience Letters 487:177-181.

Moore, B. A., L. P. Tyrrell, D. Pita, O. R. Bininda-Emonds, and E. Fernández-Juricic. 2017. Does retinal configuration make the head and eyes of foveate birds move? Scientific Reports 7:1-7.

Moore, J. M. and T. J. DeVoogd. 2017. Concerted and mosaic evolution of functional modules in songbird brains. Proceedings of the Royal Society B: Biological Sciences 284:20170469.

Morest, D. K. 1969. The growth of dendrites in the mammalian brain. Zeitschrift für Anatomie und Entwicklungsgeschichte 128:290-317.

Mullen, R. J., C. R. Buck, and A. M. Smith. 1992. NeuN, a neuronal specific nuclear protein in vertebrates. Development 116:201-211.

Noreikiene, K., G. Herczeg, A. Gonda, G. Balázs, A. Husby, and J. Merilä. 2015. Quantitative genetic analysis of brain size variation in sticklebacks: support for the mosaic model of brain evolution. Proceedings of the Royal Society B: Biological Sciences 282:20151008.

Olkowicz, S., M. Kocourek, R. K. Lučan, M. Porteš, W. T. Fitch, S. Herculano-Houzel, and P. Němec. 2016. Birds have primate-like numbers of neurons in the forebrain. Proceedings of the National Academy of Sciences 113:7255-7260.

Oscarsson, O. 1979. Functional units of the cerebellum-sagittal zones and microzones. Trends in Neurosciences 2:143-145.

Polilov, A. A. 2012. The smallest insects evolve anucleate neurons. Arthropod Structure & Development 41:29-34.

Potier, S. 2020. Visual adaptations in predatory and scavenging diurnal raptors. Diversity 12:400.

Rabenold, K. N. and P. P. Rabenold. 1985. Variation in altitudinal migration, winter segregation, and site tenacity in two subspecies of dark-eyed juncos in the southern Appalachians. The Auk 102:805-819.

Roth, G. and U. Dicke. 2005. Evolution of the brain and intelligence. Trends in Cognitive Sciences 9:250-257.

Sherwood, C. C. 2005. Comparative anatomy of the facial motor nucleus in mammals, with an analysis of neuron numbers in primates. The Anatomical Record 287A:1067-1079.

Sherwood, C. C., P. R. Hof, R. L. Holloway, K. Semendeferi, P. J. Gannon, H. D. Frahm, and K. Zilles. 2005. Evolution of the brainstem orofacial motor system in primates: a comparative study of trigeminal, facial, and hypoglossal nuclei. Journal of Human Evolution 48:45-84.

Smaers, J.B., R. S. Rothman, D. R. Hudson, A. M. Balanoff, B. Beatty, D. K. Dechmann, D. de Vries, J. C. Dunn, J. G. Fleagle, C. C. Gilbert, A. Goswami, A. N. Iwaniuk, W. L. Jungers, M. Kerney, D. T. Ksepka, P. R. Manger, C. S. Mongle, F. J. Rohlf, N. A. Smith, C. Soligo, V. Weisbecker, K. Safi. 2021. The evolution of mammalian brain size. Science Advances, 7(18).

Steinbach, M. J. and K. Money. 1972. Eye movements of the owl. Defence and Civil Inst of Environmental Medicine Downsview (Ontario).

Storks, L., B. J. Powell, and M. Leal. 2020. Peeking inside the lizard brain: Neuron numbers in *Anolis* and its implications for cognitive performance and vertebrate brain evolution. Integrative and Comparative Biology. DOI 10.1093/icb/icaa129

Striedter, G. F. 2005. Principles of brain evolution. Sinauer Associates.

Tramontin, A. D., G. T. Smith, C. W. Breuner, and E. A. Brenowitz. 1998. Seasonal plasticity and sexual dimorphism in the avian song control system: stereological measurement of neuron density and number. Journal of Comparative Neurology 396:186-192.

Tsuboi, M., W. van der Bijl, B. T. Kopperud, J. Erritzøe, K. L. Voje, A. Kotrschal, K. E. Yopak, S. P. Collin, A. N. Iwaniuk and N. Kolm. 2018. Breakdown of brain–body allometry and the encephalization of birds and mammals. Nature Ecology & Evolution, 2(9), pp.1492-1500.

Walls, G. L. 1942. The vertebrate eye. Cranbrook Institute of Science, Michigan.

Welt, C. and J. H. Abbs. 1990. Musculotopic organization of the facial motor nucleus in *Macaca fascicularis*: a morphometric and retrograde tracing study with cholera toxin B-HRP. Journal of Comparative Neurology 291:621-636.

Wylie, D. R., C. Gutiérrez-Ibáñez, A. H. Gaede, D. L. Altshuler, and A. N. Iwaniuk. 2018. Visual-cerebellar pathways and their roles in the control of avian flight. Frontiers in Neuroscience 12:223.

Yopak, K. E., T. J. Lisney, R. B. Darlington, S. P. Collin, J. C. Montgomery, and B. L. Finlay. 2010. A conserved pattern of brain scaling from sharks to primates. Proceedings of the National Academy of Sciences 107:12946-12951.

Yopak, K. E., J. Pakan, and D. Wylie. 2017. The cerebellum of nonmammalian vertebrates. In Kaas JH (ed): Evolution of Nervous Systems, 2nd ed. Oxford, Academic Press, pp. 373-386.

SUPPLEMENTARY INFORMATION

Table S2.1 Sampling interval and grid size used for each neuronal population examined: Purkinje cells, granule cells, and cerebellar nuclei neurons. For Purkinje cells and cerebellar nuclei neurons, frame size was 80 x 80 µm. For granule cells, frame size was 10 x 10 µm.

		Purkinje cells		Granule cells		Cerebellar nuclei neurons	
Order	**Species/Common name**	**Sampling interval**	**Grid size**	**Sampling interval**	**Grid size**	**Sampling interval**	**Grid size**
Accipitriformes	Collared sparrowhawk (*Accipiter cirrocephalus)*	1:16	510 x 510	1:16	1800 x 1800	1:16	300 x 300
	Wedge-tailed eagle (*Aquila audax*)	1:16	500 x 500	1:24	2400 x 2400	1:10	300 x 300
	White-bellied sea eagle (*Haliaeetus leucogaster)*	1:18	580 x 580	1:20	2200 x 2200	1:6	300 x 300
Anseriformes	American wigeon (*Anas americana*)	1:32	420 x 420	1:32	1400 x 1400	1:14	300 x 300
	Northern shoveler (*Anas clypeata*)	1:10	480 x 480	1:16	1200 x 1200	1:16	200 x 200
	Mallard (*Anas platyrhynchos*)	1:16	400 x 400	1:16	1600 x 1600	1:6	300 x 300
	Gadwall (*Anas strepera*)	1:36	420 x 420	1:32	1200 x 1200	1:16	270 x 270
	Lesser scaup (*Aythya affinis*)	1:26	400 x 400	1:26	1100 x 1100	1:12	300 x 300
	Bufflehead (*Bucephala albeola)*	1:20	380 x 380	1:16	1100 x 1100	1:10	300 x 300
	Common goldeneye (*Bucephala clangula*)	1:22	440 x 440	1:28	1400 x 1400	1:14	300 x 300
	Red-breasted merganser (*Mergus serrator*)	1:34	420 x 420	1:36	1500 x 1500	1:6	300 x 300
Caprimulgiformes	Spotted nightjar (*Eurostopodus argus*)	1:10	210 x 210	1:10	700 x 700	1:4	270 x 270
	Tawny frogmouth (*Podargus strigoides*)	1:14	360 x 360	1:14	1300 x 1300	1:4	270 x 270
Casuariiformes	Emu (*Dromaius novaehollandiae*)	1:32	620 x 620	1:32	4500 x 4500	1:32	450 x 450
Charadriiformes	Silver gull (*Larus novaehollandiae*)	1:10	300 x 300	1:12	1100 x 1100	1:4	270 x 270
	Short-billed dowitcher (*Limnodromus griseus*)	1:8	230 x 230	1:8	1000 x 1000	1:4	250 x 250
Columbiformes	Rock dove (*Columba livia*)	1:12	440 x 440	1:12	1300 x 1300	1:6	300 x 300
	Peaceful dove (*Geopelia placida*)	1:8	260 x 260	1:8	500 x 500	1:4	270 x 270
Coraciiformes	Laughing kookaburra (*Dacelo novaeguineae*)	1:14	350 x 350	1:18	1600 x 1600	1:6	300 x 300
Falconiformes	Brown falcon (*Falco berigora*)	1:14	470 x 470	1:14	1800 x 1800	1:14	120 x 120
Galliformes	Ruffed grouse (*Bonasa umbellus*)	1:20	525 x 525	1:20	1400 x 1400	1:6	300 x 300
	Japanese quail (*Coturnix japonica*)	1:16	350 x 350	1:16	1000 x 1000	1:4	250 x 250
	Spruce grouse (*Dendragapus canadensis*)	1:20	525 x 525	1:20	1000 x 1000	1:10	270 x 270
	Turkey (*Meleagris gallopavo*)	1:24	700 x 700	1:24	2000 x 2000	1:10	300 x 300
	Indian peafowl (*Pavo cristatus*)	1:20	700 x 700	1:20	1600 x 1600	1:6	300 x 300
	Grey partridge						

	(*Perdix perdix*)	1:16	525 x 525	1:16	1300 x 1300	1:8	270 x 270
	Ring-necked pheasant (*Phasianus colchicus*)	1:16	700 x 700	1:16	1600 x 1600	1:20	200 x 200
Gruiformes	American coot (*Fulica americana*)	1:12	260 x 260	1:12	1300 x 1300	1:6	300 x 300
	Dusky moorhen (*Gallinula tenebrosa*)	1:10	300 x 300	1:12	1300 x 1300	1:6	300 x 300
Otidiformes	Australian bustard (*Ardeotis australis*)	1:14	580 x 580	1:14	1700 x 1700	1:8	300 x 300
Passeriformes	Brown thornbill (*Acanthiza pusilla*)	1:6	230 x 230	1:6	700 x 700	1:2	270 x 270
	Little raven (*Corvus mellori*)	1:14	600 x 600	1:14	2200 x 2200	1:8	300 x 300
	Australian magpie (*Gymnorhina tibicen*)	1:14	420 x 420	1:14	1500 x 1500	1:6	300 x 300
	Superb lyrebird (*Menura novaehollandiae*)	1:16	580 x 580	1:16	1400 x 1400	1:6	300 x 300
	Field sparrow (*Spizella pusilla*)	1:10	260 x 260	1:10	1000 x 1000	1:4	250 x 250
Pelecaniformes	Cattle egret (*Bubulcus ibis*)	1:12	360 x 360	1:12	1200 x 1200	1:6	300 x 300
	Australian pelican (*Pelecanus conspicillatus*)	1:20	600 x 600	1:20	2200 x 2200	1:10	300 x 300
Piciformes	Scaly-throated honeyguide (*Indicator variegatus*)	1:16	280 x 280	1:16	750 x 750	1:8	200 x 200
	Yellow-bellied sapsucker (*Sphyrapicus varius*)	1:20	220 x 220	1:18	950 x 950	1:8	250 x 250
Procellariiformes	Short-tailed shearwater (*Puffinus tenuirostris*)	1:16	580 x 580	1:16	1700 x 1700	1:4	300 x 300
	Black-browed albatross (*Thalassarche melanophris*)	1:20	600 x 600	1:18	2400 x 2400	1:10	300 x 300
Psittaciformes	Australian king parrot (*Alisterus scapularis*)	1:12	360 x 360	1:12	1600 x 1600	1:4	270 x 270
	Sulphur-crested cockatoo (*Cacatua galerita*)	1:18	560 x 560	1:18	1800 x 1800	1:8	300 x 300
	Galah (*Cacatua roseicapilla*)	1:14	420 x 420	1:14	1600 x 1600	1:6	300 x 300
	Purple-crowned lorikeet (*Glossopsitta porphyrocephala*)	1:10	240 x 240	1:10	900 x 900	1:6	270 x 270
	Budgerigar (*Melopsittacus undulatus*)	1:10	240 x 240	1:10	1200 x 1200	1:4	270 x 270
	Cockatiel (*Nymphicus hollandicus*)	1:12	260 x 260	1:10	1200 x 1200	1:6	270 x 270
	Crimson rosella (*Platycercus elegans*)	1:12	260 x 260	1:12	1200 x 1200	1:4	270 x 270
	Red-rumped parrot (*Psephotus haematonotus*)	1:10	290 x 290	1:10	900 x 900	1:10	200 x 200
	Rainbow lorikeet (*Trichoglossus haematodus*)	1:10	280 x 280	1:10	1100 x 1100	1:10	200 x 200
Sphenisciformes	Little penguin (*Eudyptula minor*)	1:22	580 x 580	1:20	1300 x 1300	1:10	300 x 300
Strigiformes	Northern saw-whet owl (*Aegolius acadicus*)	1:10	280 x 280	1:8	1300 x 1300	1:4	270 x 270
	Australian boobook (*Ninox boobook*)	1:10	600 x 600	1:10	1500 x 1500	1:10	300 x 300
	Barn owl (*Tyto alba*)	1:10	480 x 480	1:14	1300 x 1300	1:6	300 x 300

Table S2.2. Details of the allometric relationships among the cerebellar measurements examined.

x-axis	y-axis	Intercept	slope	λ	F-ratio	r^2	p	Figures
Cb vol.	Molecular vol.	-0.104	1.027 ± 0.021	0	2,267	0.977	<0.01	**2.3**
	Granule vol.	-0.147	0.909 ± 0.015	0.763	3,459	0.986	<0.01	
	Wm + CbN vol	-0.756	1.058 ± 0.030	0.403	1,267	0.960	<0.01	
Cb vol.	#Purkinje cell	3.936	0.703 ± 0.035	0.346	412.6	0.886	<0.01	**2.4**
	#Granule cell	6.343	0.867 ± 0.038	0.598	507.9	0.905	<0.01	
	#CbN neuron	3.653	0.518 ± 0.027	0	353.9	0.869	<0.01	
	Purkinje cell size	2.088	0.183 ± 0.032	0.152	32.5	0.373	<0.01	
	Granule cell size	0.913	0.062 ± 0.026	0.720	5.6	0.080	0.02	
	CbN neuron size	2.327	0.091 ± 0.023	0	15.2	0.211	<0.01	
#Purkinje cell	#Granule cell	2.119	1.125 ± 0.064	0.449	311.1	0.854	<0.01	**2.6**
	#CbN neuron	1.031	0.690 ± 0.037	0	340.0	0.865	<0.01	
#Granule cell	#CbN neuron	0.407	0.534 ± 0.041	0.457	170.0	0.761	<0.01	
Purkinje cell size	Granule cell size	0.360	0.280 ± 0.073	0.770	14.6	0.205	<0.01	
	CbN neuron size	1.404	0.452 ± 0.065	0	48.0	0.470	<0.01	
Granule cell size	CbN neuron size	2.138	0.408 ± 0.116	0	12.4	0.177	<0.01	
Purkinje cell size	#Purkinje cell	2.999	1.105 ± 0.246	0.866	20.2	0.265	<0.01	**2.7**
Granule cell size	#Granule cell	-	-	-	-	-	0.424	
CbN neuron size	#CbN neuron	2.543	0.983 ± 0.311	0.835	10.0	0.145	<0.01	
Brain minus Cb vol.	Cb vol.	-0.698	0.934 ± 0.046	0.753	421.9	0.888	<0.01	**2.8**
	Purkinje layer, area	0.090	0.752 ± 0.044	0.688	297.0	0.848	<0.01	
	#Purkinje cell	3.455	0.656 ± 0.048	0.627	185.3	0.777	<0.01	
Cb vol.	Purkinje layer, area	6.711	0.788 ± 0.020	0	1,496	0.966	<0.01	**2.9**
	CFI	0.224	0.143 ± 0.014	0.872	98.3	0.647	<0.01	
Purkinje layer, area	#Purkinje cell	-1.925	0.879 ± 0.036	0.418	585.3	0.917	<0.01	
	CFI	-0.991	0.181 ± 0.015	0.876	152.5	0.741	<0.01	
#Purkinje cell	CFI	-0.502	0.189 ± 0.018	0.819	111.3	0.675	<0.01	

Table S2.3. Multiple allometric models with number of Purkinje cells as the dependent variable, and surface area of the Purkinje cell layer, and cerebellar volume as the predictor variables. #PC = number of Purkinje cells; PCL area = surface area of the Purkinje cell layer; Cbvol = cerebellum volume

Full model: #PC ~ PCL area + Cbvol				
p	**λ**	**r^2**	**AIC**	
<0.01	0.417	0.915	-111.31	
Sequential SS Anova			**Mean sq.**	**p**
PCL area			0.04	<0.01*
Cbvol			<0.01	0.97
Residuals			<0.01	

Model 1: #PC ~ PCL area				
P	**λ**	**r^2**	**AIC**	
<0.01	0.418	0.917	-113.30	
Sequential SS Anova			**Mean sq.**	**p**
PCL			0.04	<0.01*
Residuals			<0.01	

Model 2: #PC ~ Cbvol				
P	**λ**	**r^2**	**AIC**	
<0.01	0.346	0.886	-95.24	
Sequential SS Anova			**Mean sq.**	**p**
Cbvol			0.04	<0.01*
Residuals			<0.01	

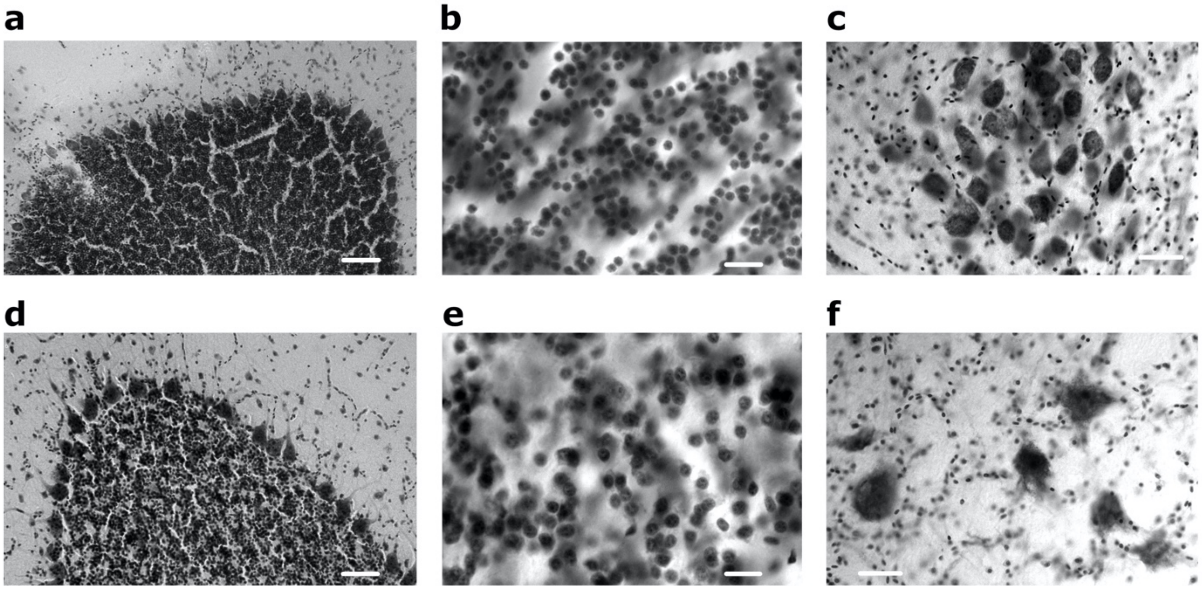

Figure S2.1. A comparison of the sizes of Purkinje cells, granule cells, and cerebellar nuclei neurons in two species, **A-C** the brown thornbill (Acanthiza pusilla), and **D-F** the little penguin (Eudyptula minor). For each species, Purkinje cells are shown in **A** and **D** (scale-bar = 50 µm); granule cells in **B** and **E** (scale-bar = 10 µm), and cerebellar nuclei neuron in **C** and **F** (scale-bar = 30 µm).